R O S E T T A

FLIGHT REPORTS
of RPC–MAG

RO–IGEP–TR–0025

Issue: 4 Revision: 0

January 24, 2019

Report of the

STEINS Flyby

Time period: September 01 - 10, 2008

Karl-Heinz Glassmeier
Ingo Richter

Institut für Geophysik und extraterrestrische Physik
Technische Universität Braunschweig
Mendelssohnstraße 3, 38106 Braunschweig
Germany

Contents

1 Introduction

ROSETTA's Flyby at asteroid 2867 STEINS happened on September 05, 2008. RPC-MAG was switched on in the time between 2008-09-01T00:10:00 and 2008-09-10T06:01:00. The Closest Approach (CA) took place at 2008-09-05T18:38:19.3 (Onboard UTC). The instrument performance was flawlessly. There were no problems from the instrument side.

This document gives a brief description of the executed activities and show the obtained data. Housekeeping data (Temperature of the OB & IB sensor, Filter Stages A & B, Filter configuration register, Reference voltage, negative and positive 5V supply voltage, and the coarse HK sampled magnetic field data of the OB sensor) are presented as well as magnetic field science data of the OB and IB sensor in the activated modes. Magnetic field data are plotted in s/c coordinates and ECLIPJ2000 coordinates if not otherwise stated. They are calibrated according to the results of the ground calibration and the results of the inflight temperature model 009 using the actual flight data. Sensitivity, Misalignment, and Temperature effects are taken into account. The s/c residual field is not subtracted.

The spectra of the magnetic field data measured by the OB sensor are plotted in section 5. As usual an influence of ROSETTAs reaction wheels (refer to section 6) can be seen in Burstmode.

From time to time there are also horizontal lines in the dynamic spectrum to be seen. These lines represent constant frequencies and are caused by the LAP instrument. This behavior was investigated and proofed during the PC10 campaign in November 2010. See RO-IGEP-TR0030 for further details.

The data quality and a comparison between OB and IB sensor is presented in section 4.

The activation of the LANDER was combined with the test of some heaters associated to the MUPUS experiment. Unfortunately this caused magnetic disturbances which are also discussed in section 4.

The Rotation Angles of the Solar Arrays and the High Gain Antenna have been plotted in section 7 for the assessment of their influence to the magnetic field data.

A temperature profile for the whole Fly–By is shown in section 8.

2 The Fly–By Geometry

This section gives an overview about the trajectory during the Fly–By.

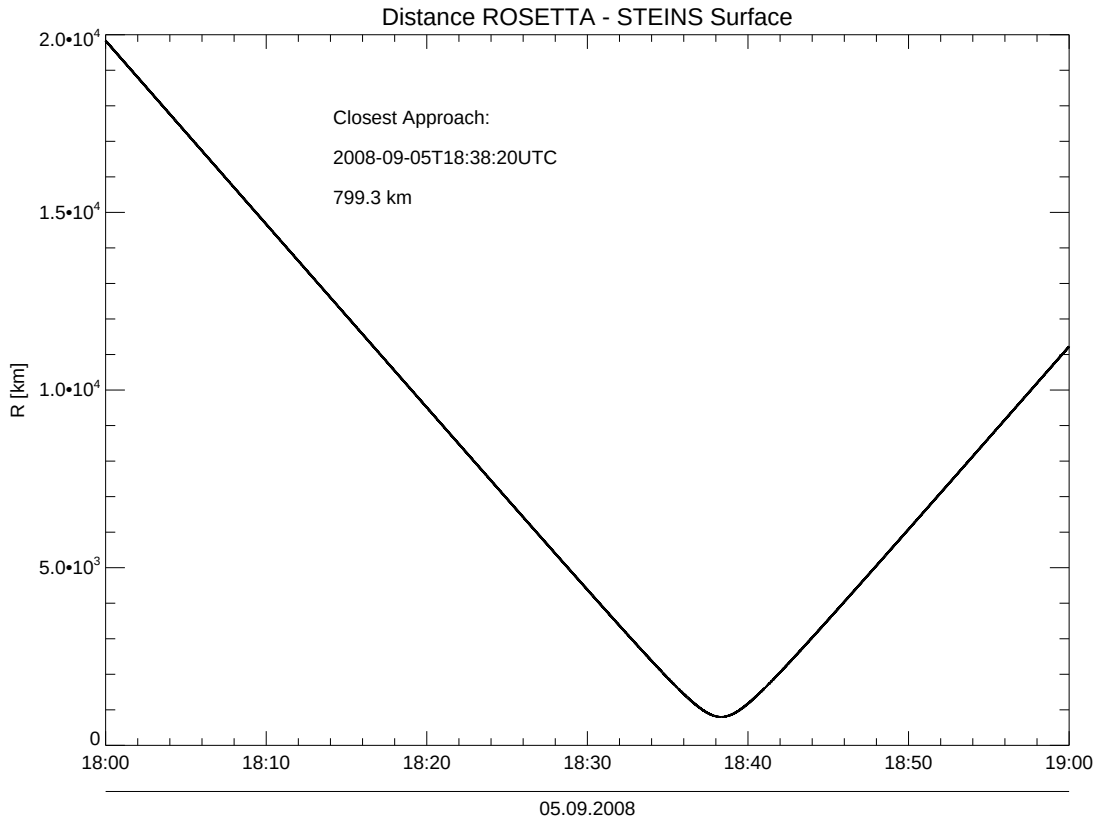

Figure 1: ROSETTA'S Distance to the STEINS Surface

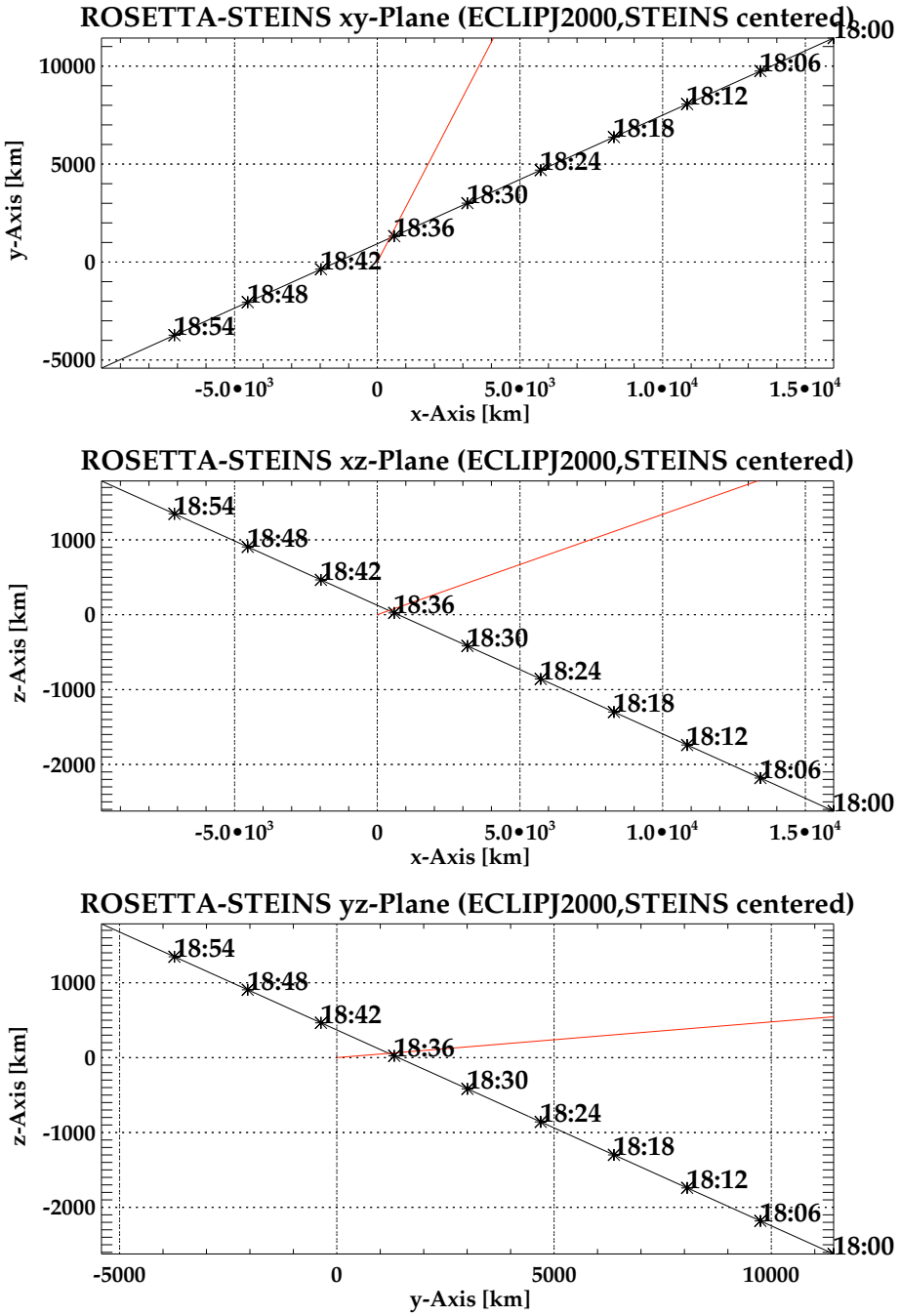

Figure 2: ROSETTA'S Fly-By Trajectory in ECLIPJ2000 coordinates. Red Line: SUN Direction

3 Activities and data plots of the STEINS Fly By

This chapter presents all relevant data /data types measured by RPCMAG day by day:

- Housekeeping data (HK).
- Calibrated LEVEL_B data (s/c coordinates) of the IB and OB sensor with the original sampling frequency.
- Calibrated LEVEL_C data (ECLIPJ2000 coordinates) of the IB and OB sensor with the original sampling frequency.

3.1 September 01, 2008:

3.1.1 Actions

MAG was switched on immediately after PIU and set to HK mode at 00:02. The normal mode SID 2 was set at 00:10. All commands passed smoothly and the instrument followed in the expected way.

3.2 Plots of Calibrated Data

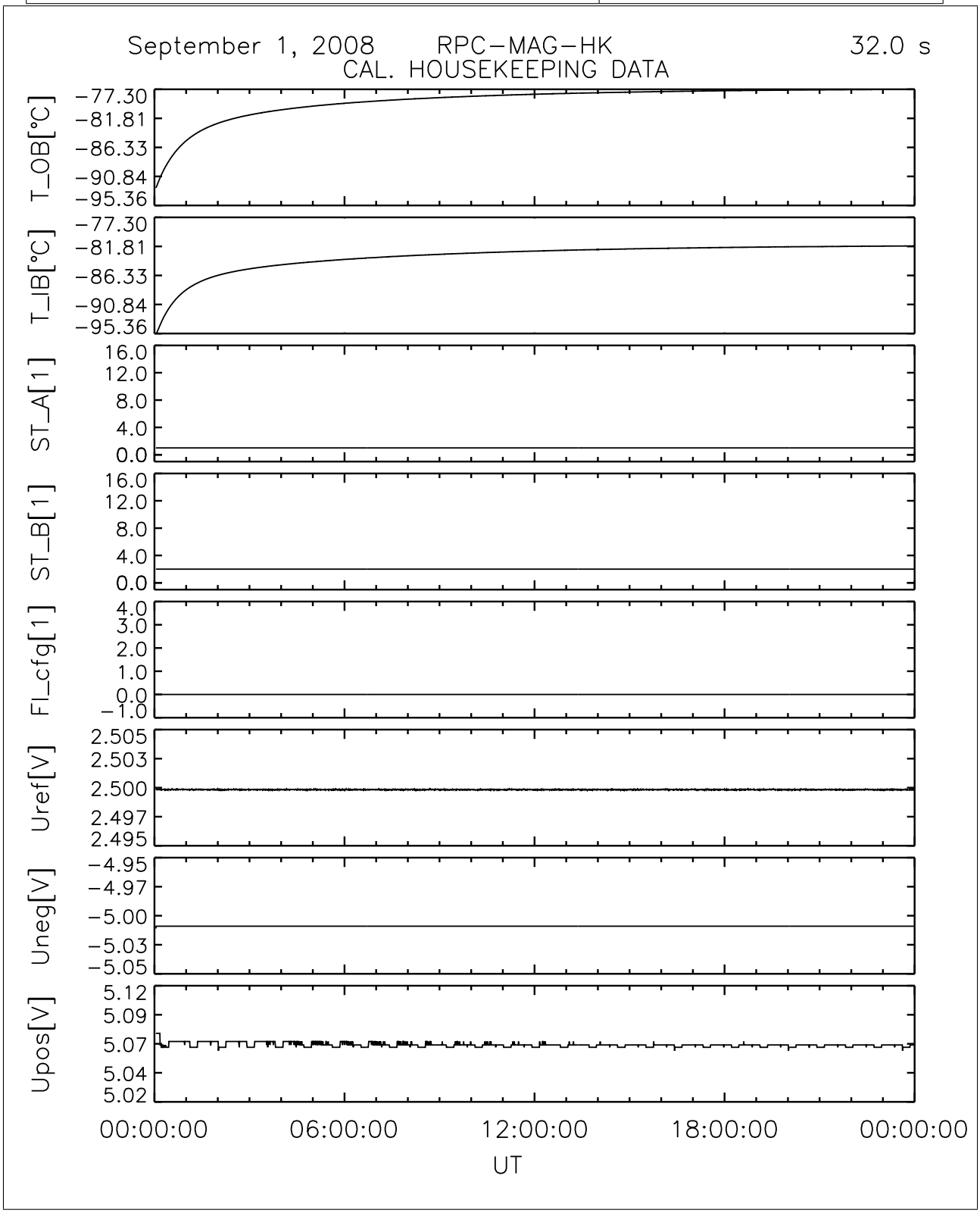

Figure 3: File: RPCMAG080901T0002_CLA_HK_P0000_2400

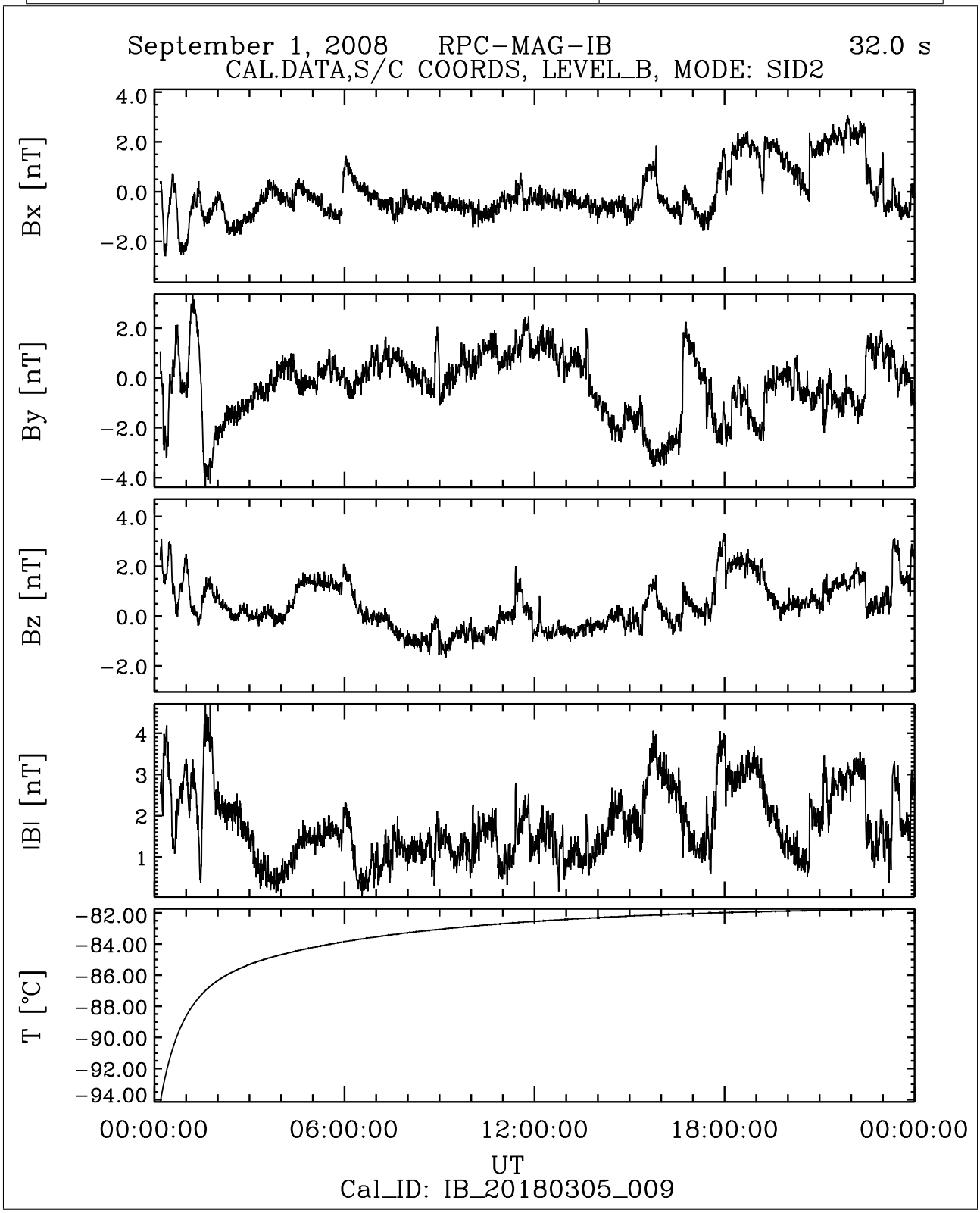

Figure 4: File: RPCMAG080901T0010_CLB_IB_M2_T0000_2400_009

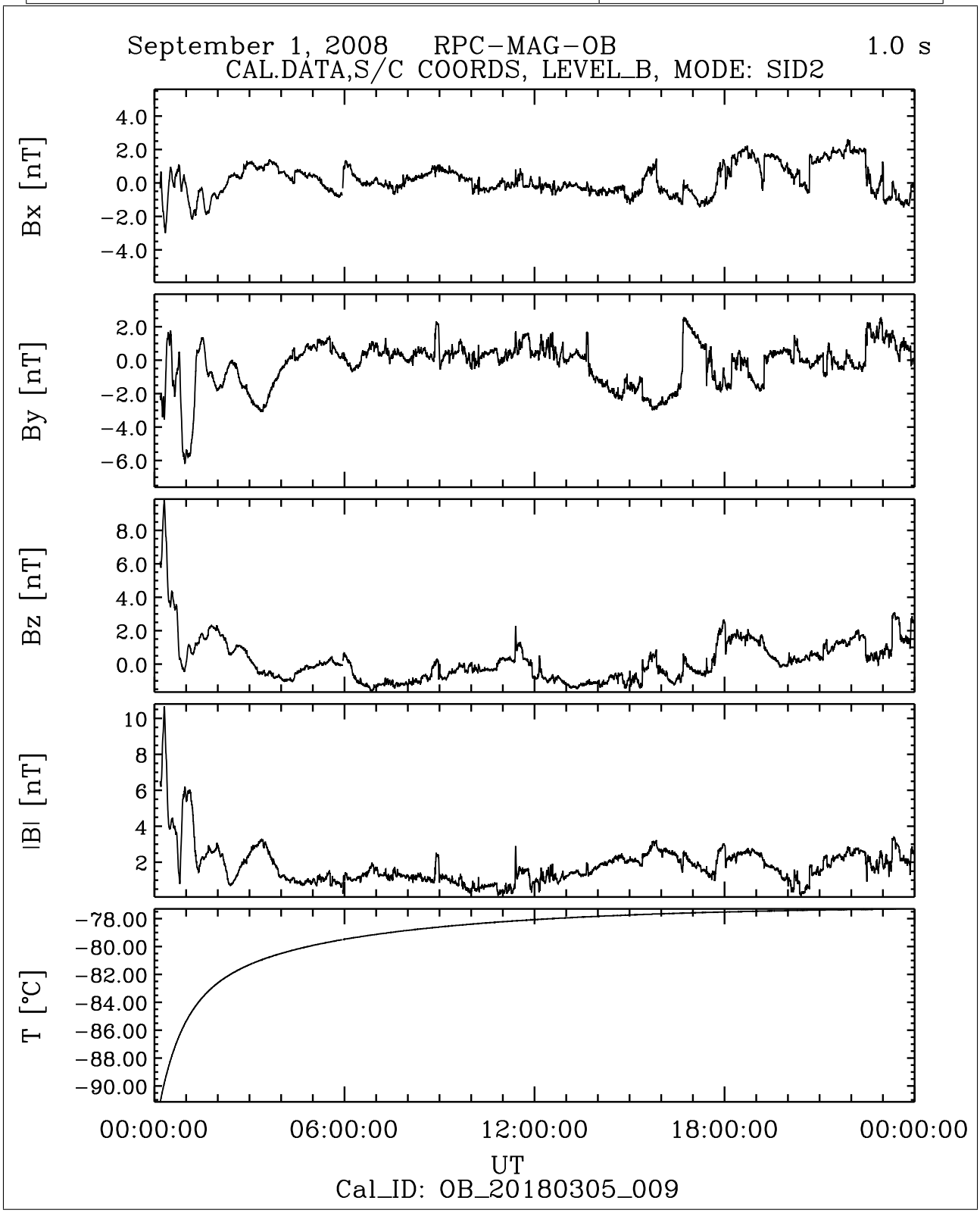

Figure 5: File: RPCMAG080901T0010_CLB_OB_M2_T0000_2400_009

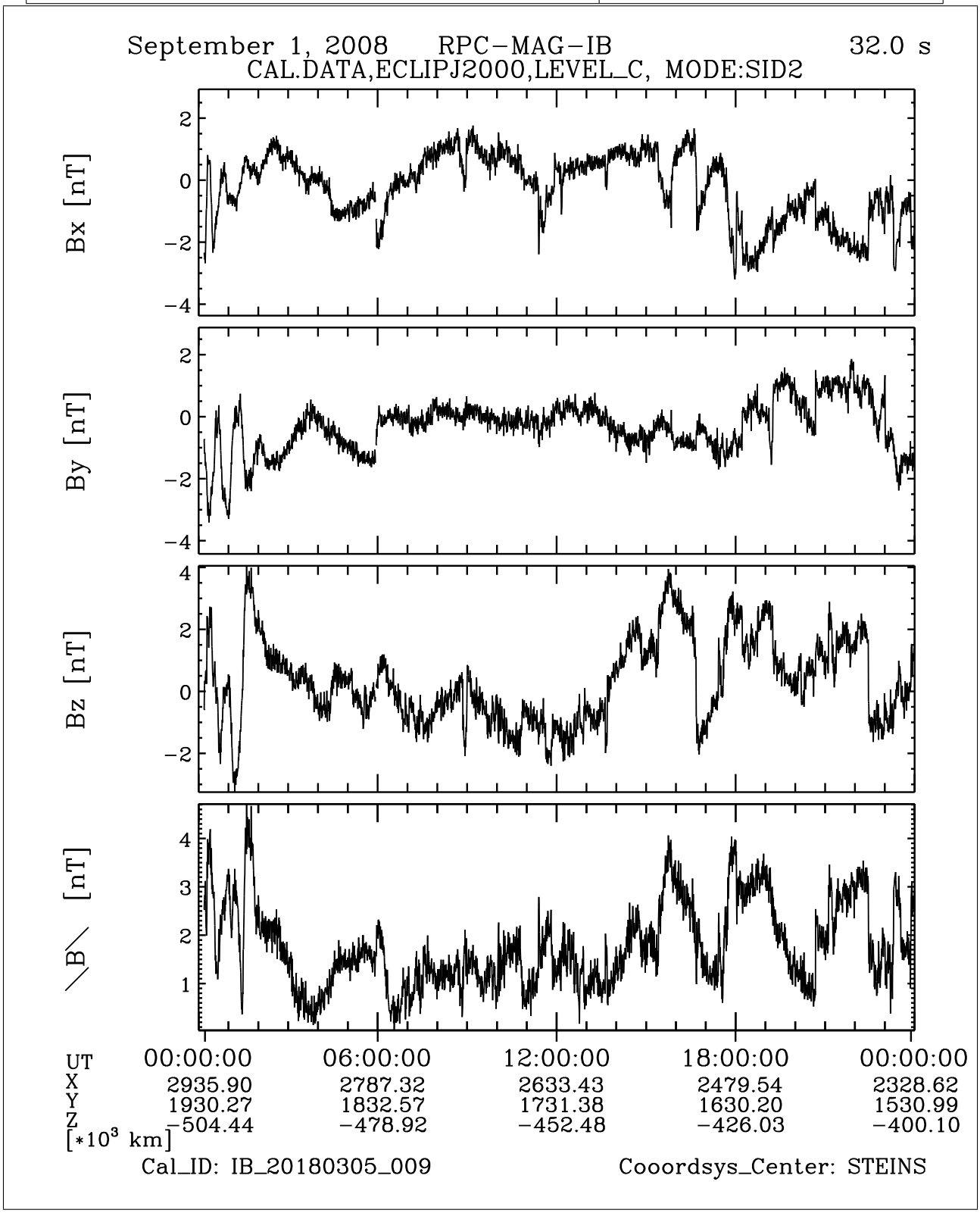

Figure 6: File: RPCMAG080901T0010_CLC_IB_M2_T0000_2400_009

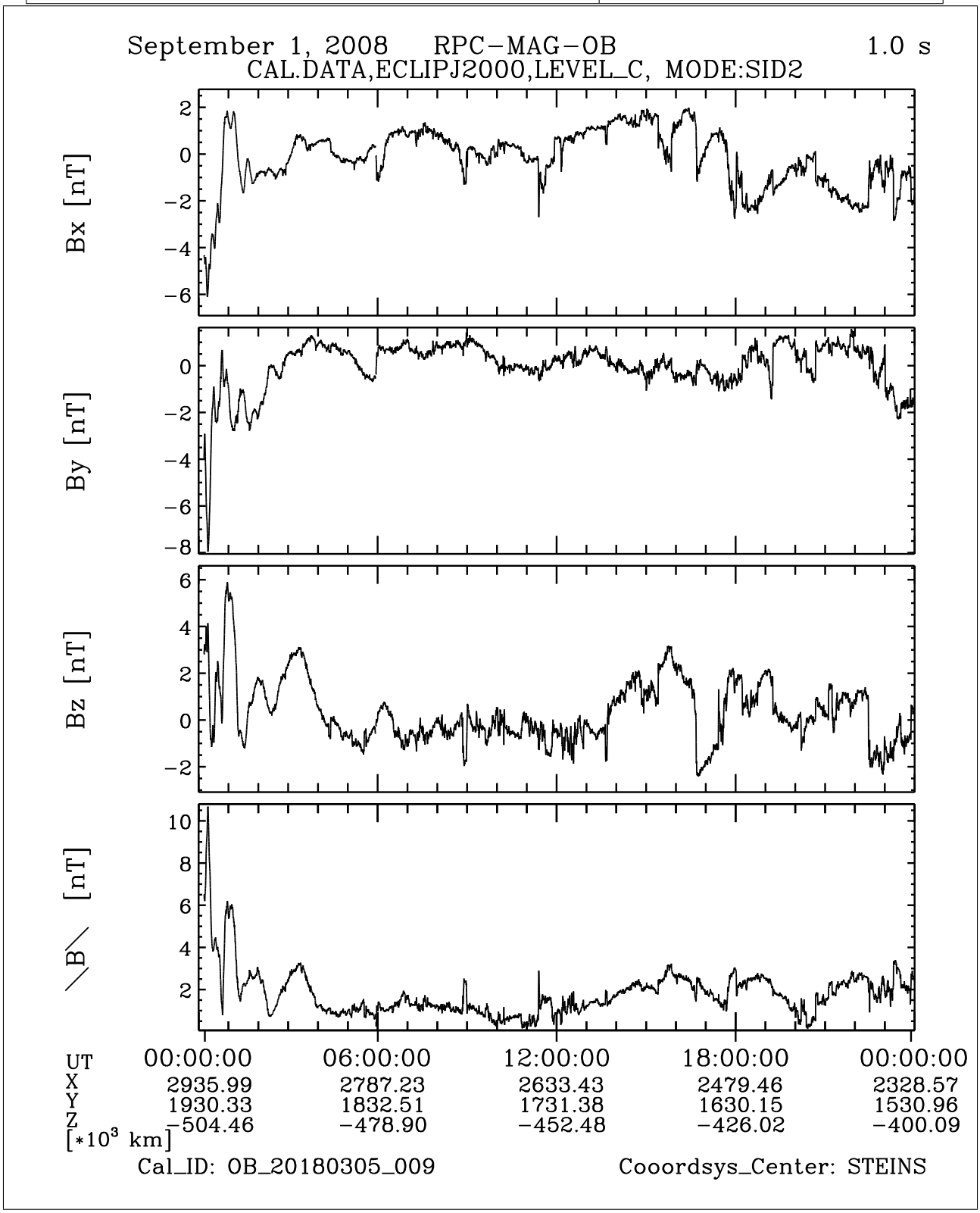

Figure 7: File: RPCMAG080901T0010_CLC_OB_M2_T0000_2400_009

3.3 September 02, 2008:

3.3.1 Actions

MAG stayed in SID 2. No problems occurred.

3.3.2 Plots of Calibrated Data

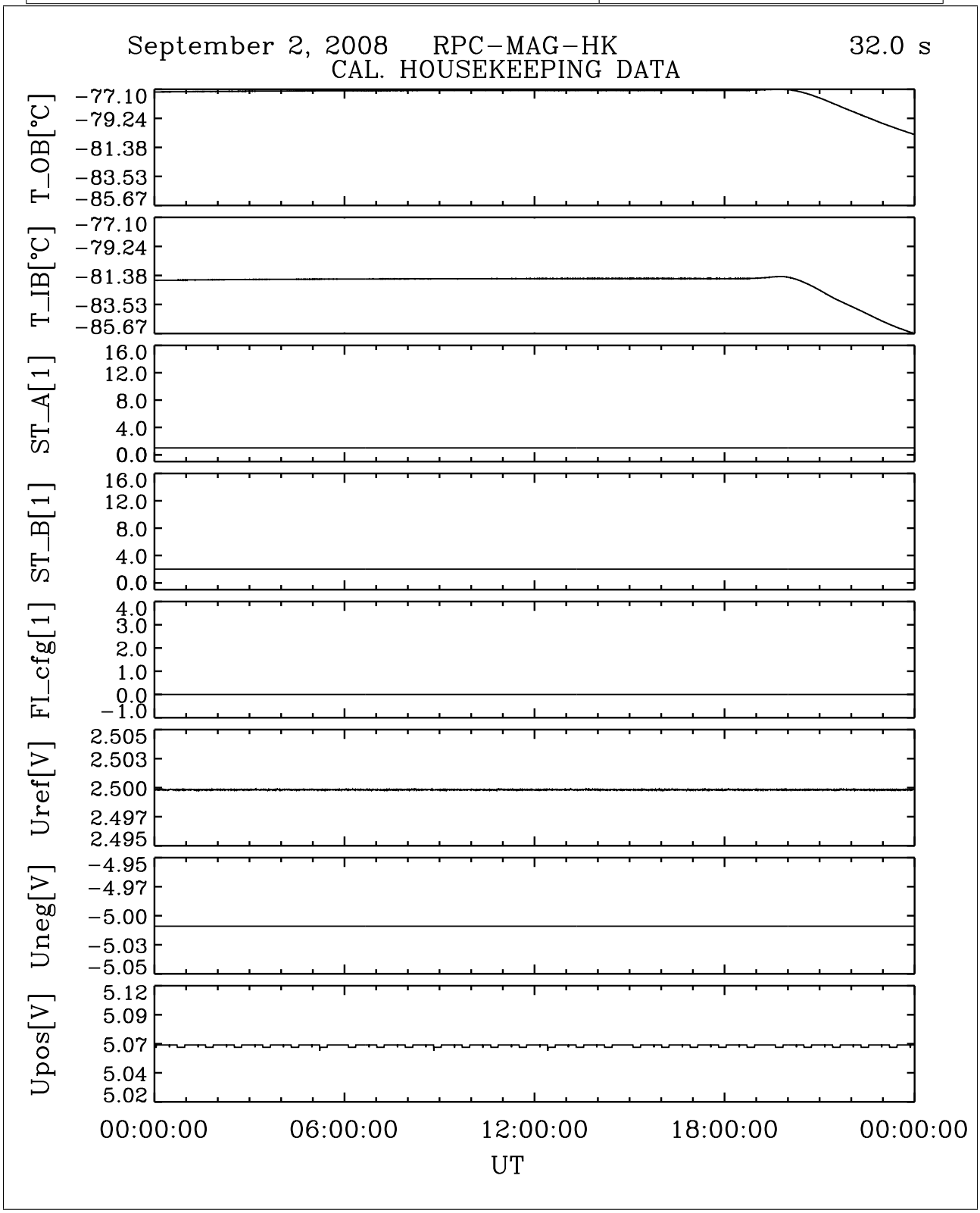

Figure 8: File: RPCMAG080902T0000_CLA_HK_P0000_2400

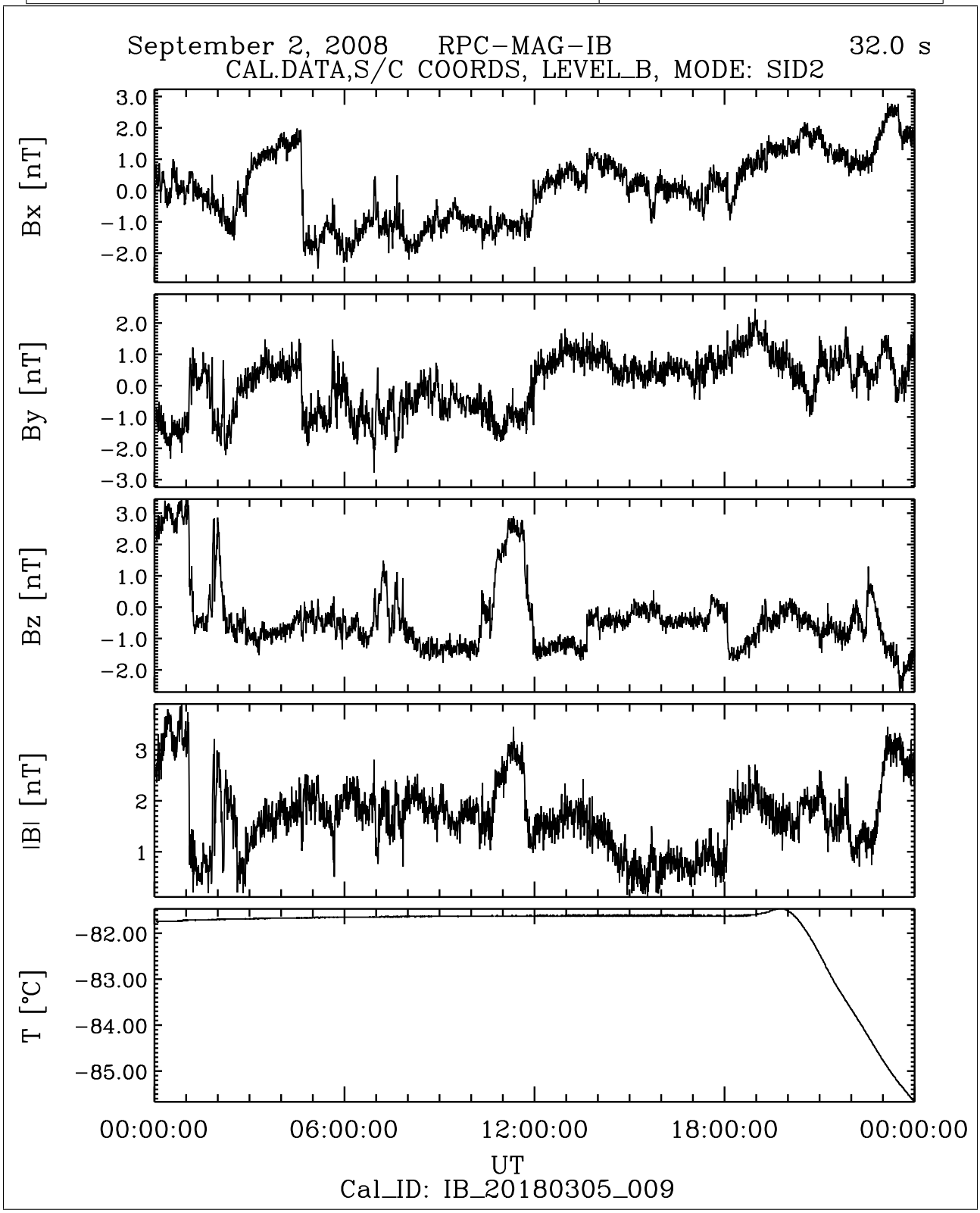

Figure 9: File: RPCMAG080902T0000_CLB_IB_M2_T0000_2400_009

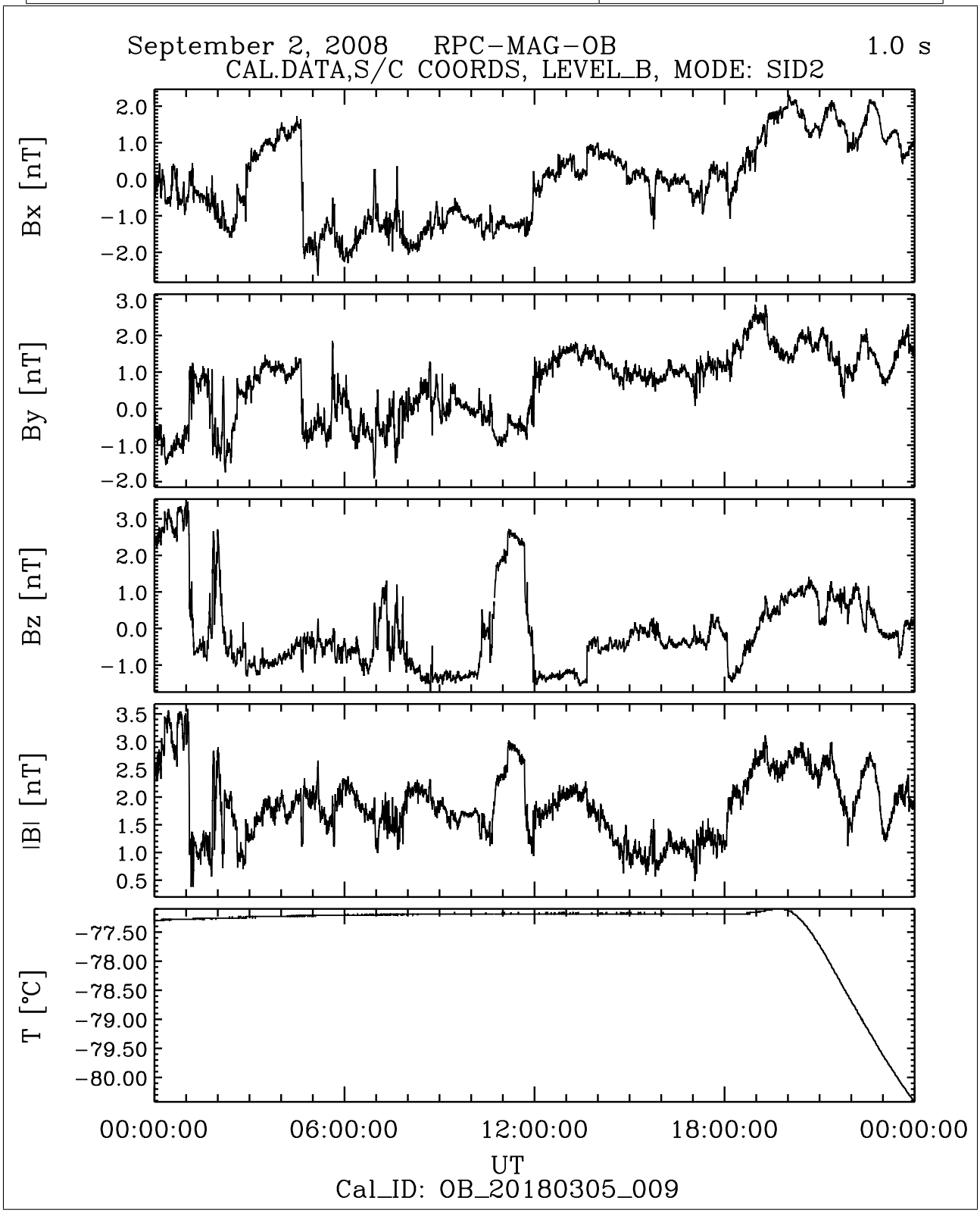

Figure 10: File: RPCMAG080902T0000_CLB_OB_M2_T0000_2400_009

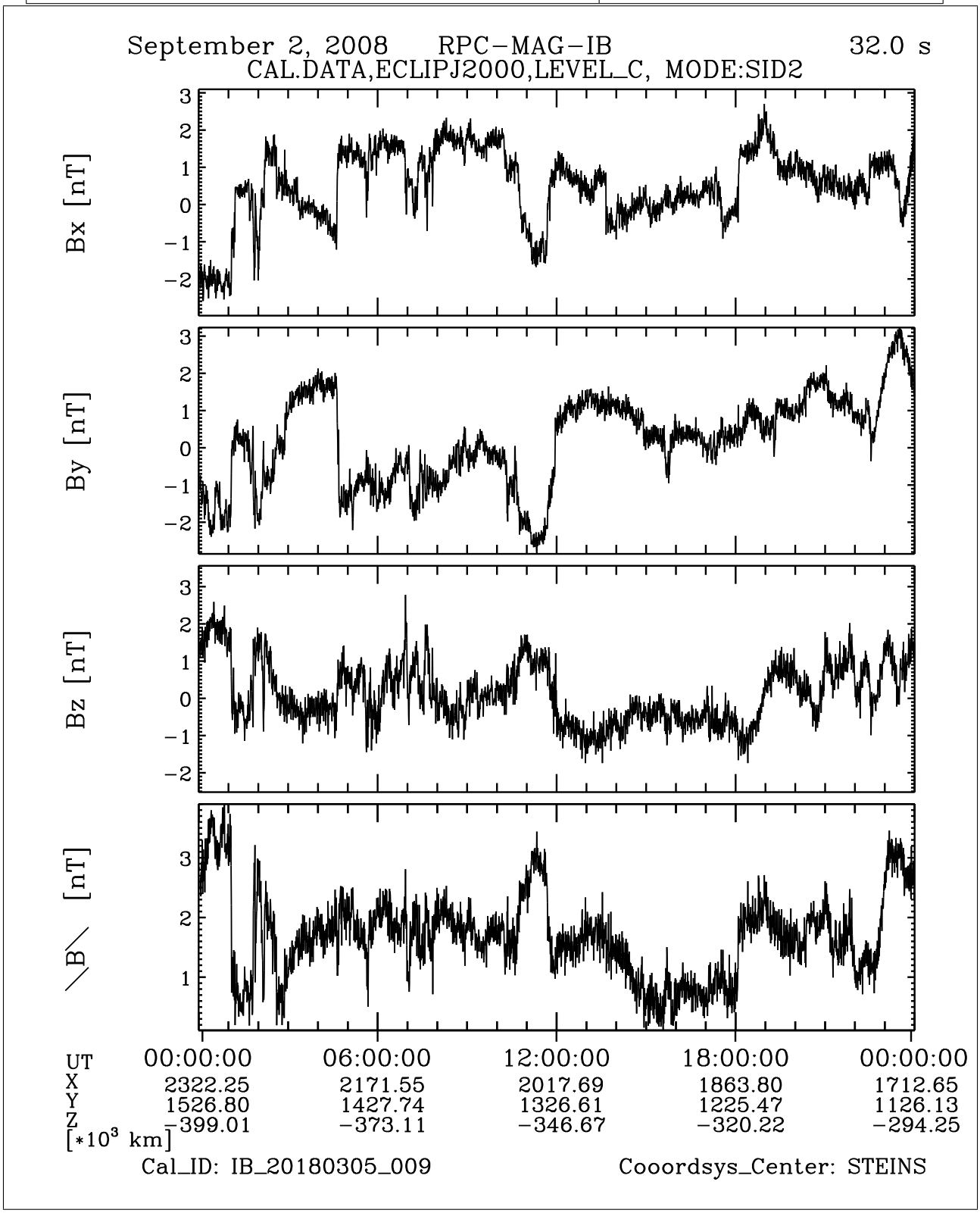

Figure 11: File: RPCMAG080902T0000_CLC_IB_M2_T0000_2400_009

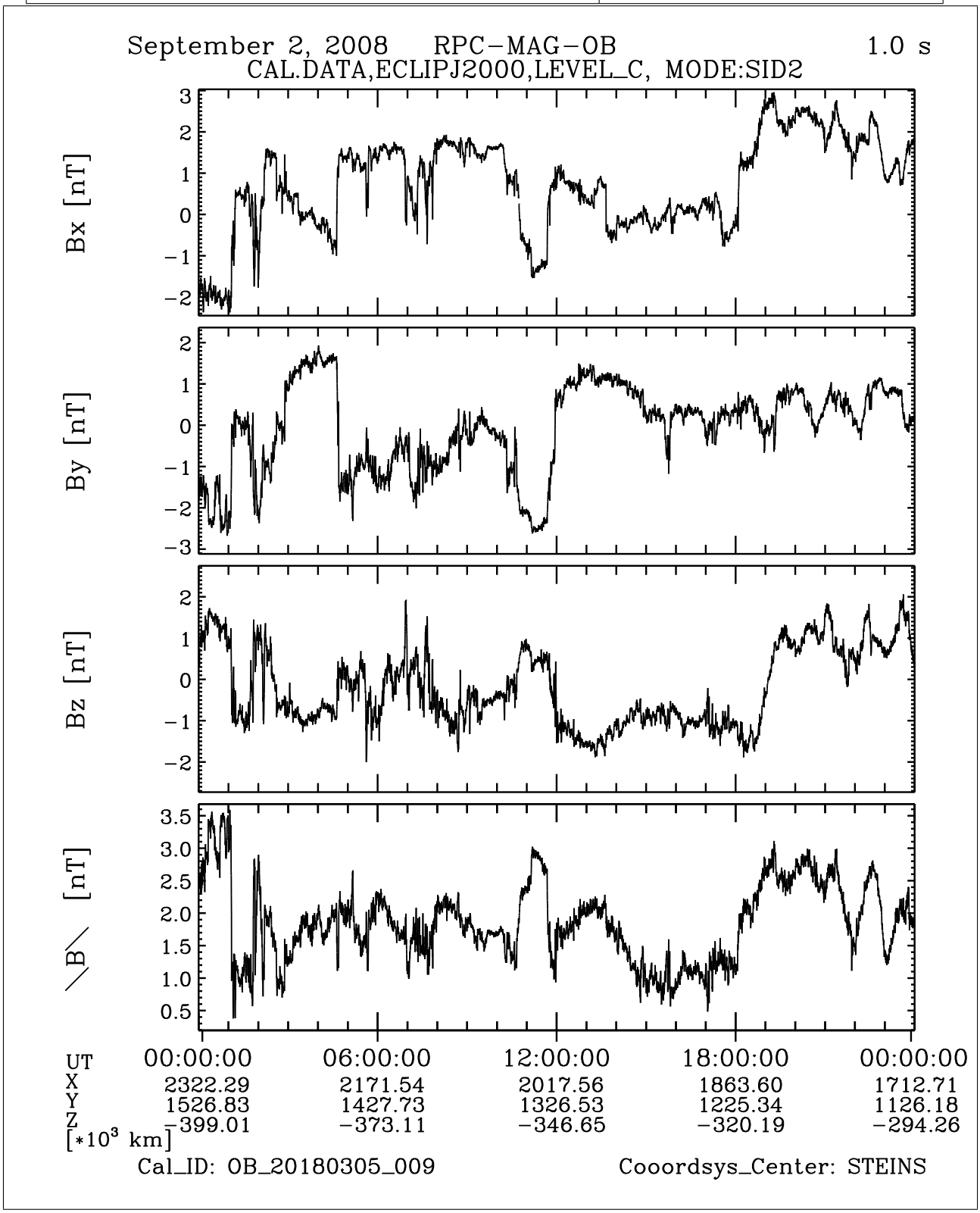

Figure 12: File: RPCMAG080902T0000_CLC_OB_M2_T0000_2400_009

3.4 September 03, 2008:

3.4.1 Actions

MAG stayed in SID 2. No problems occurred.

3.4.2 Plots of Calibrated Data

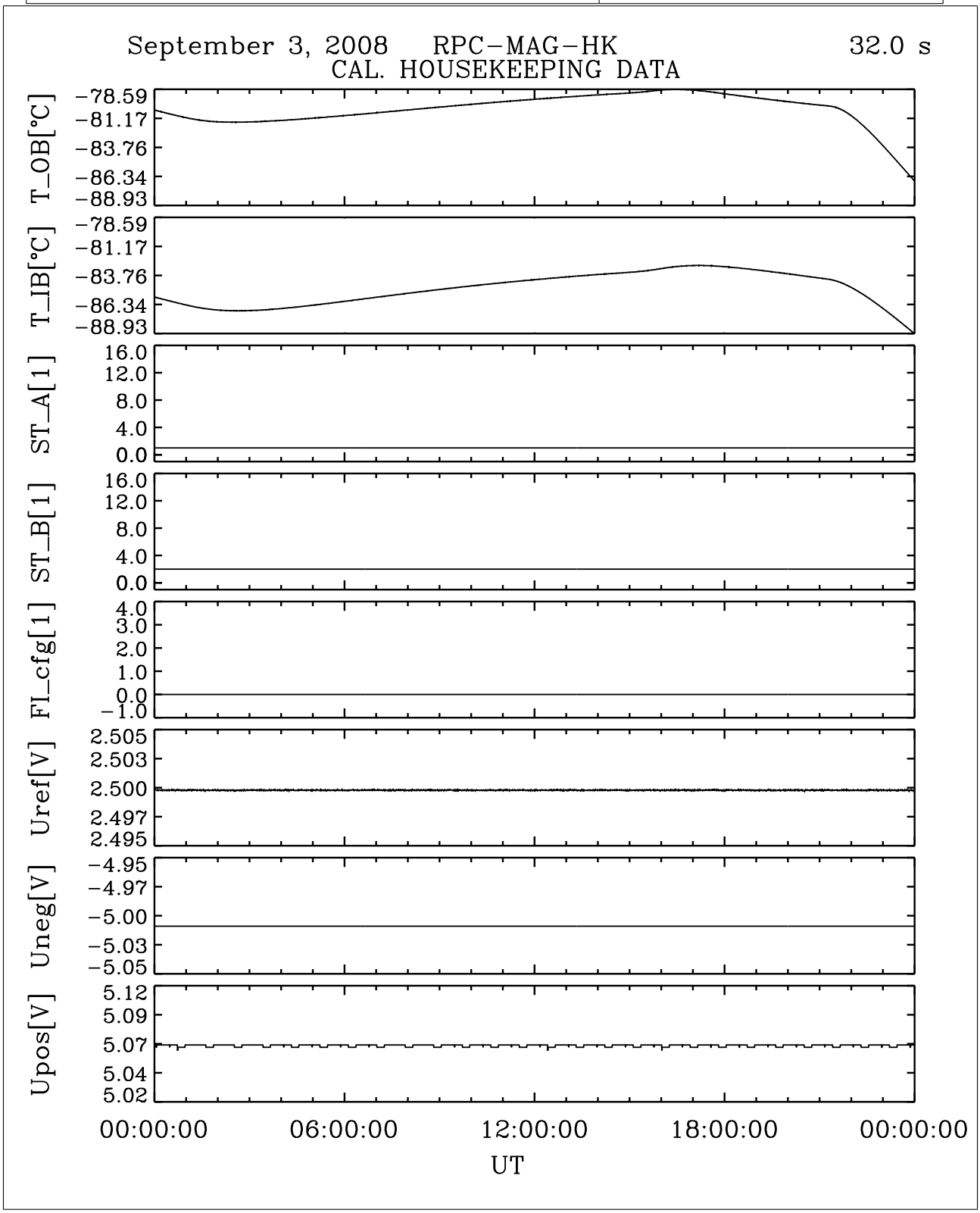

Figure 13: File: RPCMAG080903T0000_CLA_HK_P0000_2400

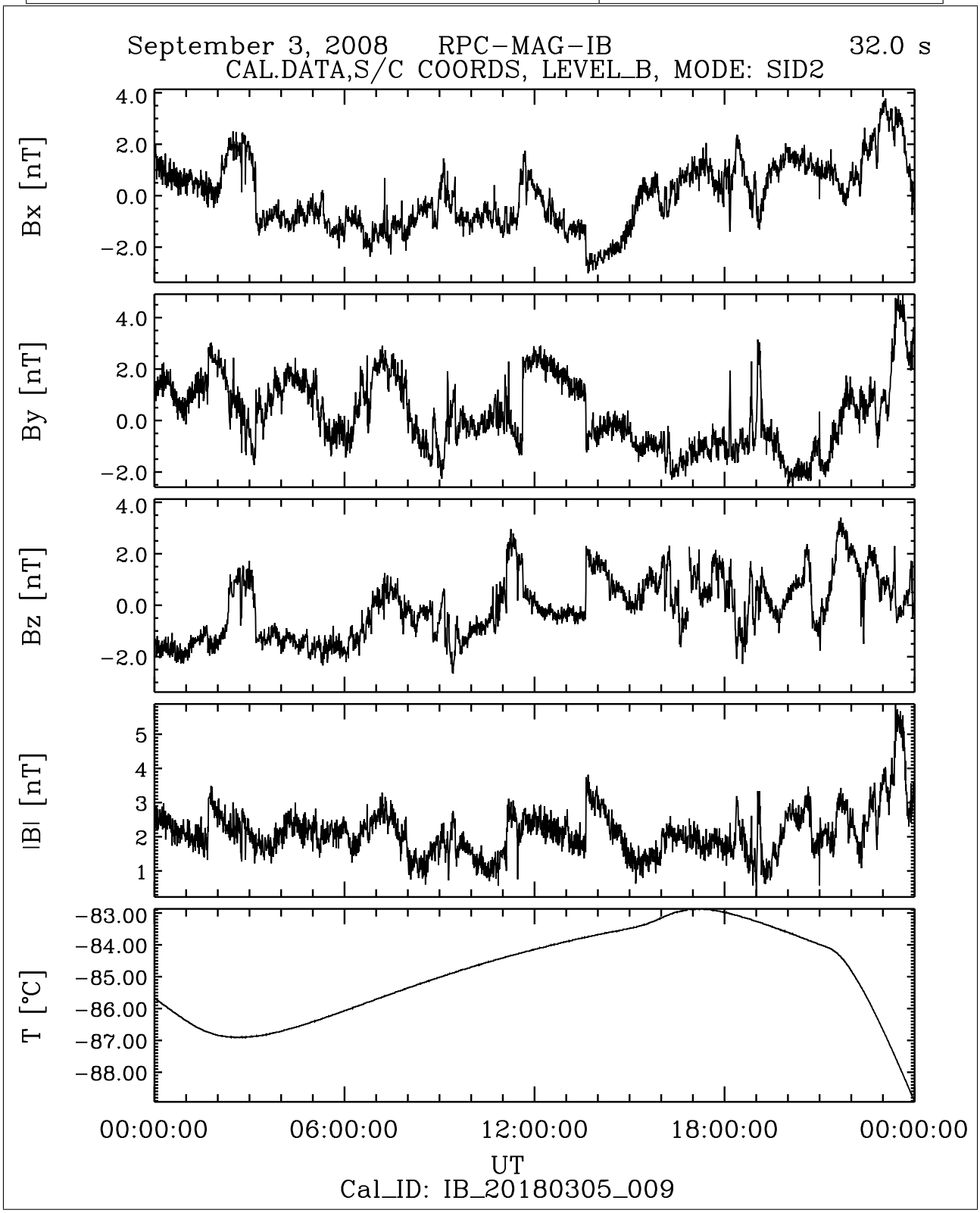

Figure 14: File: RPCMAG080903T0000_CLB_IB_M2_T0000_2400_009

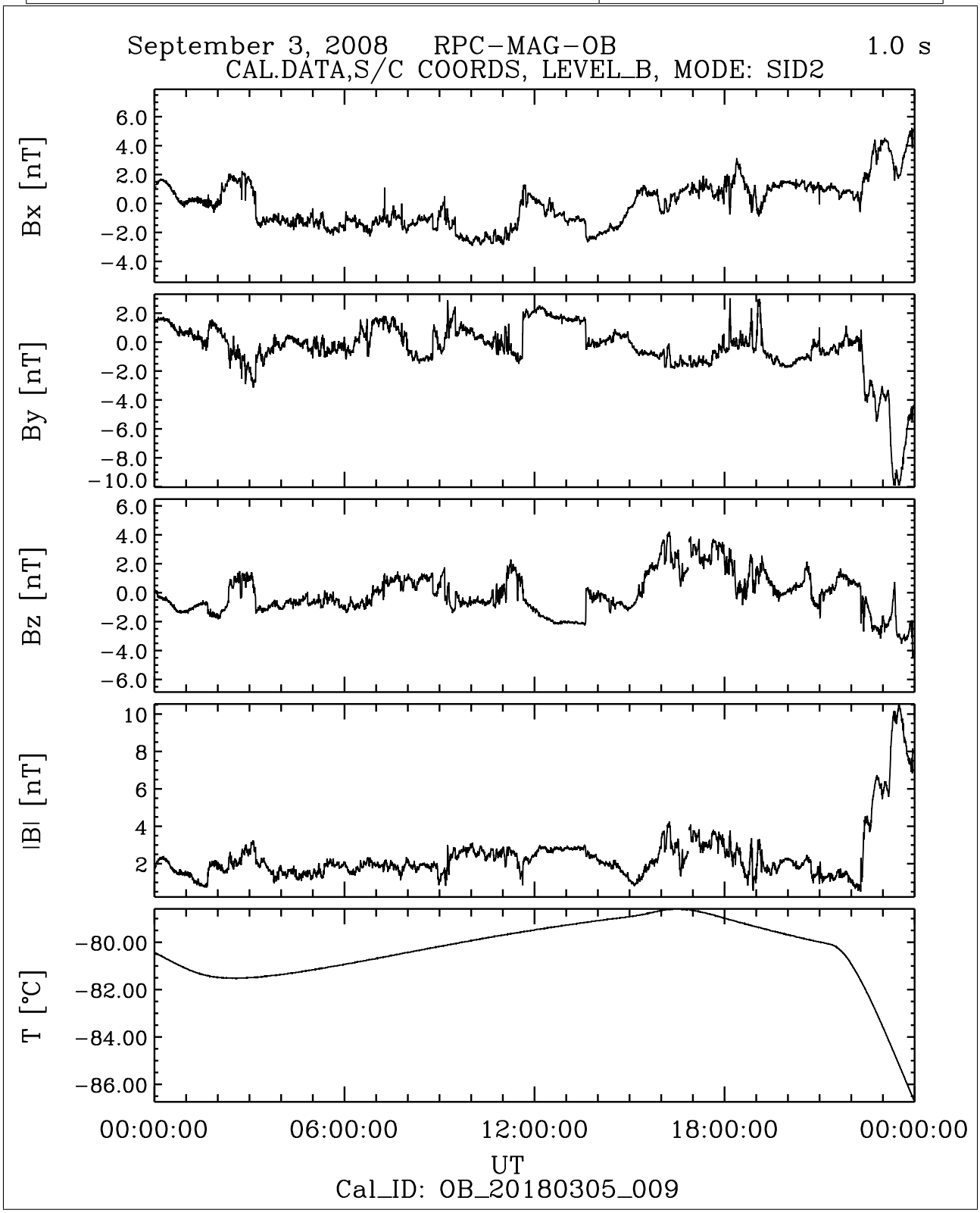

Figure 15: File: RPCMAG080903T0000_CLB_OB_M2_T0000_2400_009

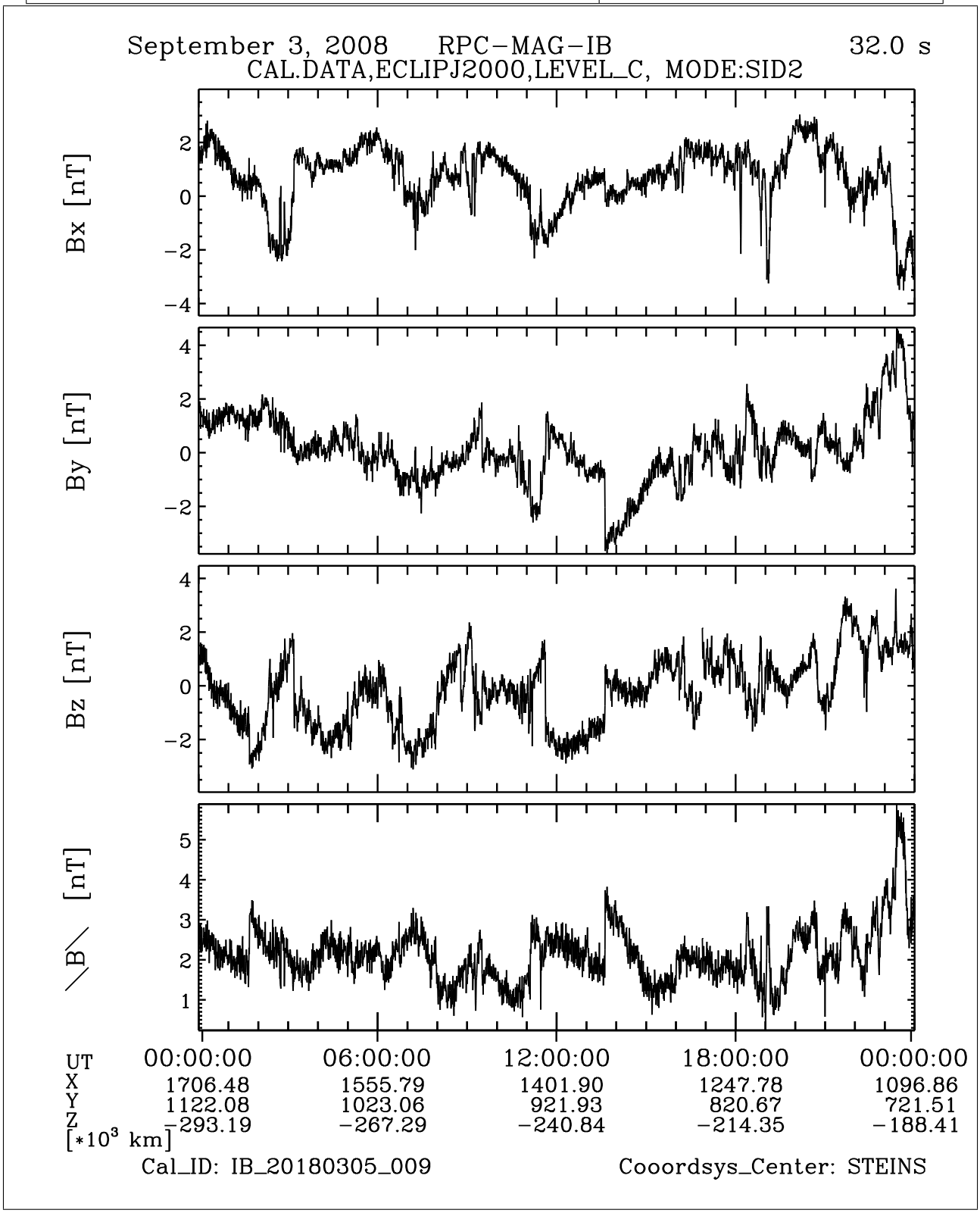

Figure 16: File: RPCMAG080903T0000_CLC_IB_M2_T0000_2400_009

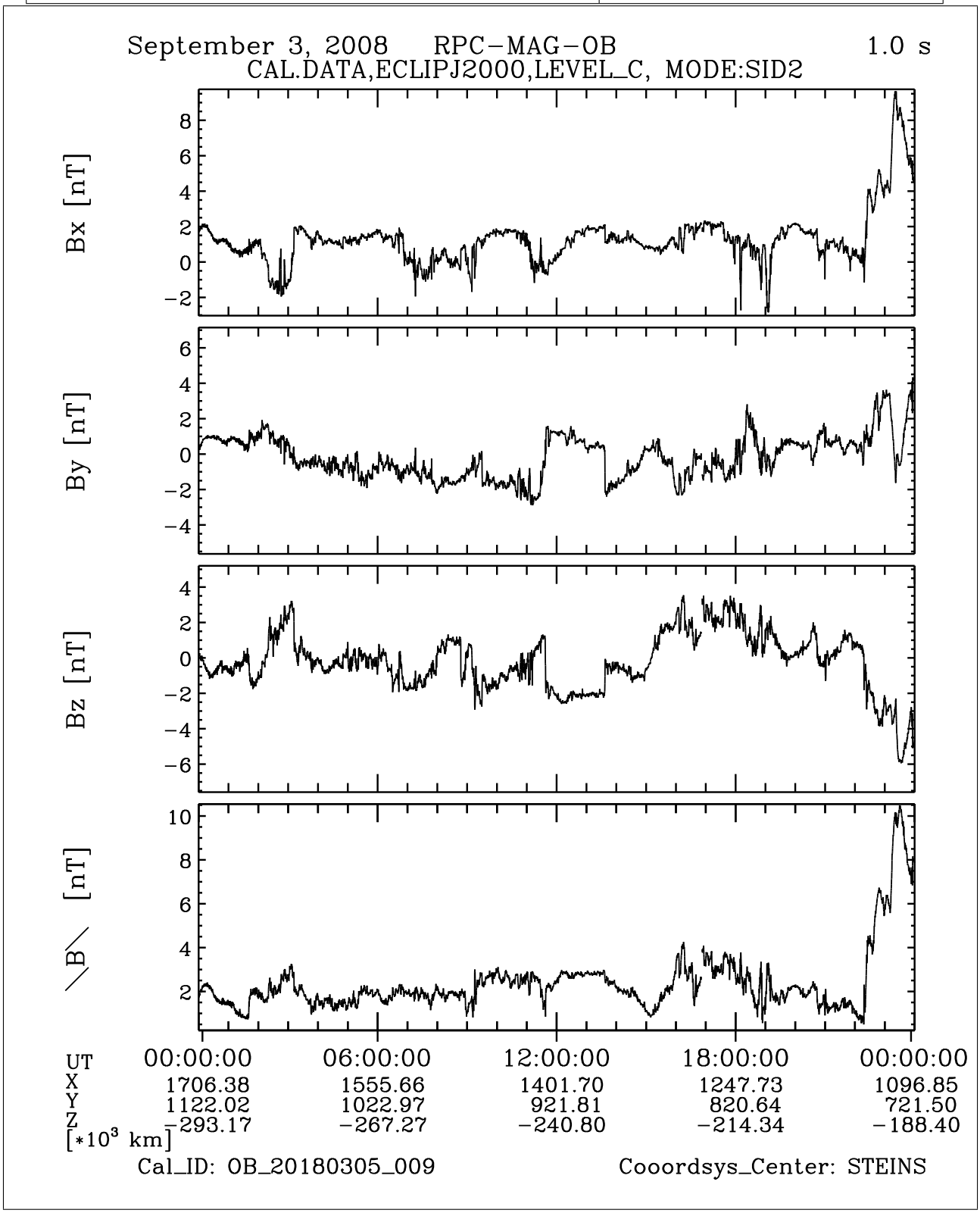

Figure 17: File: RPCMAG080903T0000_CLC_OB_M2_T0000_2400_009

3.5 September 04, 2008:

3.5.1 Actions

MAG stayed in SID 2. No problems occurred.

3.5.2 Plots of Calibrated Data

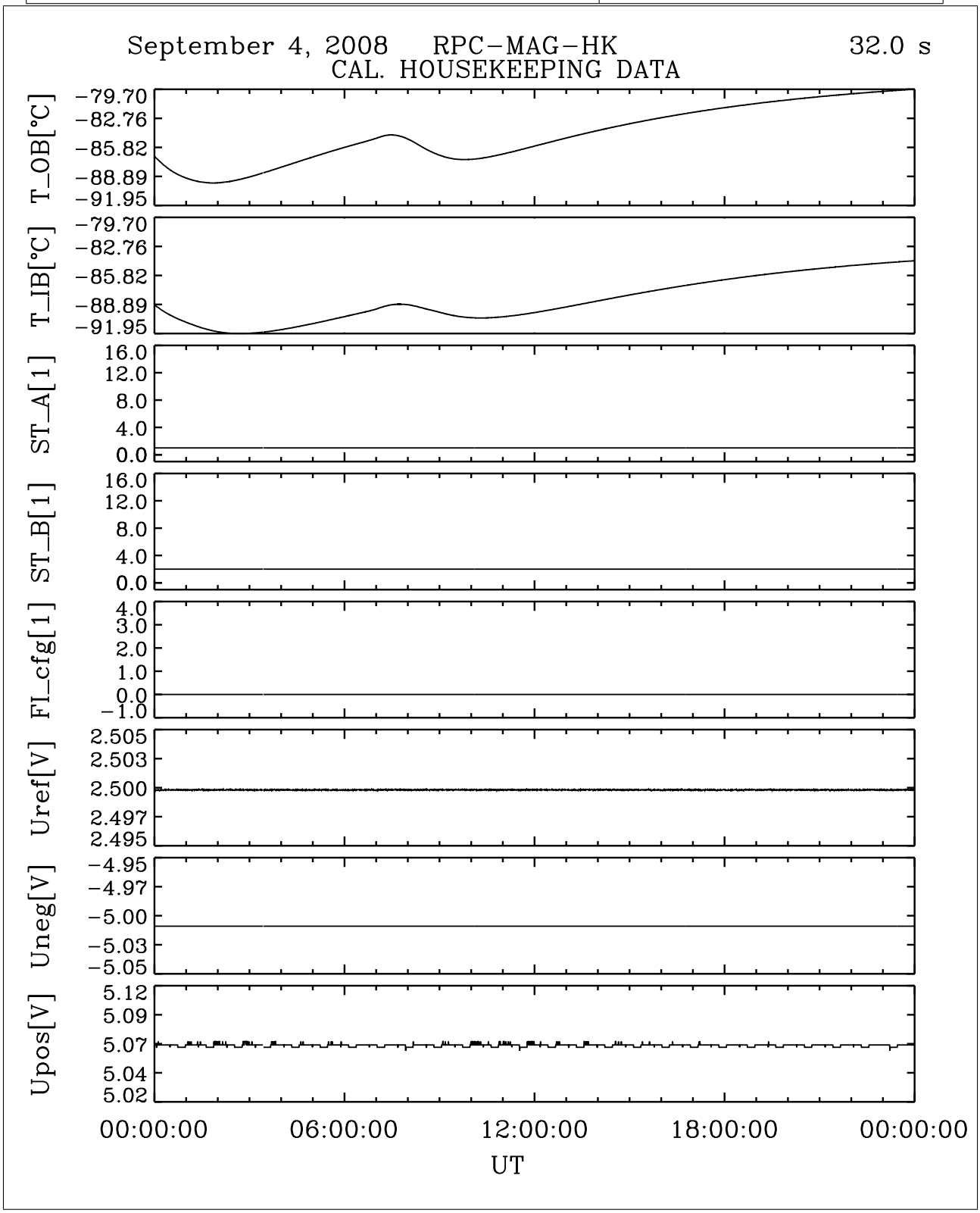

Figure 18: File: RPCMAG080904T0000_CLA_HK_P0000_2400

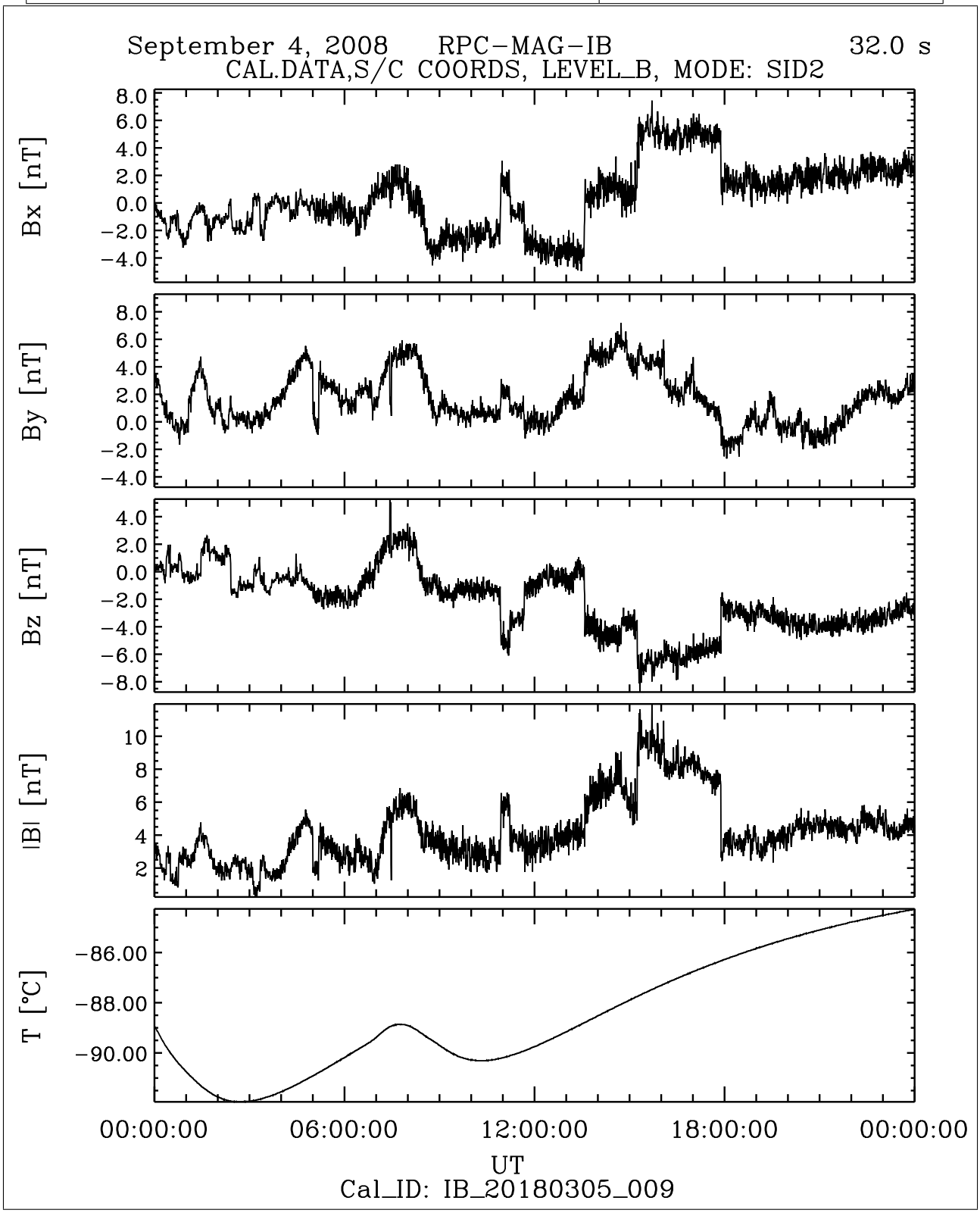

Figure 19: File: RPCMAG080904T0000_CLB_IB_M2_T0000_2400_009

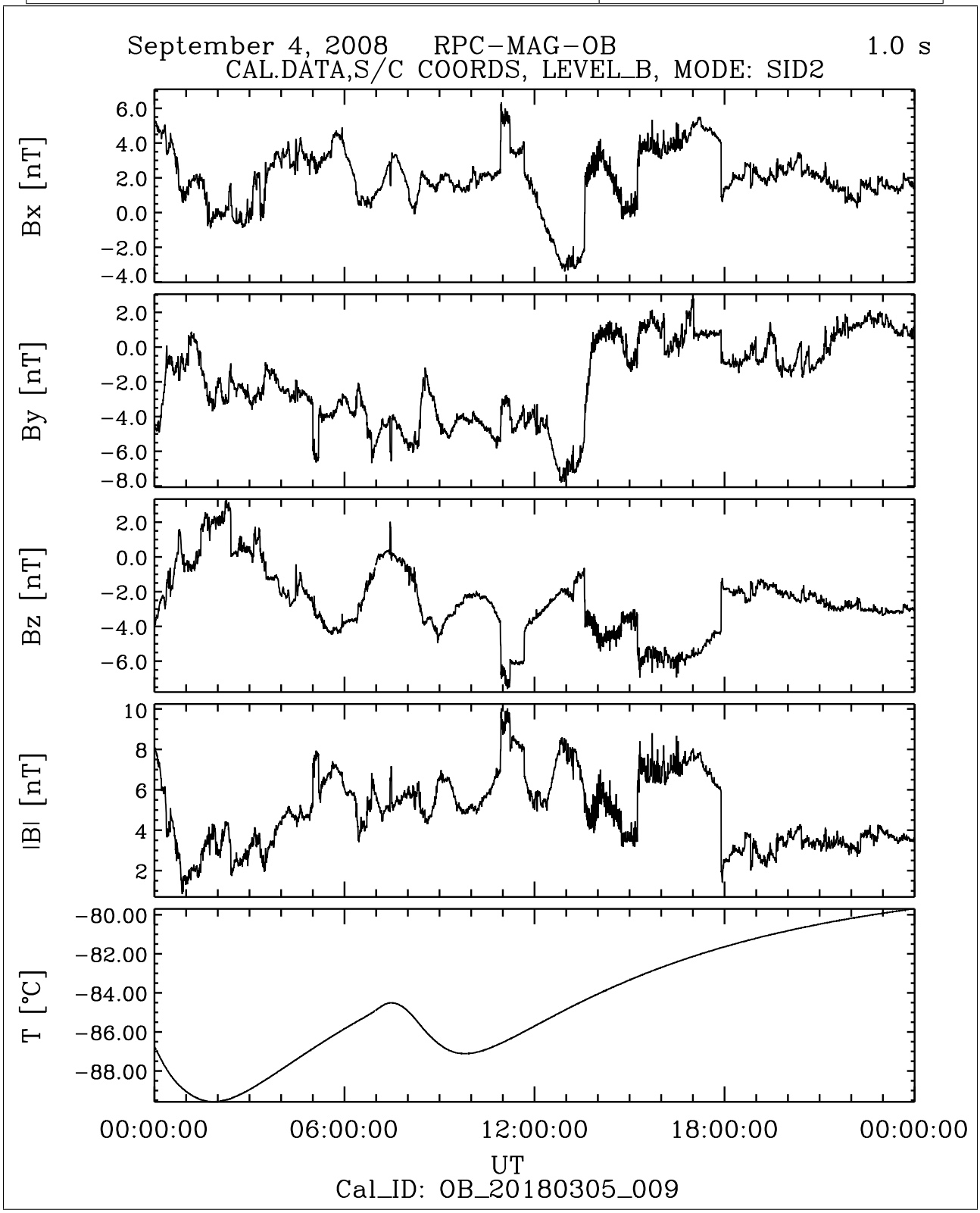

Figure 20: File: RPCMAG080904T0000_CLB_OB_M2_T0000_2400_009

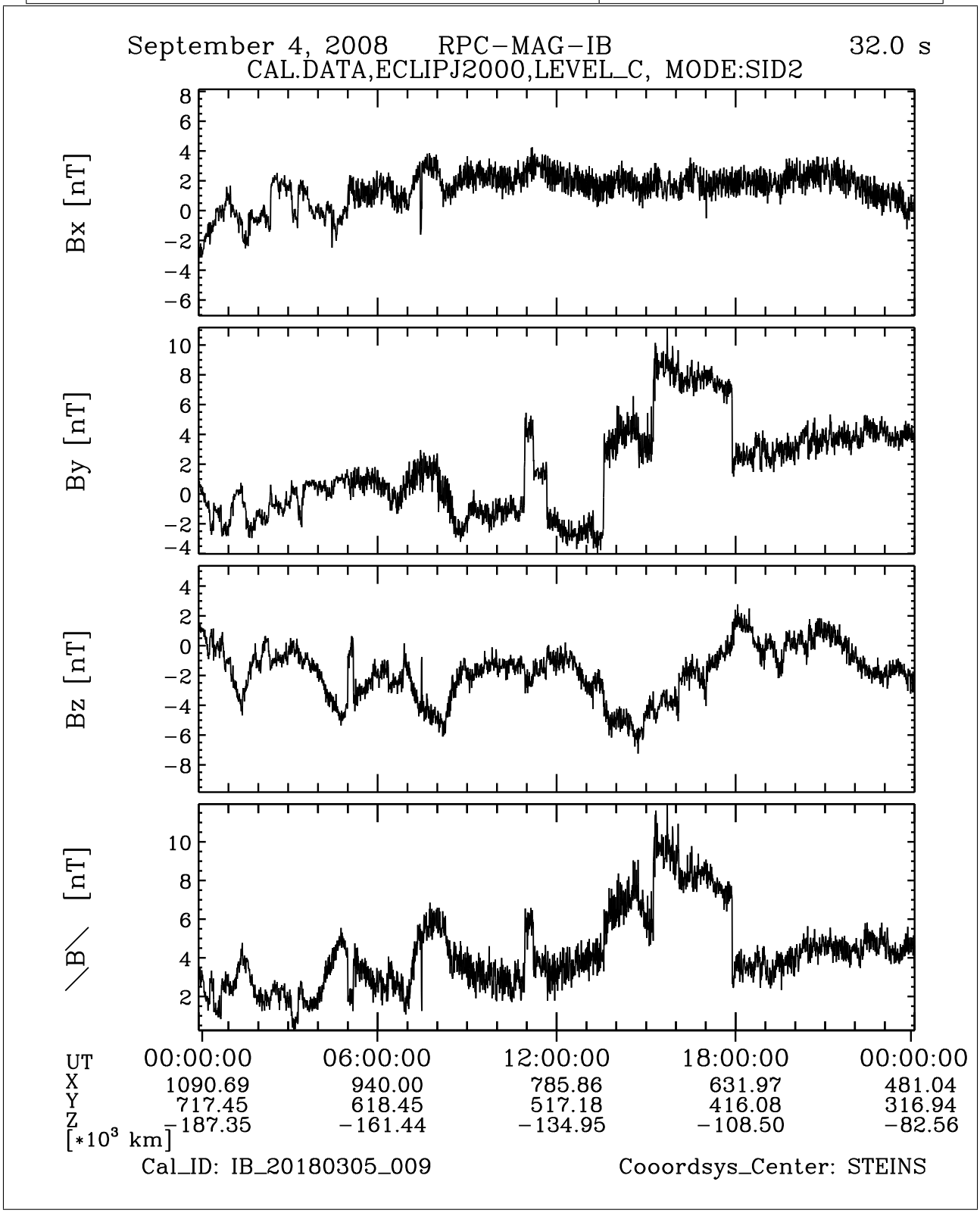

Figure 21: File: RPCMAG080904T0000_CLC_IB_M2_T0000_2400_009

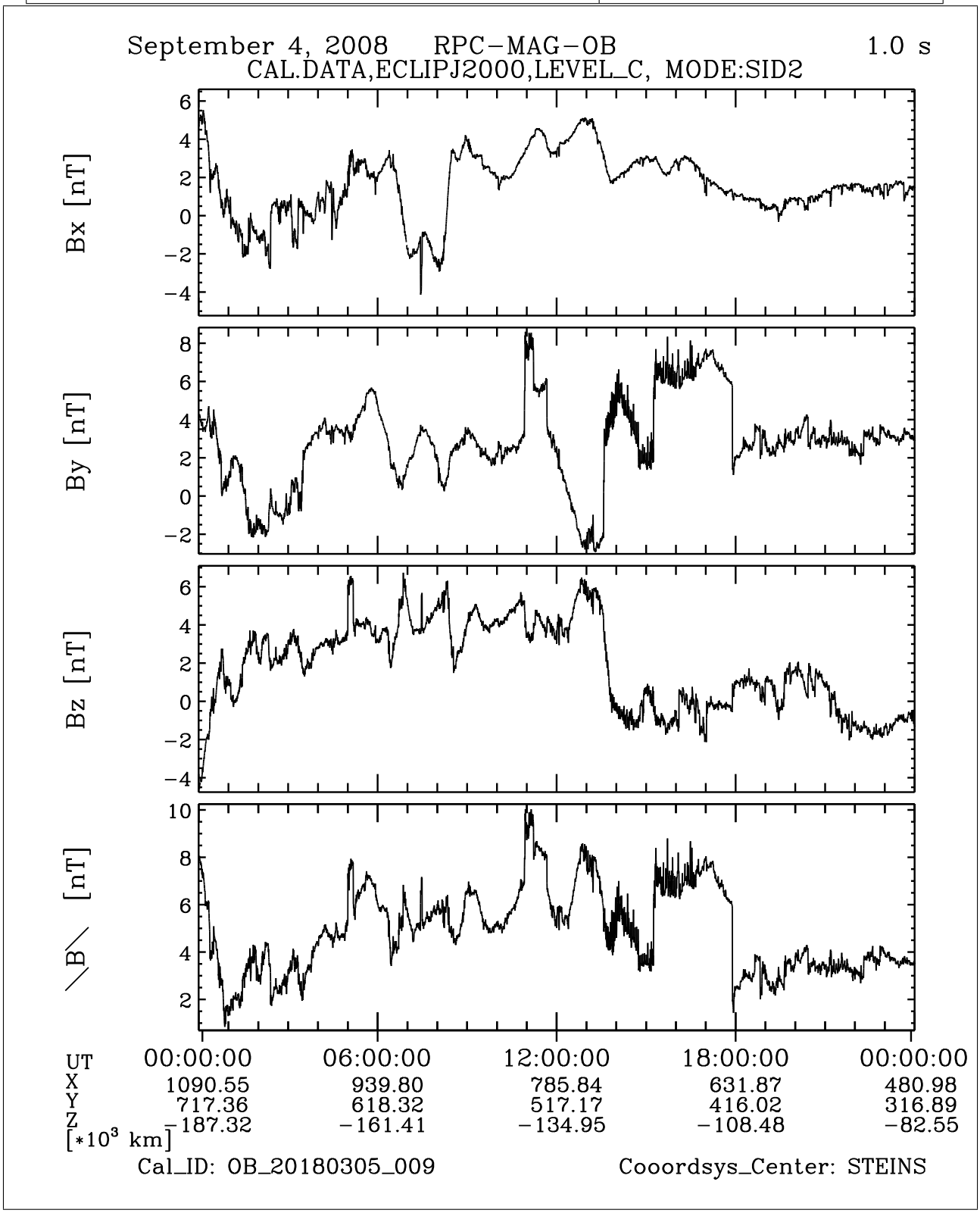

Figure 22: File: RPCMAG080904T0000_CLC_OB_M2_T0000_2400_009

3.6 September 05, 2008:

3.6.1 Actions

MAG stayed in SID 2 until 04:38. Then the instrument was set into BURST mode, SID3. No problems occurred.

3.6.2 Plots of Calibrated Data

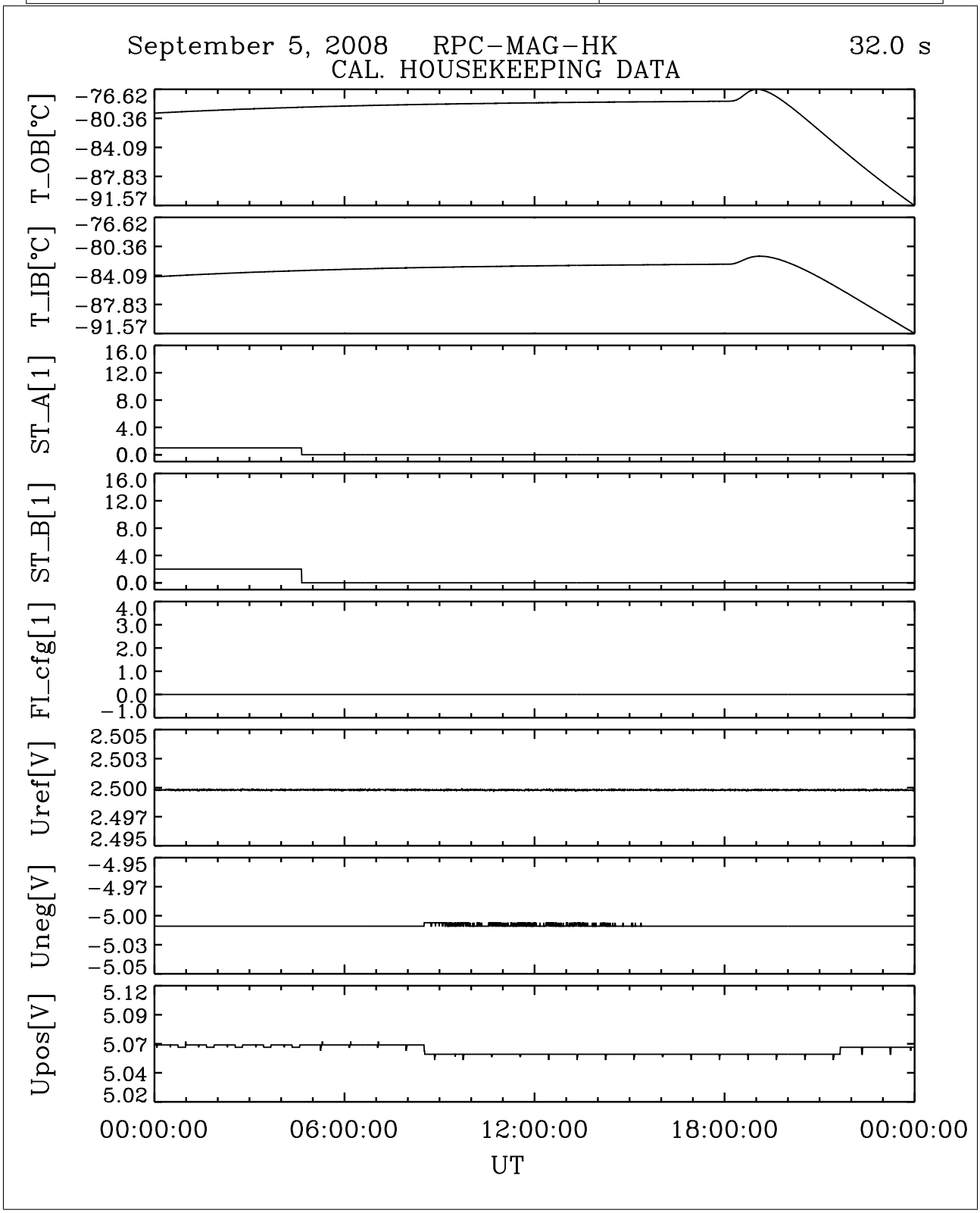

Figure 23: File: RPCMAG080905T0000_CLA_HK_P0000_2400

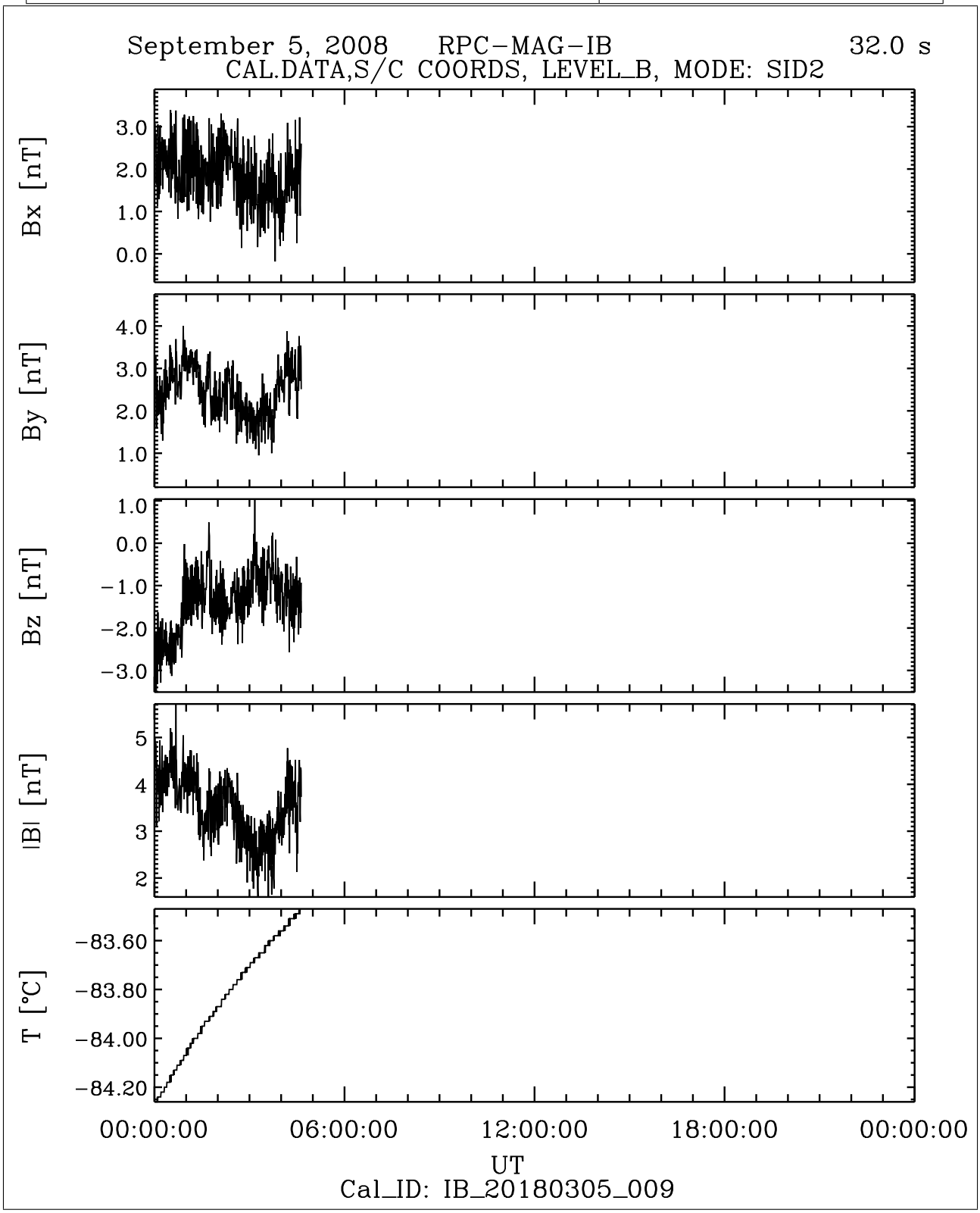

Figure 24: File: RPCMAG080905T0000_CLB_IB_M2_T0000_2400_009

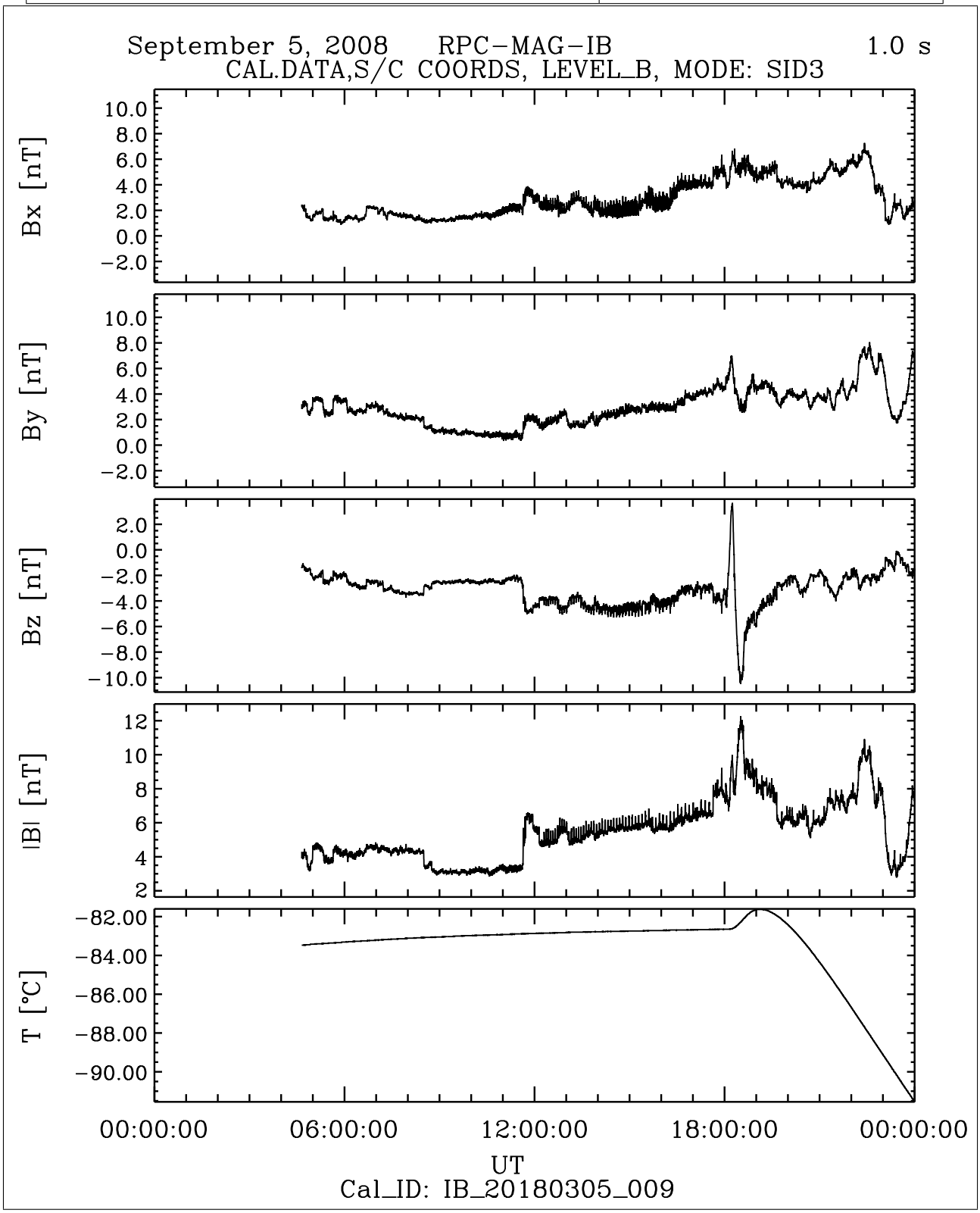

Figure 25: File: RPCMAG080905T0438_CLB_IB_M3_T0000_2400_009

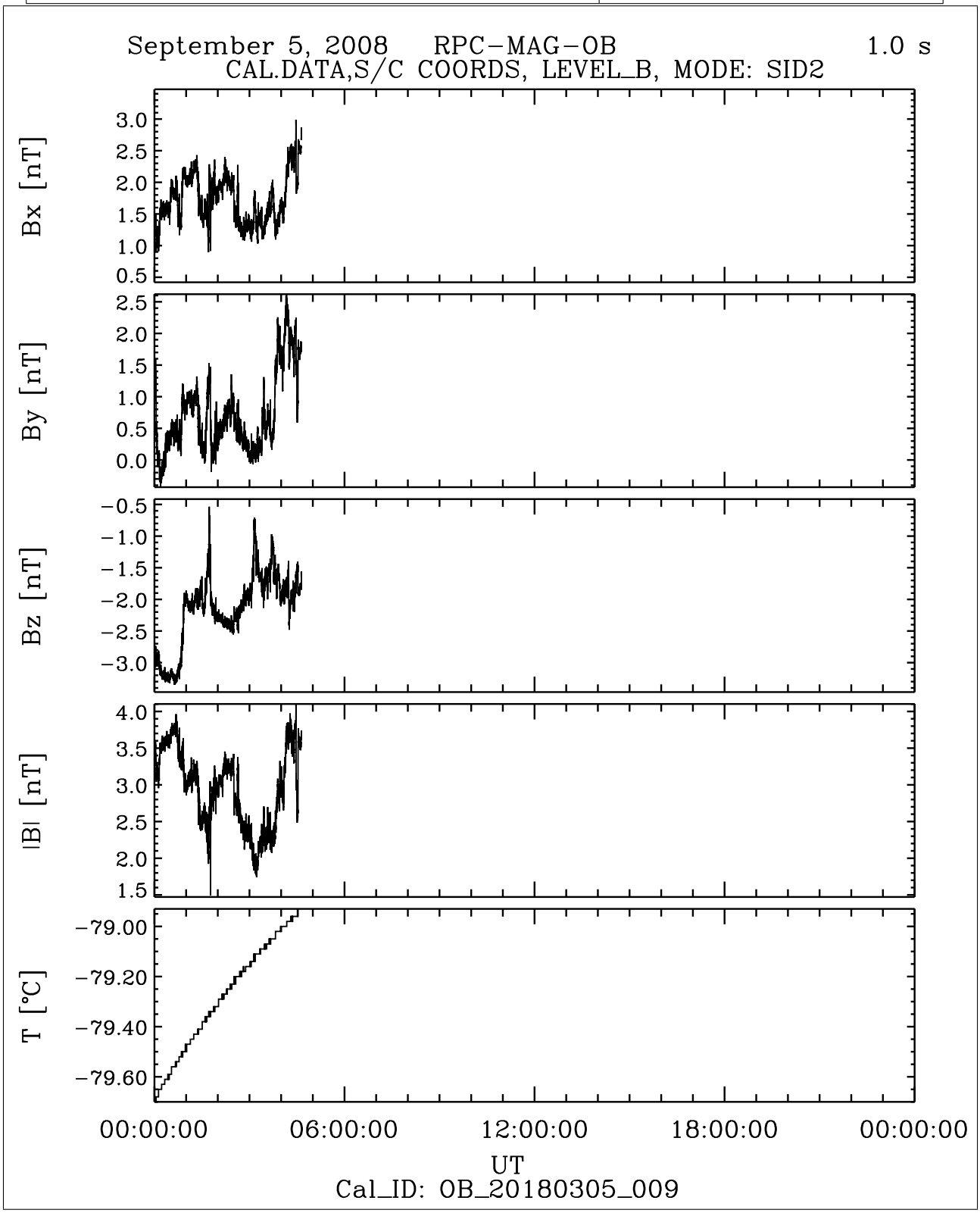

Figure 26: File: RPCMAG080905T0000_CLB_OB_M2_T0000_2400_009

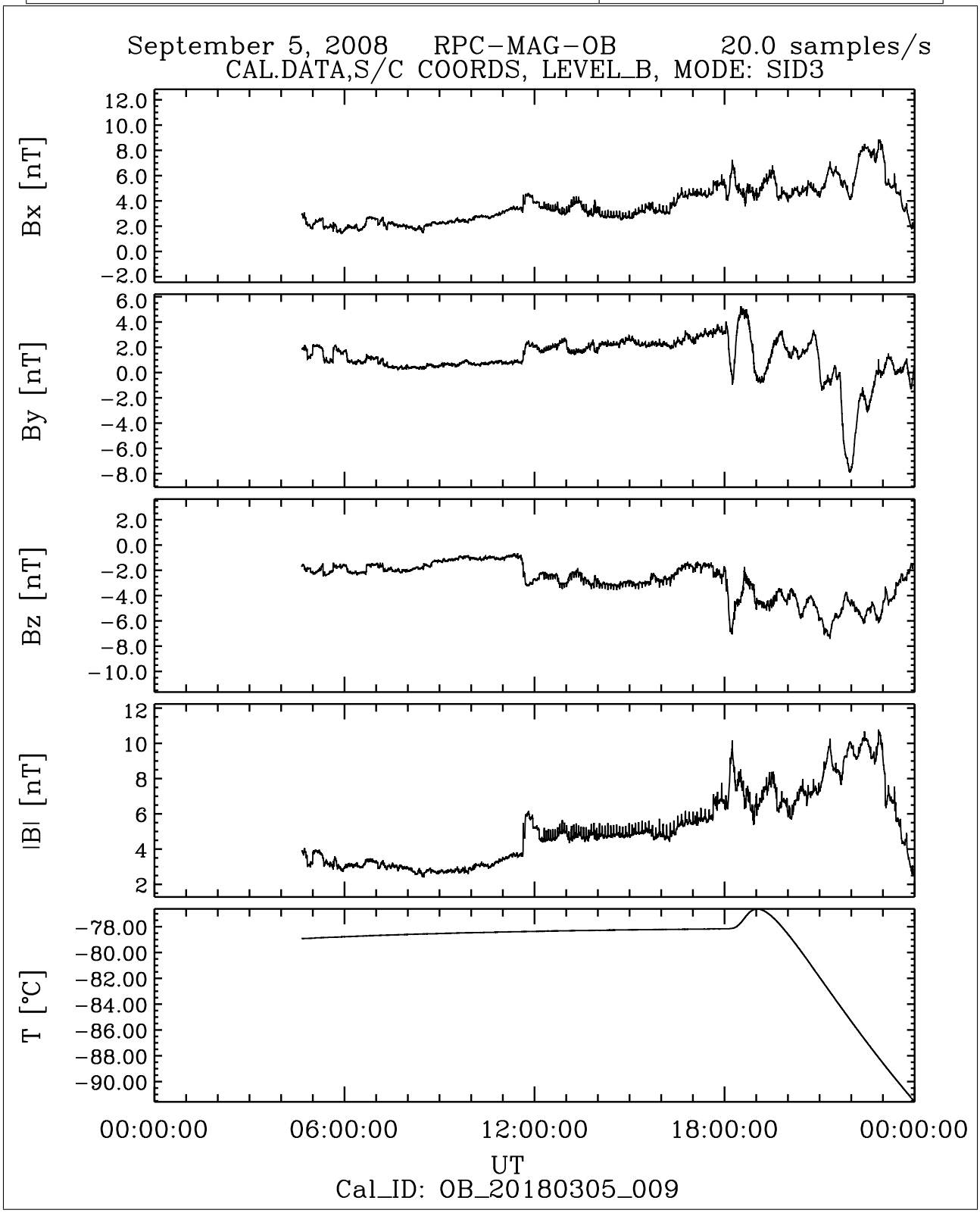

Figure 27: File: RPCMAG080905T0438_CLB_OB_M3_T0000_2400_009

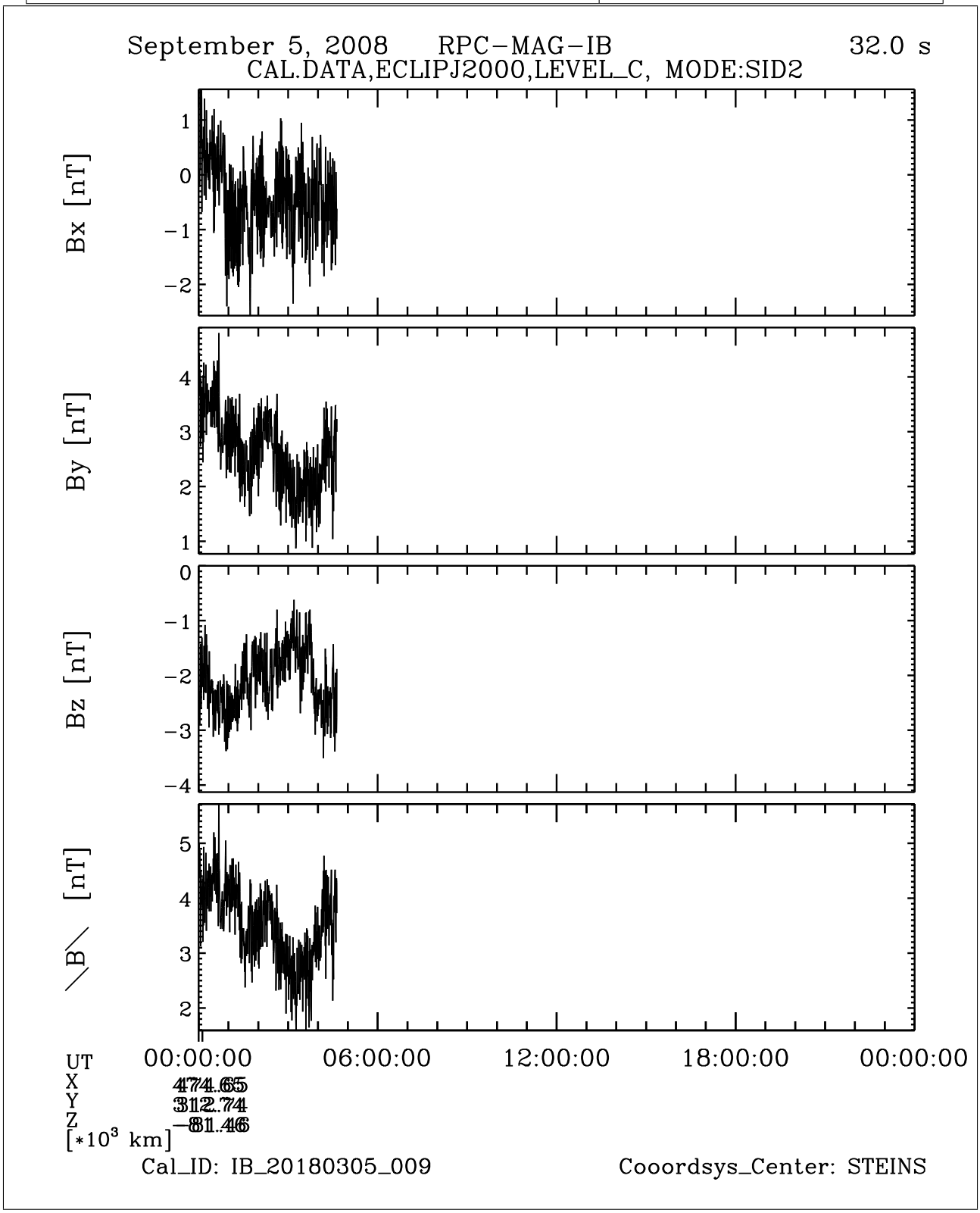

Figure 28: File: RPCMAG080905T0000_CLC_IB_M2_T0000_2400_009

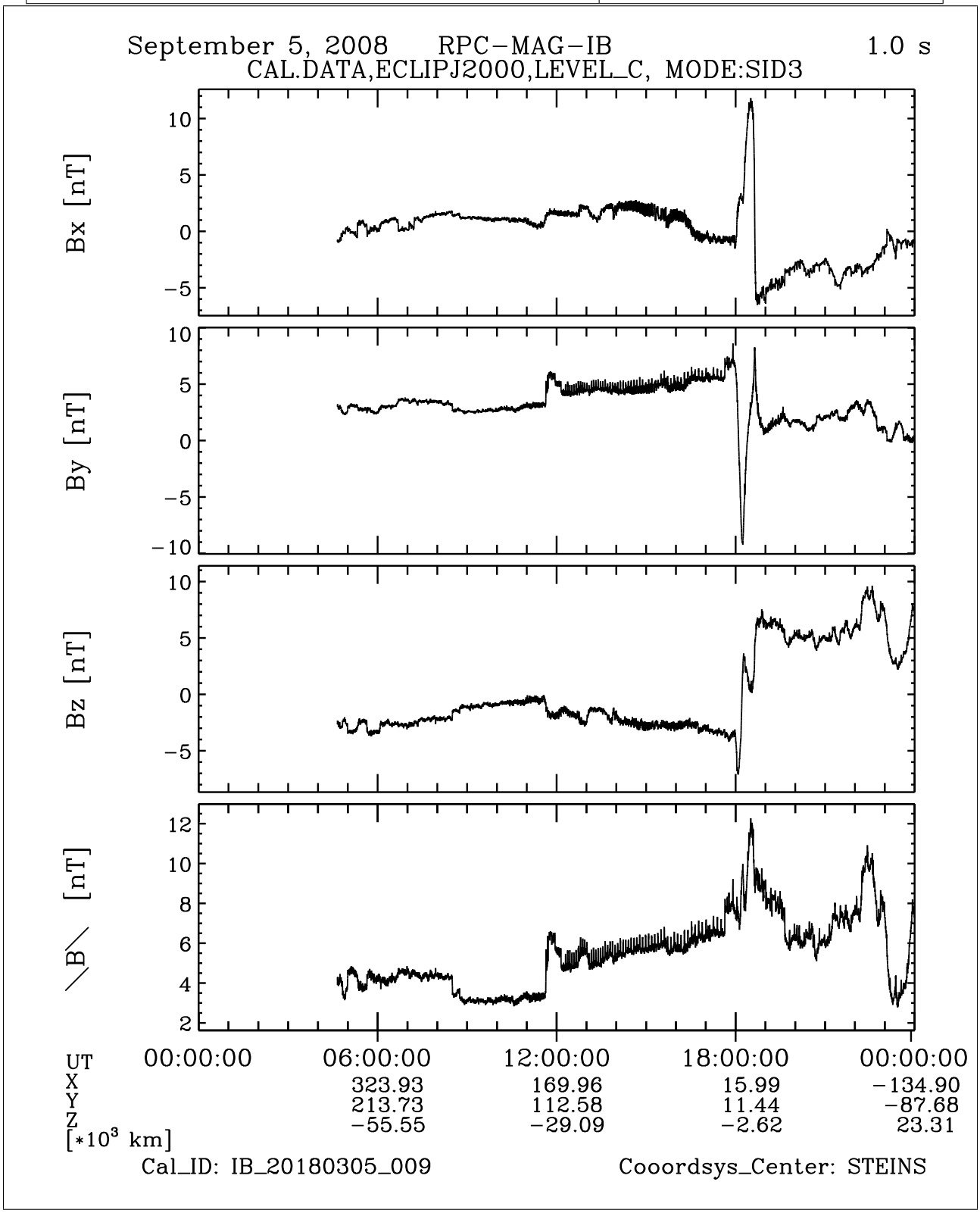

Figure 29: File: RPCMAG080905T0438_CLC_IB_M3_T0000_2400_009

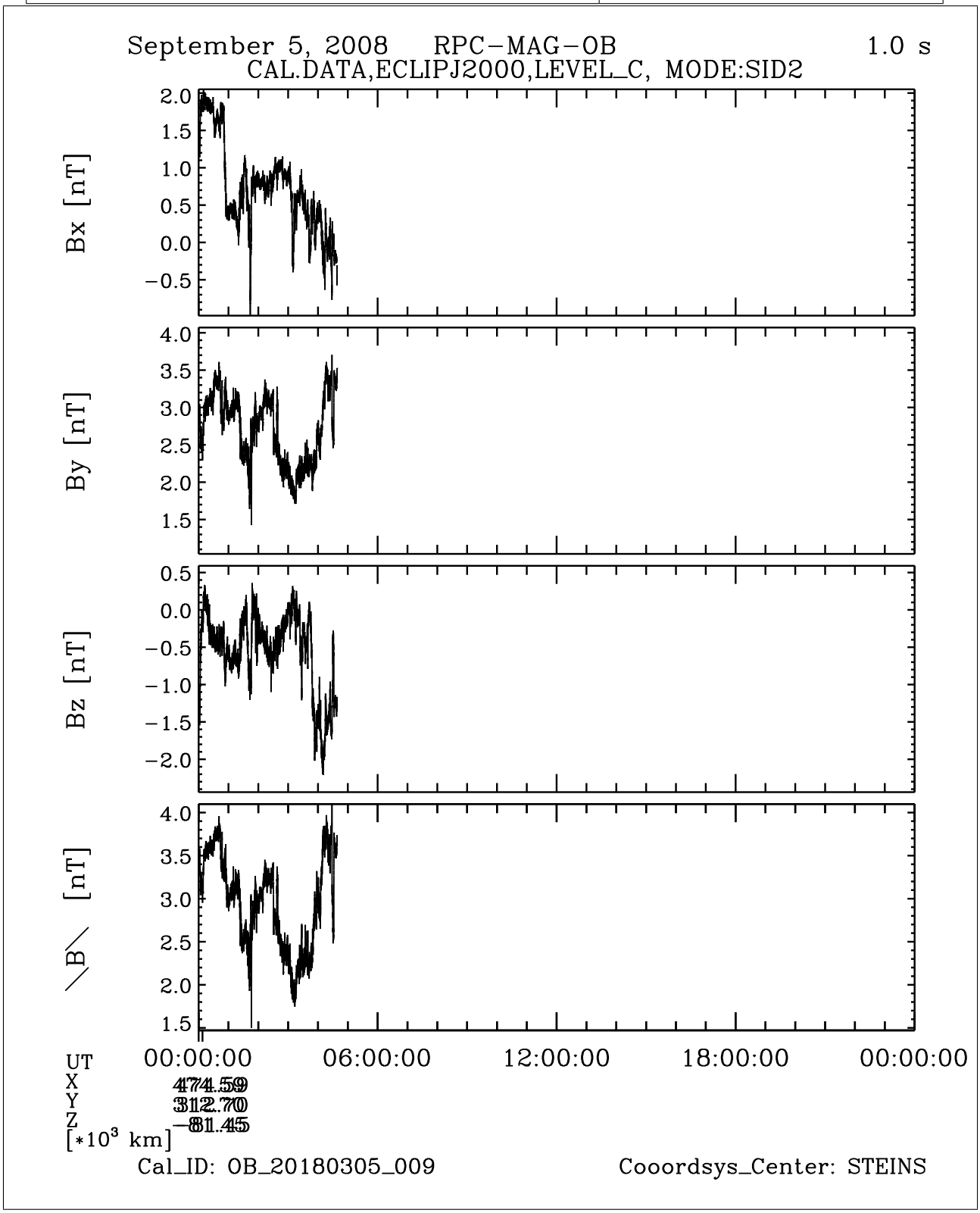

Figure 30: File: RPCMAG080905T0000_CLC_OB_M2_T0000_2400_009

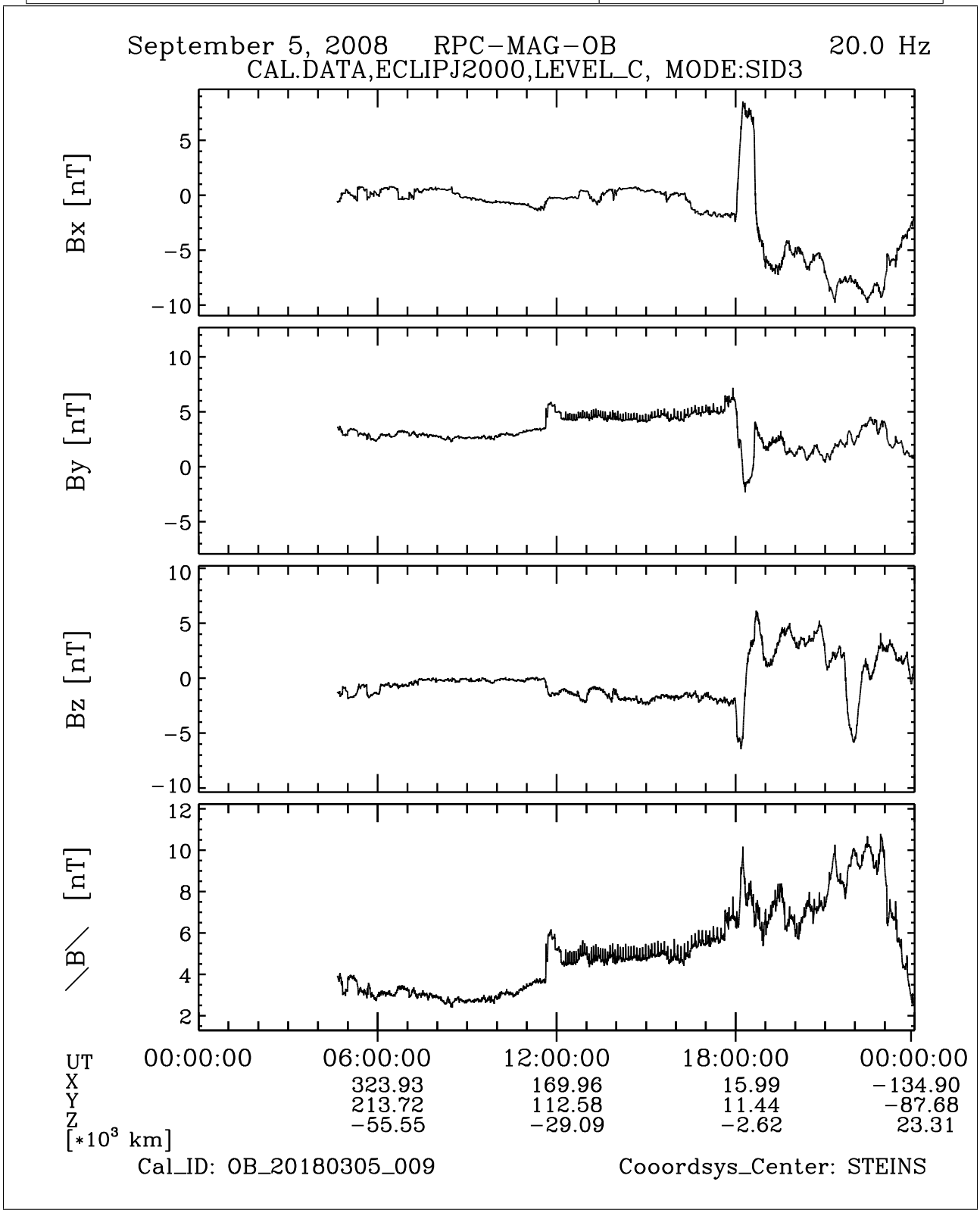

Figure 31: File: RPCMAG080905T0438_CLC_OB_M3_T0000_2400_009

3.7 September 06, 2008:

3.7.1 Actions

MAG stayed in SID 3 until 06:38. Then the instrument was switched back to NORMAL mode SID2. No problems occurred.

3.7.2 Plots of Calibrated Data

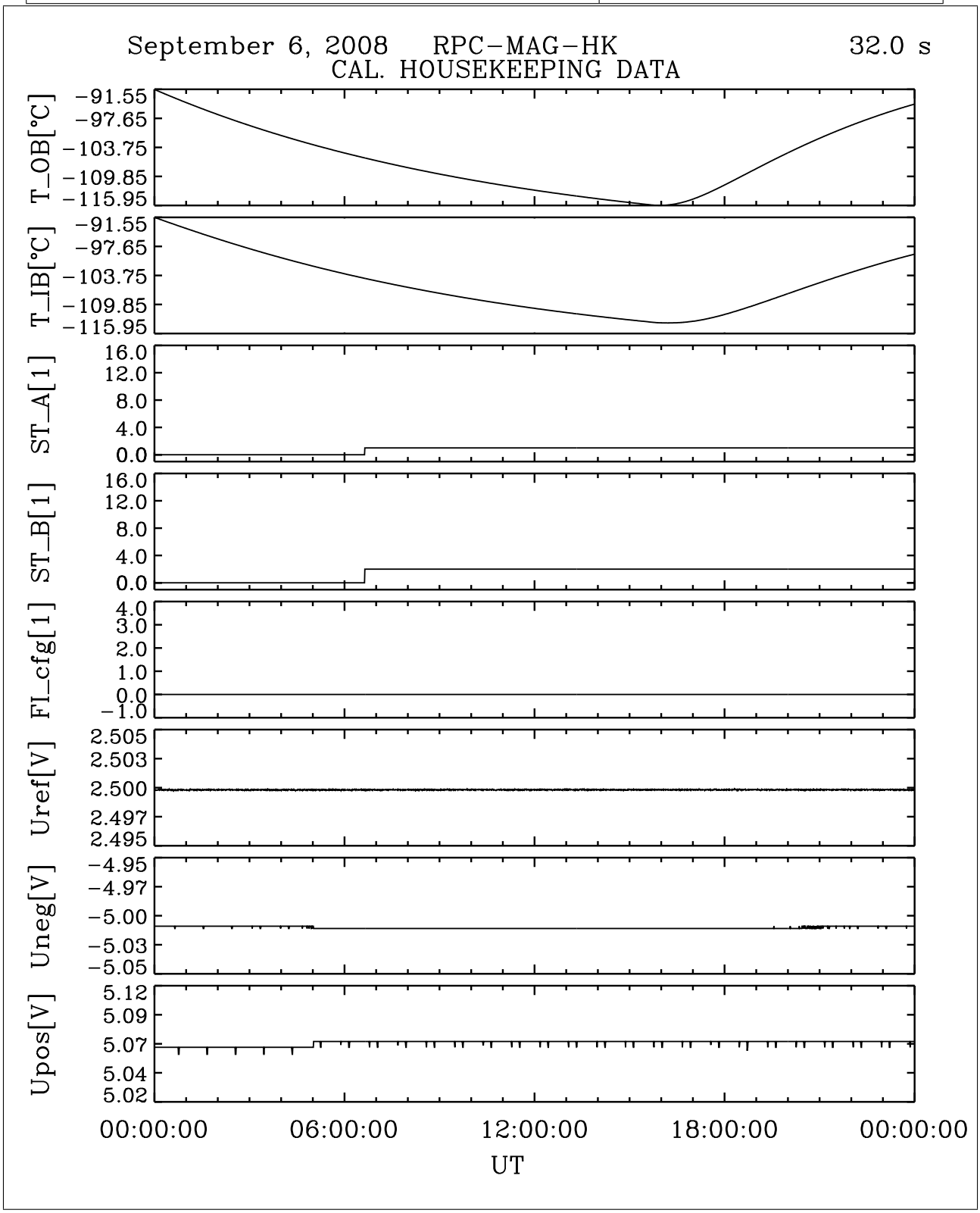

Figure 32: File: RPCMAG080906T0000_CLA_HK_P0000_2400

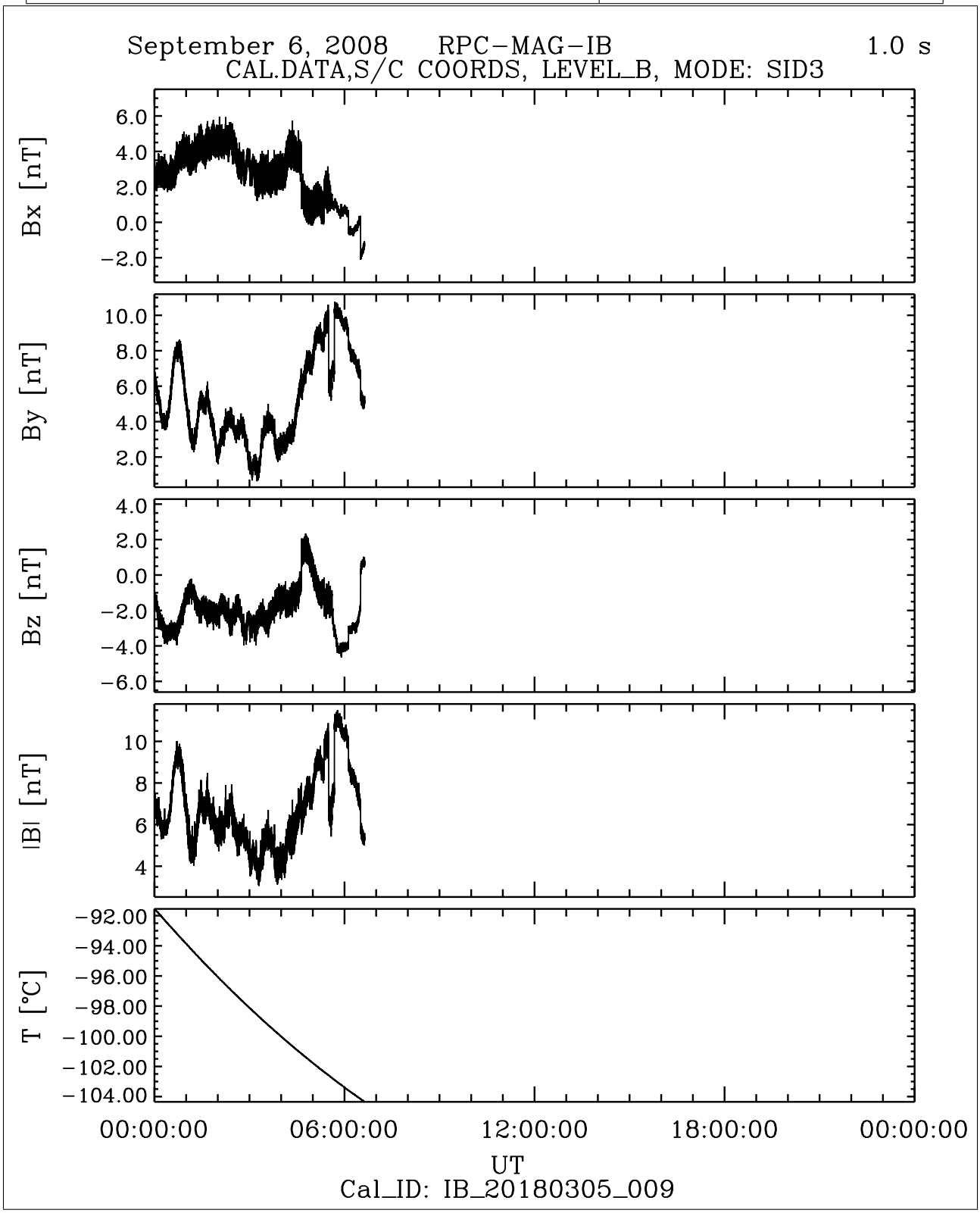

Figure 33: File: RPCMAG080906T0000_CLB_IB_M3_T0000_2400_009

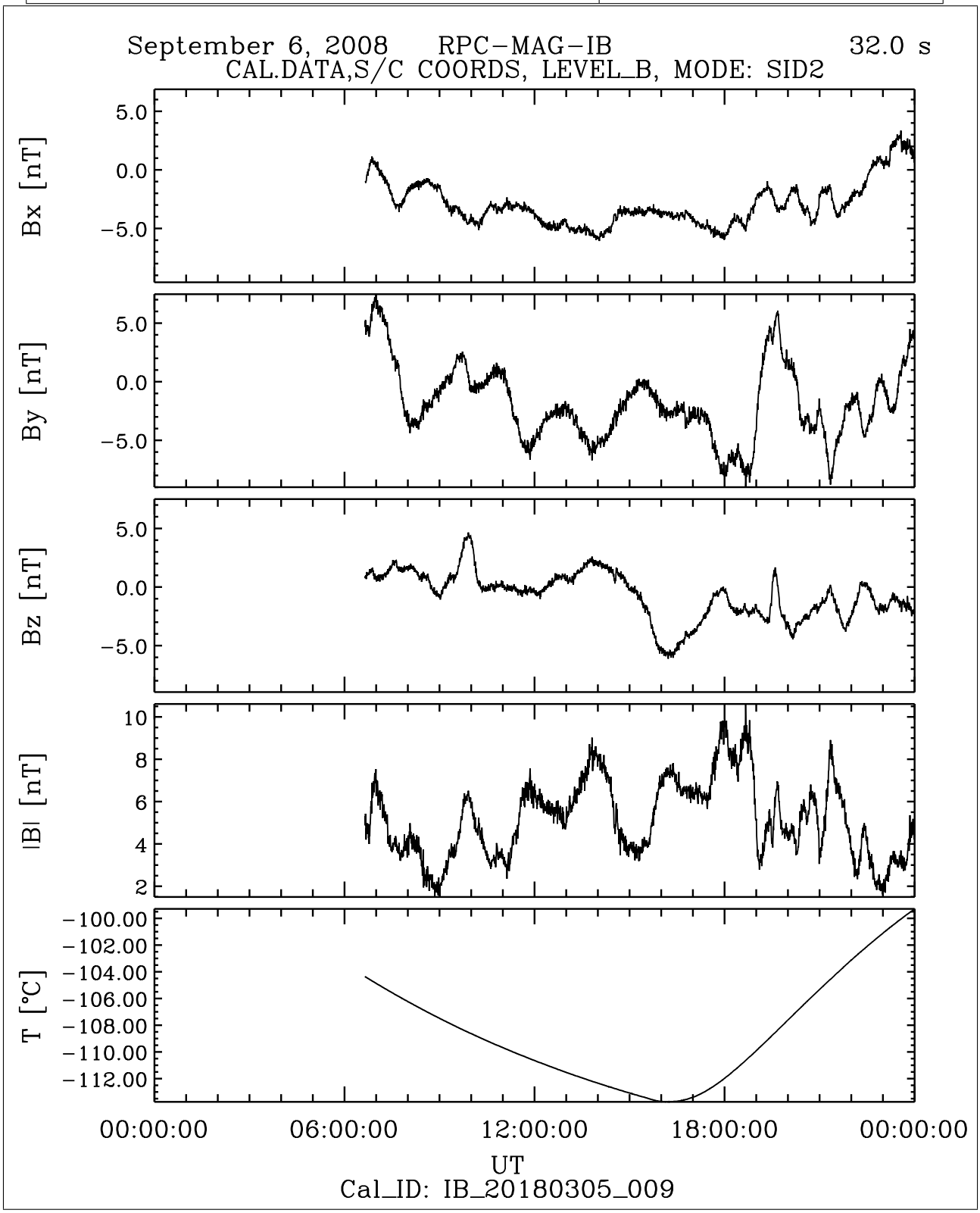

Figure 34: File: RPCMAG080906T0638_CLB_IB_M2_T0000_2400_009

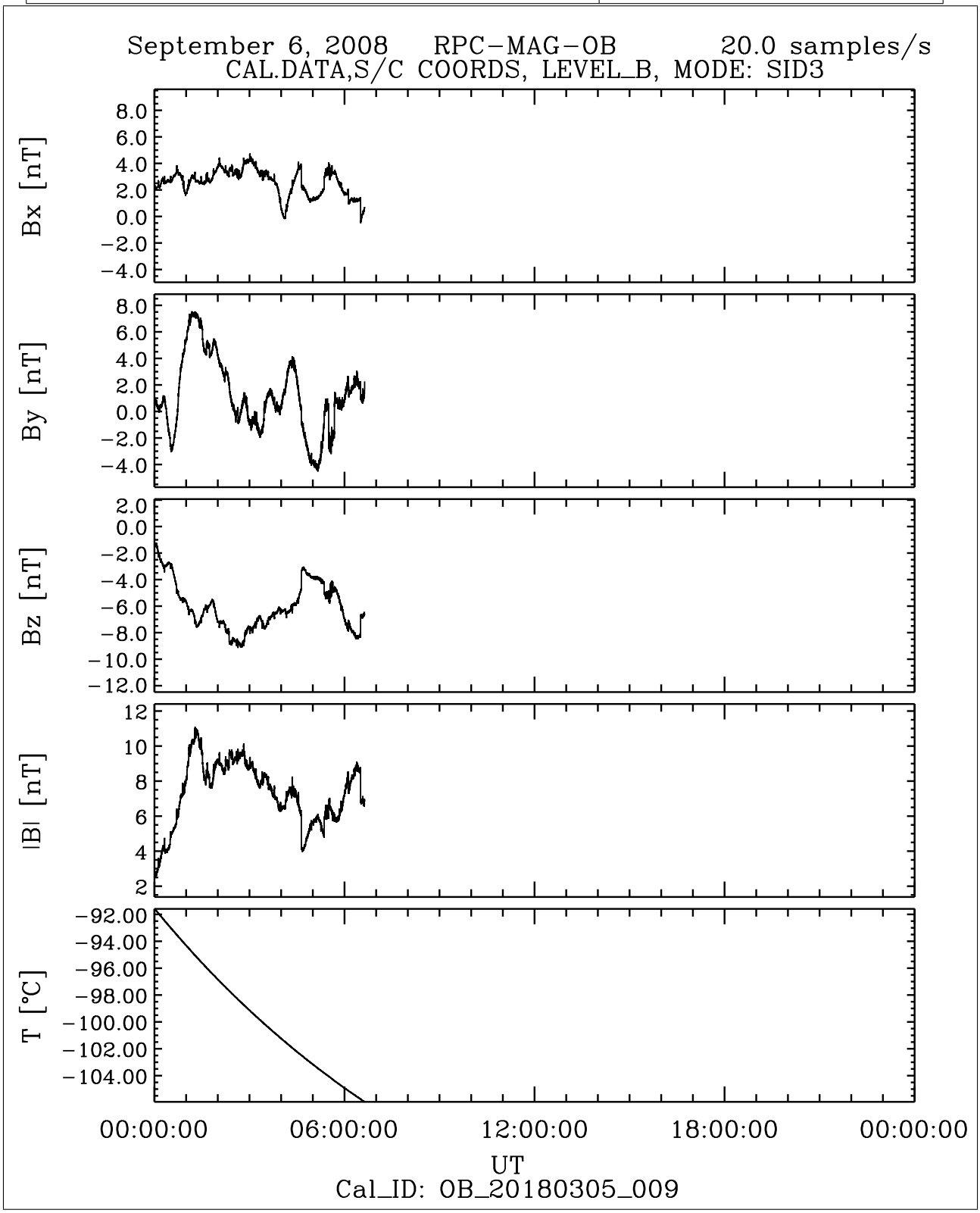

Figure 35: File: RPCMAG080906T0000_CLB_OB_M3_T0000_2400_009

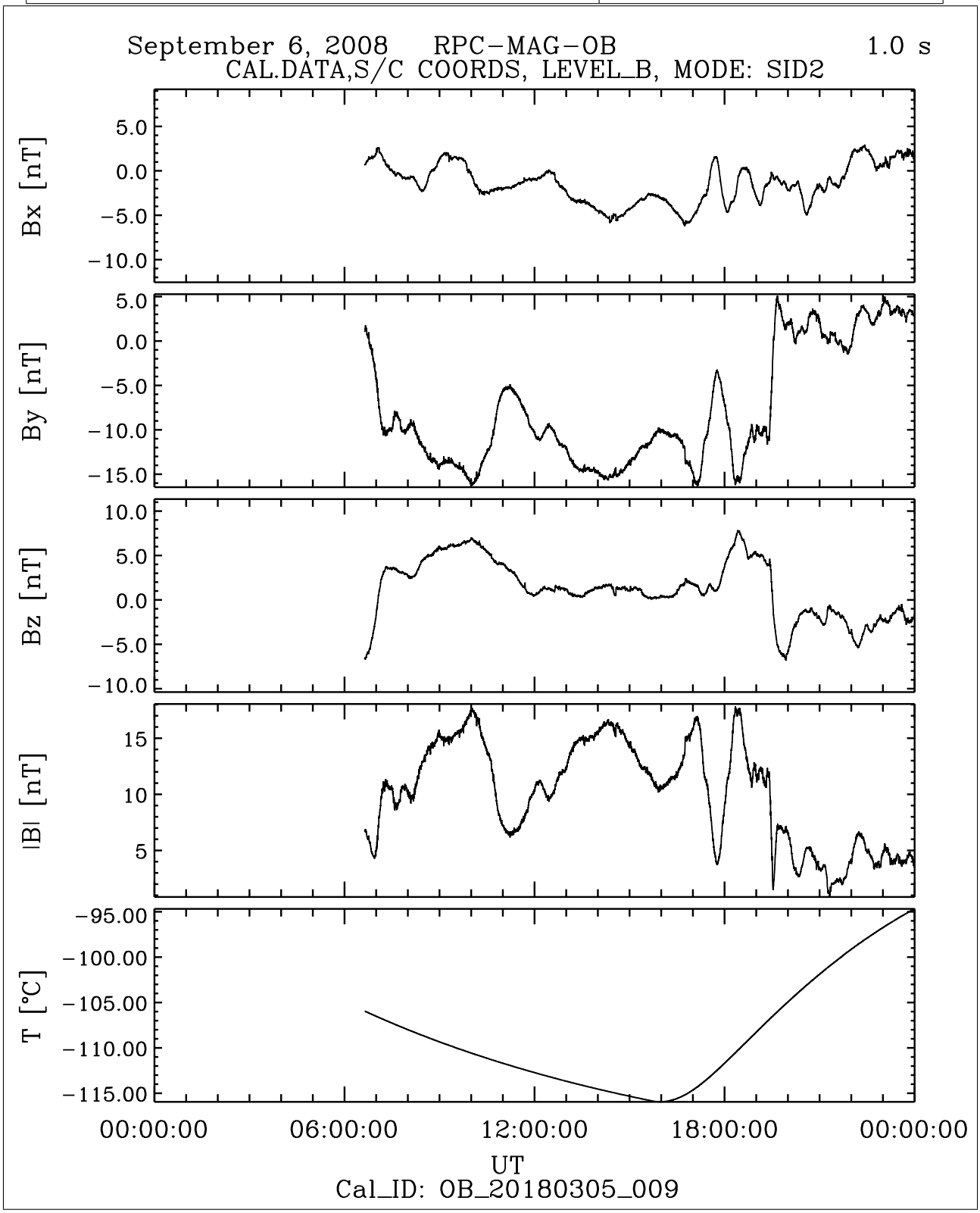

Figure 36: File: RPCMAG080906T0638_CLB_OB_M2_T0000_2400_009

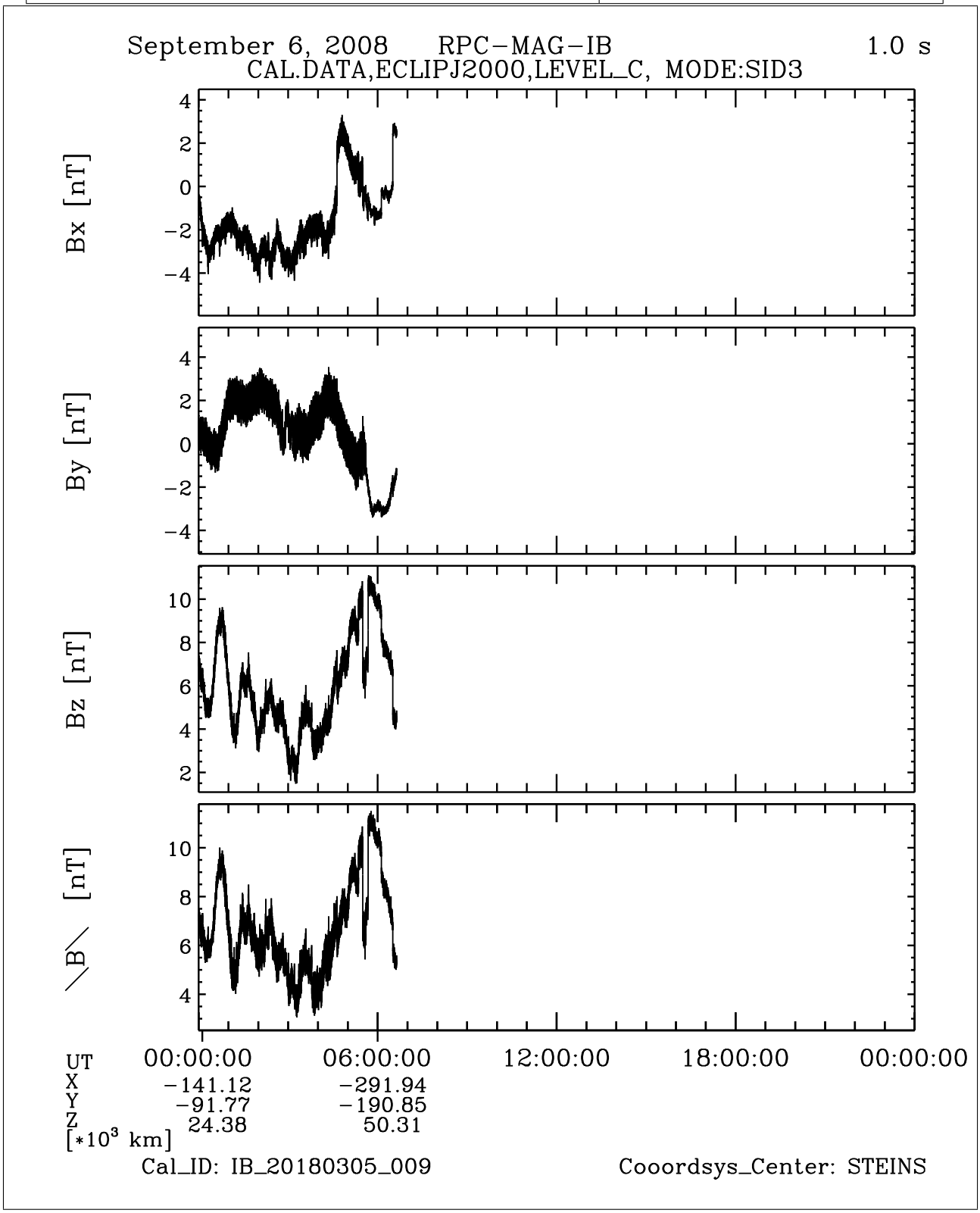

Figure 37: File: RPCMAG080906T0000_CLC_IB_M3_T0000_2400_009

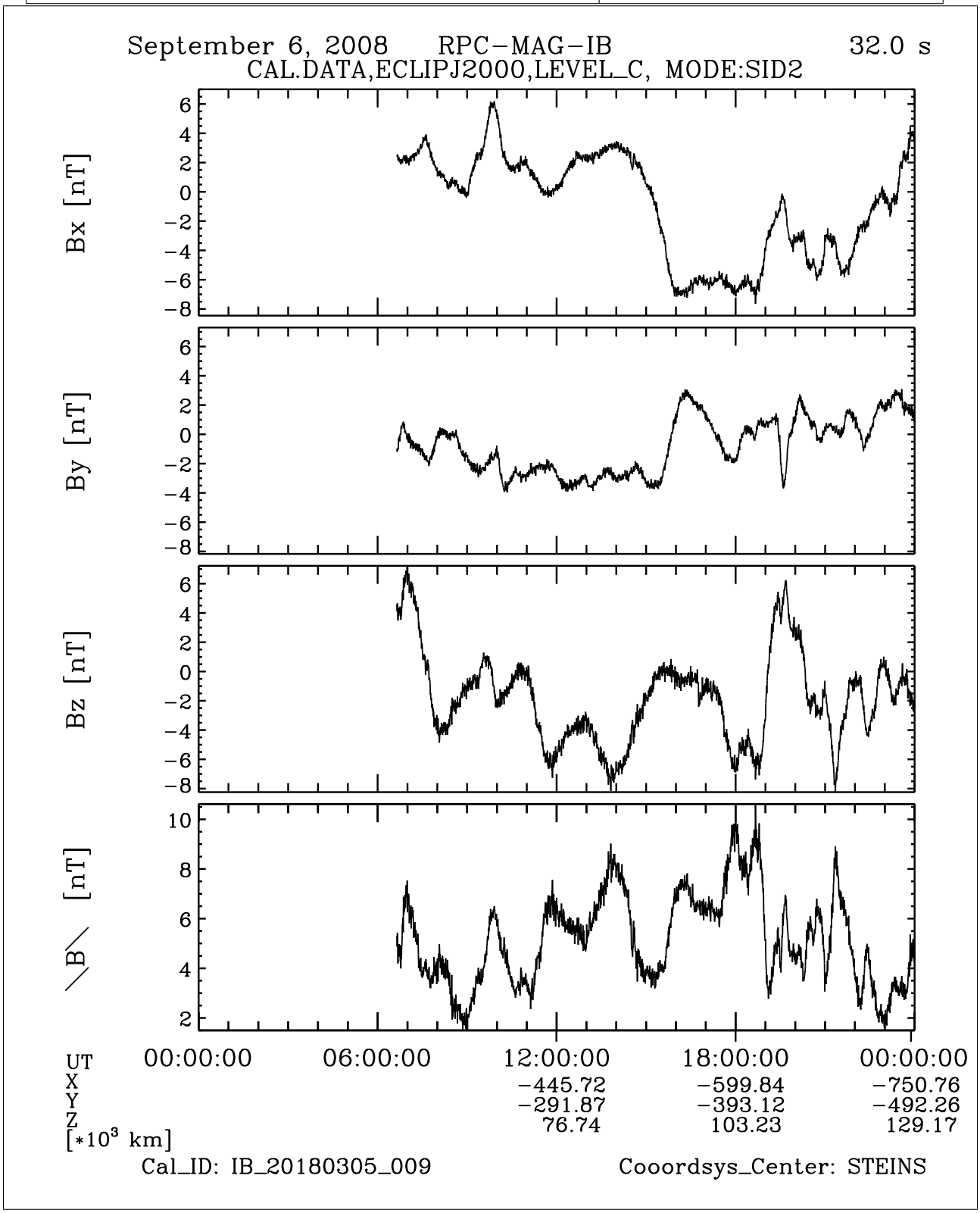

Figure 38: File: RPCMAG080906T0638_CLC_IB_M2_T0000_2400_009

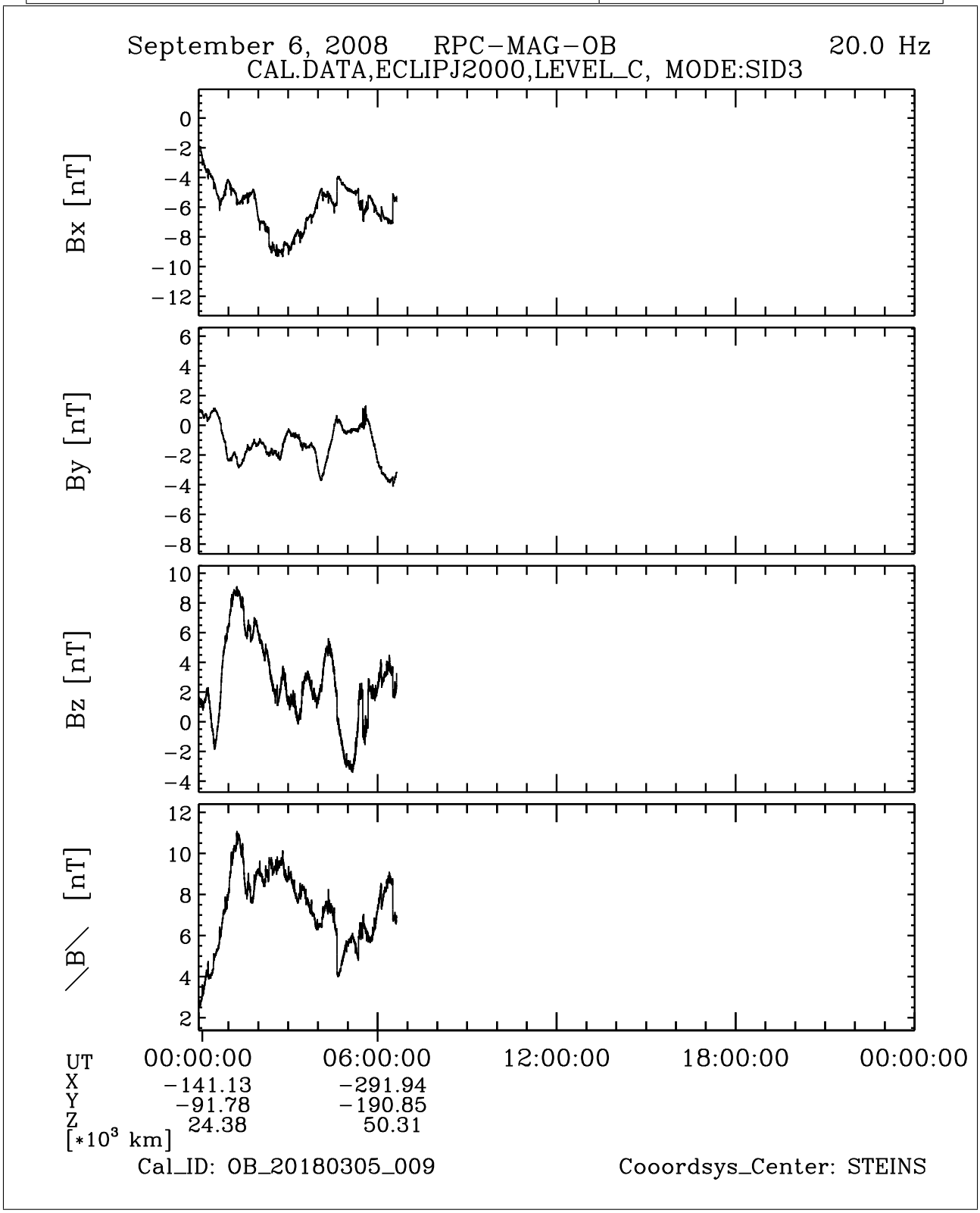

Figure 39: File: RPCMAG080906T0000_CLC_OB_M3_T0000_2400_009

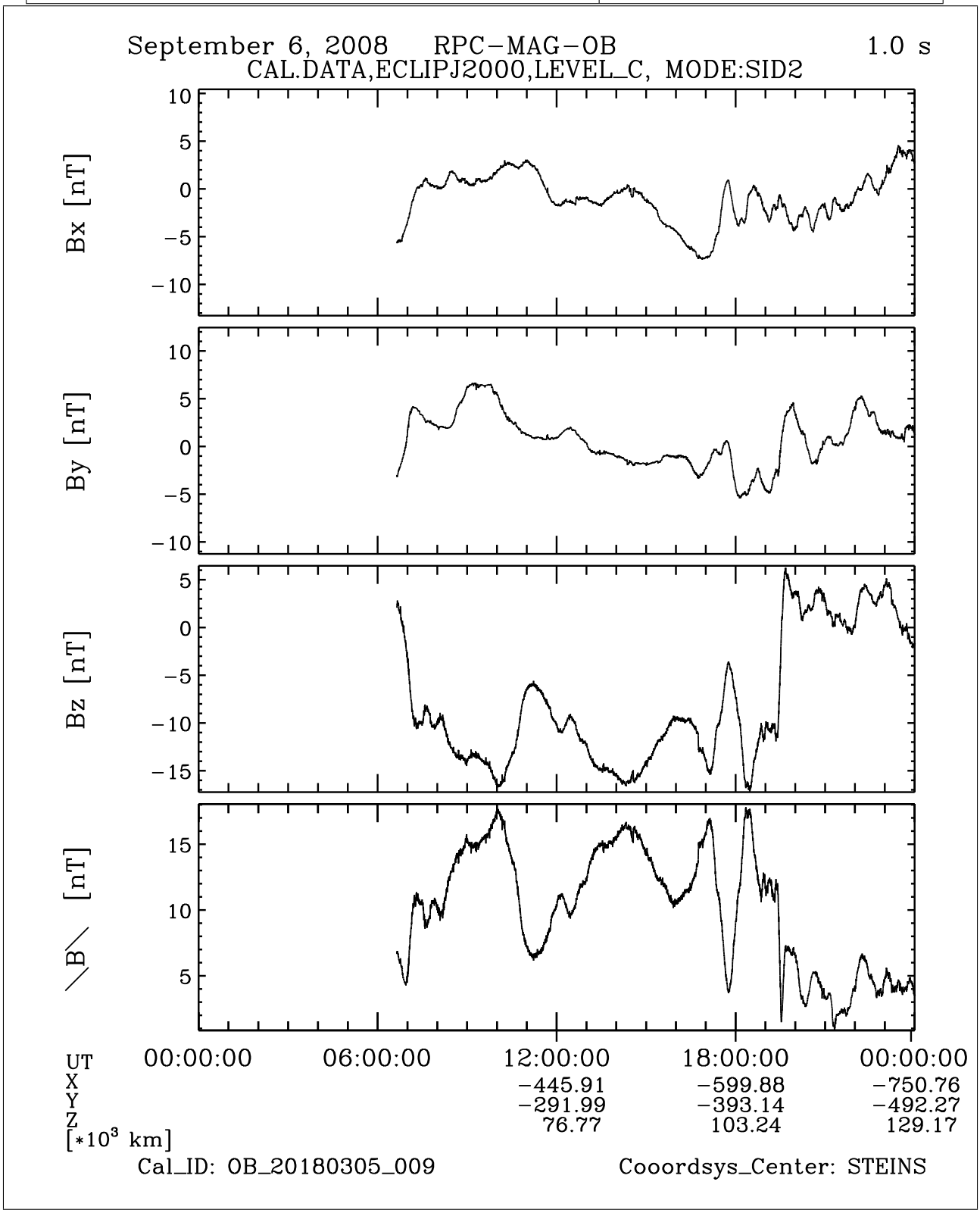

Figure 40: File: RPCMAG080906T0638_CLC_OB_M2_T0000_2400_009

3.8 September 07, 2008:

3.8.1 Actions

MAG stayed in SID 2. No problems occurred.

3.8.2 Plots of Calibrated Data

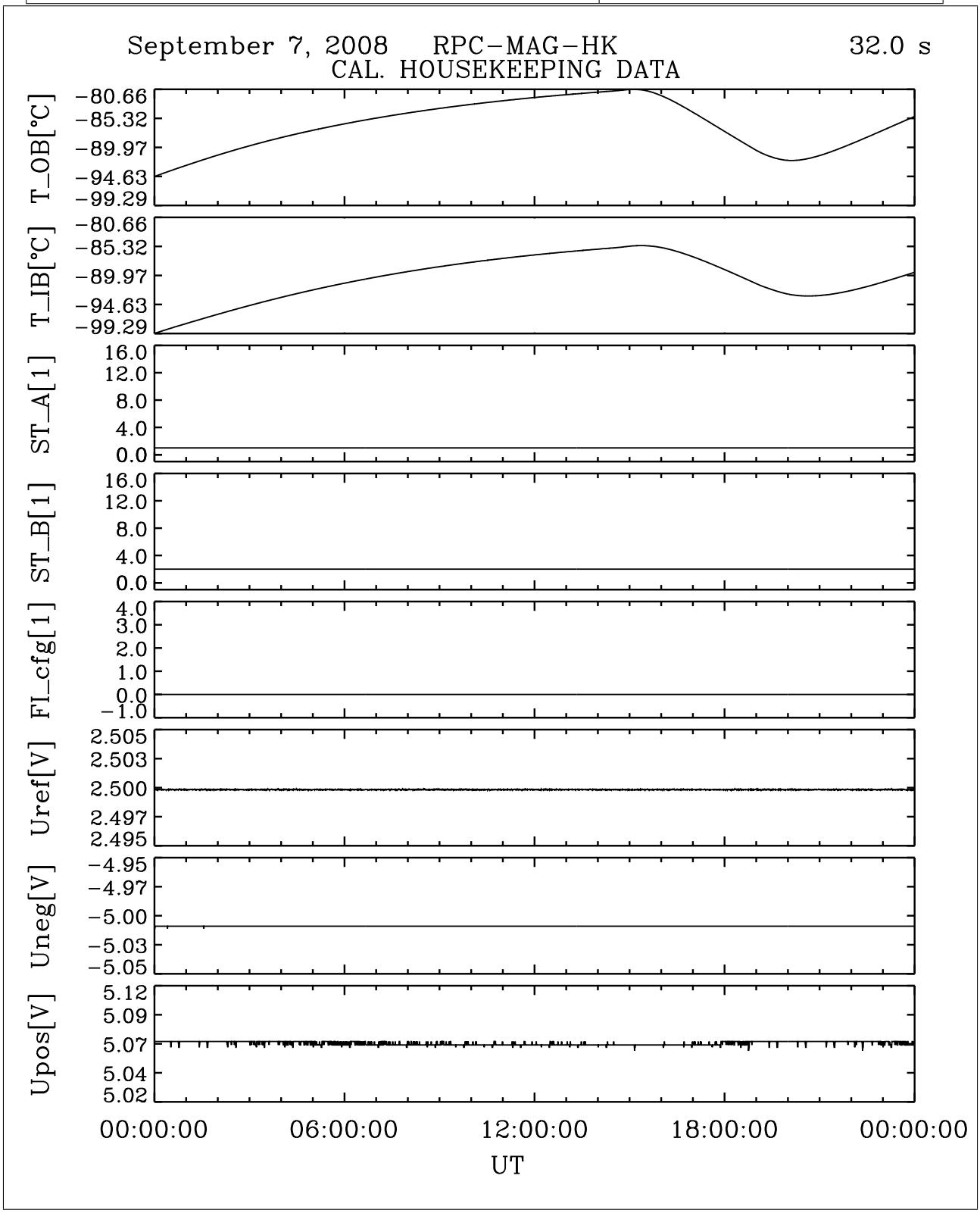

Figure 41: File: RPCMAG080907T0000_CLA_HK_P0000_2400

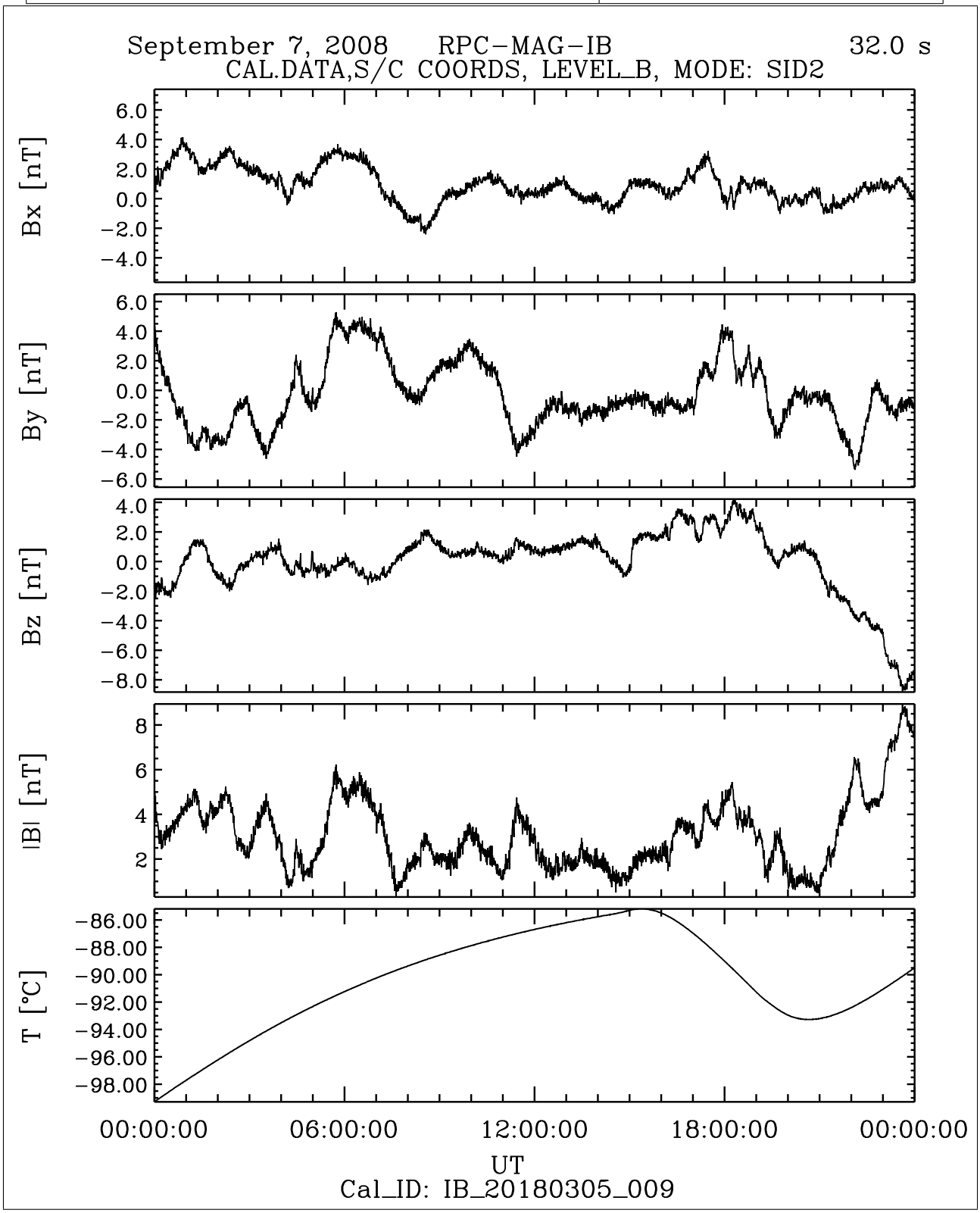

Figure 42: File: RPCMAG080907T0000_CLB_IB_M2_T0000_2400_009

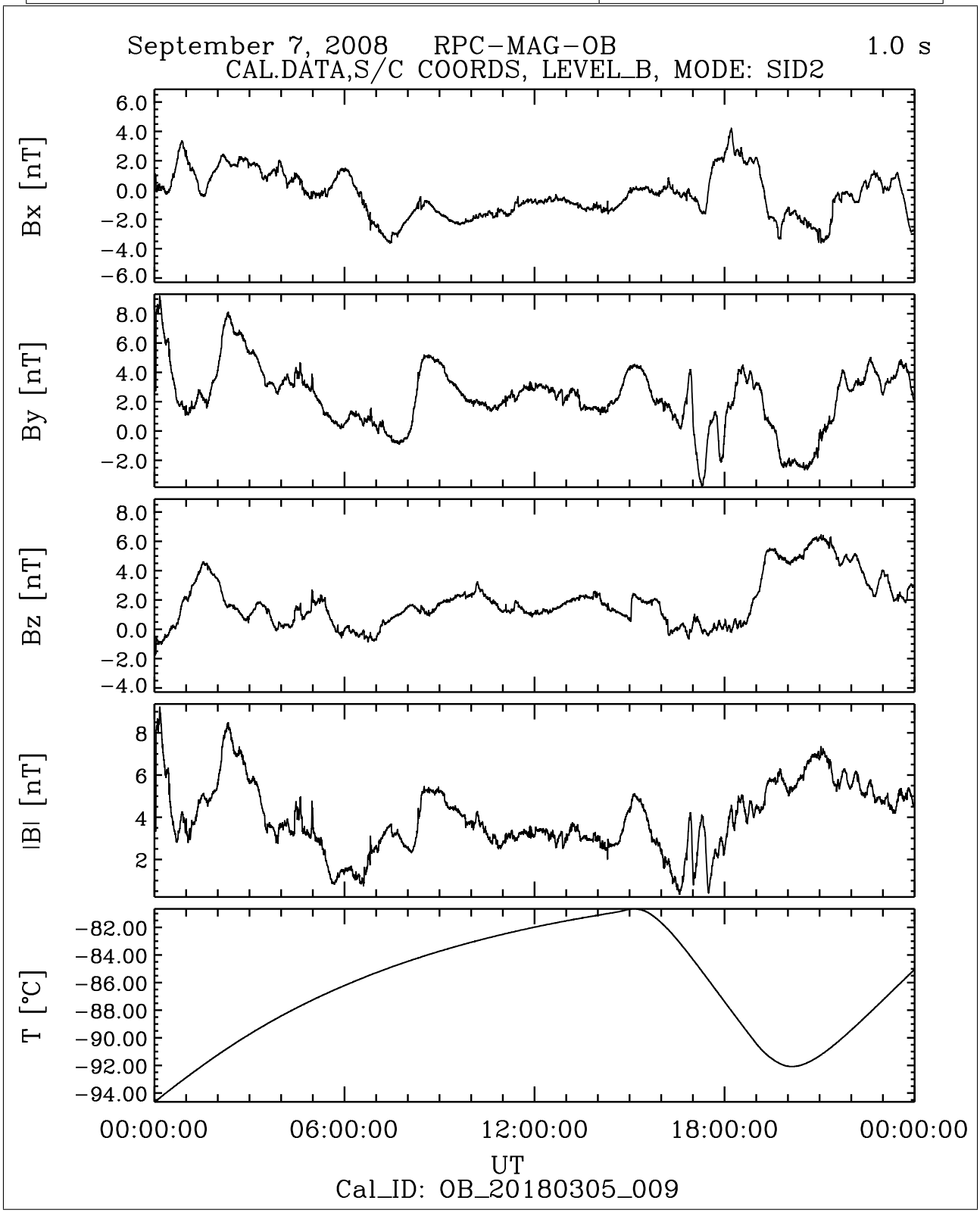

Figure 43: File: RPCMAG080907T0000_CLB_OB_M2_T0000_2400_009

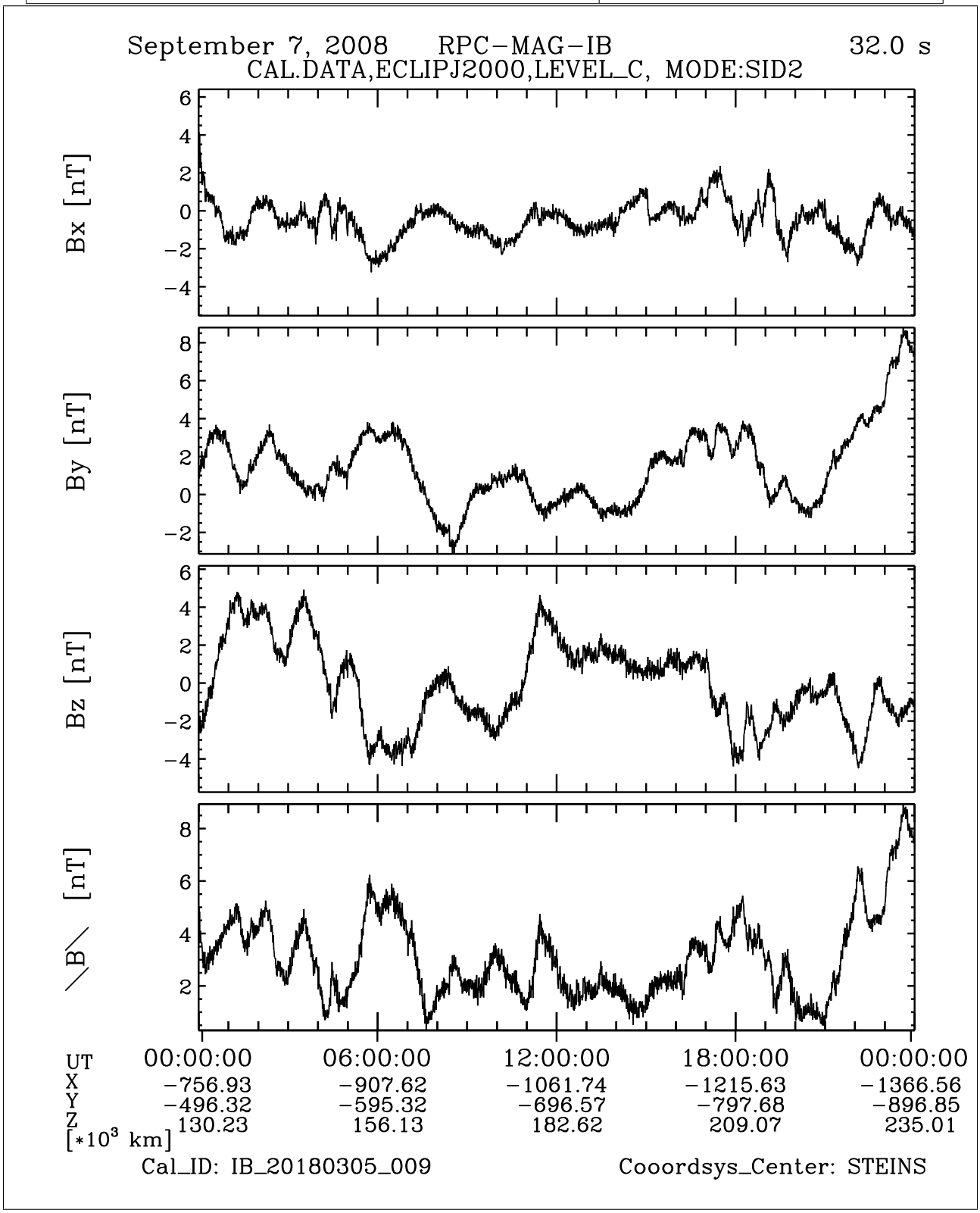

Figure 44: File: RPCMAG080907T0000_CLC_IB_M2_T0000_2400_009

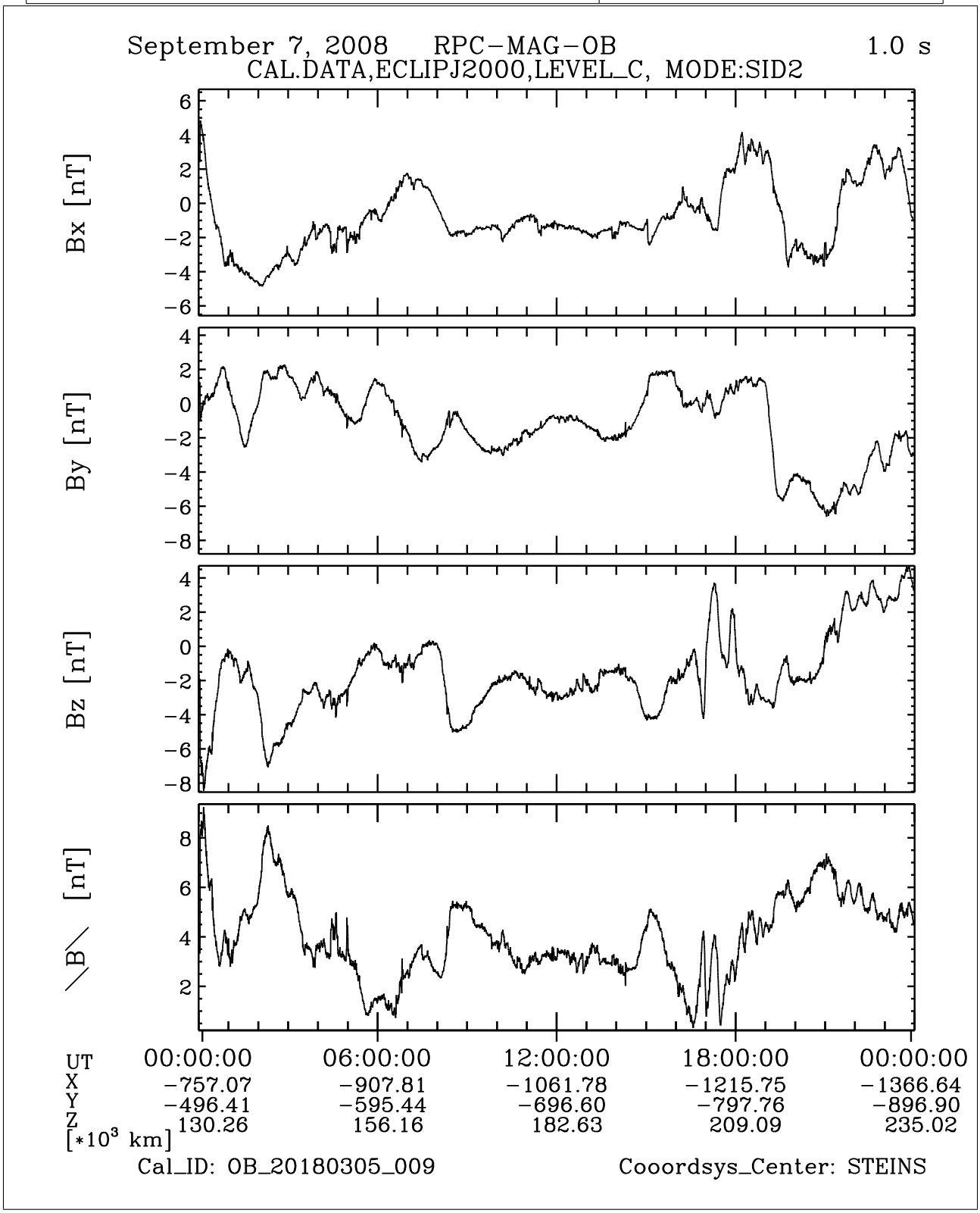

Figure 45: File: RPCMAG080907T0000_CLC_OB_M2_T0000_2400_009

3.9 September 08, 2008:

3.9.1 Actions

MAG stayed in SID 2. No problems occurred.

3.9.2 Plots of Calibrated Data

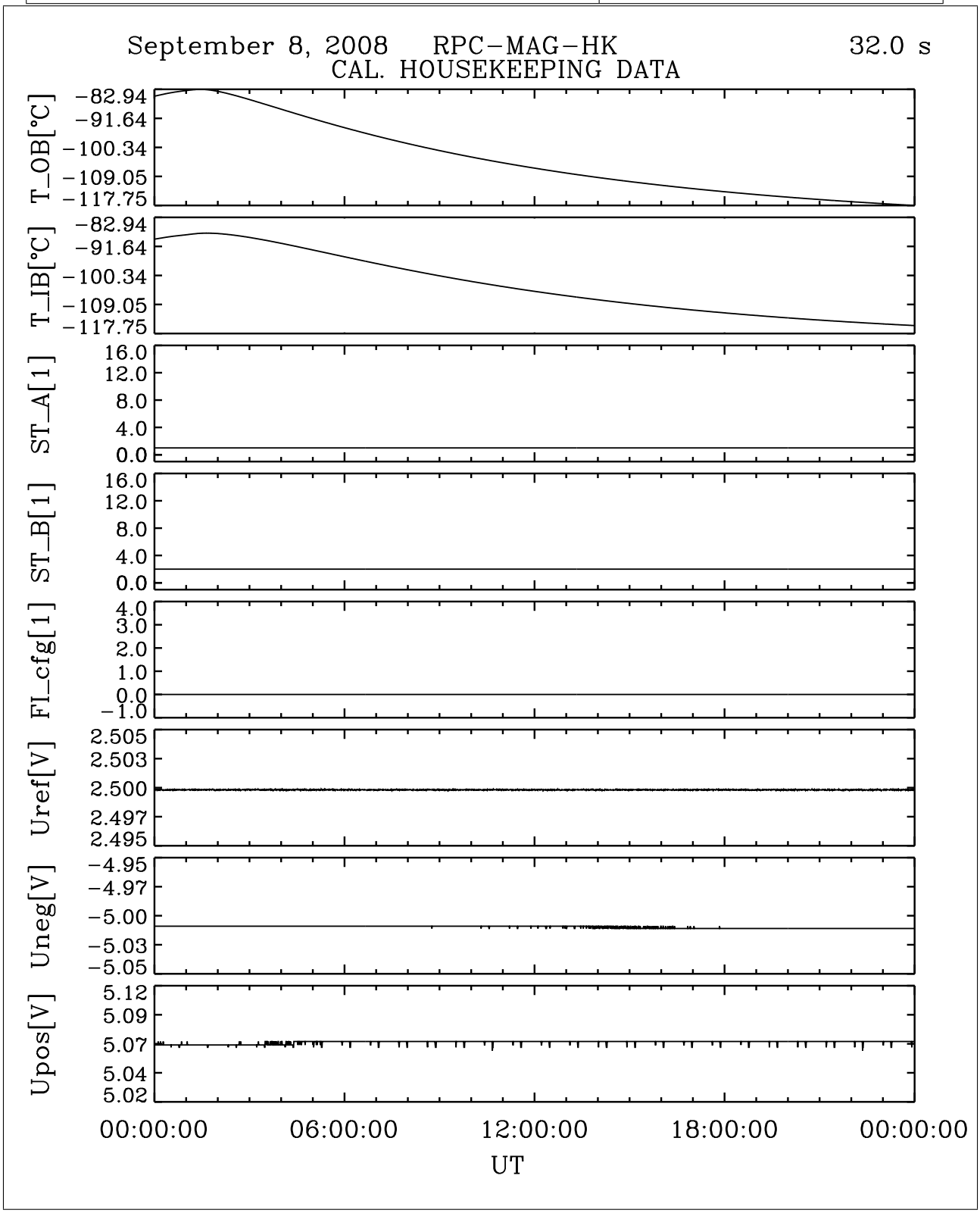

Figure 46: File: RPCMAG080908T0000_CLA_HK_P0000_2400

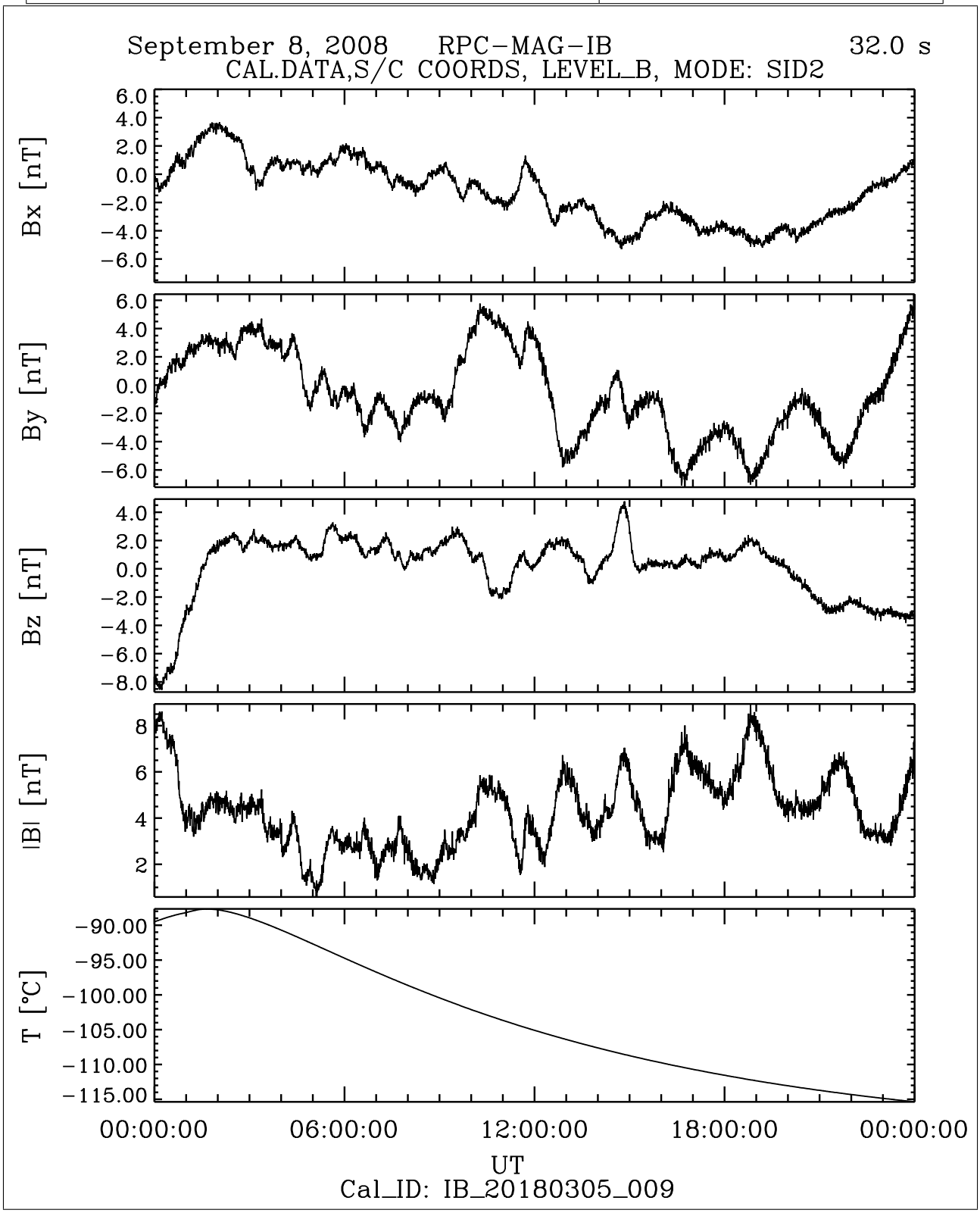

Figure 47: File: RPCMAG080908T0000_CLB_IB_M2_T0000_2400_009

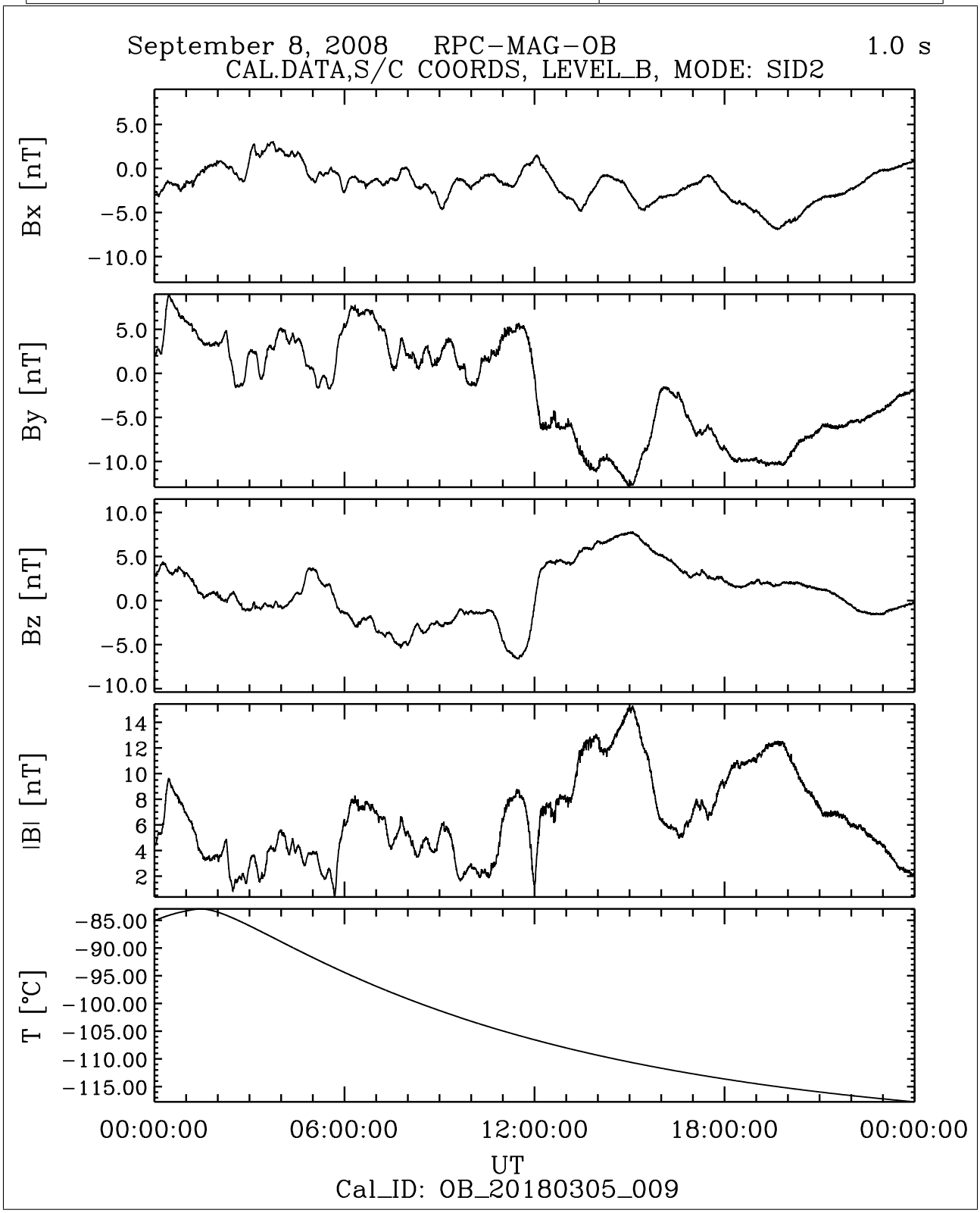

Figure 48: File: RPCMAG080908T0000_CLB_OB_M2_T0000_2400_009

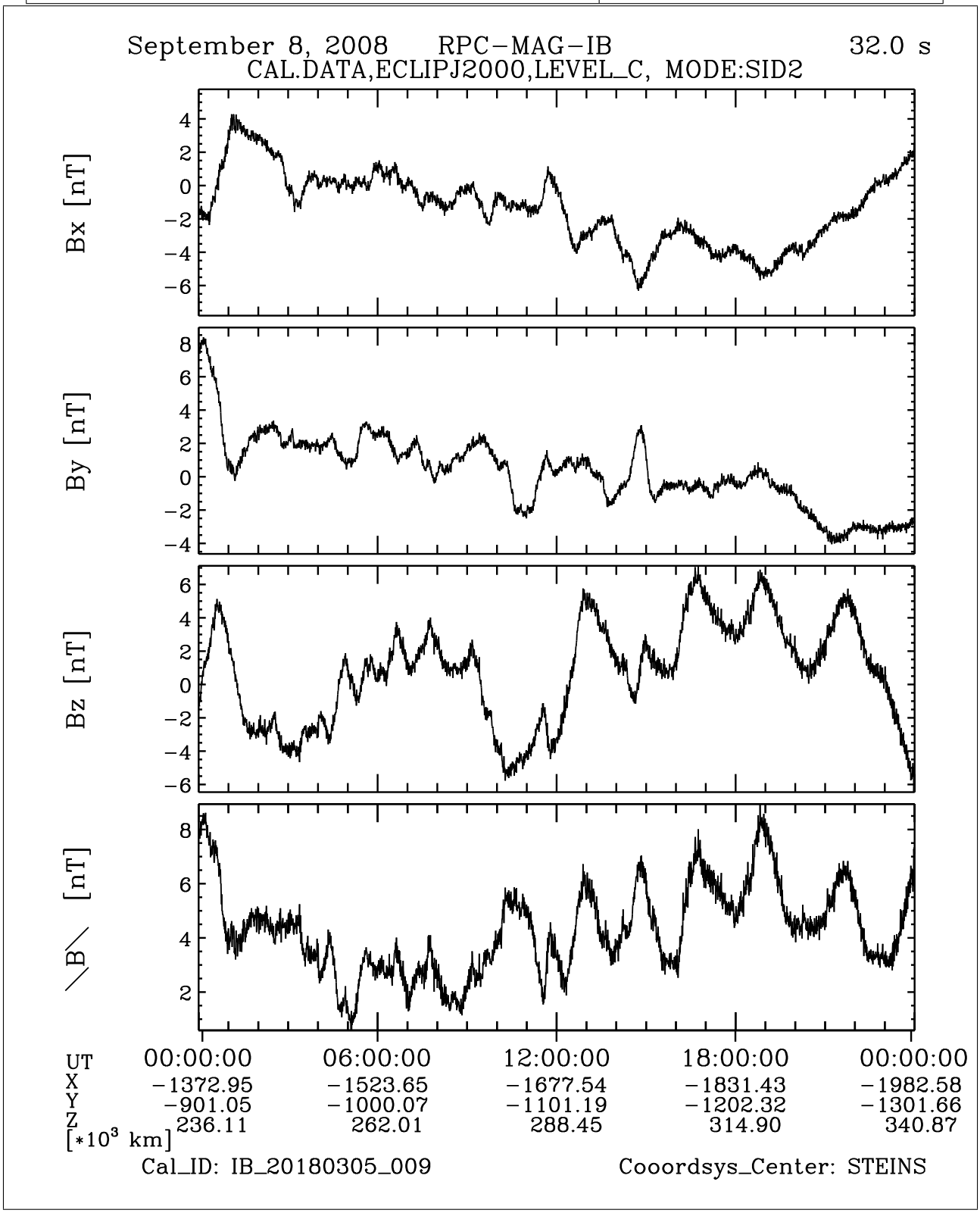

Figure 49: File: RPCMAG080908T0000_CLC_IB_M2_T0000_2400_009

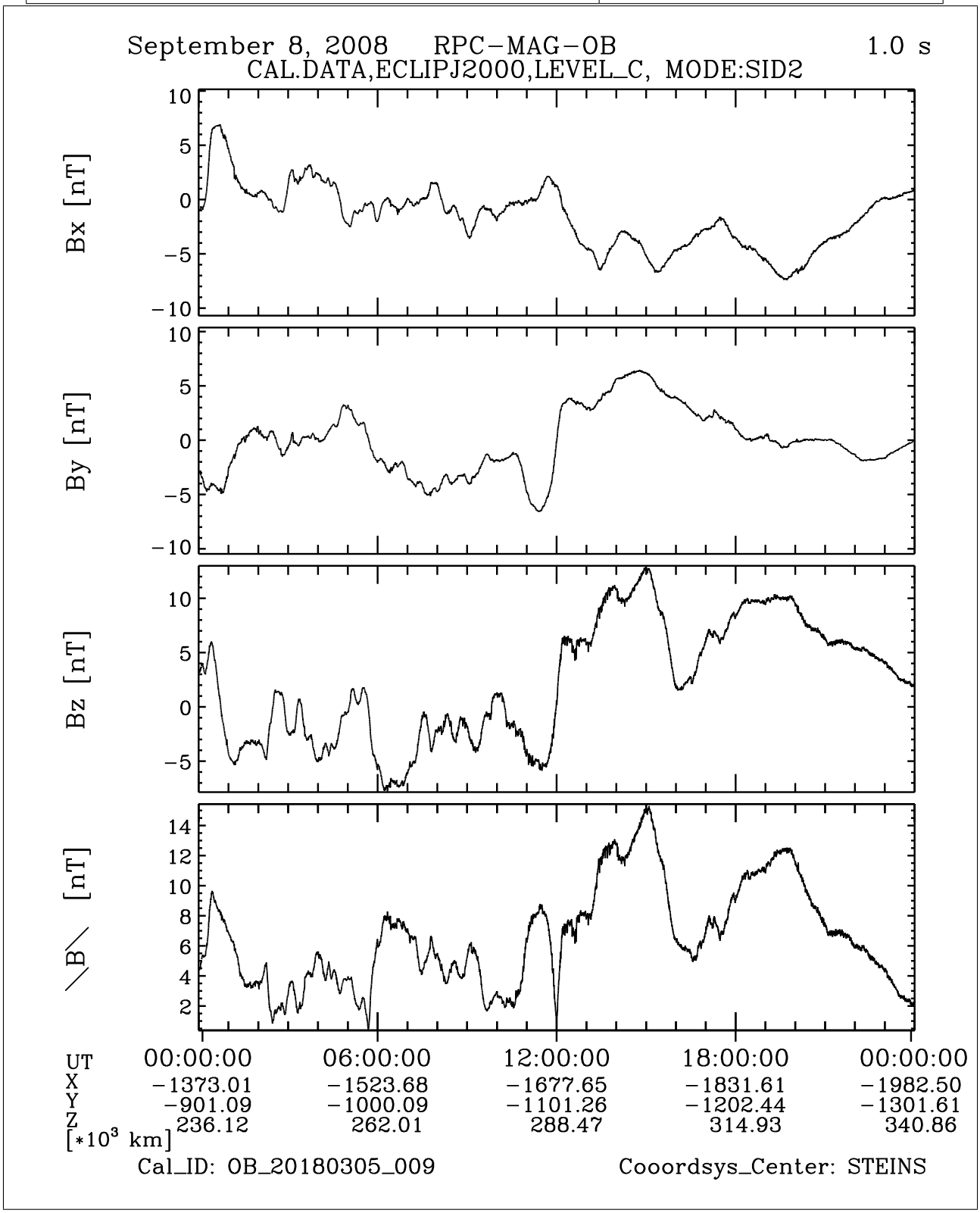

Figure 50: File: RPCMAG080908T0000_CLC_OB_M2_T0000_2400_009

3.10 September 09, 2008:

3.10.1 Actions

MAG stayed in SID 2. No problems occurred.

3.10.2 Plots of Calibrated Data

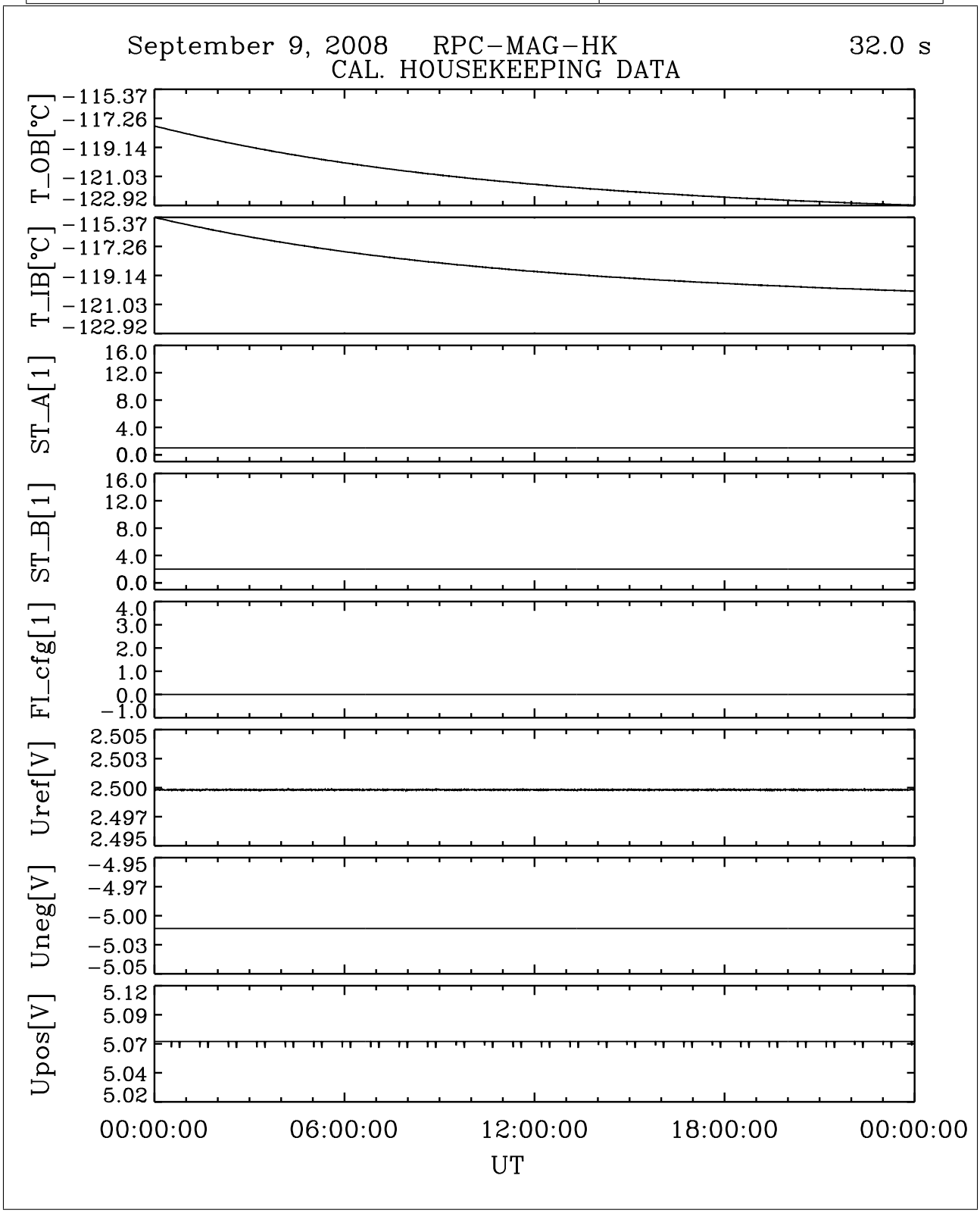

Figure 51: File: RPCMAG080909T0000_CLA_HK_P0000_2400

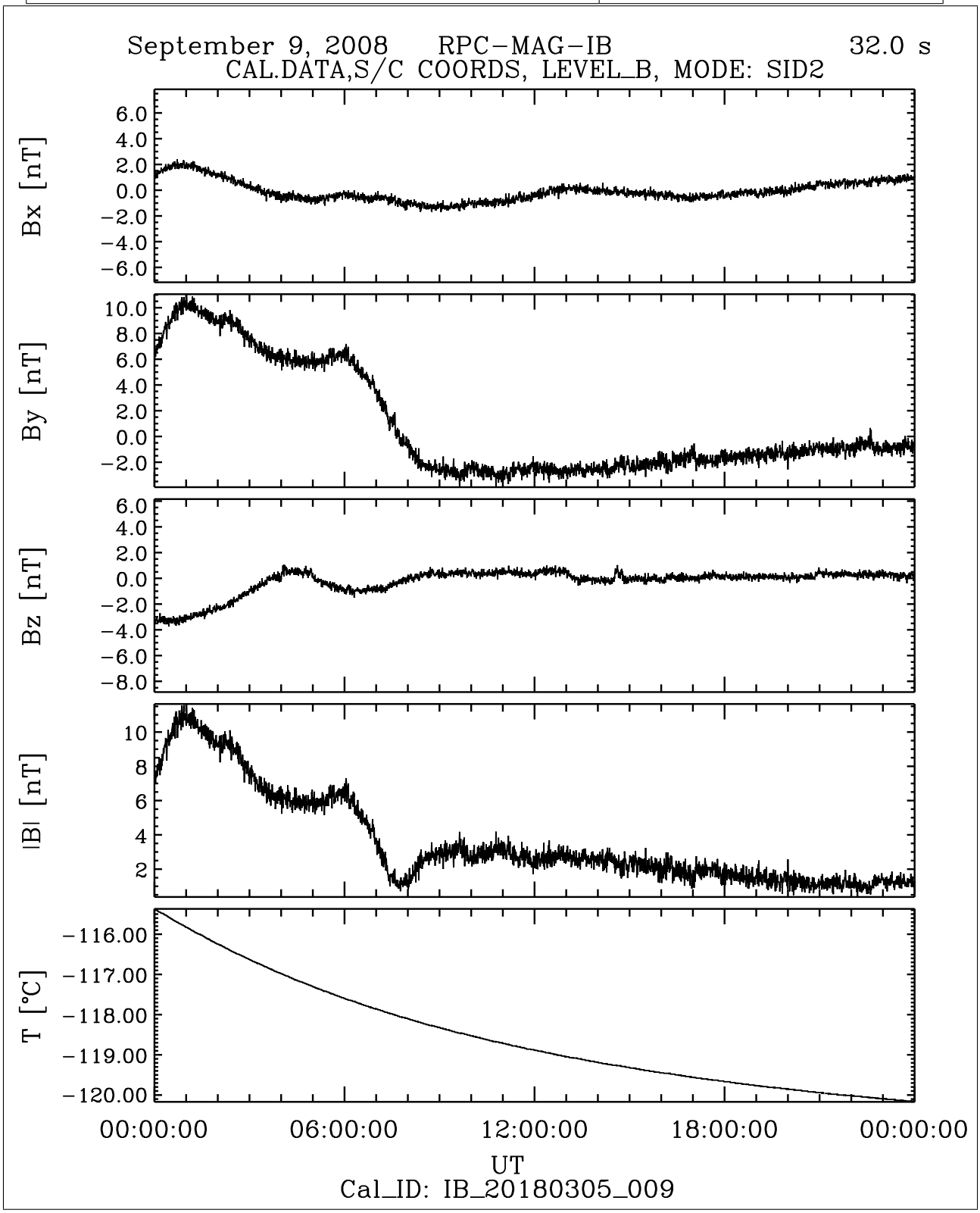

Figure 52: File: RPCMAG080909T0000_CLB_IB_M2_T0000_2400_009

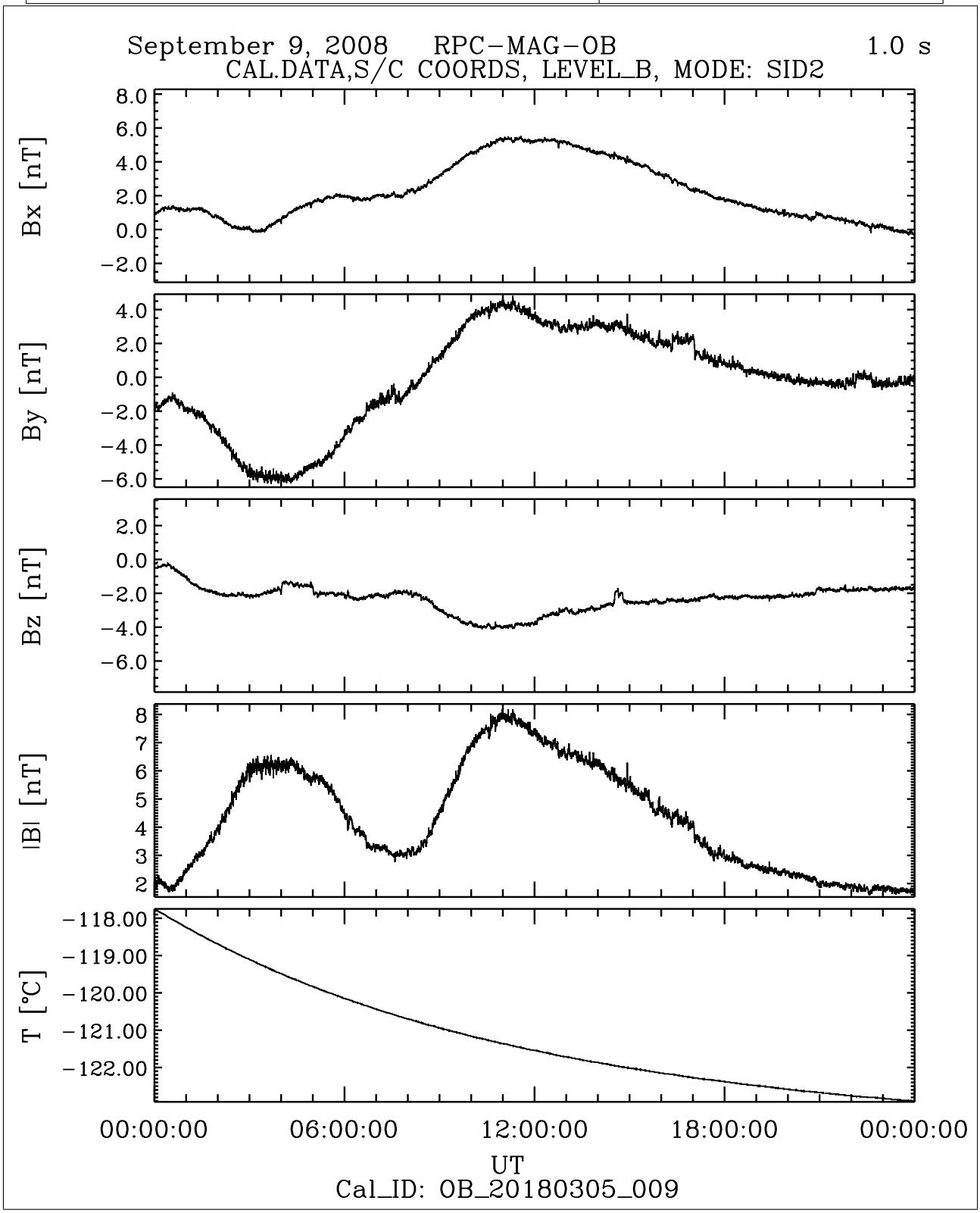

Figure 53: File: RPCMAG080909T0000_CLB_OB_M2_T0000_2400_009

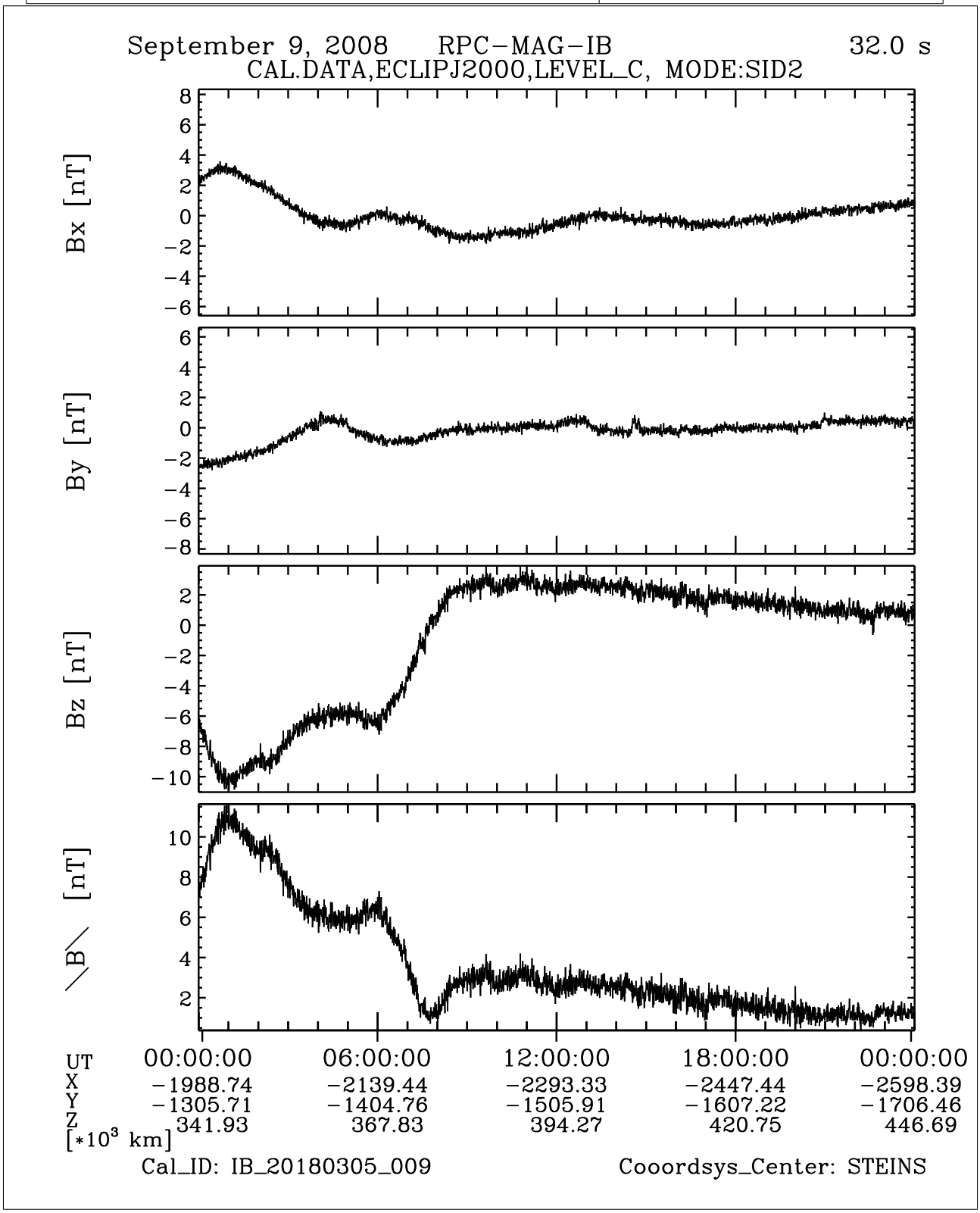

Figure 54: File: RPCMAG080909T0000_CLC_IB_M2_T0000_2400_009

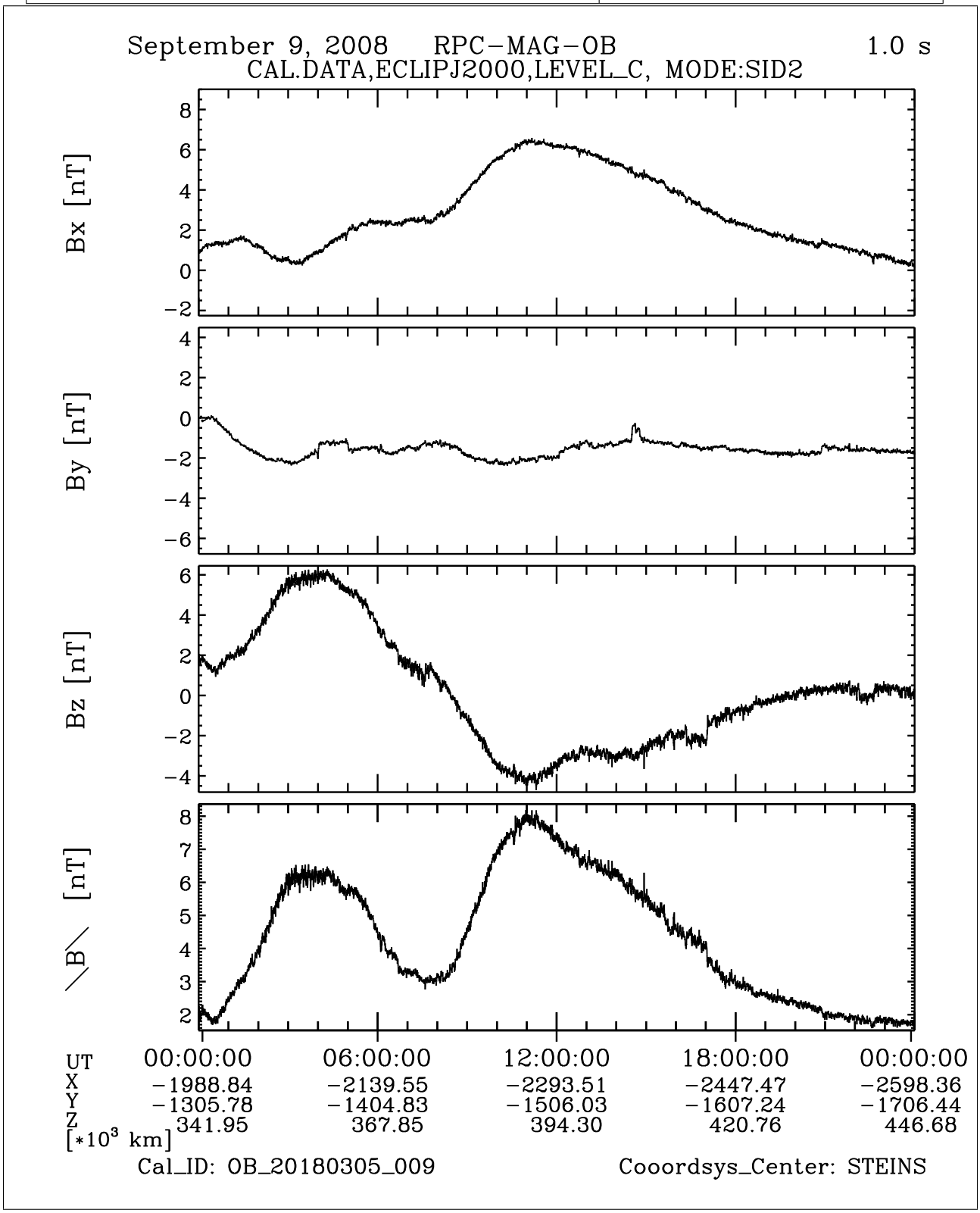

Figure 55: File: RPCMAG080909T0000_CLC_OB_M2_T0000_2400_009

3.11 September 10, 2008:

3.11.1 Actions

MAG stayed in SID 2. No problems occurred.

3.11.2 Plots of Calibrated Data

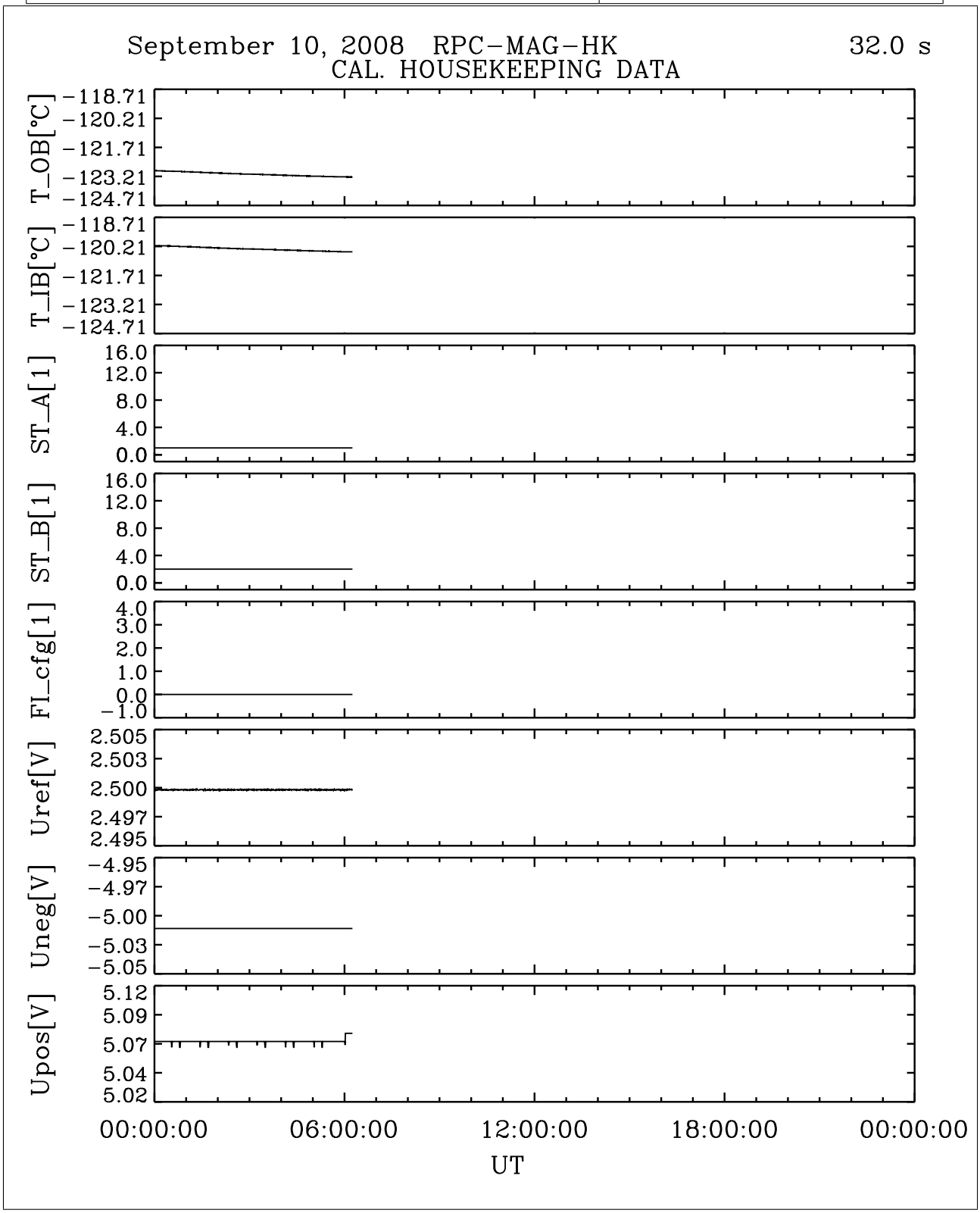

Figure 56: File: RPCMAG080910T0000_CLA_HK_P0000_2400

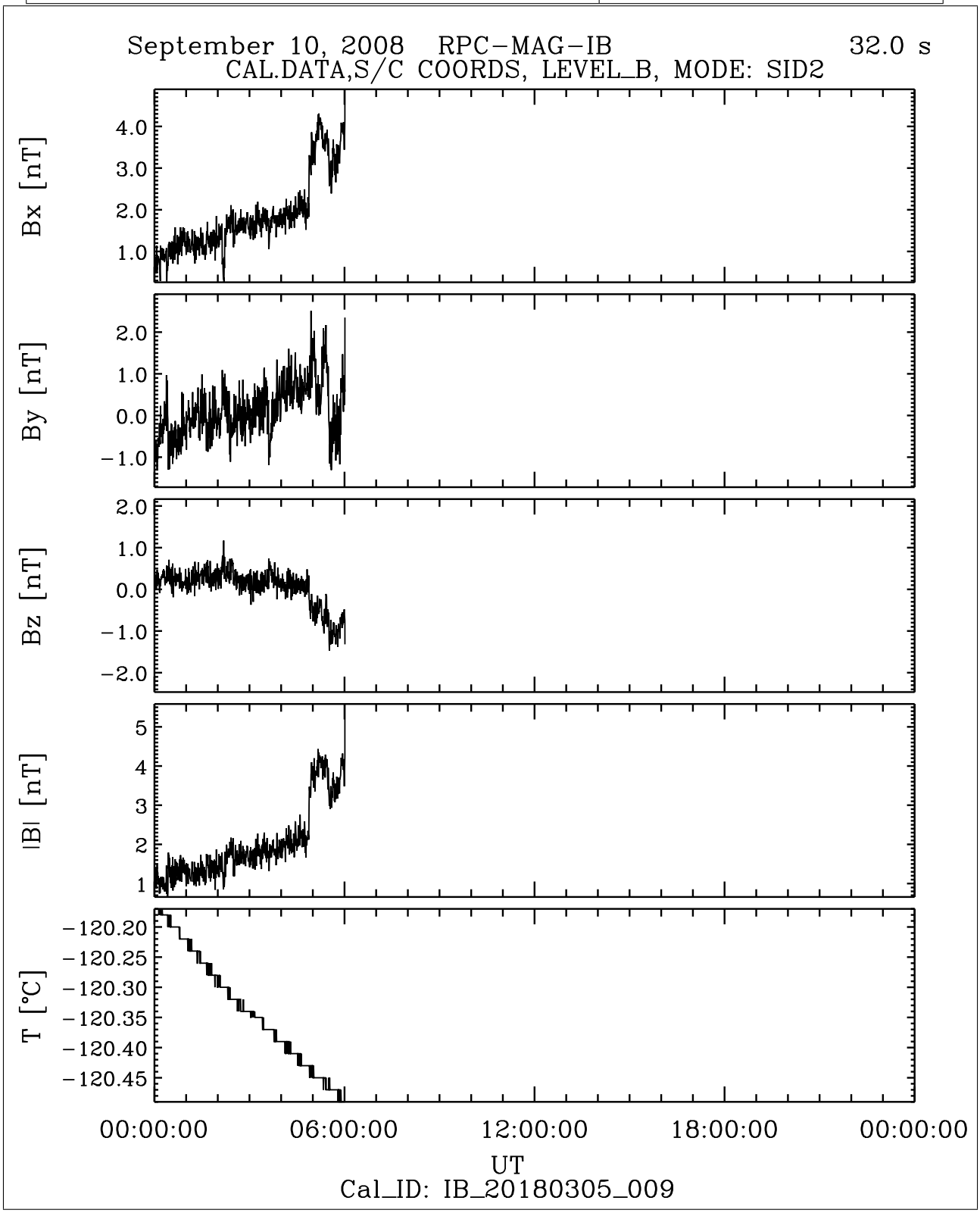

Figure 57: File: RPCMAG080910T0000_CLB_IB_M2_T0000_2400_009

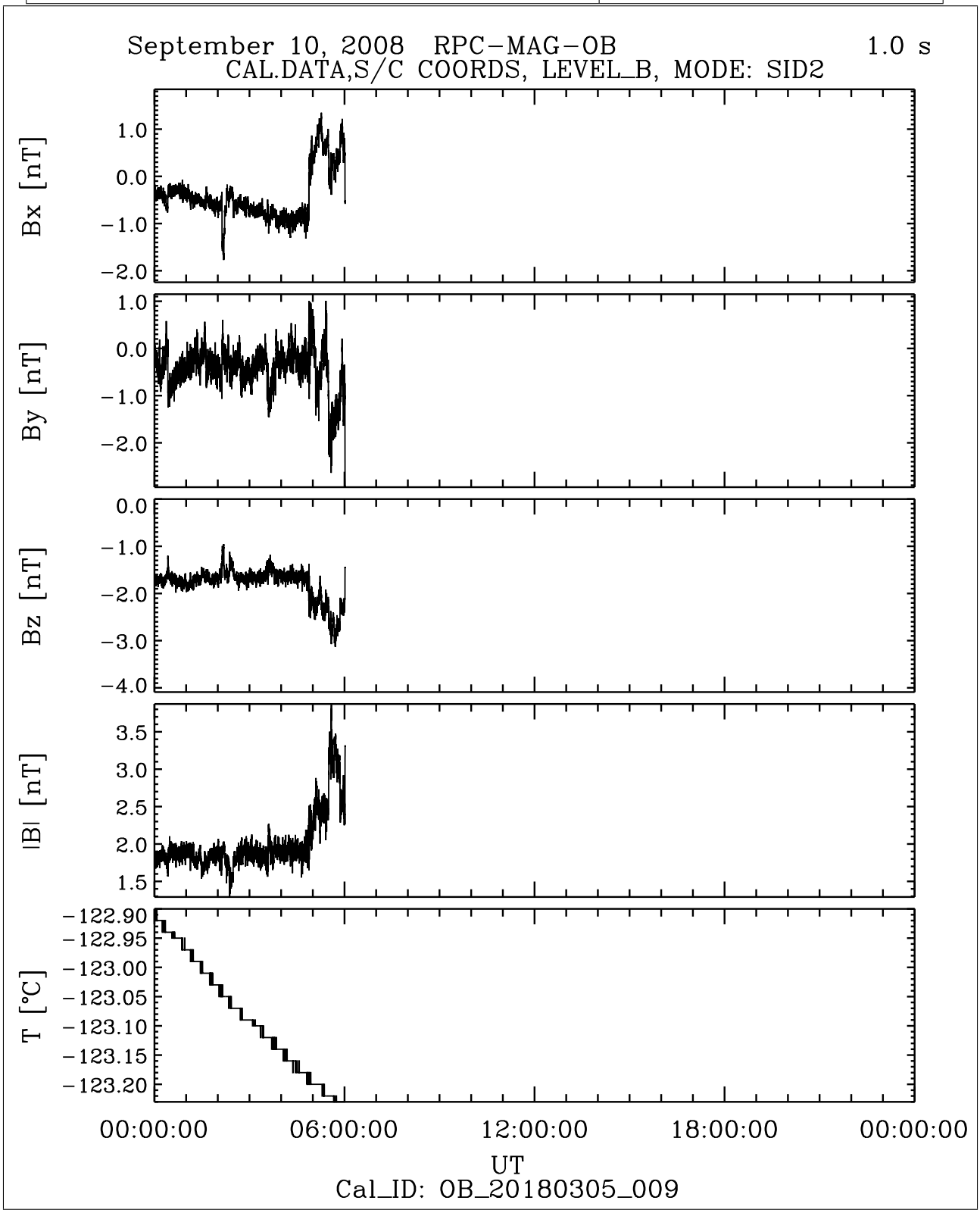

Figure 58: File: RPCMAG080910T0000_CLB_OB_M2_T0000_2400_009

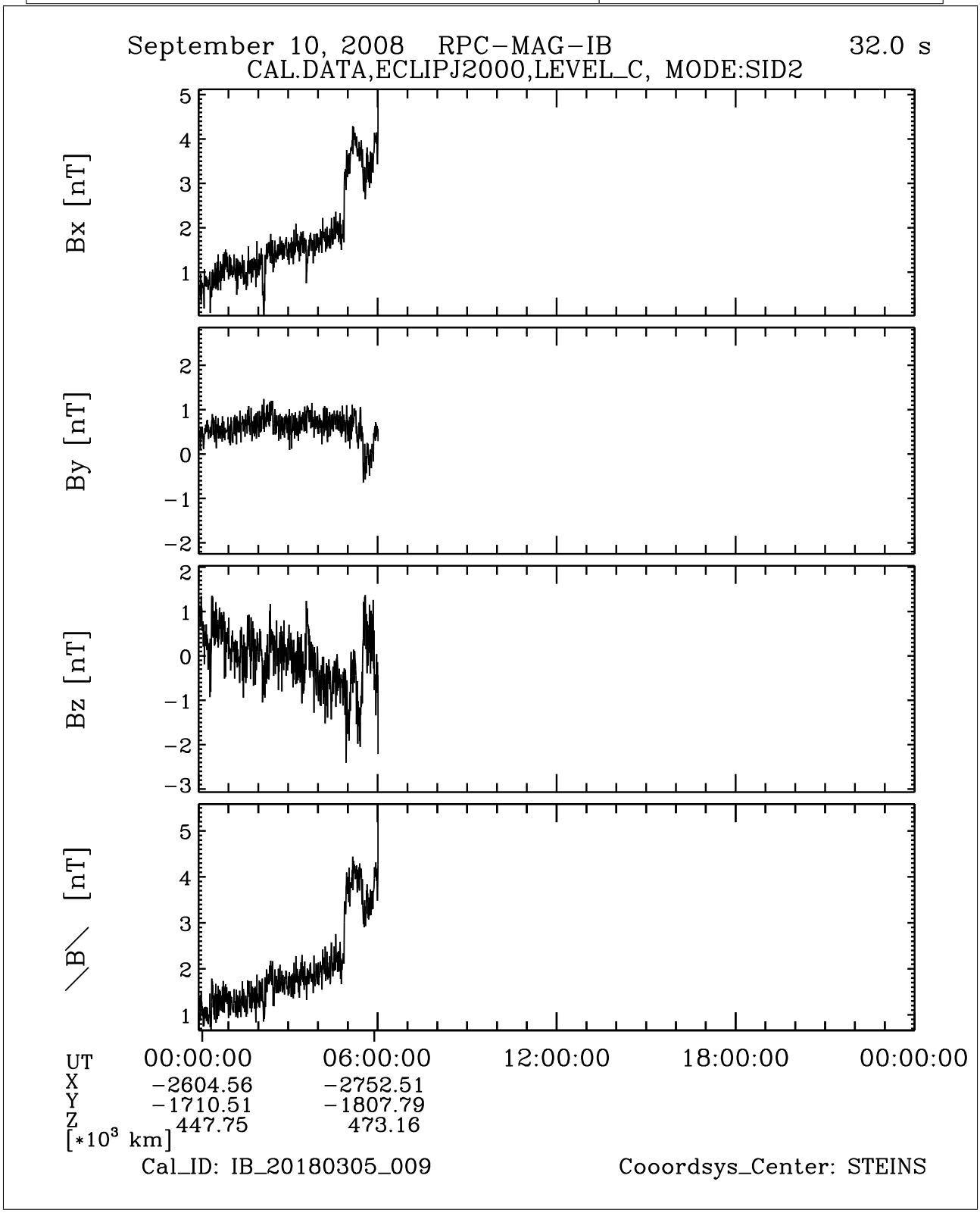

Figure 59: File: RPCMAG080910T0000_CLC_IB_M2_T0000_2400_009

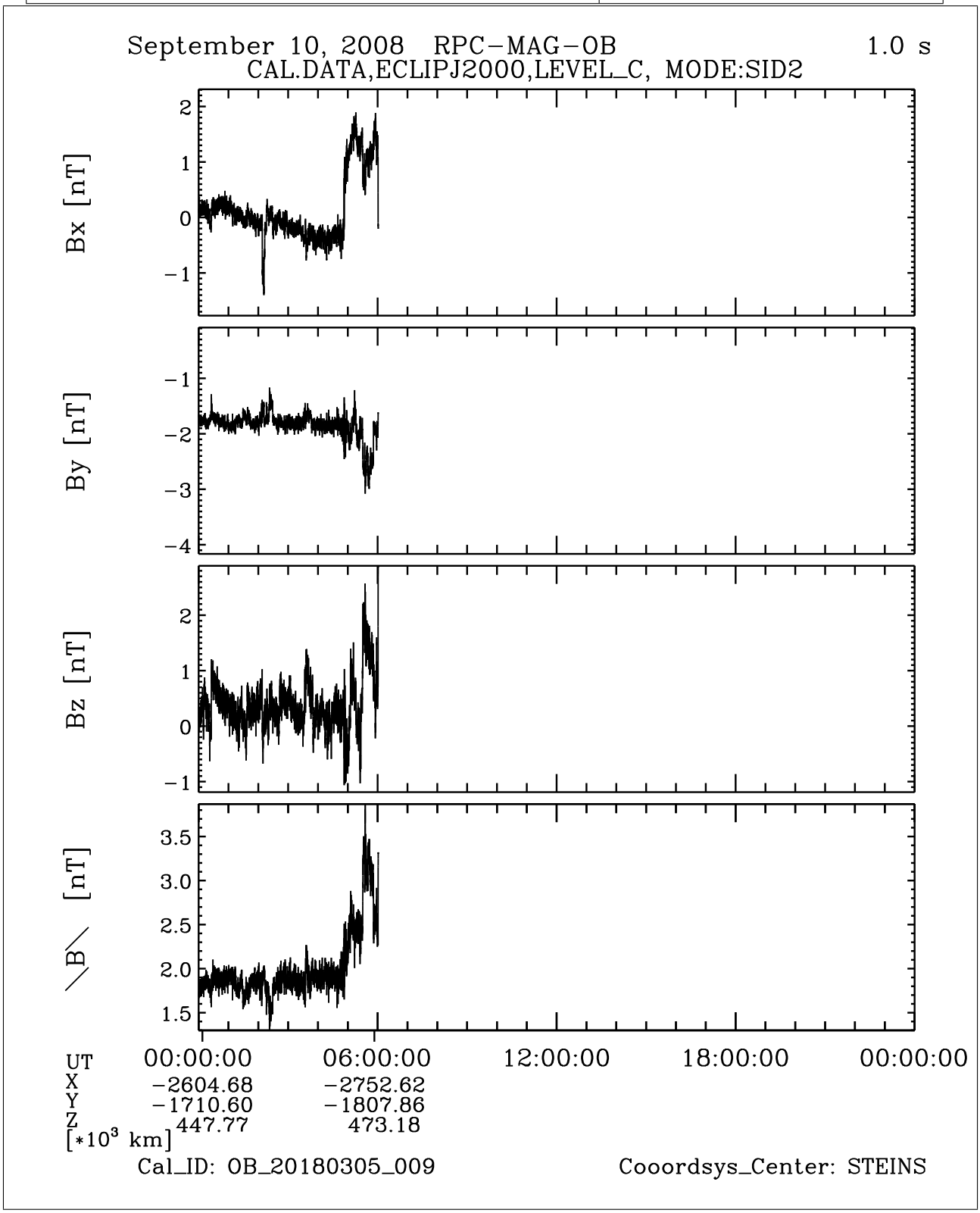

Figure 60: File: RPCMAG080910T0000_CLC_OB_M2_T0000_2400_009

4 Comparison between OB and IB: The Influence of the Sensor Temperature and of other Disturbers

In this section we compare the measured data of the OB Sensor with the IB ones. The investigation is done with 1 s averaged LEVEL_F data (s/c coordinates) for various days.

From earlier mission phases we know, that the OB and IB data match very well at times where the both sensors feel the same temperature *variation*. When the temperature changes are different, then the magnetic field data diverge as well. We do see this effect although a 3rd order temperature calibration has been applied. On short time scales, however, different heat capacities and micro physical hysteresis effects of the sensors core material may cause this behavior.

At the actual mission phase we see, however, that the OB and IB data are sometimes different also if the temperature behavior is the same. This leads to the assumption that there are active disturbers on the s/c.

One of the disturbance sources is the MUPUS experiment on the Lander.This can clearly be seen in Figure 25 and in the spectrum shown in Figure 66. The disturbance lasts from 12:00 - 20:00 on September 5th, and has an amplitude of about 1 nT. The ROMAP magnetic field sensor sees about 100 nT disturbance. An explanation of this signature was given by the MUPUS PI: MUPUS was operated in the standard temperature measurement mode (TEM) during the flyby. As the Temperature must not fall below -50°C a background heating routine was executed, which pulsed some heaters every 4-5 minutes for 1 minute with a current of about 100 mA, which generated a disturbing magnetic field.

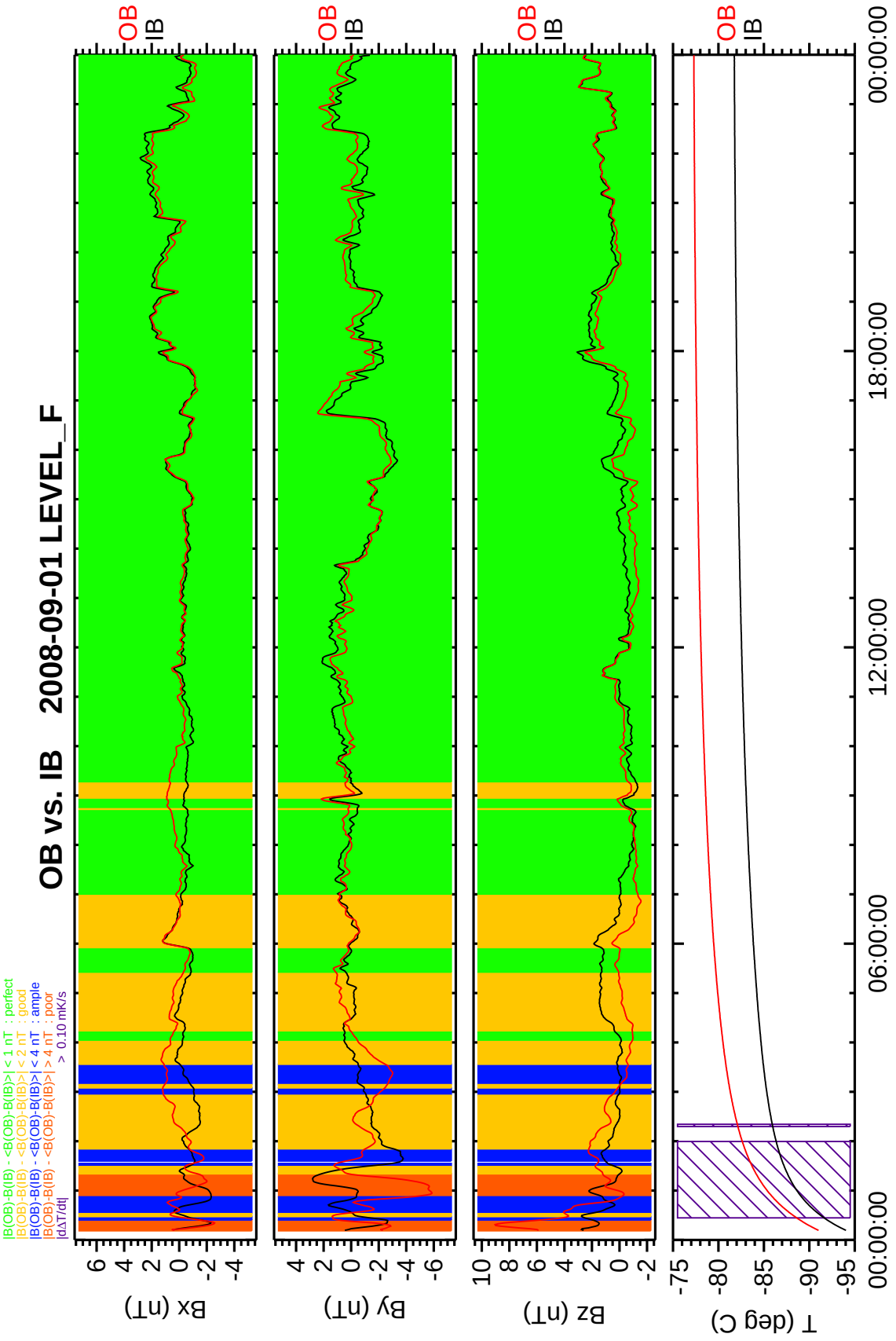
OB vs. IB 2008-09-01 LEVEL_F
|B(OB)-B(IB) - <B(OB)-B(IB)>| < 1 nT : perfect
|B(OB)-B(IB) - <B(OB)-B(IB)>| < 2 nT : good
|B(OB)-B(IB) - <B(OB)-B(IB)>| < 4 nT : ample
|B(OB)-B(IB) - <B(OB)-B(IB)>| > 4 nT : poor
|dΔT/dt| > 0.10 mK/s
OB
IB
Bx (nT)
By (nT)
Bz (nT)
T (deg C)
00:00:00
06:00:00
12:00:00
18:00:00
00:00:00

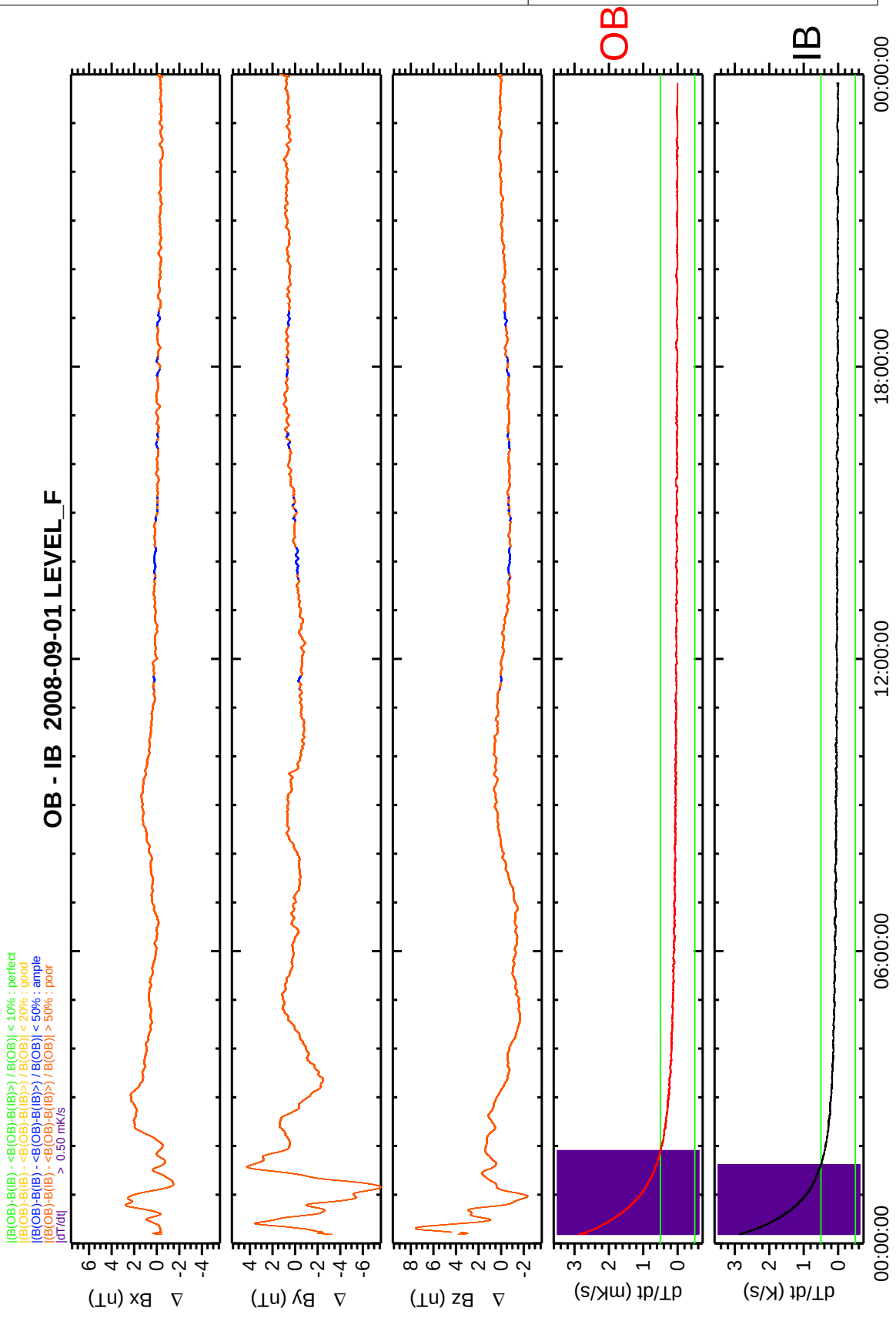
OB - IB 2008-09-01 LEVEL_F
OB
IB
Δ Bx (nT)
Δ By (nT)
Δ Bz (nT)
dT/dt (mK/s)
dT/dt (K/s)
00:00:00
06:00:00
12:00:00
18:00:00
00:00:00
|(B(OB)-B(IB) - <B(OB)-B(IB)>) / B(OB)| < 10% : perfect
|(B(OB)-B(IB) - <B(OB)-B(IB)>) / B(OB)| < 20% : good
|(B(OB)-B(IB) - <B(OB)-B(IB)>) / B(OB)| < 50% : ample
|(B(OB)-B(IB) - <B(OB)-B(IB)>) / B(OB)| > 50% : poor
|dT/dt| > 0.50 mK/s

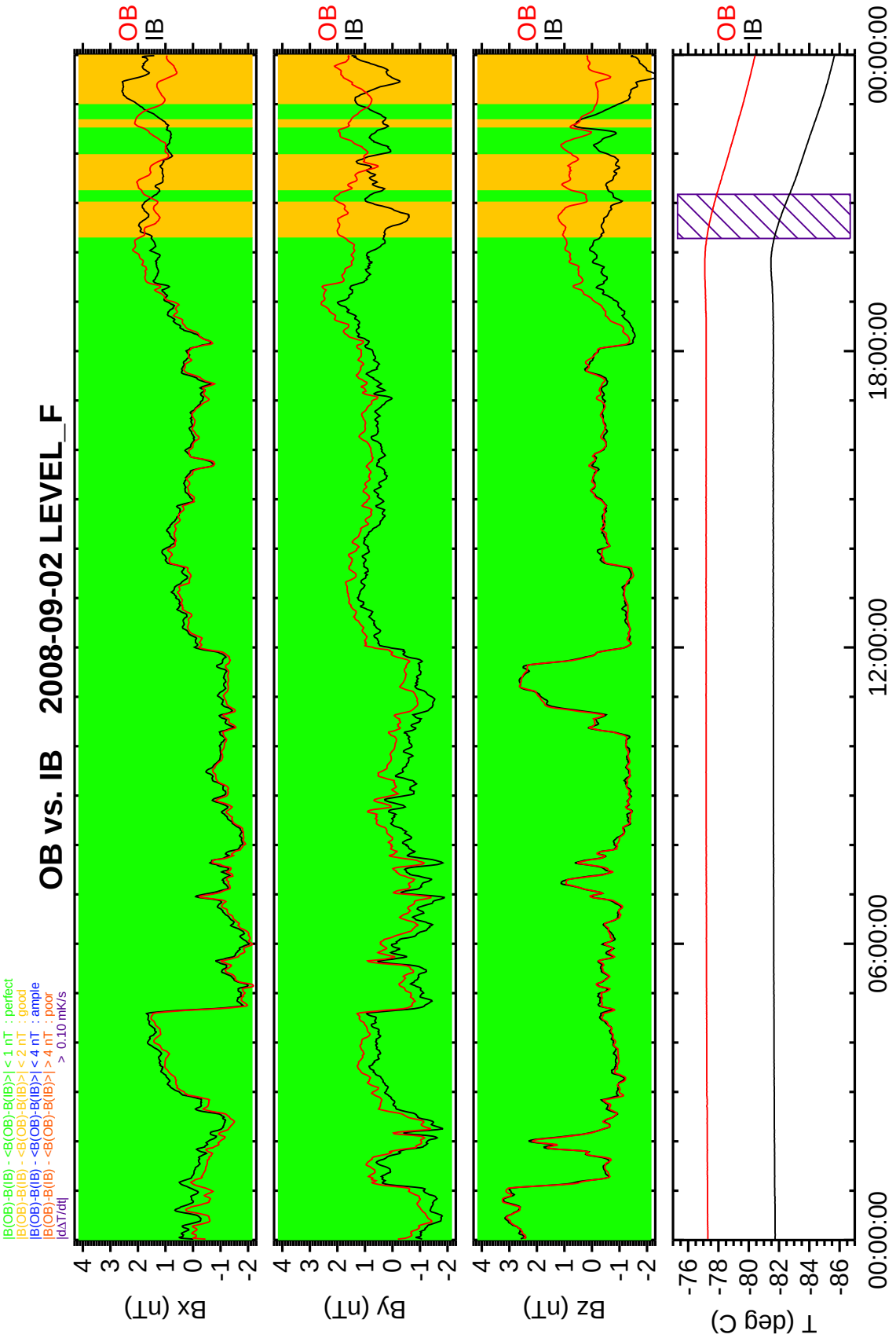
OB vs. IB 2008-09-02 LEVEL_F
|B(OB)-B(IB) - <B(OB)-B(IB)>| < 1 nT : perfect
|B(OB)-B(IB) - <B(OB)-B(IB)>| < 2 nT : good
|B(OB)-B(IB) - <B(OB)-B(IB)>| < 4 nT : ample
|B(OB)-B(IB) - <B(OB)-B(IB)>| > 4 nT : poor
|dΔT/dt| > 0.10 mK/s
OB
IB
Bx (nT)
By (nT)
Bz (nT)
T (deg C)
4
3
2
1
0
-1
-2
-76
-78
-80
-82
-84
-86
00:00:00
06:00:00
12:00:00
18:00:00
00:00:00

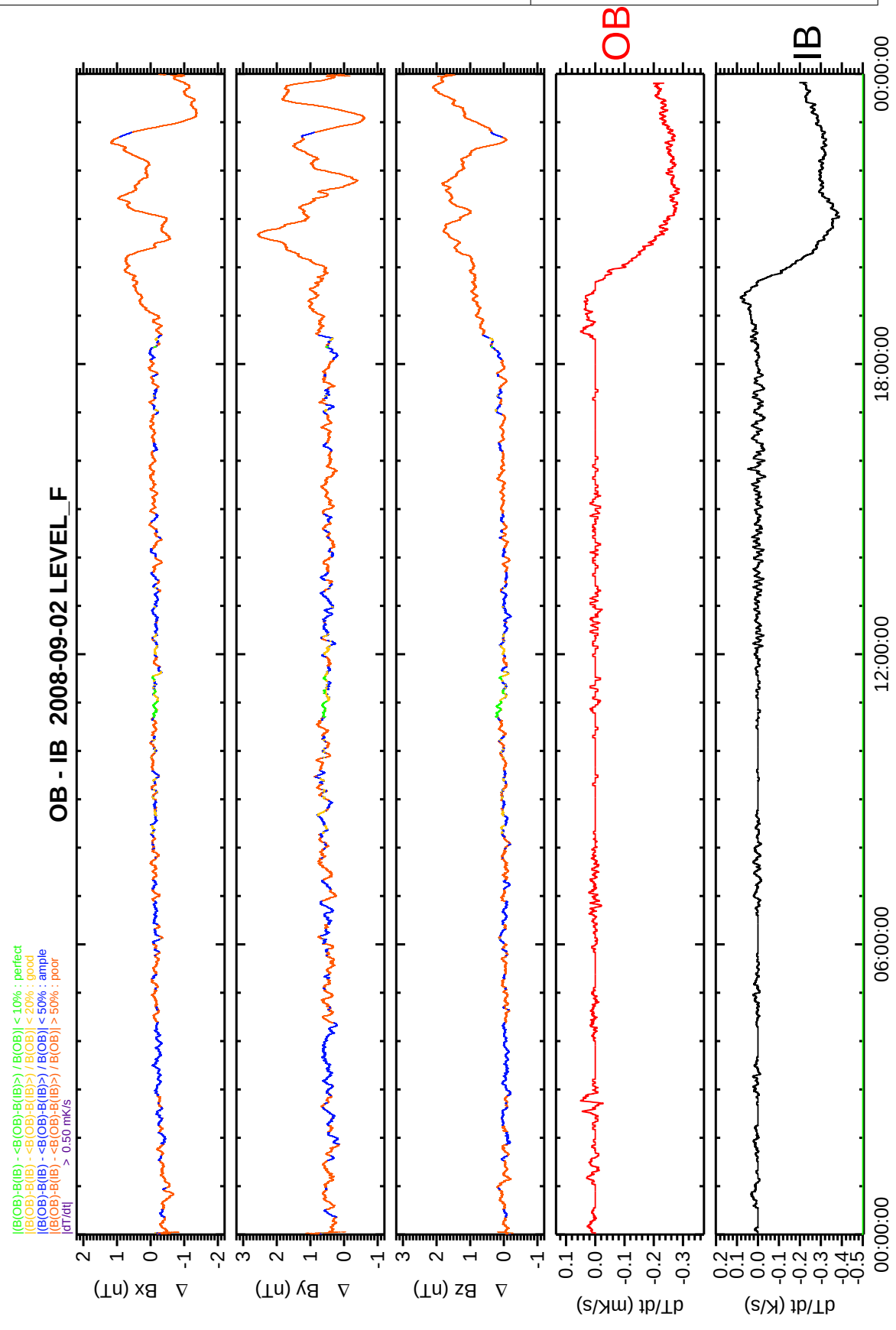
OB - IB 2008-09-02 LEVEL_F
OB
IB
Δ Bx (nT)
Δ By (nT)
Δ Bz (nT)
dT/dt (mK/s)
dT/dt (K/s)
00:00:00
06:00:00
12:00:00
18:00:00
00:00:00
|(B(OB)-B(IB) - <B(OB)-B(IB)>) / B(OB)| < 10% : perfect
|(B(OB)-B(IB) - <B(OB)-B(IB)>) / B(OB)| < 20% : good
|(B(OB)-B(IB) - <B(OB)-B(IB)>) / B(OB)| < 50% : ample
|(B(OB)-B(IB) - <B(OB)-B(IB)>) / B(OB)| > 50% : poor
|dT/dt| > 0.50 mK/s

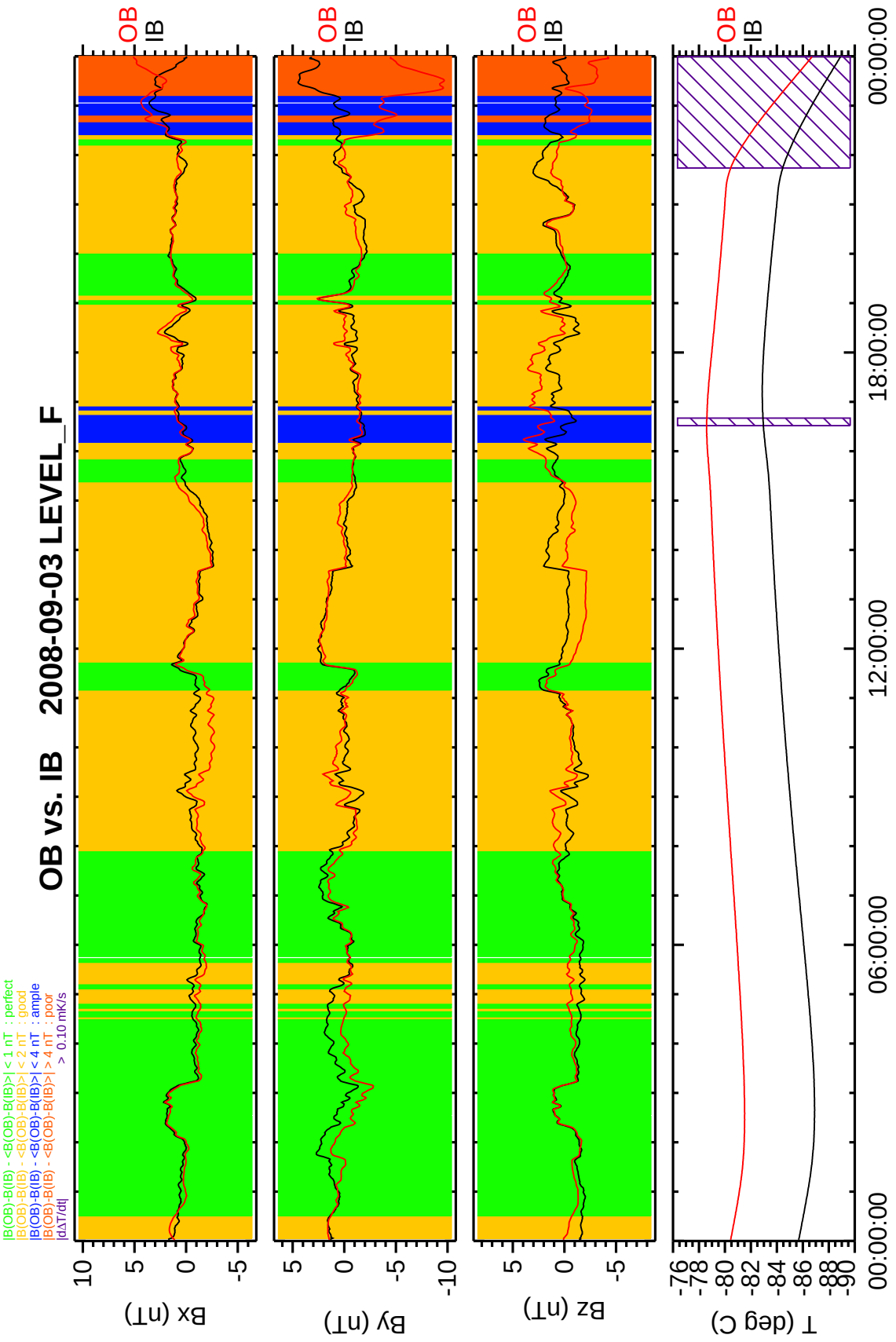
OB vs. IB 2008-09-03 LEVEL_F
|B(OB)-B(IB) - <B(OB)-B(IB)>| < 1 nT : perfect
|B(OB)-B(IB) - <B(OB)-B(IB)>| < 2 nT : good
|B(OB)-B(IB) - <B(OB)-B(IB)>| < 4 nT : ample
|B(OB)-B(IB) - <B(OB)-B(IB)>| > 4 nT : poor
|dΔT/dt| > 0.10 mK/s
OB
IB
Bx (nT)
By (nT)
Bz (nT)
T (deg C)
00:00:00
06:00:00
12:00:00
18:00:00
00:00:00

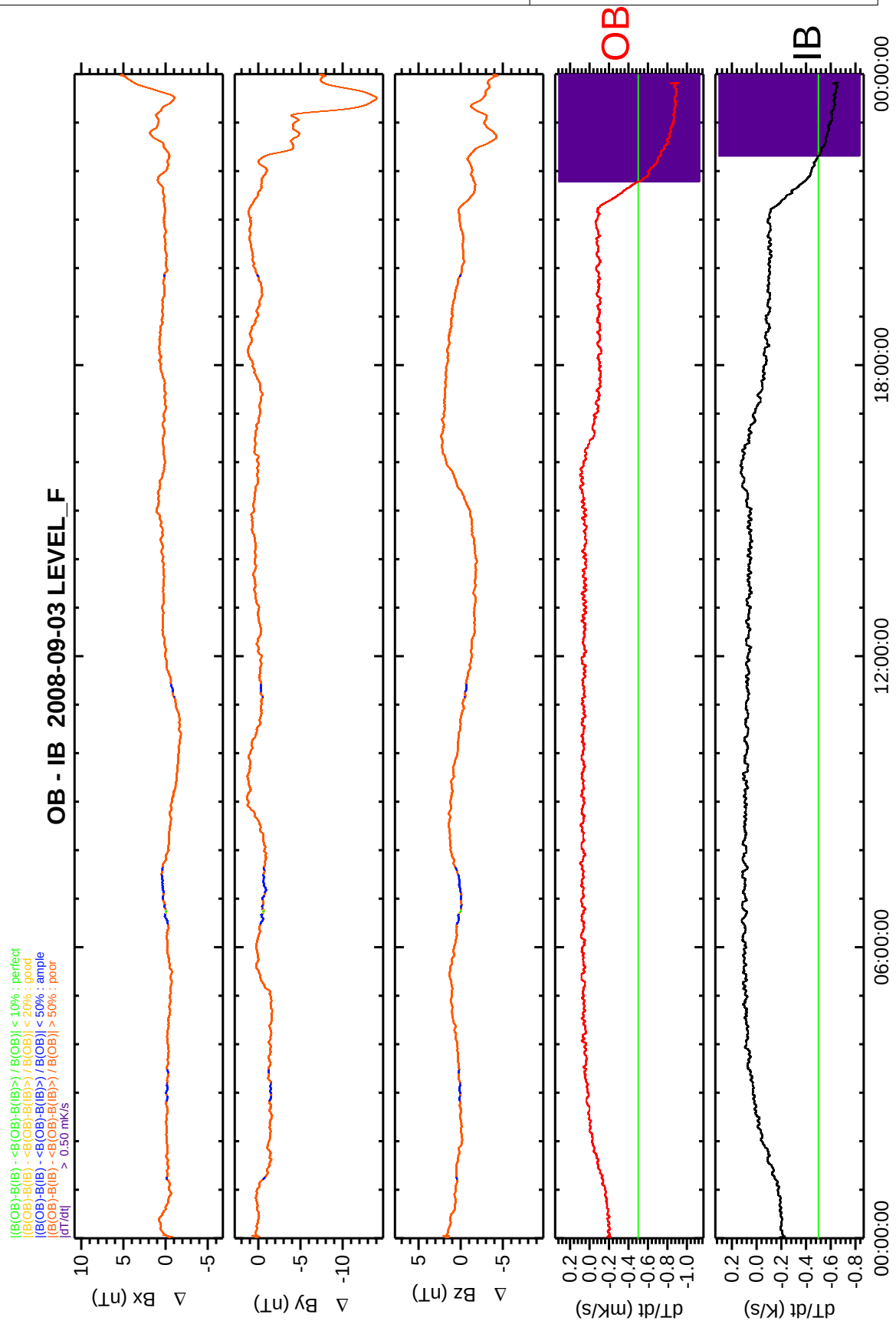
OB - IB 2008-09-03 LEVEL_F
OB
IB
Δ Bx (nT)
Δ By (nT)
Δ Bz (nT)
dT/dt (mK/s)
dT/dt (K/s)
00:00:00
06:00:00
12:00:00
18:00:00
00:00:00
|(B(OB)-B(IB) - <B(OB)-B(IB)>) / B(OB)| < 10% : perfect
|(B(OB)-B(IB) - <B(OB)-B(IB)>) / B(OB)| < 20% : good
|(B(OB)-B(IB) - <B(OB)-B(IB)>) / B(OB)| < 50% : ample
|(B(OB)-B(IB) - <B(OB)-B(IB)>) / B(OB)| > 50% : poor
|dT/dt| > 0.50 mK/s

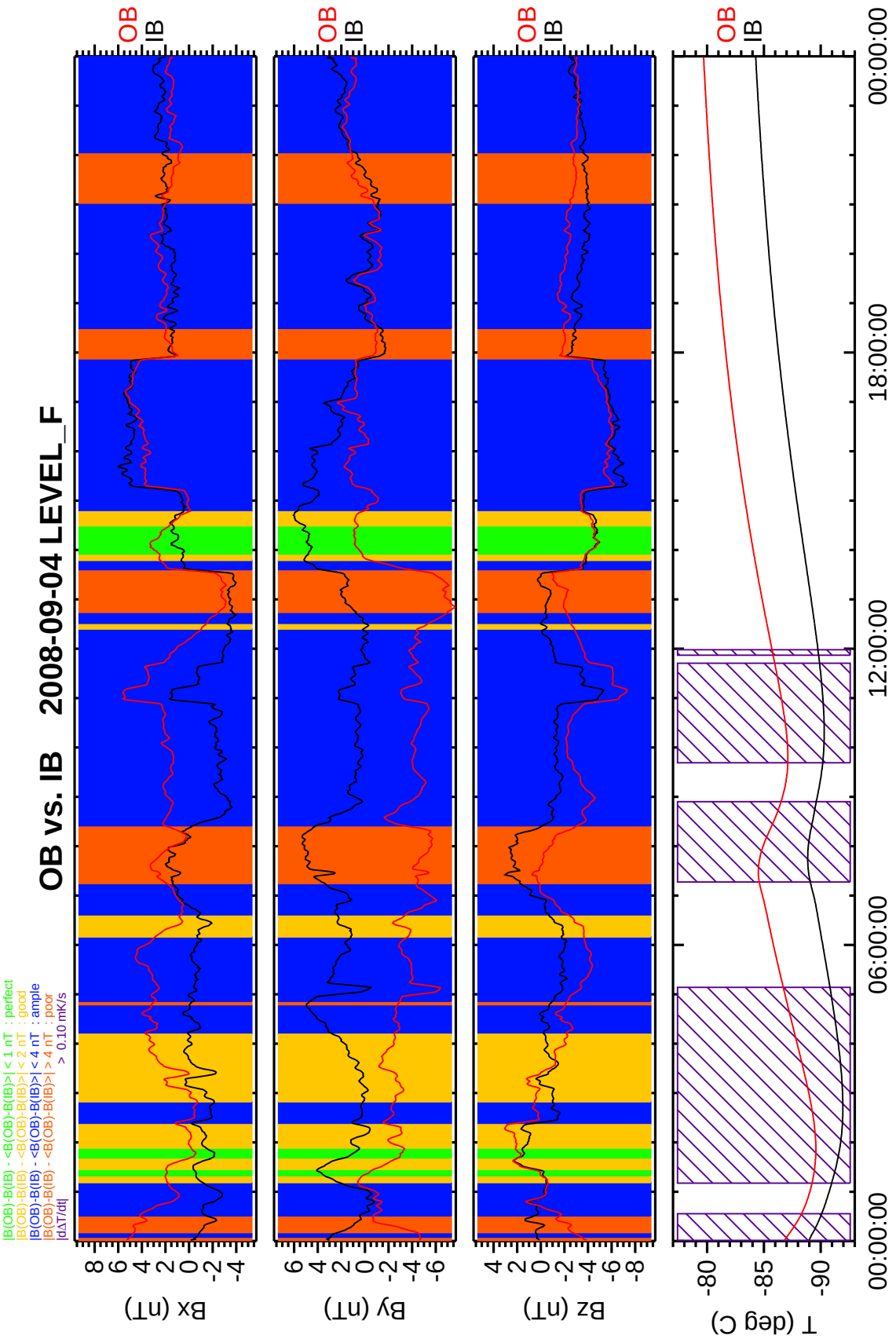
OB vs. IB 2008-09-04 LEVEL_F
|B(OB)-B(IB) - <B(OB)-B(IB)>| < 1 nT : perfect
|B(OB)-B(IB) - <B(OB)-B(IB)>| < 2 nT : good
|B(OB)-B(IB) - <B(OB)-B(IB)>| < 4 nT : ample
|B(OB)-B(IB) - <B(OB)-B(IB)>| > 4 nT : poor
|dΔT/dt| > 0.10 mK/s
OB
IB
Bx (nT)
By (nT)
Bz (nT)
T (deg C)
00:00:00
06:00:00
12:00:00
18:00:00
00:00:00

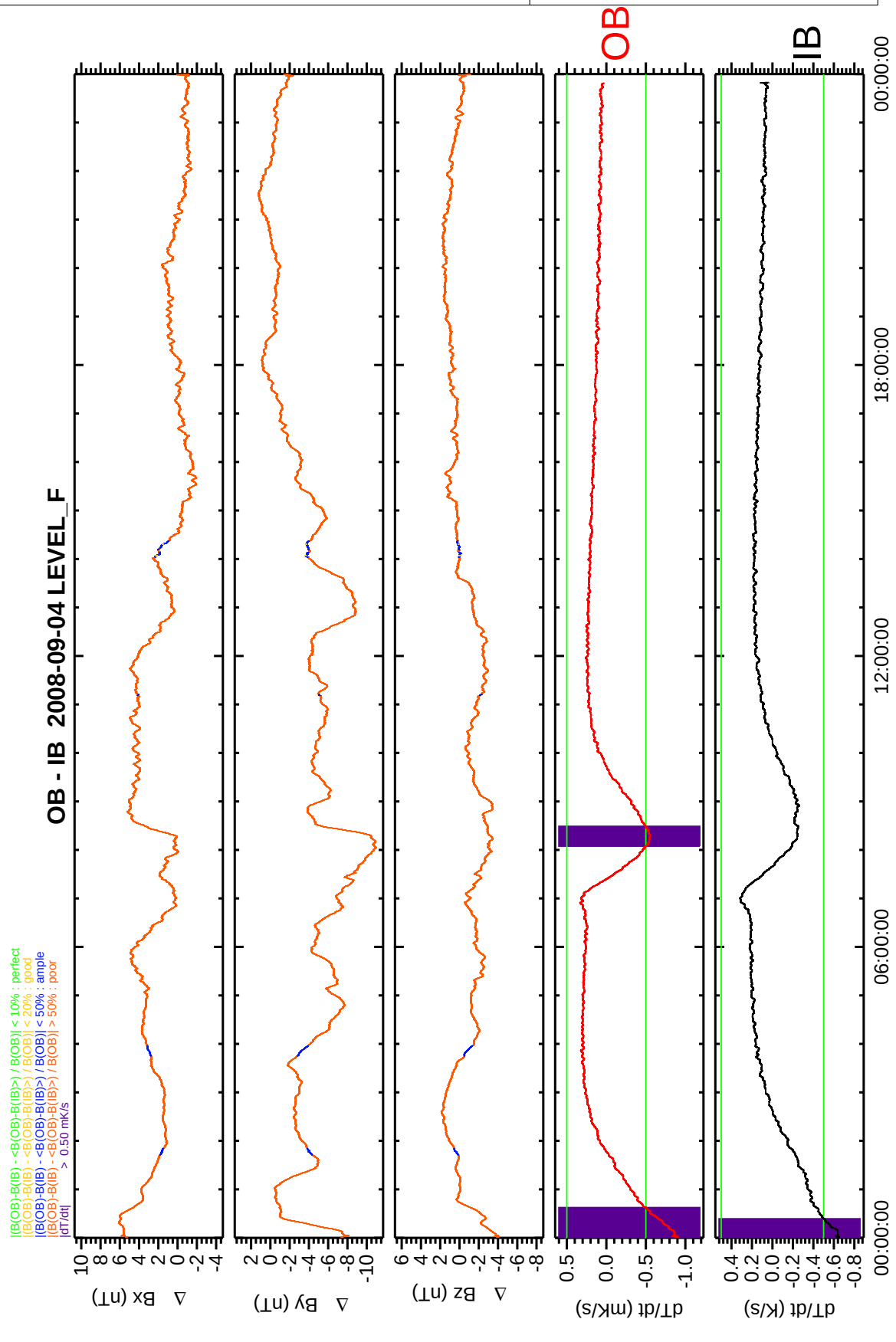
OB - IB 2008-09-04 LEVEL_F
OB
IB
Δ Bx (nT)
Δ By (nT)
Δ Bz (nT)
dT/dt (mK/s)
dT/dt (K/s)
00:00:00
06:00:00
12:00:00
18:00:00
00:00:00
|(B(OB)-B(IB) - <B(OB)-B(IB)>) / B(OB)| < 10% : perfect
|(B(OB)-B(IB) - <B(OB)-B(IB)>) / B(OB)| < 20% : good
|(B(OB)-B(IB) - <B(OB)-B(IB)>) / B(OB)| < 50% : ample
|(B(OB)-B(IB) - <B(OB)-B(IB)>) / B(OB)| > 50% : poor
|dT/dt| > 0.50 mK/s

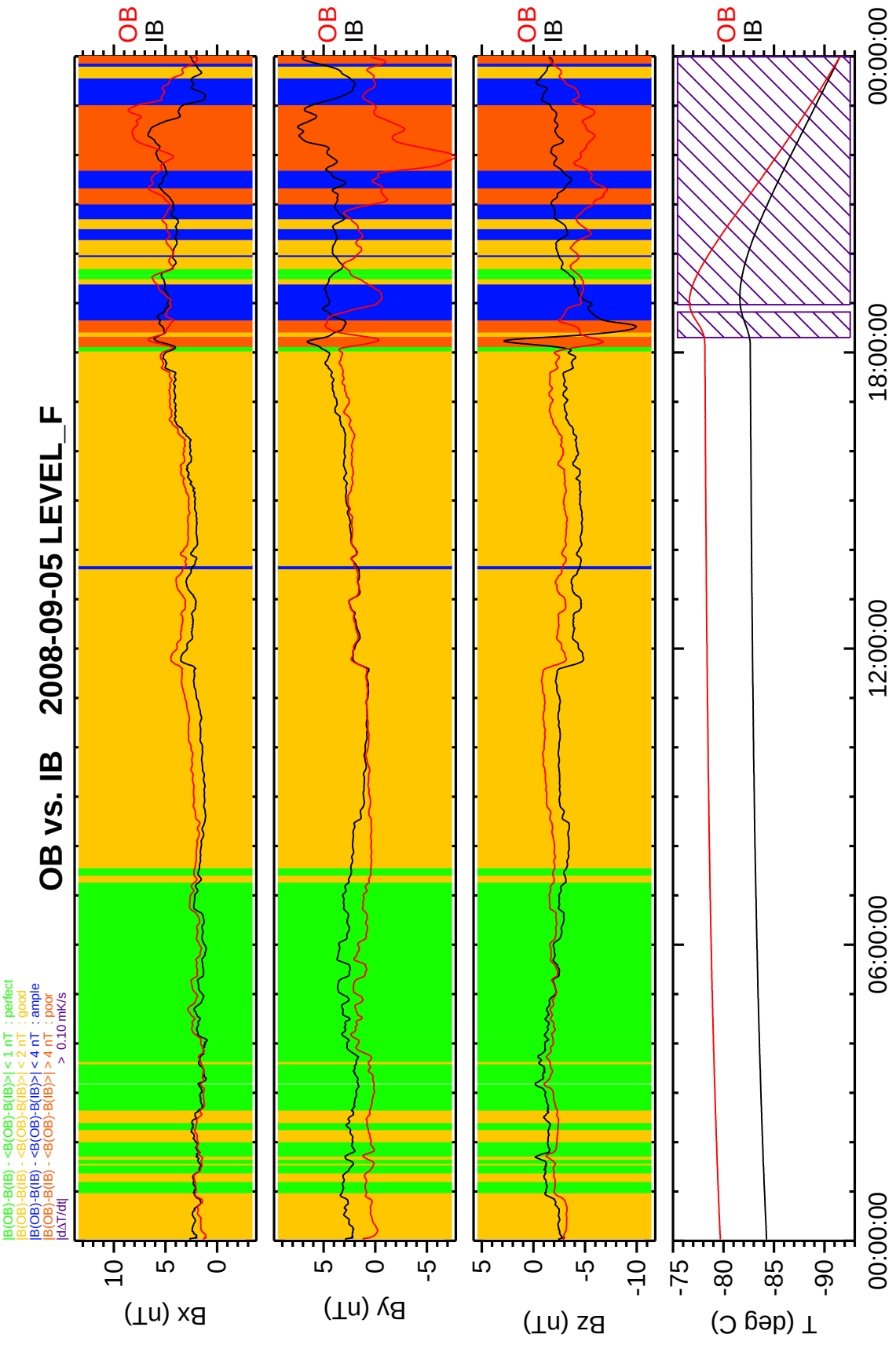
OB vs. IB 2008-09-05 LEVEL_F
|B(OB)-B(IB) - <B(OB)-B(IB)>| < 1 nT : perfect
|B(OB)-B(IB) - <B(OB)-B(IB)>| < 2 nT : good
|B(OB)-B(IB) - <B(OB)-B(IB)>| < 4 nT : ample
|B(OB)-B(IB) - <B(OB)-B(IB)>| > 4 nT : poor
|dΔT/dt| > 0.10 mK/s
OB
IB
Bx (nT)
By (nT)
Bz (nT)
T (deg C)
00:00:00
06:00:00
12:00:00
18:00:00
00:00:00

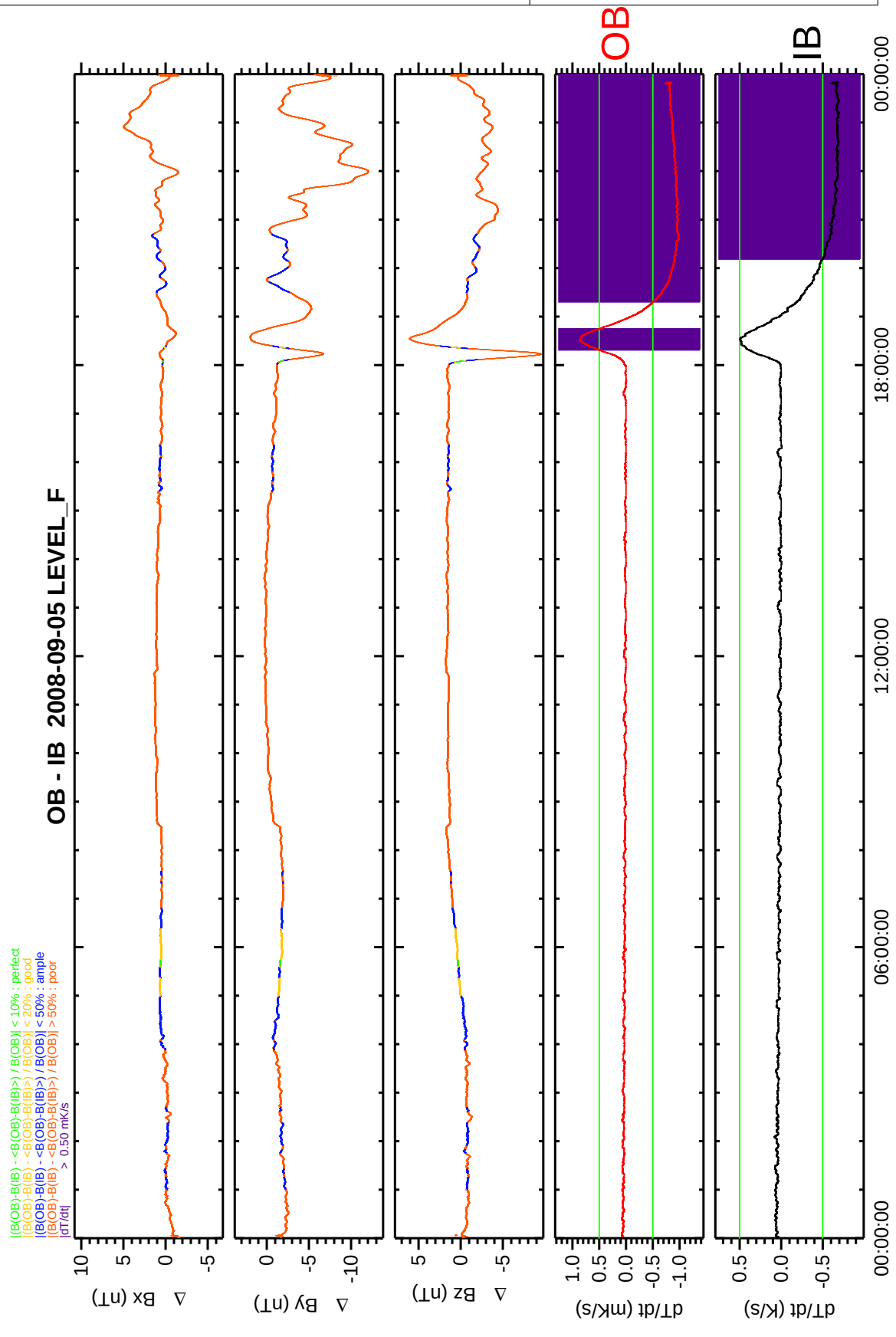
OB - IB 2008-09-05 LEVEL_F
OB
IB
Δ Bx (nT)
Δ By (nT)
Δ Bz (nT)
dT/dt (mK/s)
dT/dt (K/s)
00:00:00
06:00:00
12:00:00
18:00:00
00:00:00
|(B(OB)-B(IB) - <B(OB)-B(IB)>) / B(OB)| < 10% : perfect
|(B(OB)-B(IB) - <B(OB)-B(IB)>) / B(OB)| < 20% : good
|(B(OB)-B(IB) - <B(OB)-B(IB)>) / B(OB)| < 50% : ample
|(B(OB)-B(IB) - <B(OB)-B(IB)>) / B(OB)| > 50% : poor
|dT/dt| > 0.50 mK/s

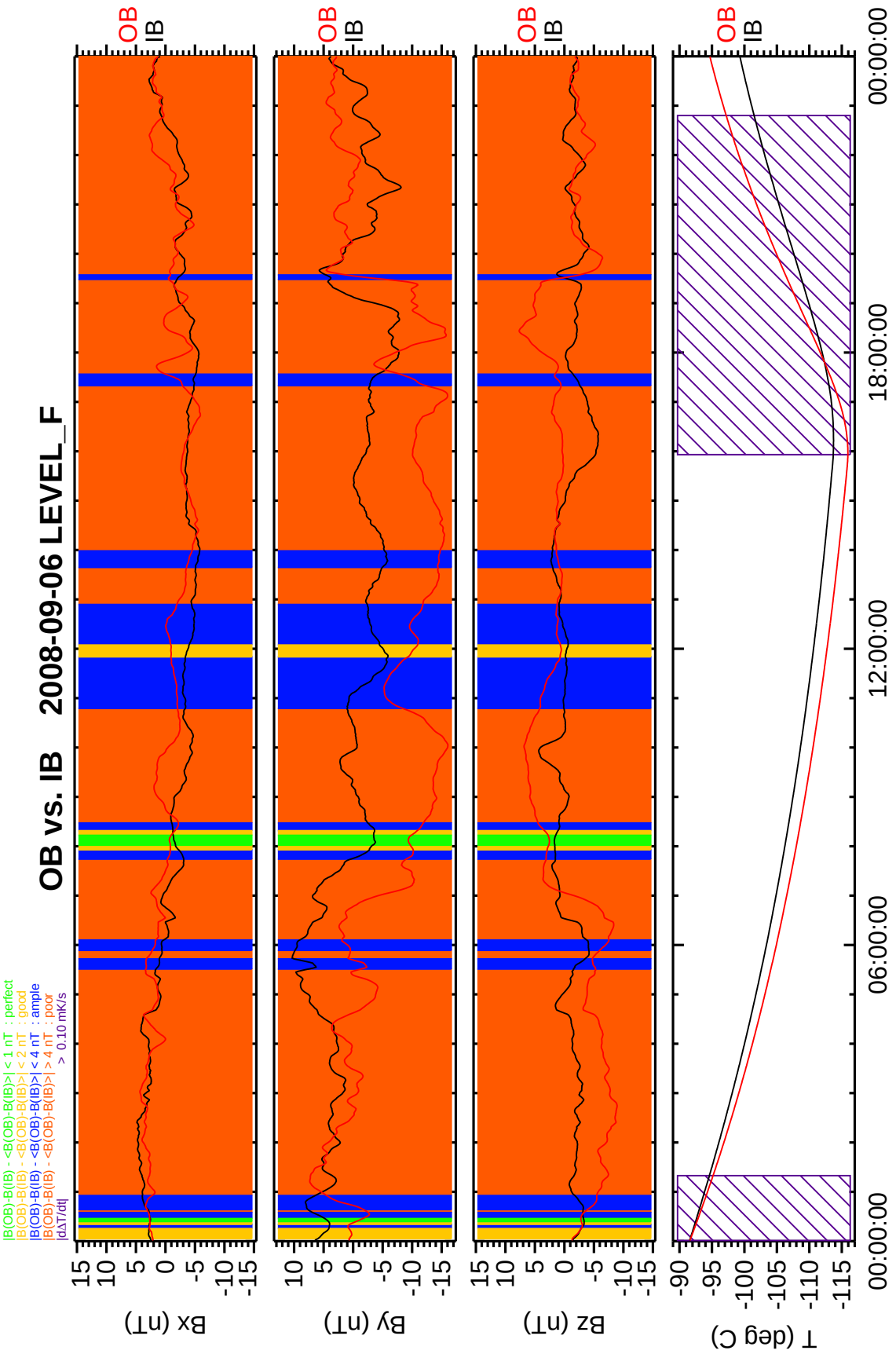
OB vs. IB 2008-09-06 LEVEL_F
|B(OB)-B(IB) - <B(OB)-B(IB)>| < 1 nT : perfect
|B(OB)-B(IB) - <B(OB)-B(IB)>| < 2 nT : good
|B(OB)-B(IB) - <B(OB)-B(IB)>| < 4 nT : ample
|B(OB)-B(IB) - <B(OB)-B(IB)>| > 4 nT : poor
|dΔT/dt| > 0.10 mK/s
OB
IB
Bx (nT)
By (nT)
Bz (nT)
T (deg C)
00:00:00
06:00:00
12:00:00
18:00:00
00:00:00

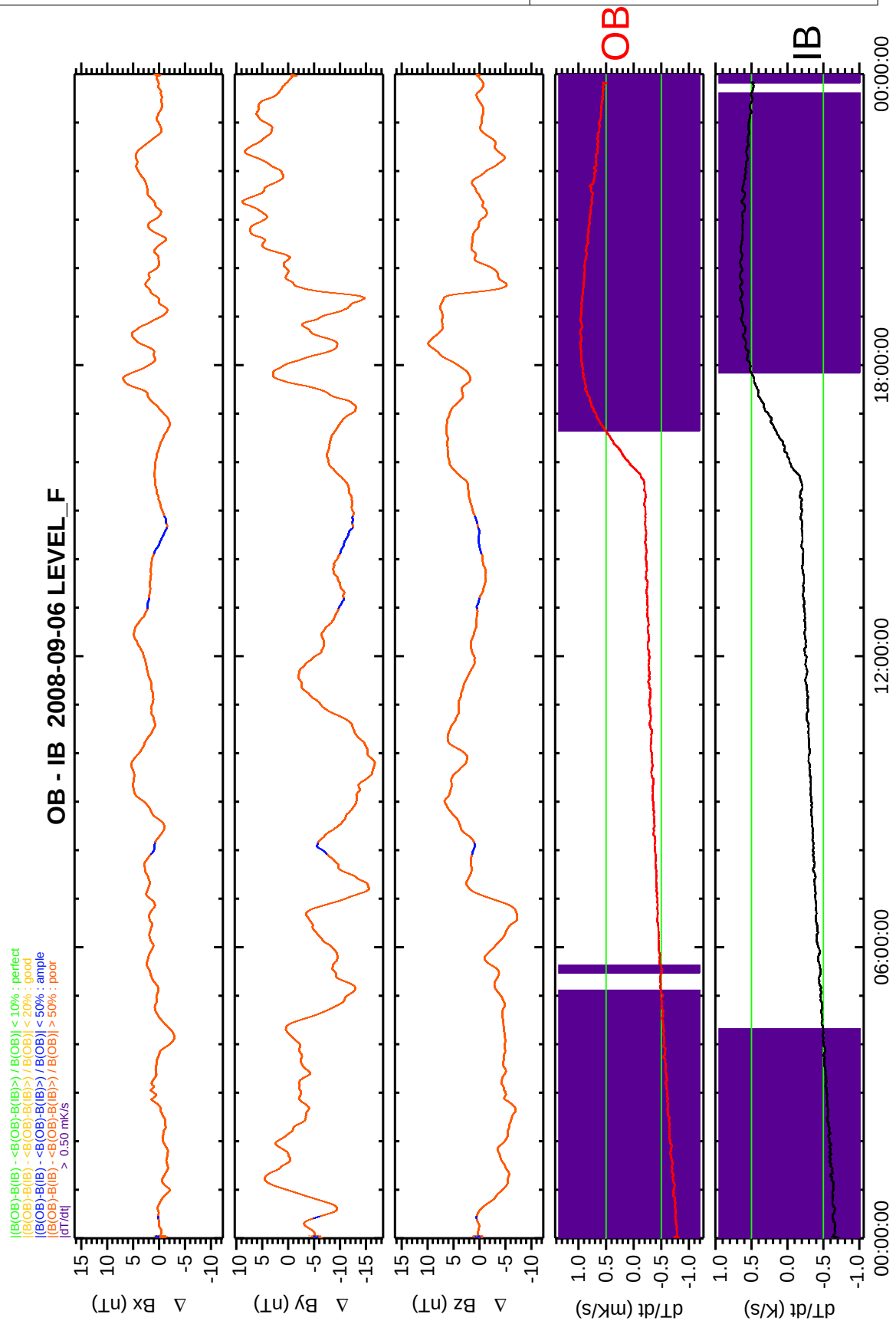
OB - IB 2008-09-06 LEVEL_F
OB
IB
Δ Bx (nT)
Δ By (nT)
Δ Bz (nT)
dT/dt (mK/s)
dT/dt (K/s)
00:00:00
06:00:00
12:00:00
18:00:00
00:00:00
|(B(OB)-B(IB) - <B(OB)-B(IB)>) / B(OB)| < 10% : perfect
|(B(OB)-B(IB) - <B(OB)-B(IB)>) / B(OB)| < 20% : good
|(B(OB)-B(IB) - <B(OB)-B(IB)>) / B(OB)| < 50% : ample
|(B(OB)-B(IB) - <B(OB)-B(IB)>) / B(OB)| > 50% : poor
|dT/dt| > 0.50 mK/s

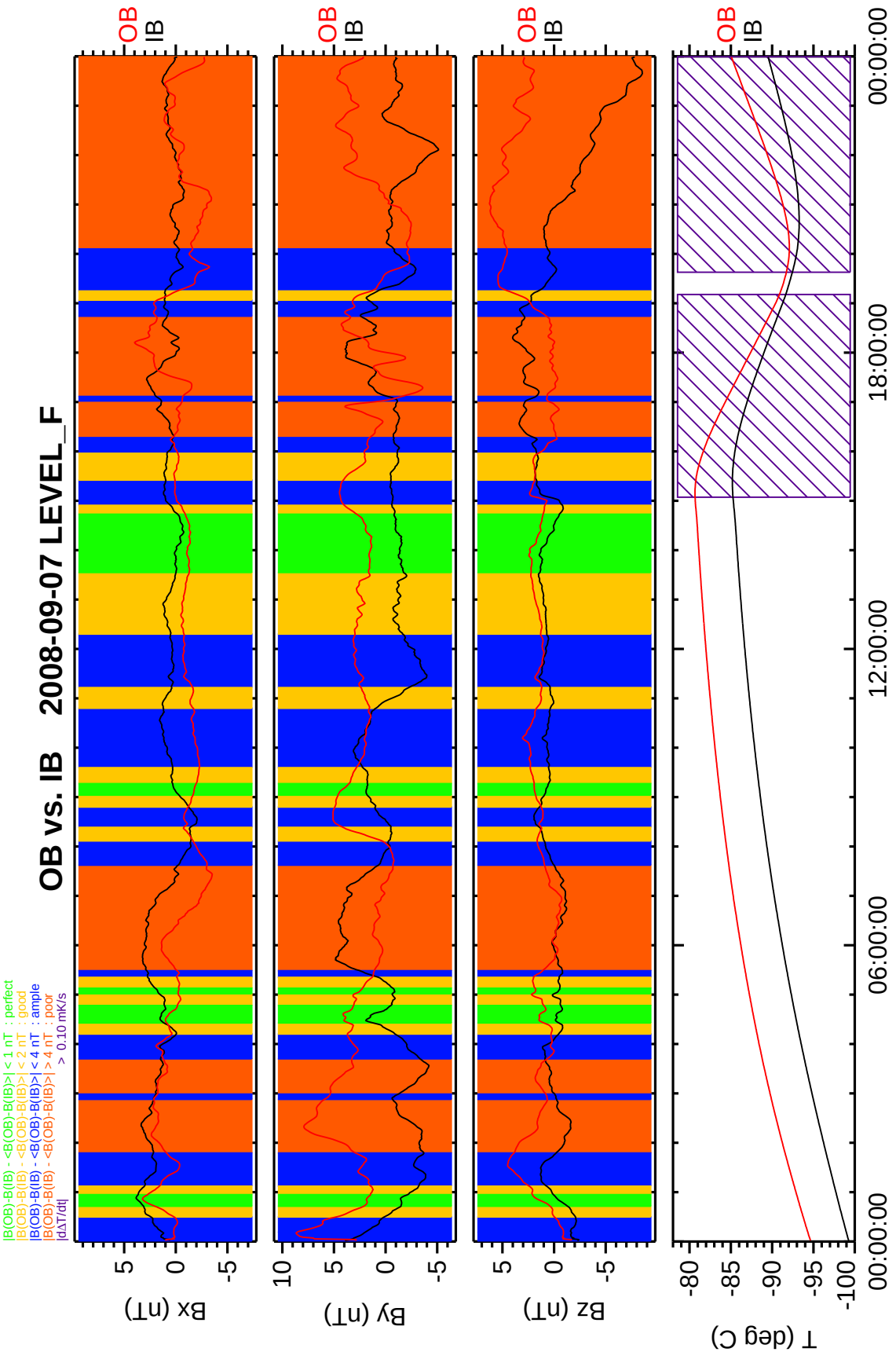
OB vs. IB 2008-09-07 LEVEL_F
|B(OB)-B(IB) - <B(OB)-B(IB)>| < 1 nT : perfect
|B(OB)-B(IB) - <B(OB)-B(IB)>| < 2 nT : good
|B(OB)-B(IB) - <B(OB)-B(IB)>| < 4 nT : ample
|B(OB)-B(IB) - <B(OB)-B(IB)>| > 4 nT : poor
|dΔT/dt| > 0.10 mK/s
OB
IB
Bx (nT)
By (nT)
Bz (nT)
T (deg C)
00:00:00
06:00:00
12:00:00
18:00:00
00:00:00

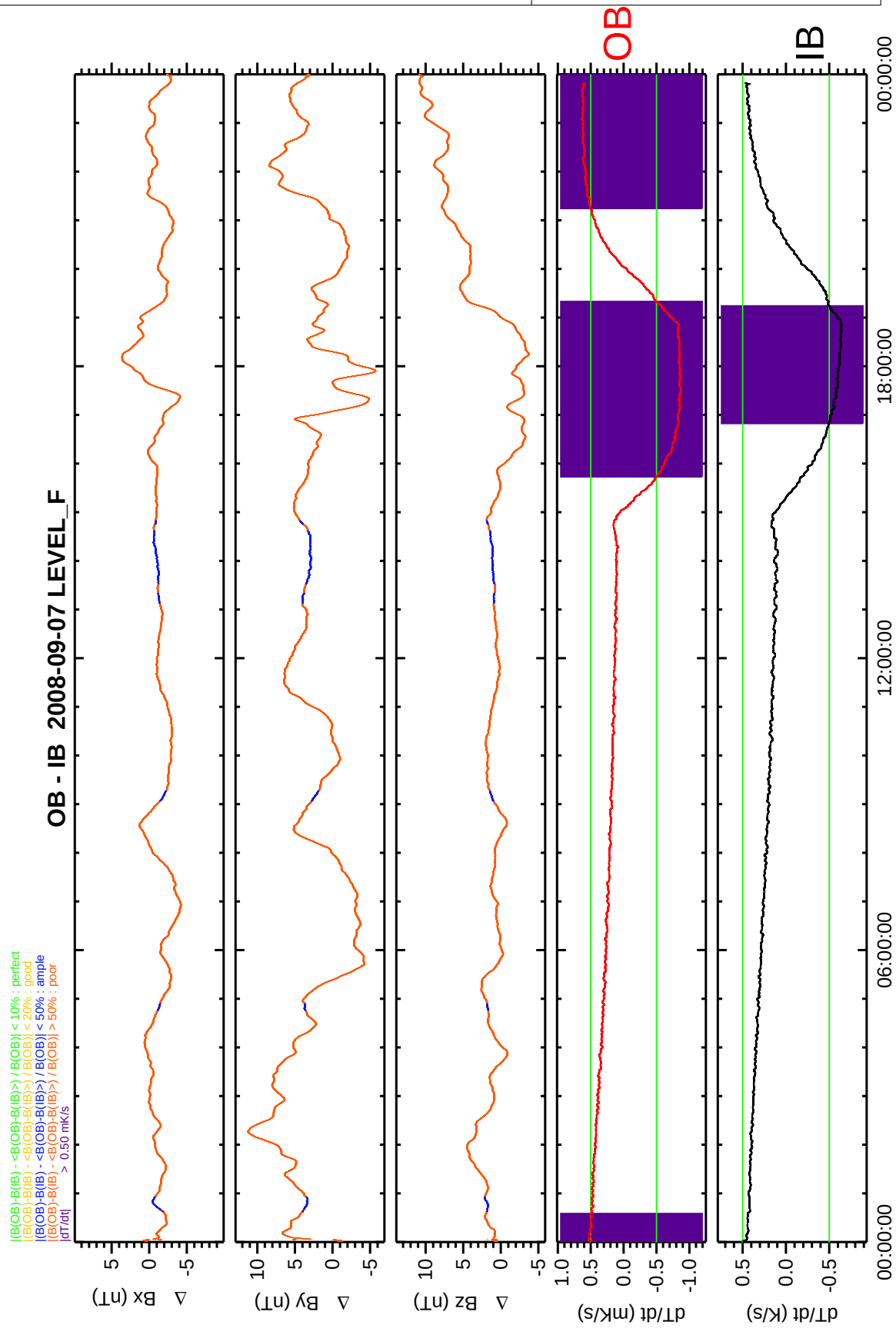
OB - IB 2008-09-07 LEVEL_F
OB
IB
Δ Bx (nT)
Δ By (nT)
Δ Bz (nT)
dT/dt (mK/s)
dT/dt (K/s)
00:00:00
06:00:00
12:00:00
18:00:00
00:00:00
|(B(OB)-B(IB) - <B(OB)-B(IB)>) / B(OB)| < 10% : perfect
|(B(OB)-B(IB) - <B(OB)-B(IB)>) / B(OB)| < 20% : good
|(B(OB)-B(IB) - <B(OB)-B(IB)>) / B(OB)| < 50% : ample
|(B(OB)-B(IB) - <B(OB)-B(IB)>) / B(OB)| > 50% : poor
|dT/dt| > 0.50 mK/s

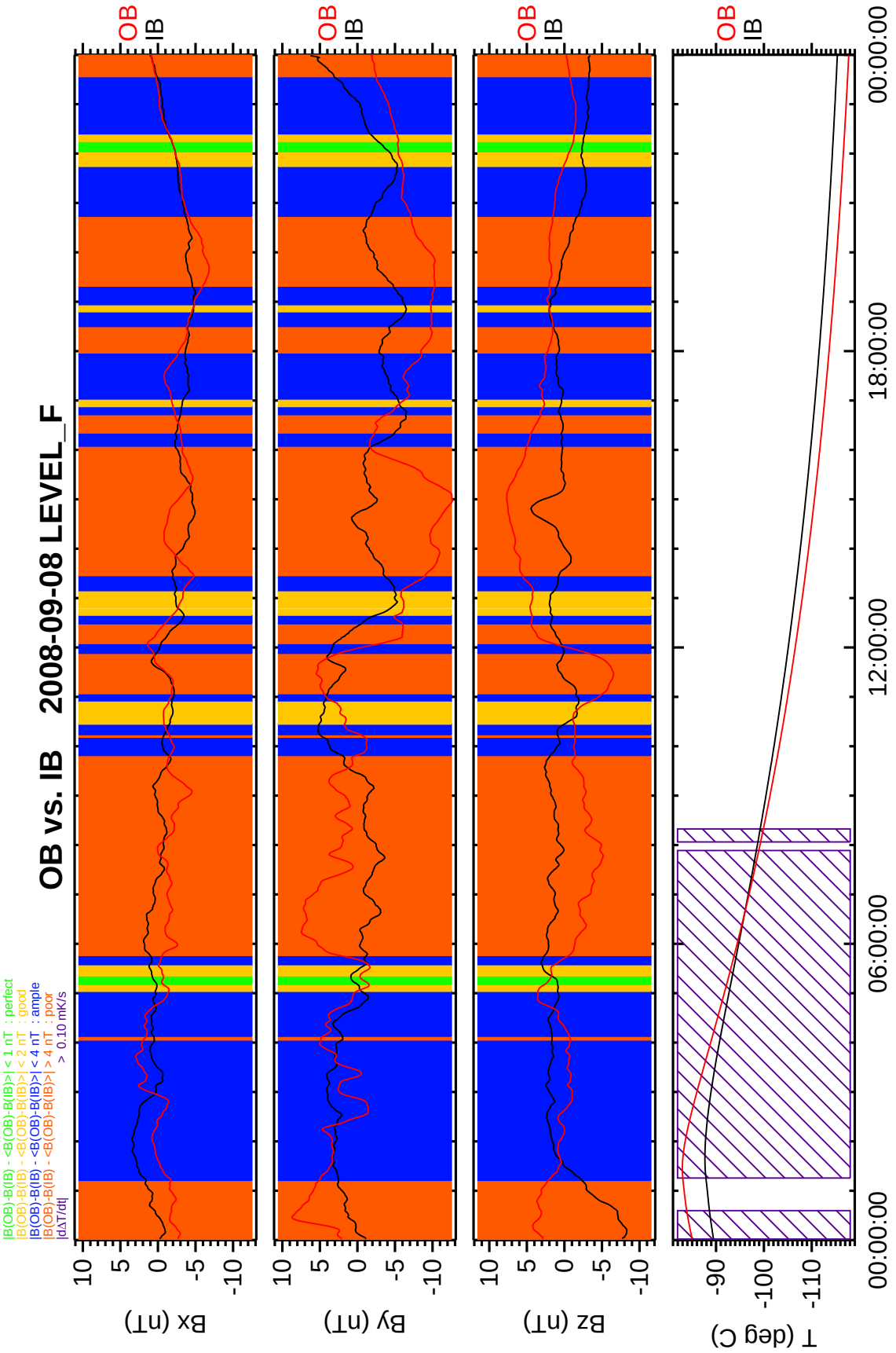
OB vs. IB 2008-09-08 LEVEL_F
|B(OB)-B(IB) - <B(OB)-B(IB)>| < 1 nT : perfect
|B(OB)-B(IB) - <B(OB)-B(IB)>| < 2 nT : good
|B(OB)-B(IB) - <B(OB)-B(IB)>| < 4 nT : ample
|B(OB)-B(IB) - <B(OB)-B(IB)>| > 4 nT : poor
|dΔT/dt| > 0.10 mK/s
OB
IB
Bx (nT)
By (nT)
Bz (nT)
T (deg C)
10
5
0
-5
-10
-90
-100
-110
00:00:00
06:00:00
12:00:00
18:00:00
00:00:00

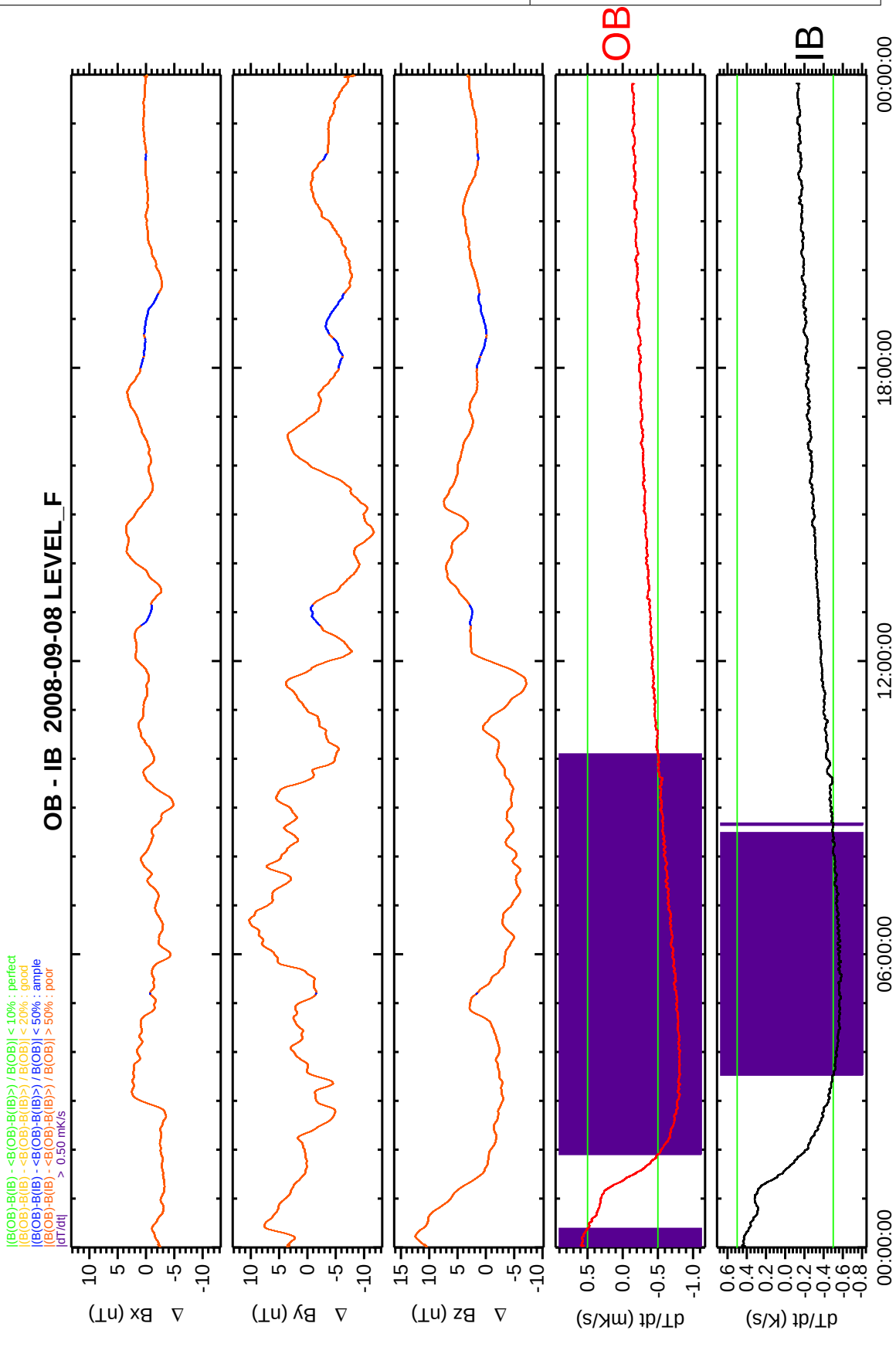
OB - IB 2008-09-08 LEVEL_F
OB
IB
Δ Bx (nT)
Δ By (nT)
Δ Bz (nT)
dT/dt (mK/s)
dT/dt (K/s)
00:00:00
06:00:00
12:00:00
18:00:00
00:00:00
|(B(OB)-B(IB) - <B(OB)-B(IB)>) / B(OB)| < 10% : perfect
|(B(OB)-B(IB) - <B(OB)-B(IB)>) / B(OB)| < 20% : good
|(B(OB)-B(IB) - <B(OB)-B(IB)>) / B(OB)| < 50% : ample
|(B(OB)-B(IB) - <B(OB)-B(IB)>) / B(OB)| > 50% : poor
|dT/dt| > 0.50 mK/s

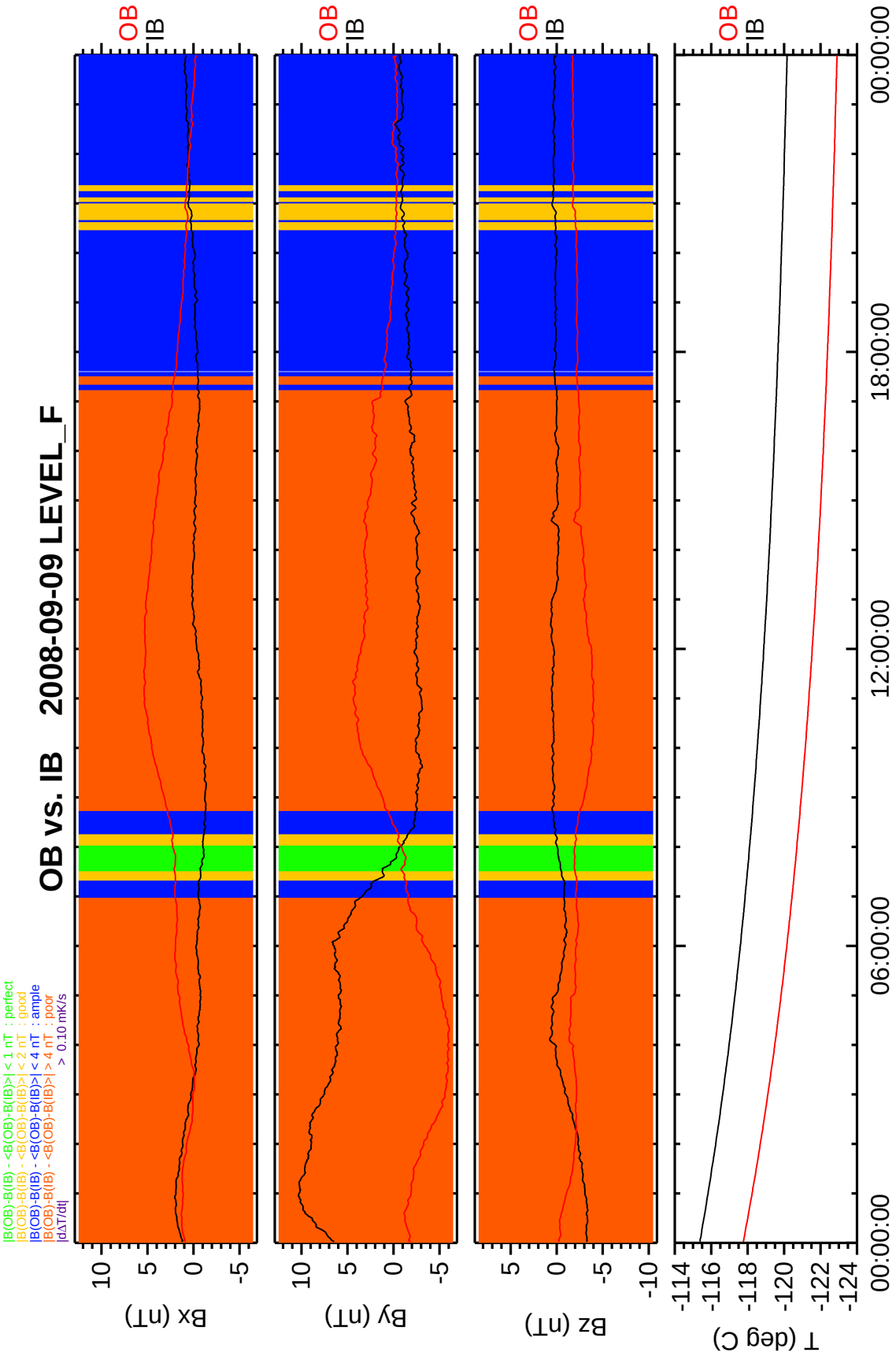
OB vs. IB 2008-09-09 LEVEL_F
|B(OB)-B(IB) - <B(OB)-B(IB)>| < 1 nT : perfect
|B(OB)-B(IB) - <B(OB)-B(IB)>| < 2 nT : good
|B(OB)-B(IB) - <B(OB)-B(IB)>| < 4 nT : ample
|B(OB)-B(IB) - <B(OB)-B(IB)>| > 4 nT : poor
|dΔT/dt| > 0.10 mK/s
OB
IB
Bx (nT)
By (nT)
Bz (nT)
T (deg C)
00:00:00
06:00:00
12:00:00
18:00:00
00:00:00

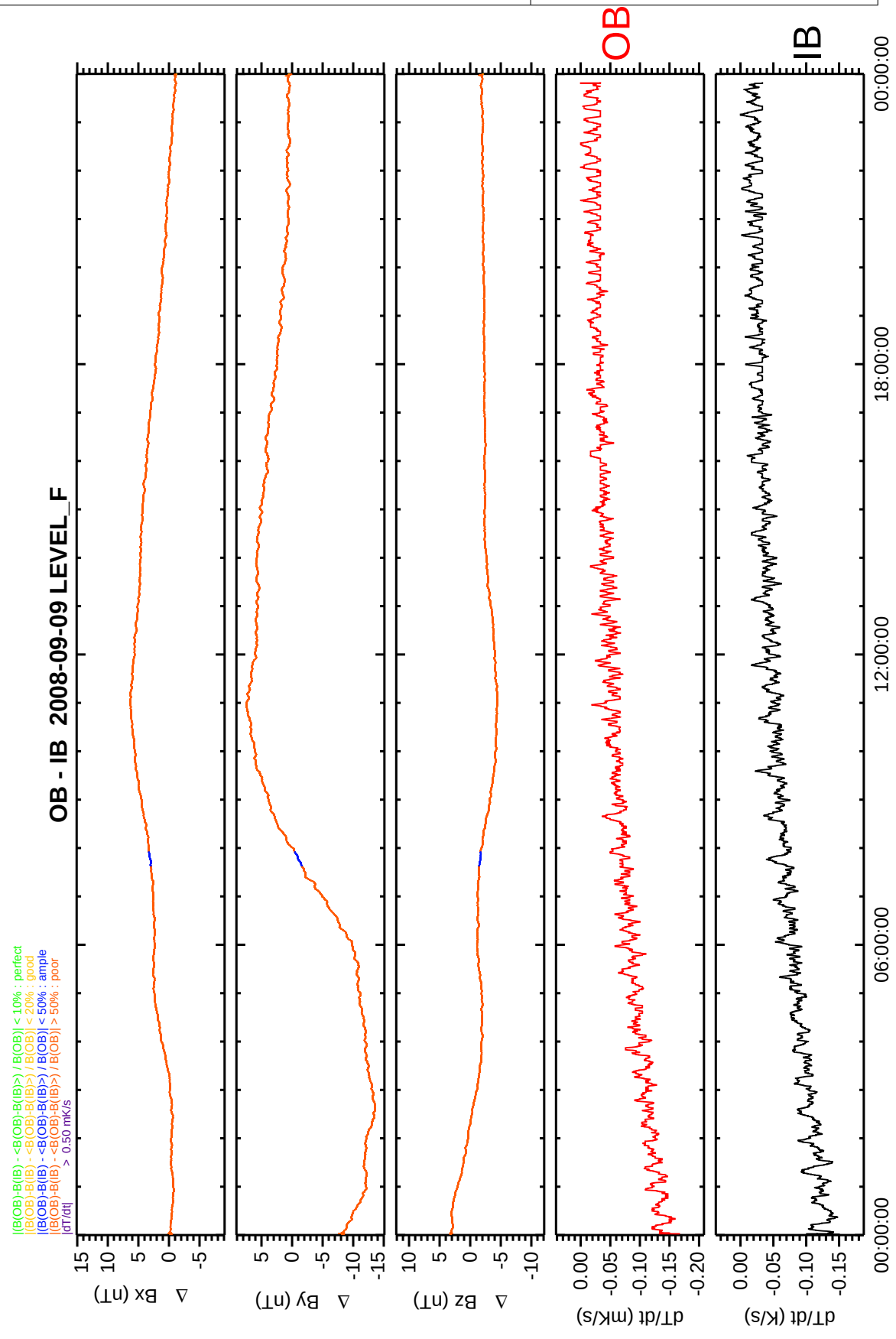
OB - IB 2008-09-09 LEVEL_F
OB
IB
Δ Bx (nT)
Δ By (nT)
Δ Bz (nT)
dT/dt (mK/s)
dT/dt (K/s)
00:00:00
06:00:00
12:00:00
18:00:00
00:00:00
|(B(OB)-B(IB) - <B(OB)-B(IB)>) / B(OB)| < 10% : perfect
|(B(OB)-B(IB) - <B(OB)-B(IB)>) / B(OB)| < 20% : good
|(B(OB)-B(IB) - <B(OB)-B(IB)>) / B(OB)| < 50% : ample
|(B(OB)-B(IB) - <B(OB)-B(IB)>) / B(OB)| > 50% : poor
|dT/dt| > 0.50 mK/s

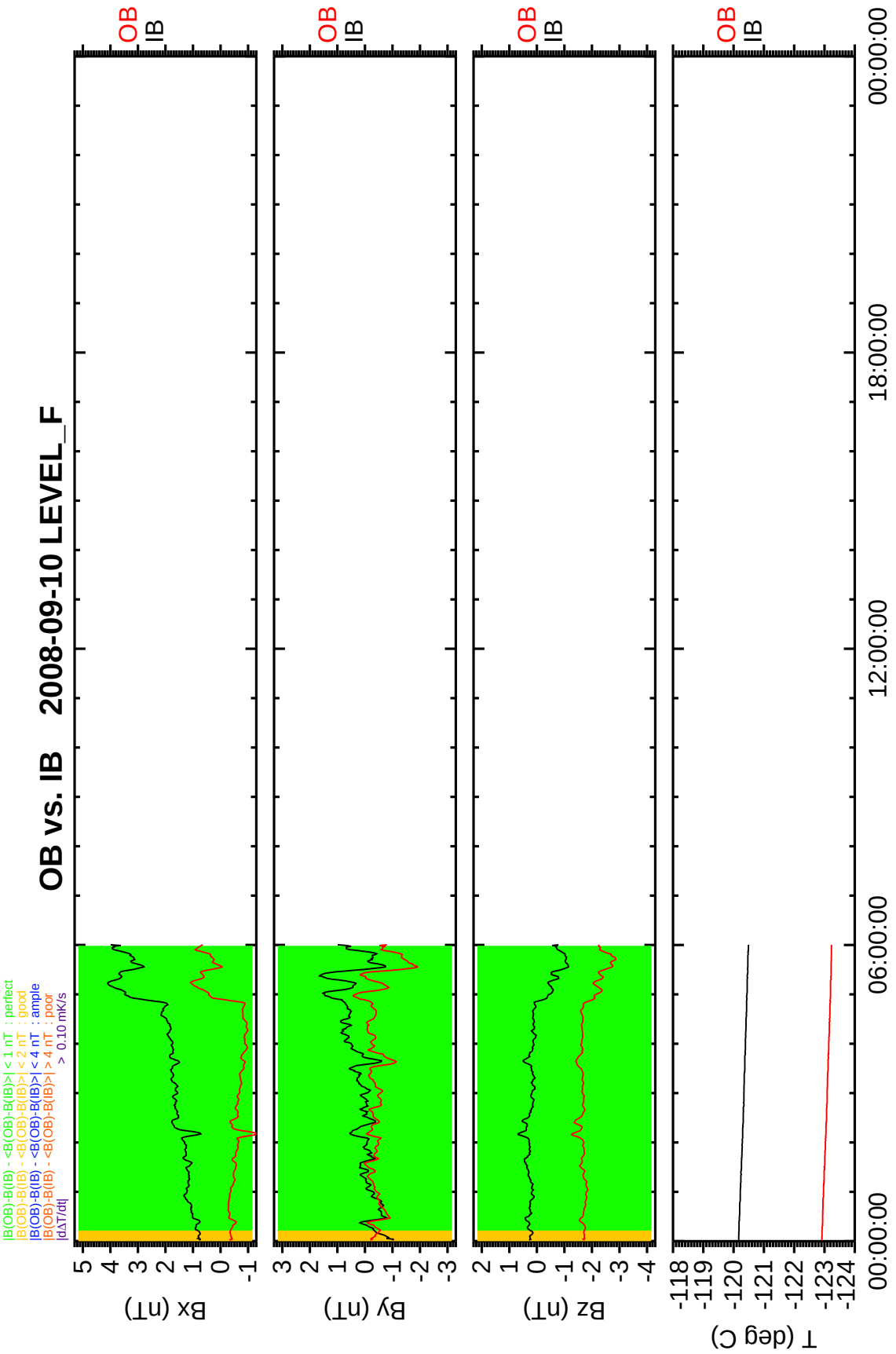
OB vs. IB 2008-09-10 LEVEL_F
|B(OB)-B(IB) - <B(OB)-B(IB)>| < 1 nT : perfect
|B(OB)-B(IB) - <B(OB)-B(IB)>| < 2 nT : good
|B(OB)-B(IB) - <B(OB)-B(IB)>| < 4 nT : ample
|B(OB)-B(IB) - <B(OB)-B(IB)>| > 4 nT : poor
|dΔT/dt| > 0.10 mK/s
OB
IB
Bx (nT)
By (nT)
Bz (nT)
T (deg C)
00:00:00
06:00:00
12:00:00
18:00:00
00:00:00

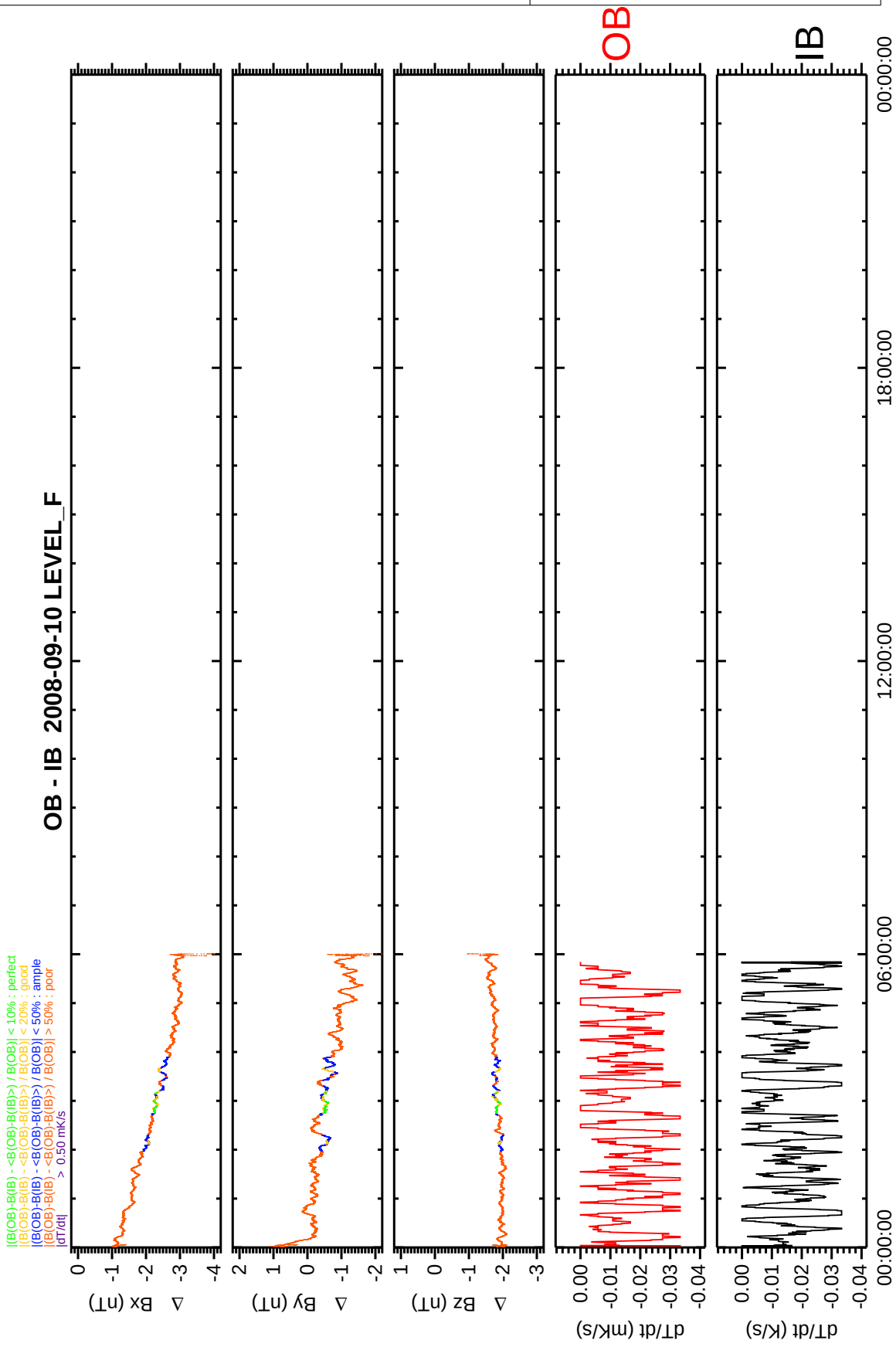
OB - IB 2008-09-10 LEVEL_F
OB
IB
Δ Bx (nT)
Δ By (nT)
Δ Bz (nT)
dT/dt (mK/s)
dT/dt (K/s)
00:00:00
06:00:00
12:00:00
18:00:00
00:00:00
|(B(OB)-B(IB) - <B(OB)-B(IB)>) / B(OB)| < 10% : perfect
|(B(OB)-B(IB) - <B(OB)-B(IB)>) / B(OB)| < 20% : good
|(B(OB)-B(IB) - <B(OB)-B(IB)>) / B(OB)| < 50% : ample
|(B(OB)-B(IB) - <B(OB)-B(IB)>) / B(OB)| > 50% : poor
|dT/dt| > 0.50 mK/s

5 Dynamic Spectra of the Fly-By

This section shows the dynamic spectra of the OB sensor in LEVEL_C = ECLIPJ2000 coordinates. As the sensor was operated as primary sensor in NORMAL mode, SID2, for most of the time the maximum resolvable frequency is 0.5 Hz. Around the closest approach time (2008-09-05T18:38:19) RPCMAG was set to Burstmode (20 Hz sampling rate) starting at 2008-09-05T04:38 and ending at 2008-09-06T06:38.

The spectra show significant structures from 2008-09-05T12:00 until 2008-09-06T20:00. These disturbances are caused by the MUPUS heaters.

All the tilted lines in the spectra are caused by the Reaction wheels as usual. The 3.2 Hz lines is most likely caused by the LAP instrument.

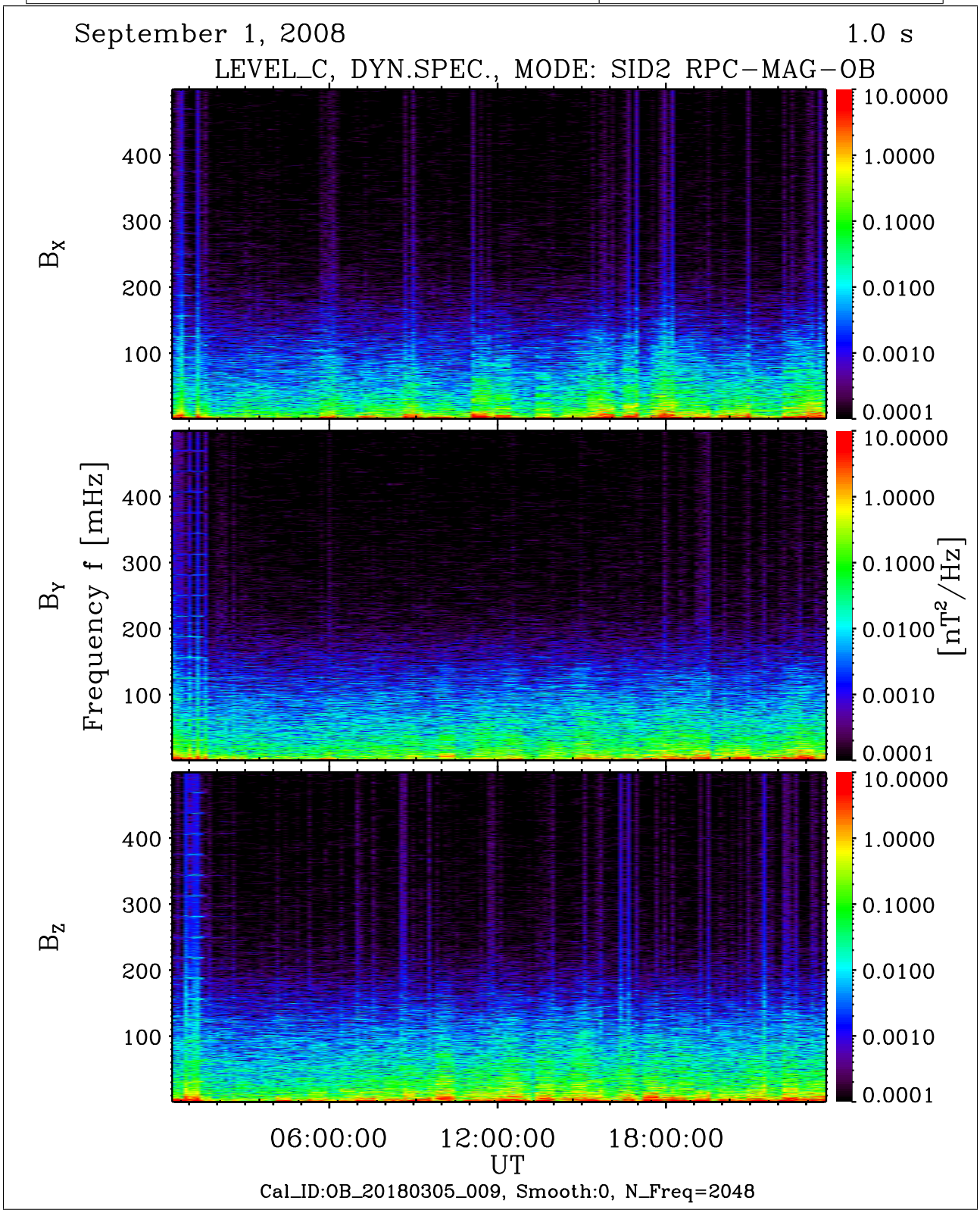

Figure 61: File: RPCMAG080901T0010_CLC_OB_M2_DS0_500_009

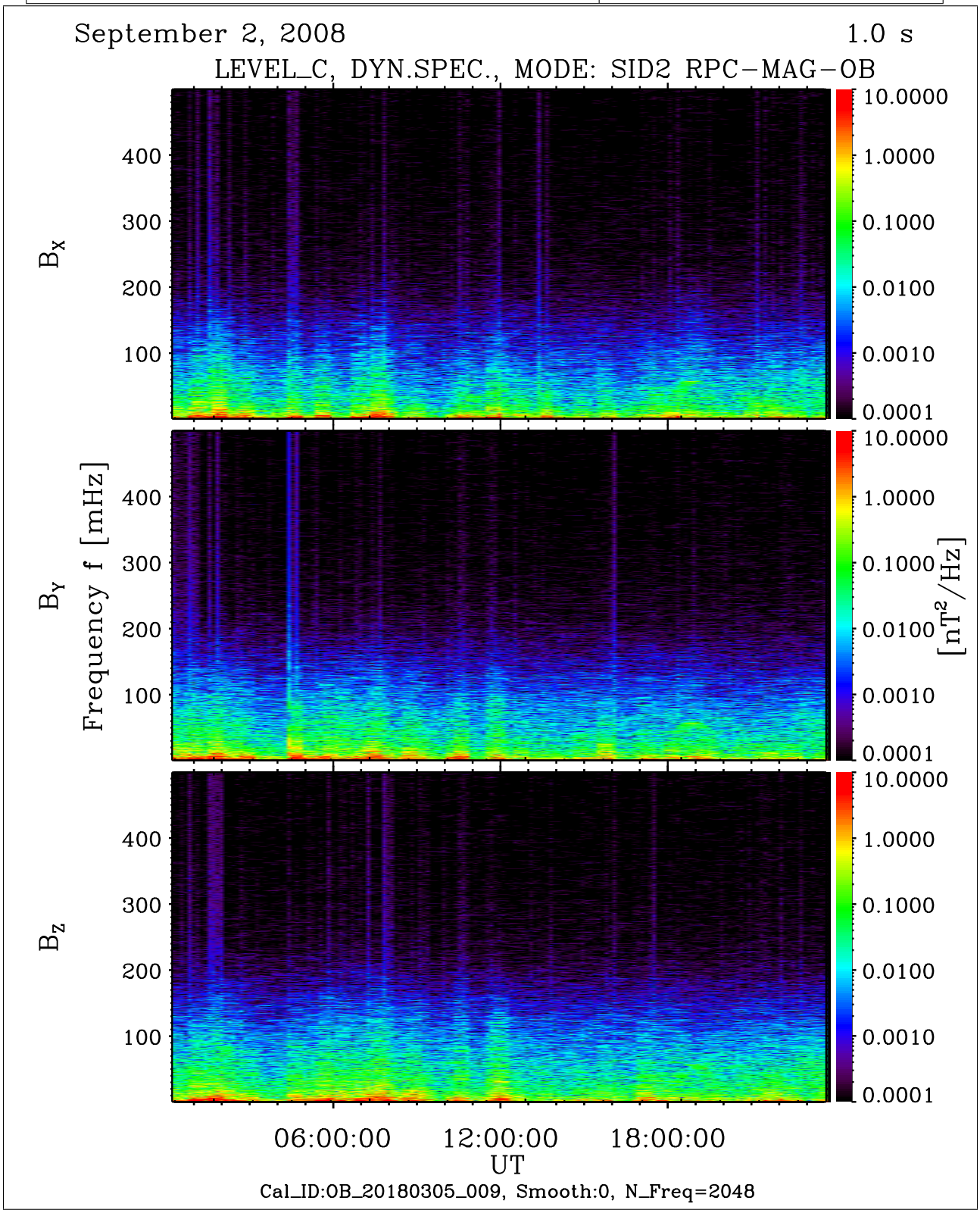

Figure 62: File: RPCMAG080902T0000_CLC_OB_M2_DS0_500_009

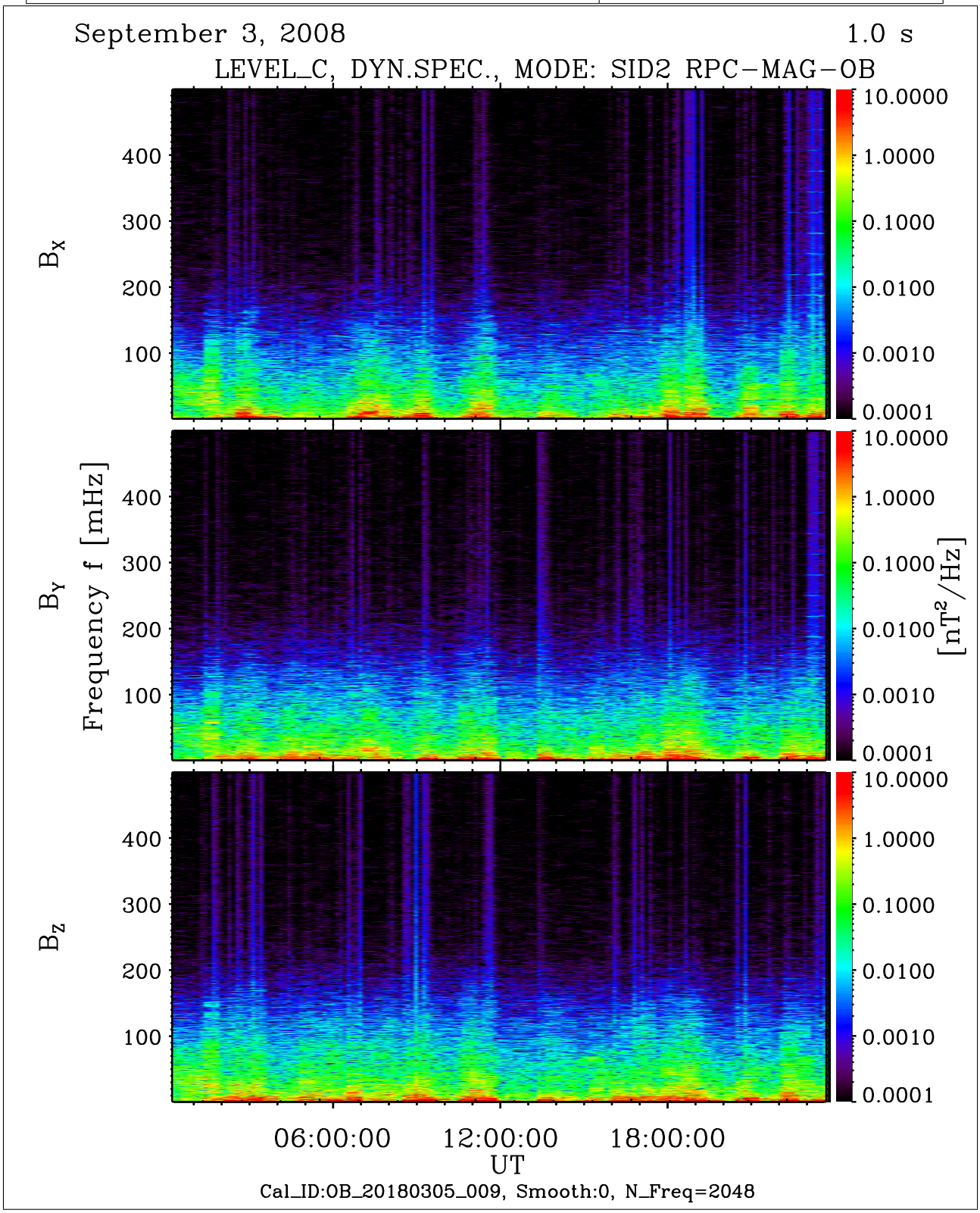

Figure 63: File: RPCMAG080903T0000_CLC_OB_M2_DS0_500_009

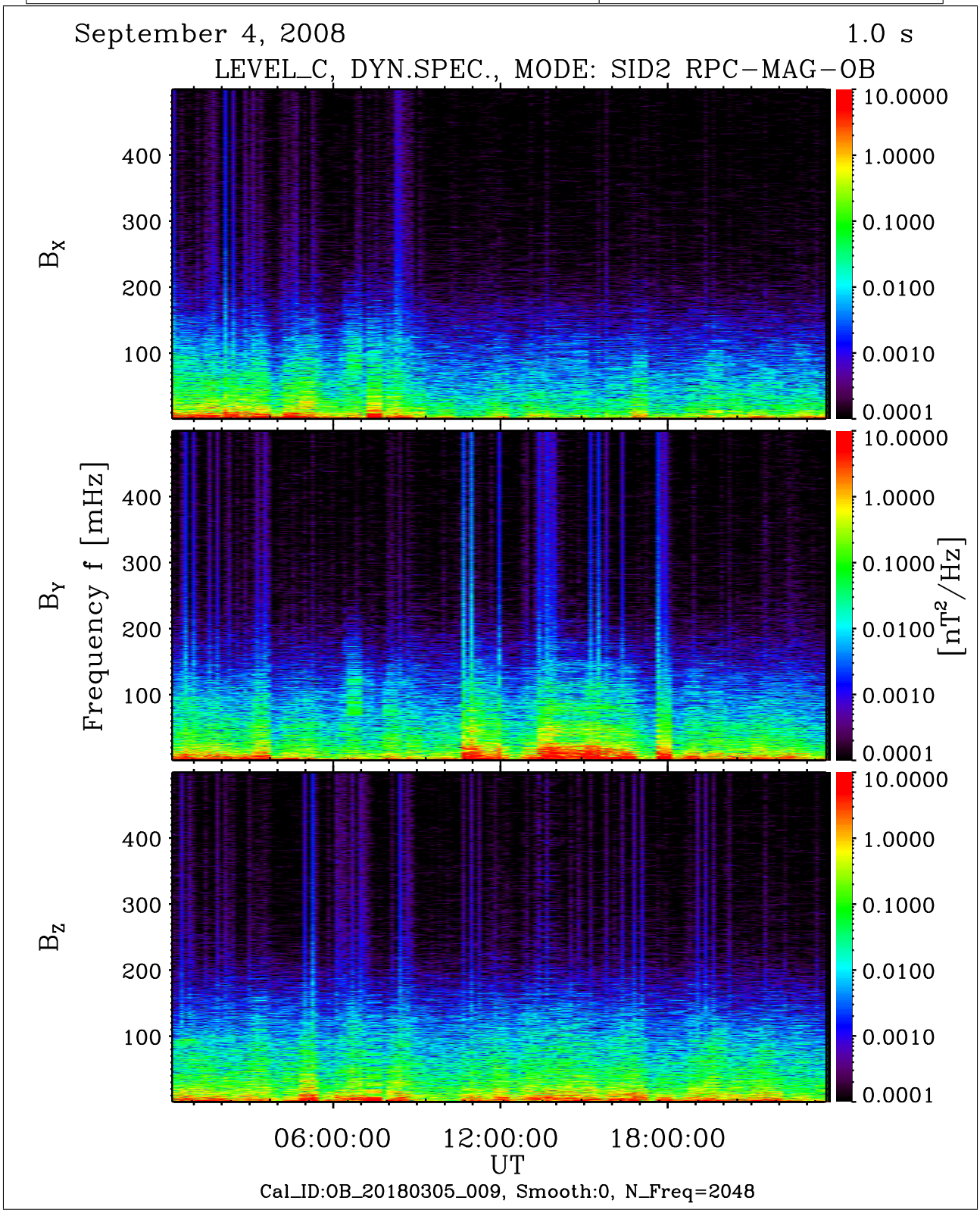

Figure 64: File: RPCMAG080904T0000_CLC_OB_M2_DS0_500_009

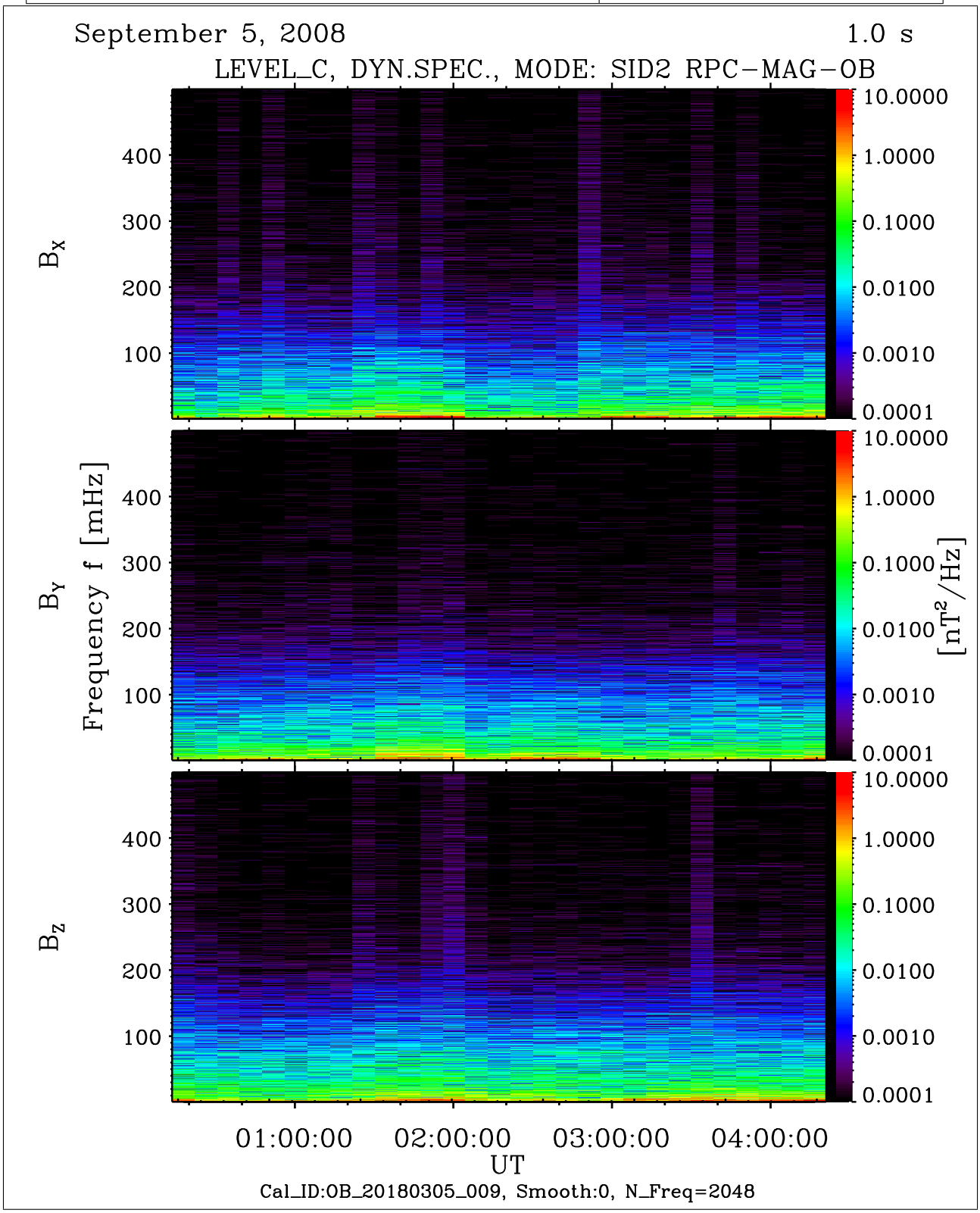

Figure 65: File: RPCMAG080905T0000_CLC_OB_M2_DS0_500_009

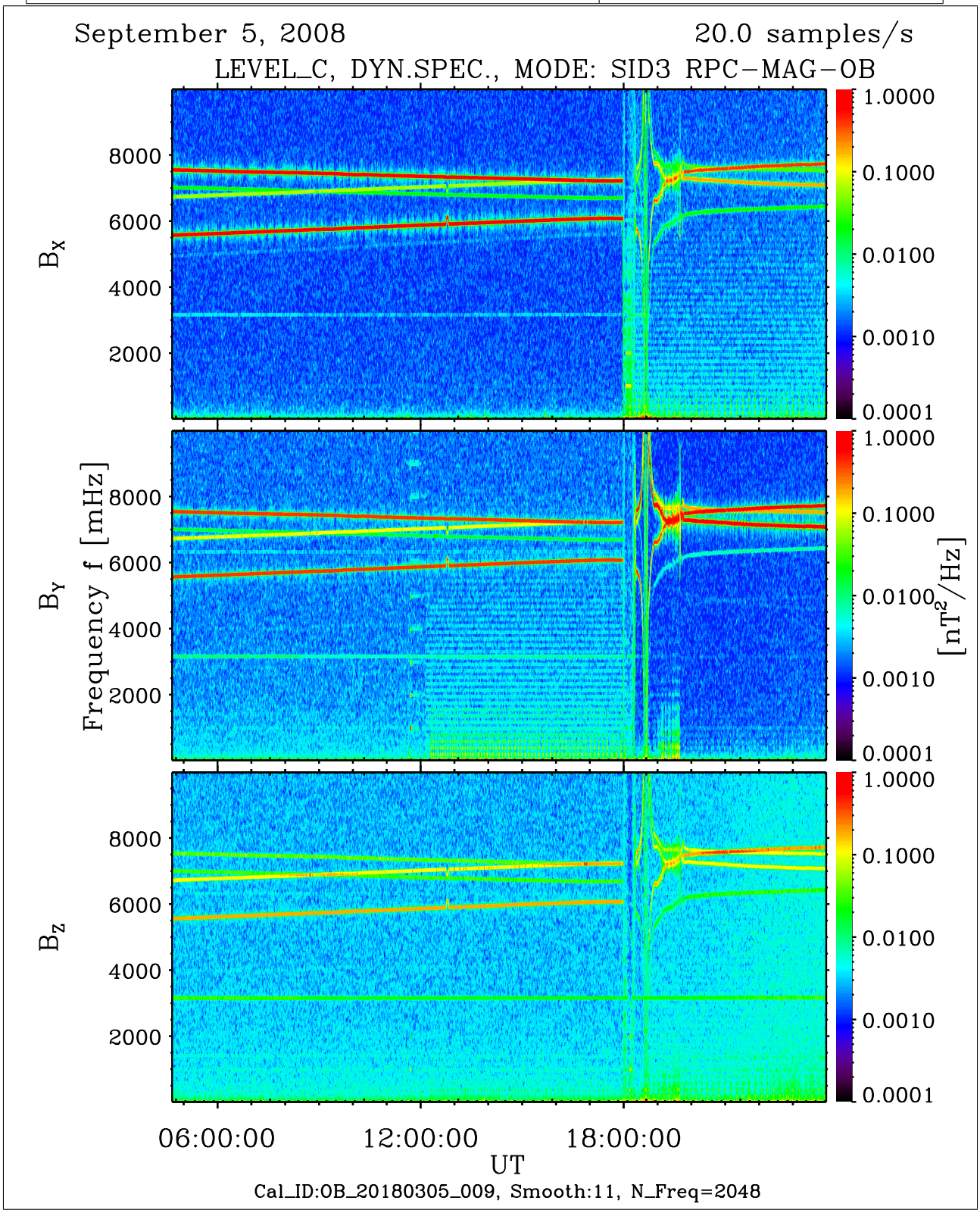

Figure 66: File: RPCMAG080905T0438_CLC_OB_M3_DS0_10000_009

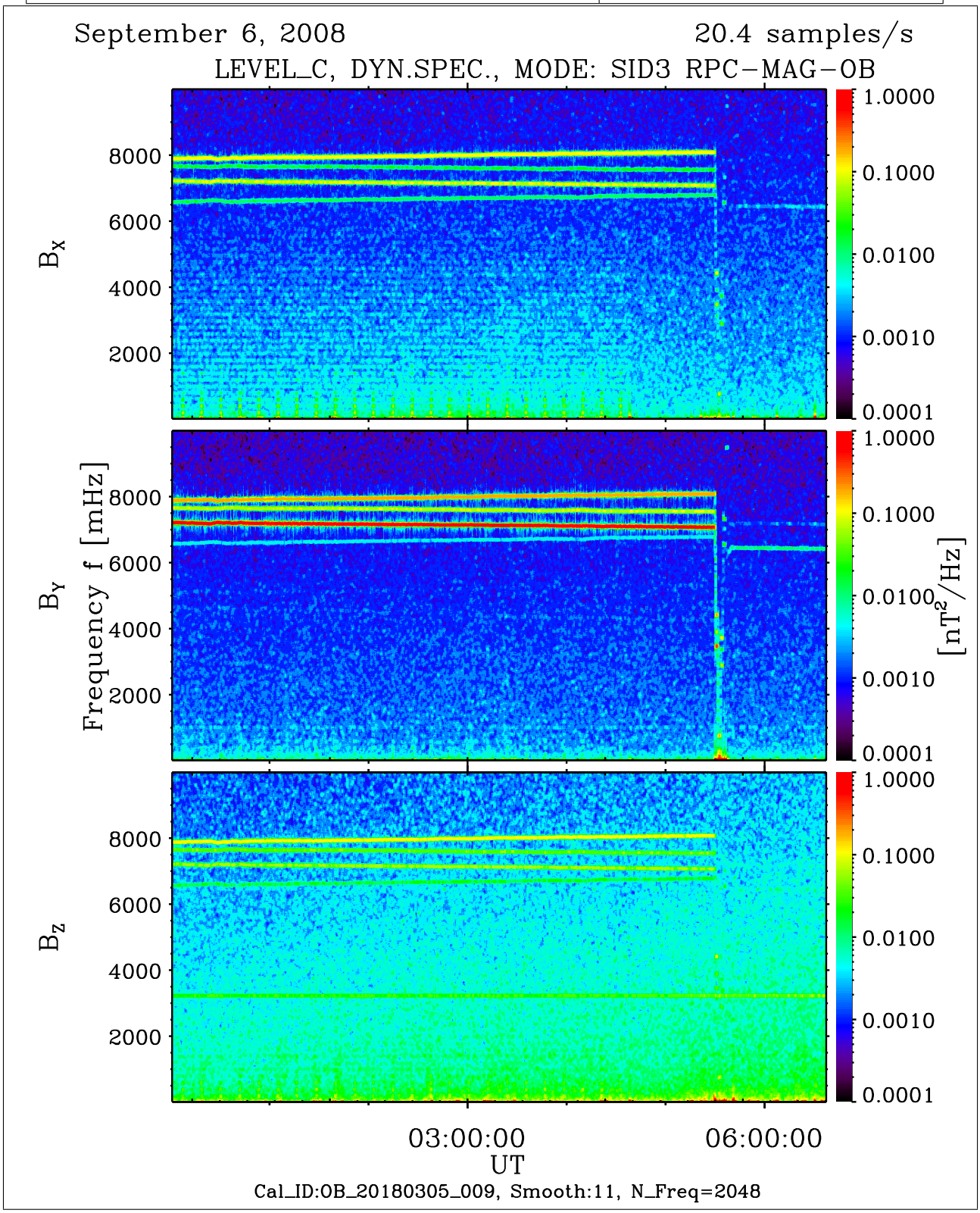

Figure 67: File: RPCMAG080906T0000_CLC_OB_M3_DS0_10000_009

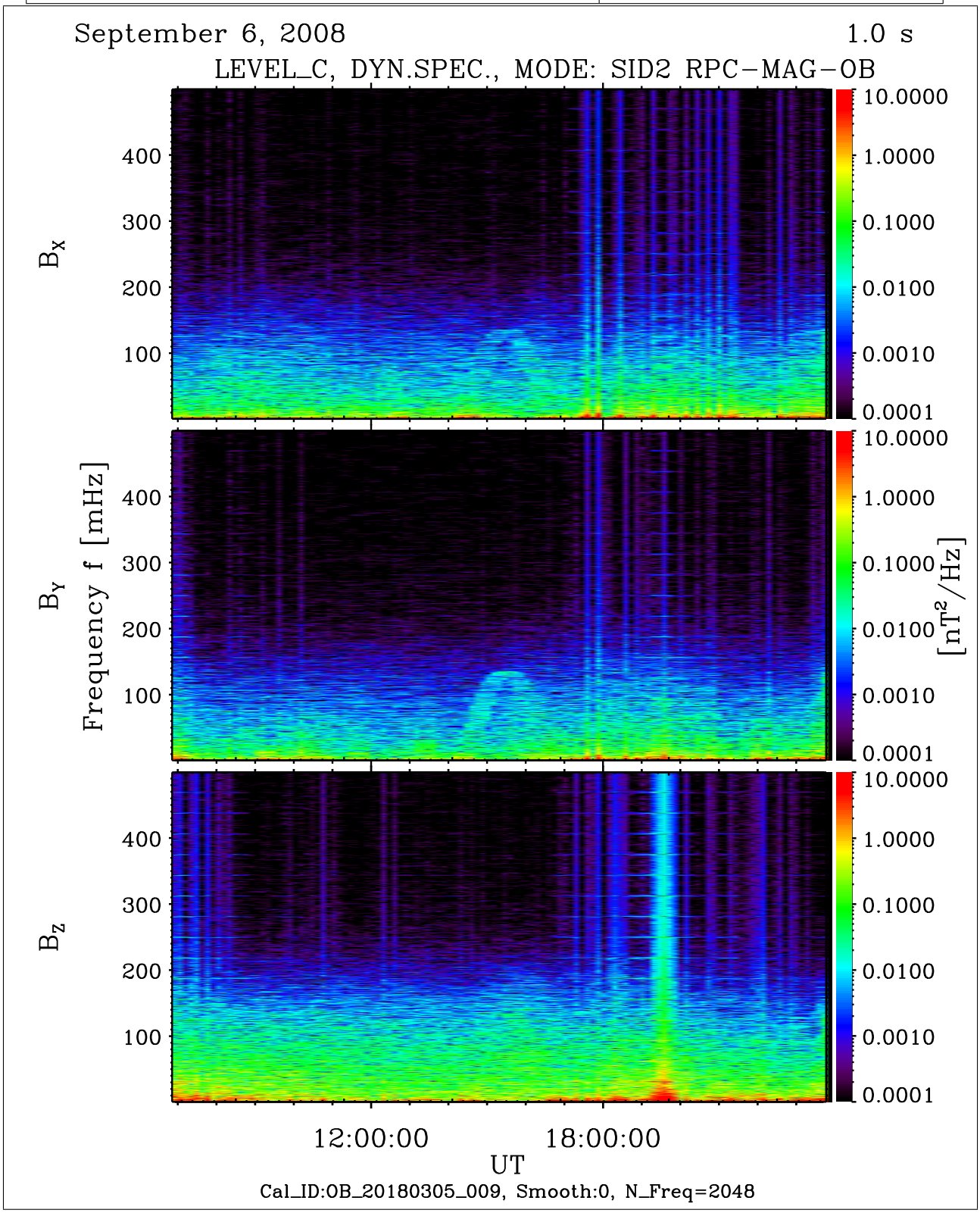

Figure 68: File: RPCMAG080906T0638_CLC_OB_M2_DS0_500_009

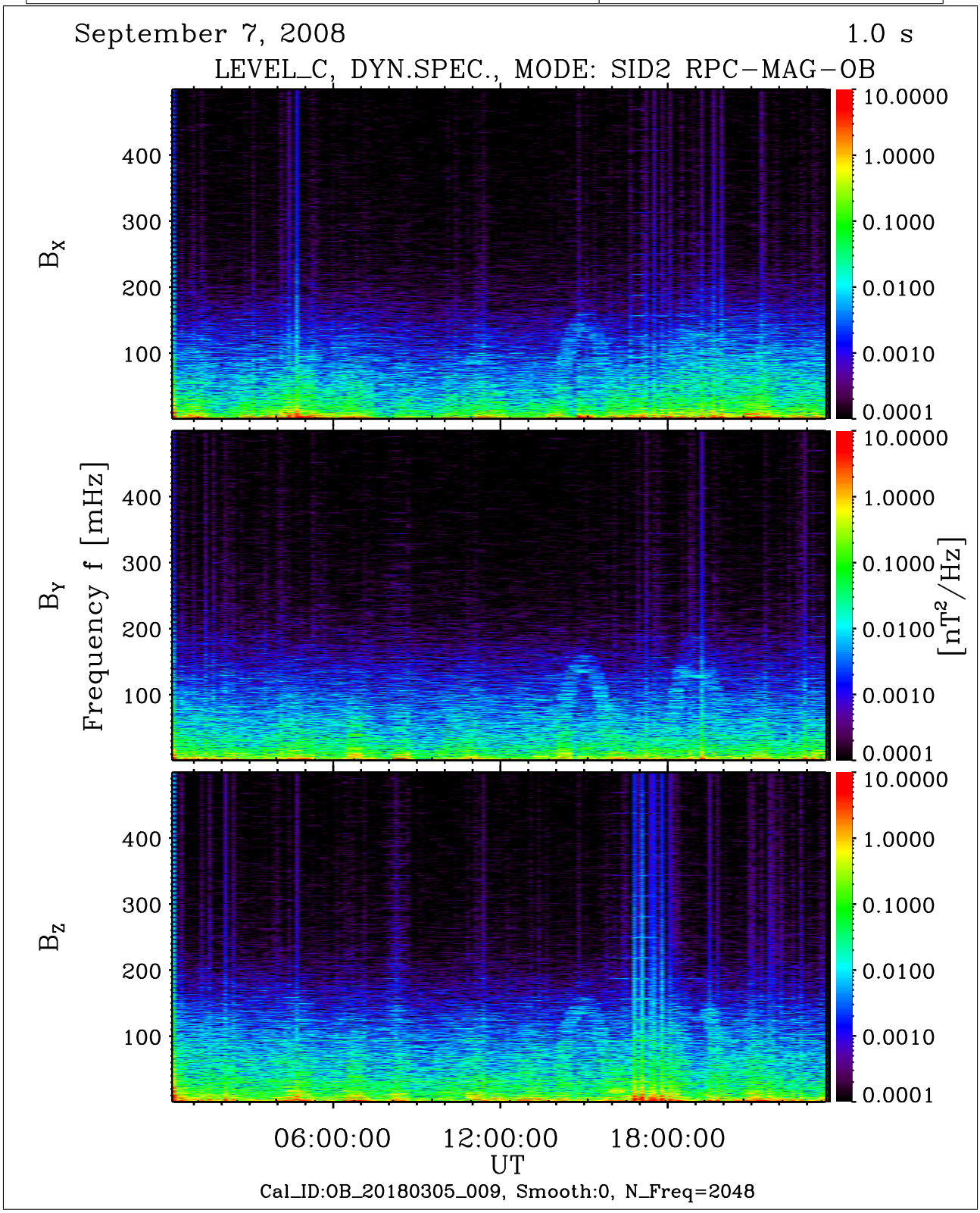

Figure 69: File: RPCMAG080907T0000_CLC_OB_M2_DS0_500_009

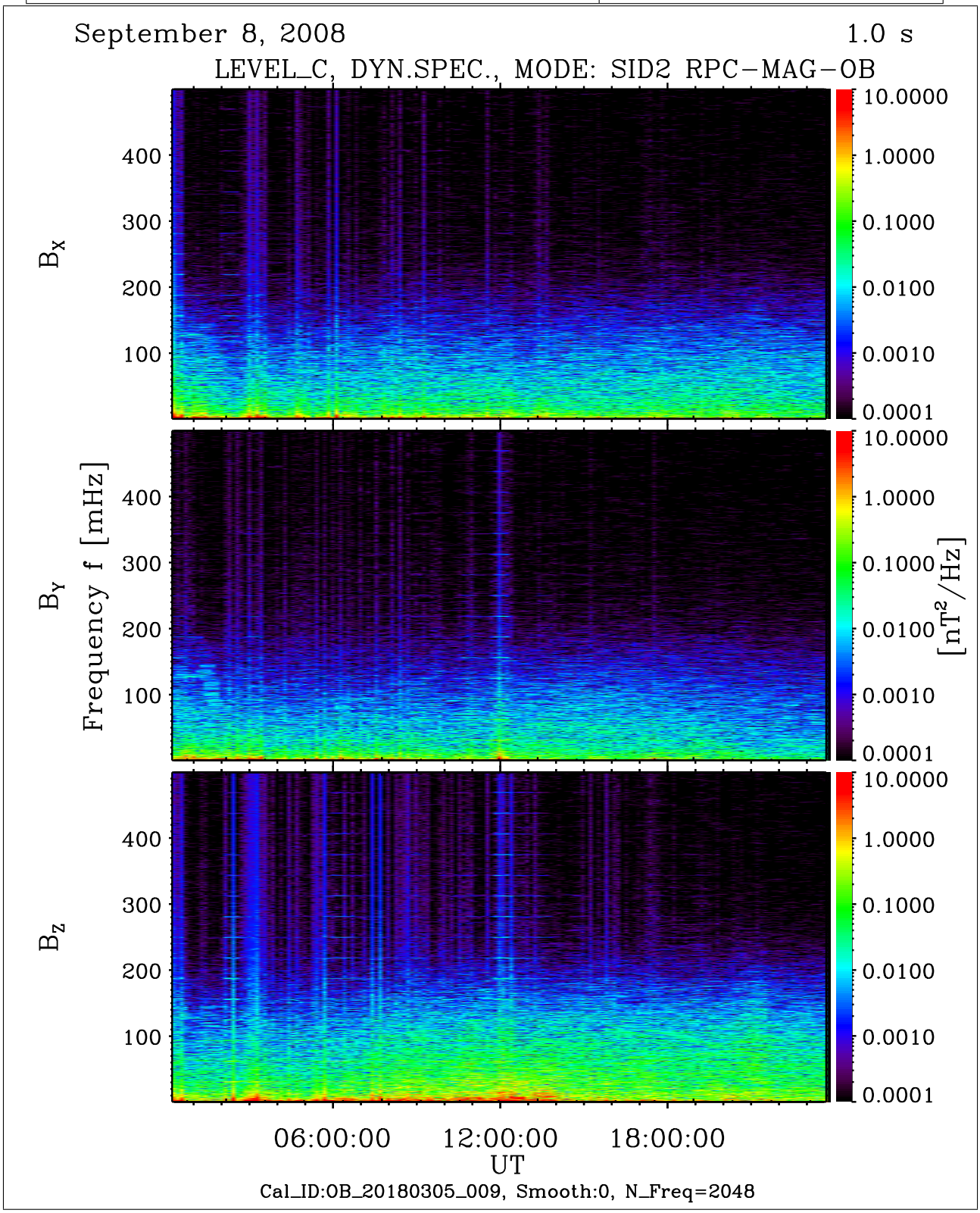

Figure 70: File: RPCMAG080908T0000_CLC_OB_M2_DS0_500_009

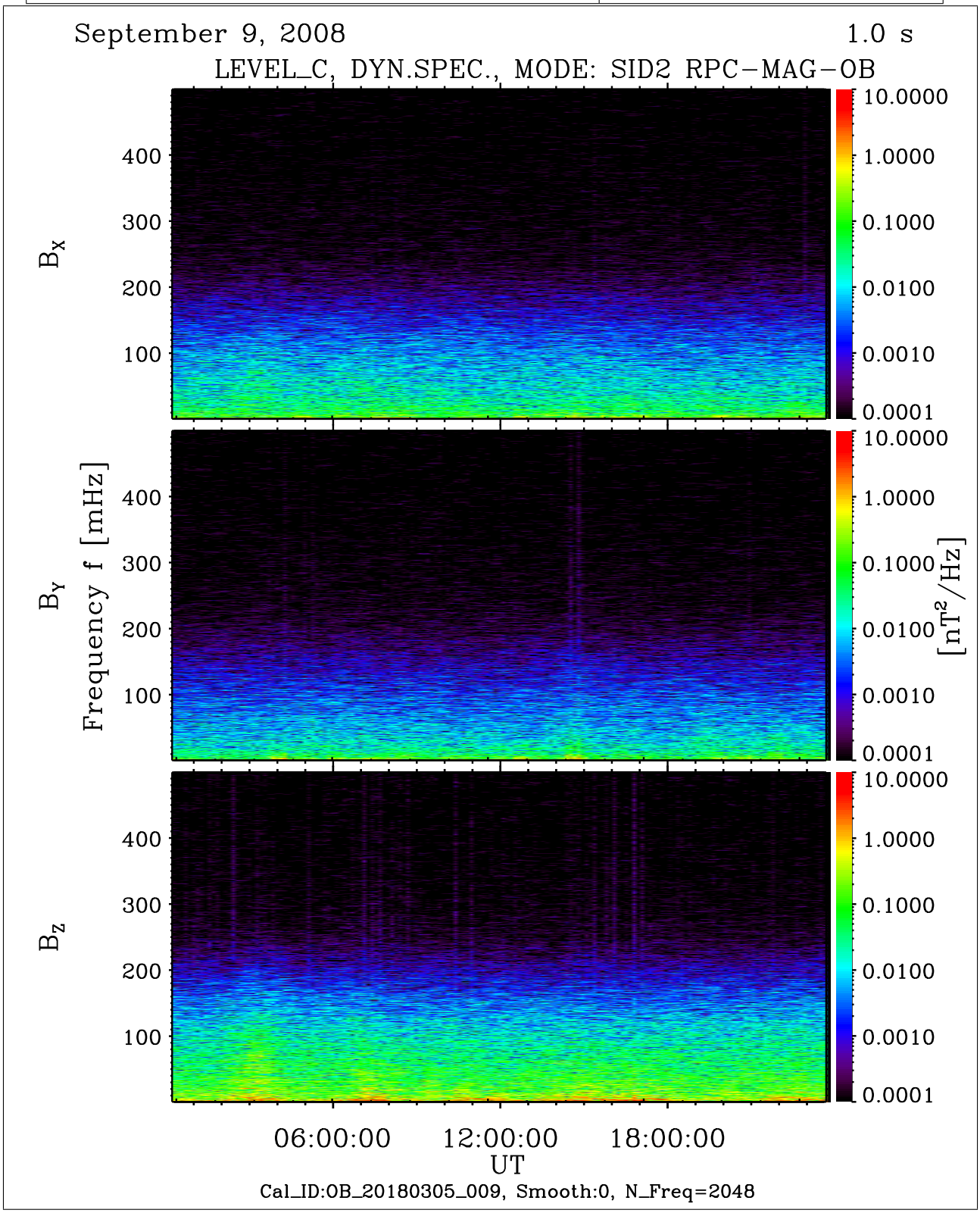

Figure 71: File: RPCMAG080909T0000_CLC_OB_M2_DS0_500_009

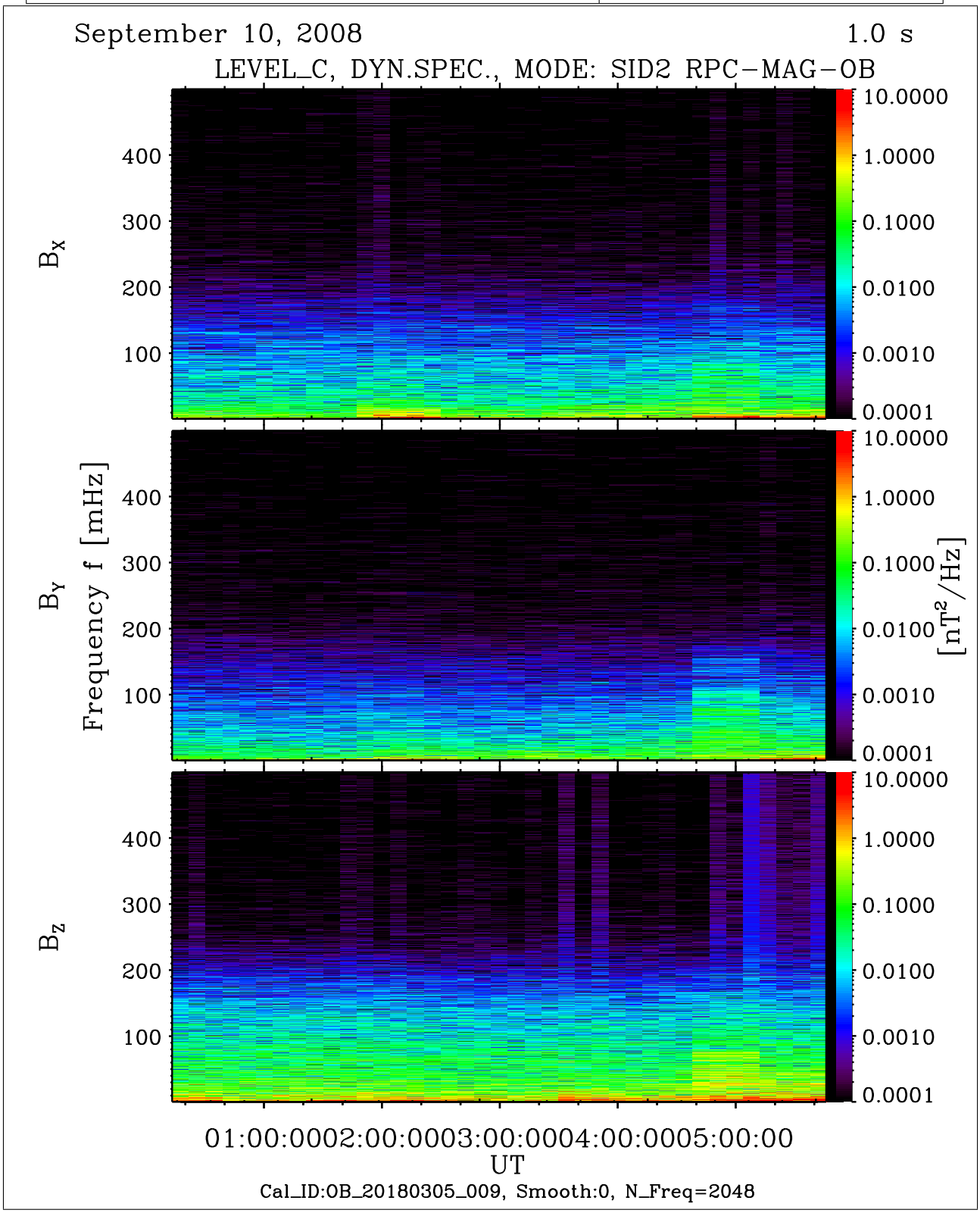

Figure 72: File: RPCMAG080910T0000_CLC_OB_M2_DS0_500_009

6 Dynamic Spectra of ROSETTAs REACTION WHEELS

This section shows the spectra of ROSETTAs Reaction Wheels (RW). There are 4 different wheels rotating with different frequencies. The plots do not show the original rotation frequencies but the signatures that would be expected using an data acquisition system operating at 1 Hz sampling frequency (or 20 Hz in Burst mode) without any aliasing filter. These signatures are expected to be seen on the OB sensor operated in NORMAL mode (sometimes) and always in BURST mode.

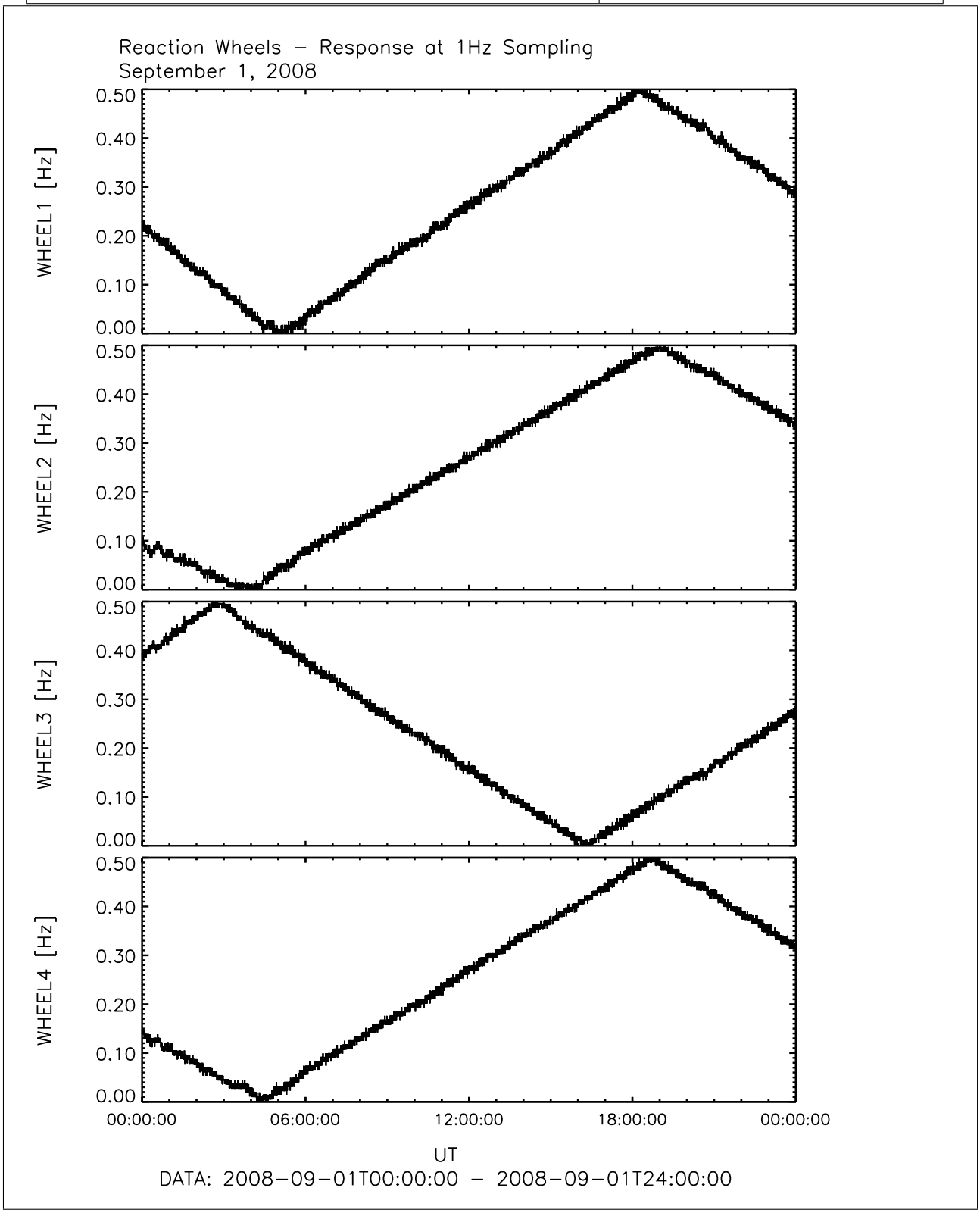

Figure 73: File: wheels_1Hz_Sampling2008-09-01T00-00

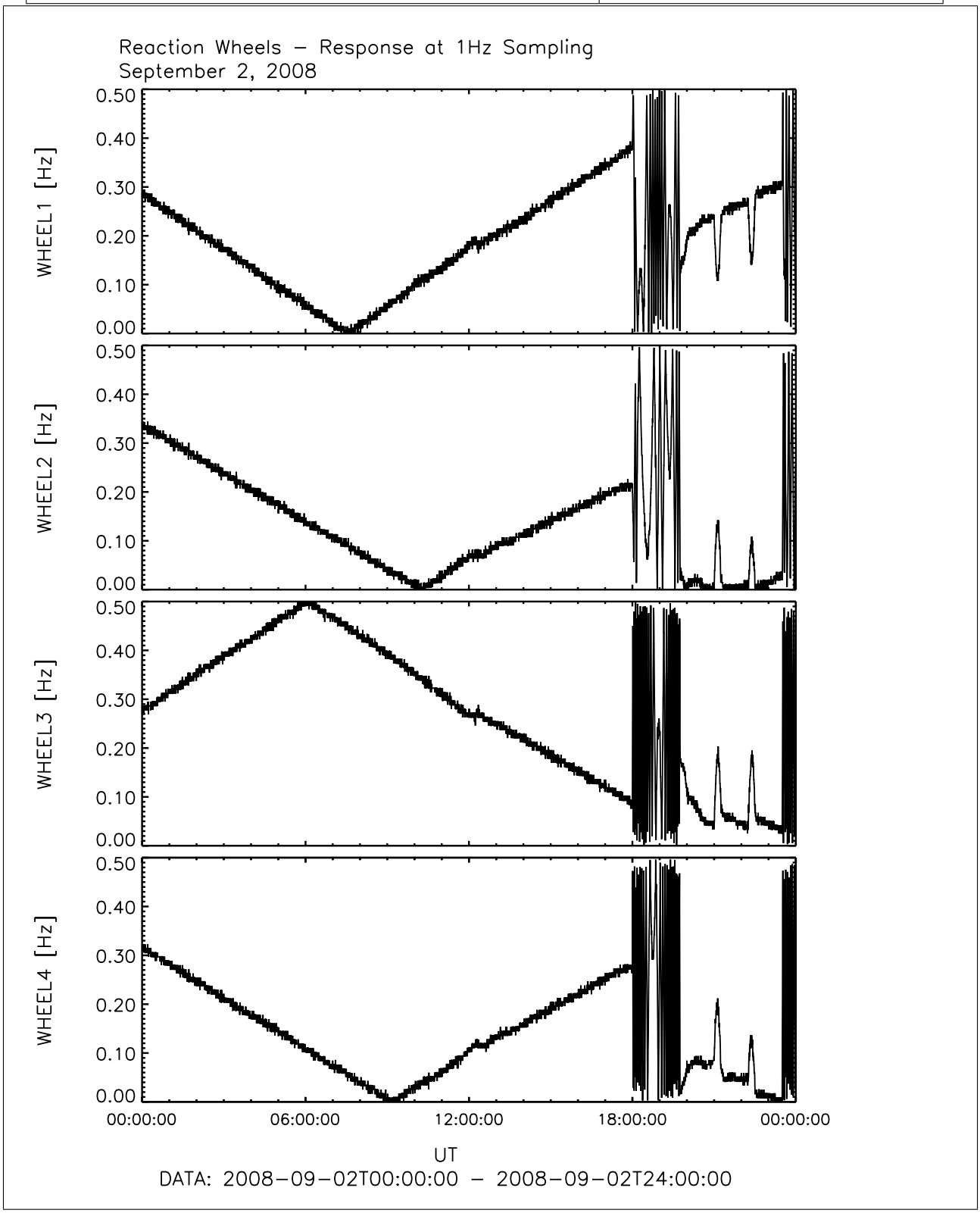

Figure 74: File: wheels_1Hz_Sampling2008-09-02T00-00

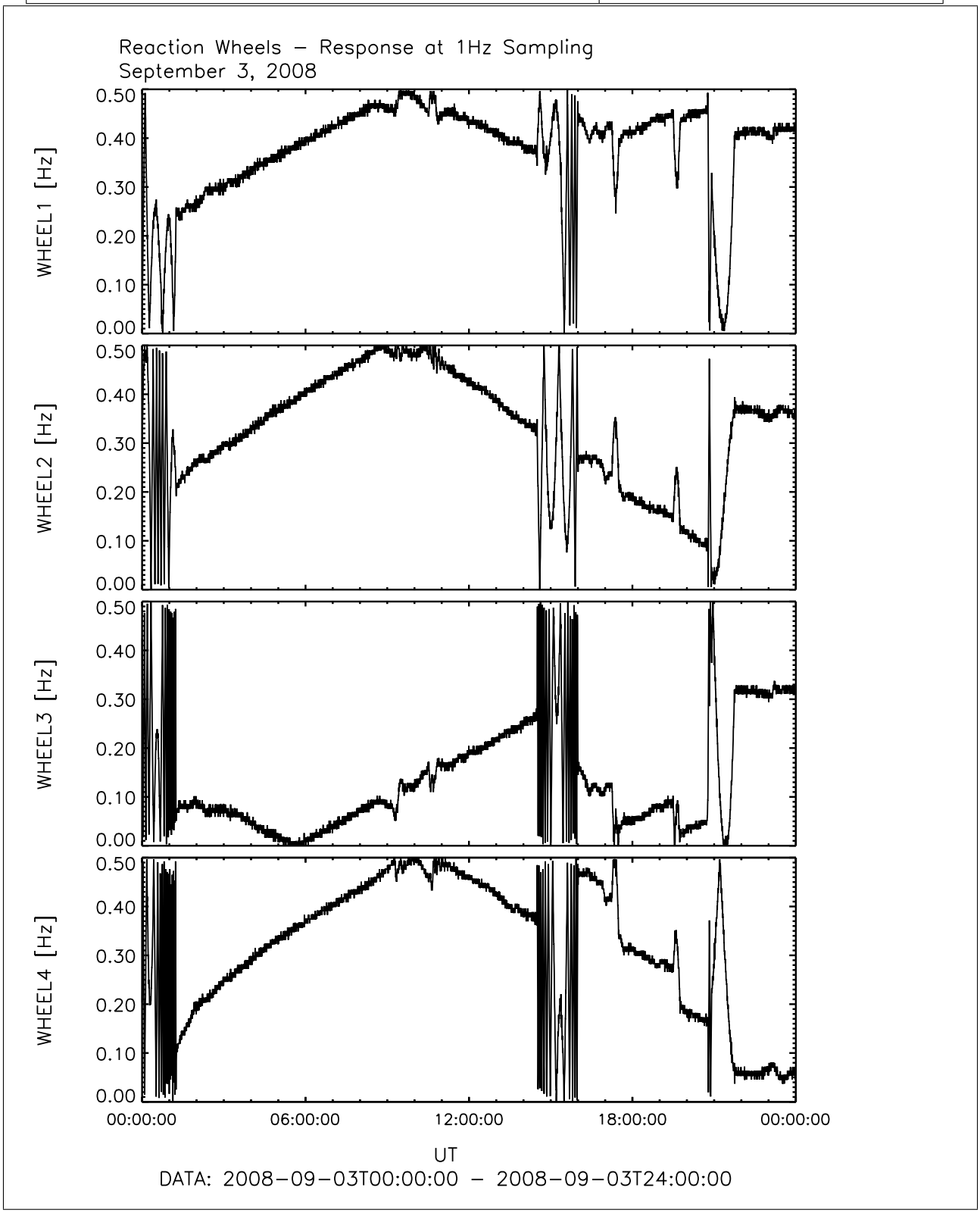

Figure 75: File: wheels_1Hz_Sampling2008-09-03T00-00

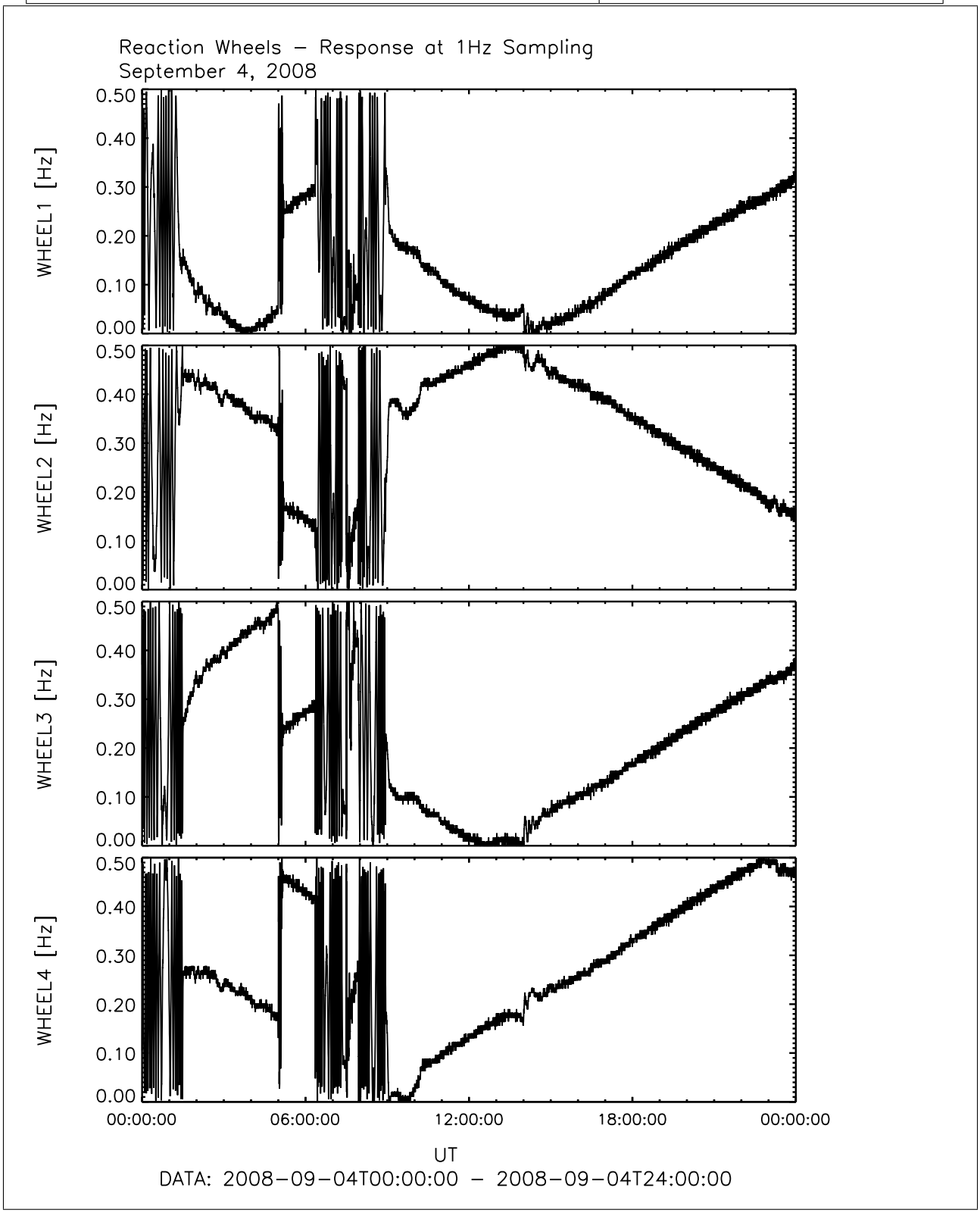

Figure 76: File: wheels_1Hz_Sampling2008-09-04T00-00

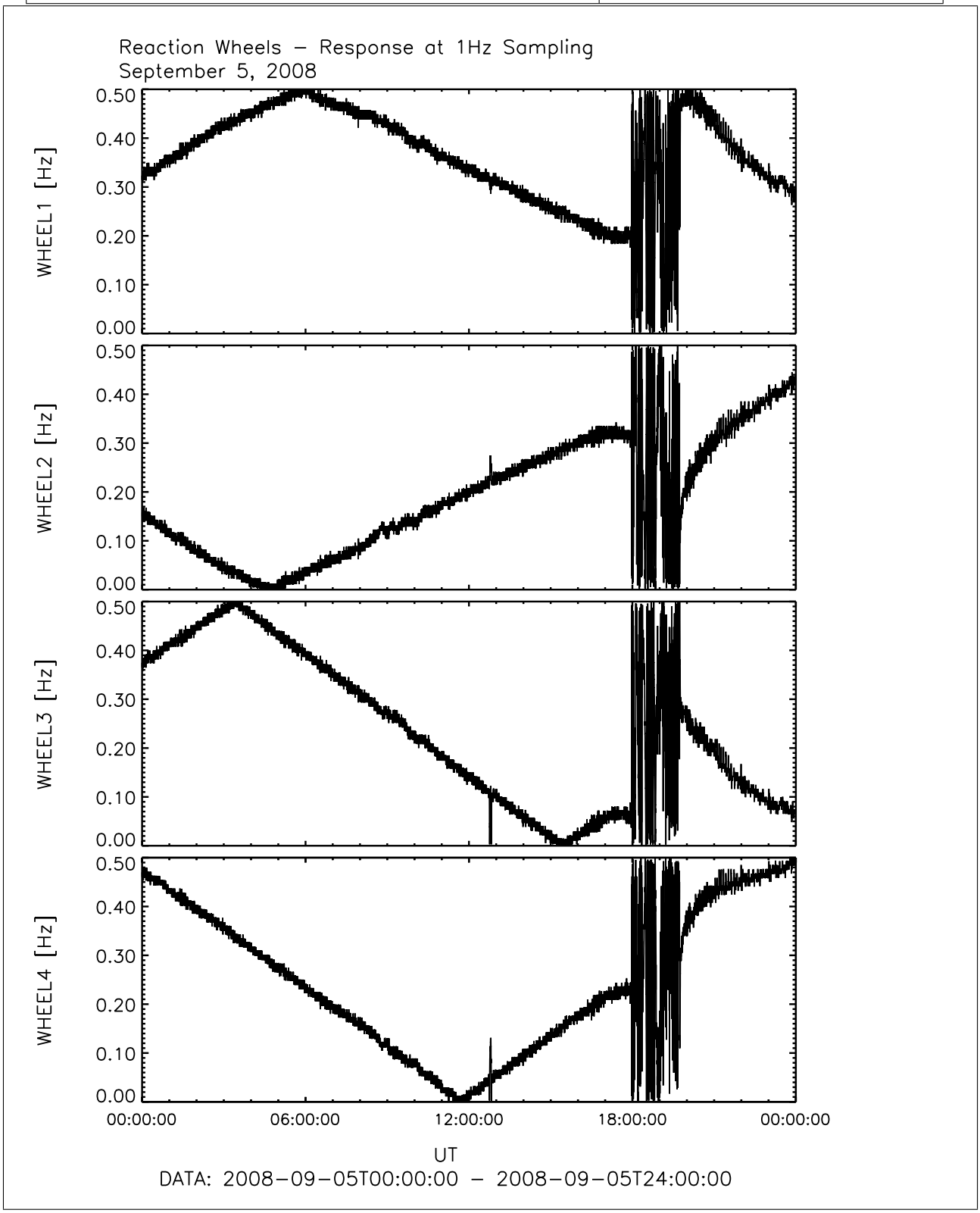

Figure 77: File: wheels_1Hz_Sampling2008-09-05T00-00

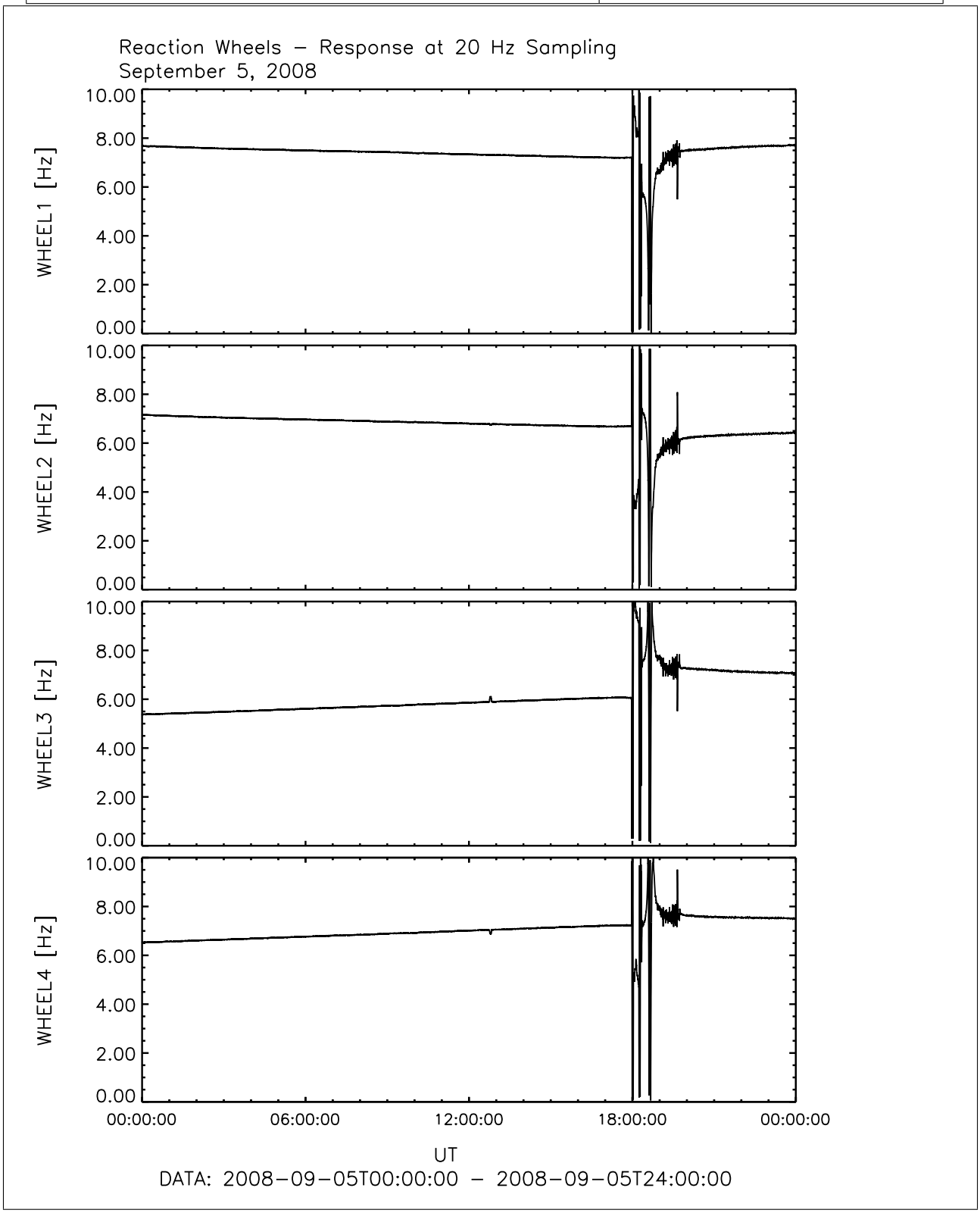

Figure 78: File: wheels_20Hz_Sampling2008-09-05T00-00

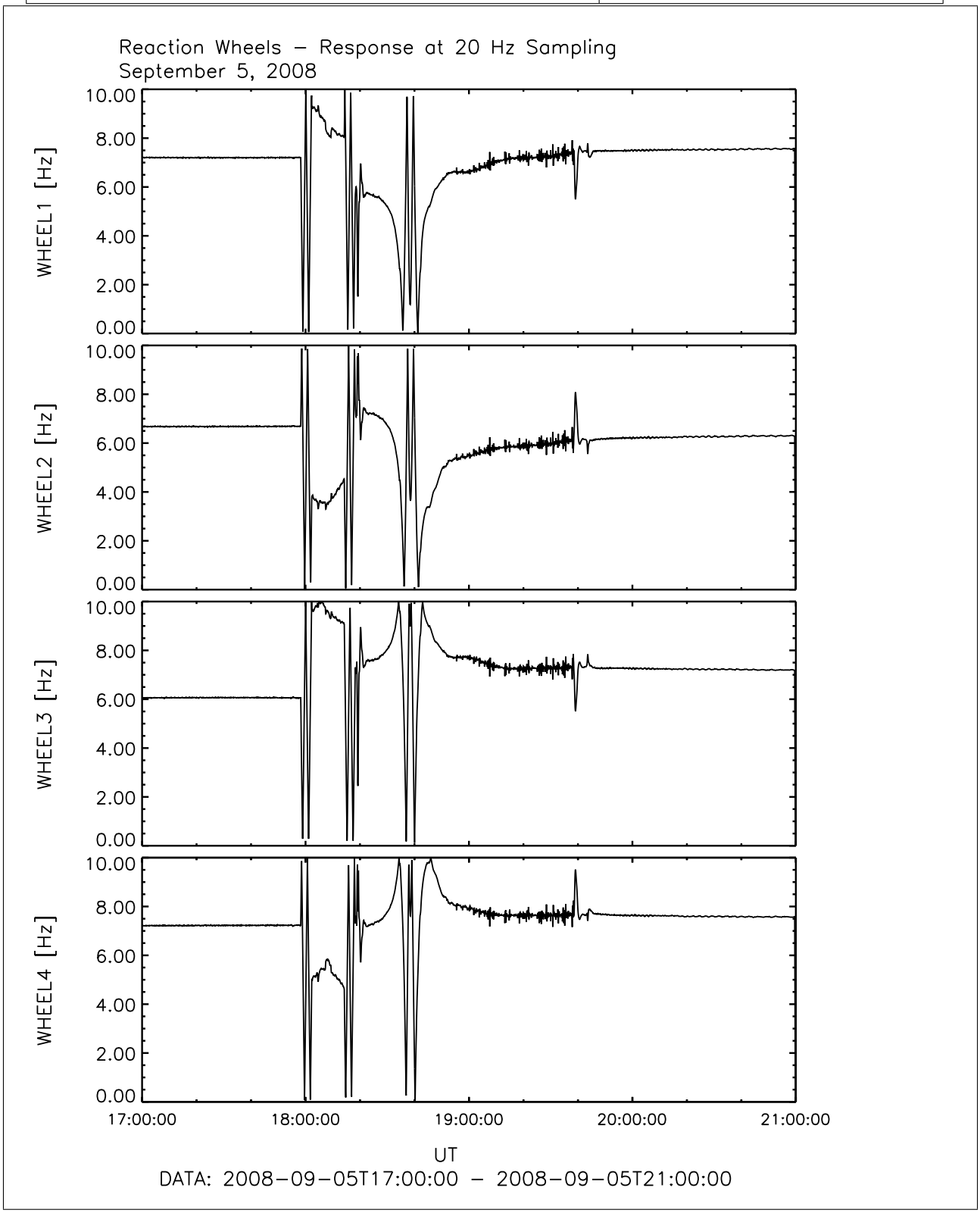

Figure 79: File: wheels_20Hz_Sampling2008-09-05T17-00

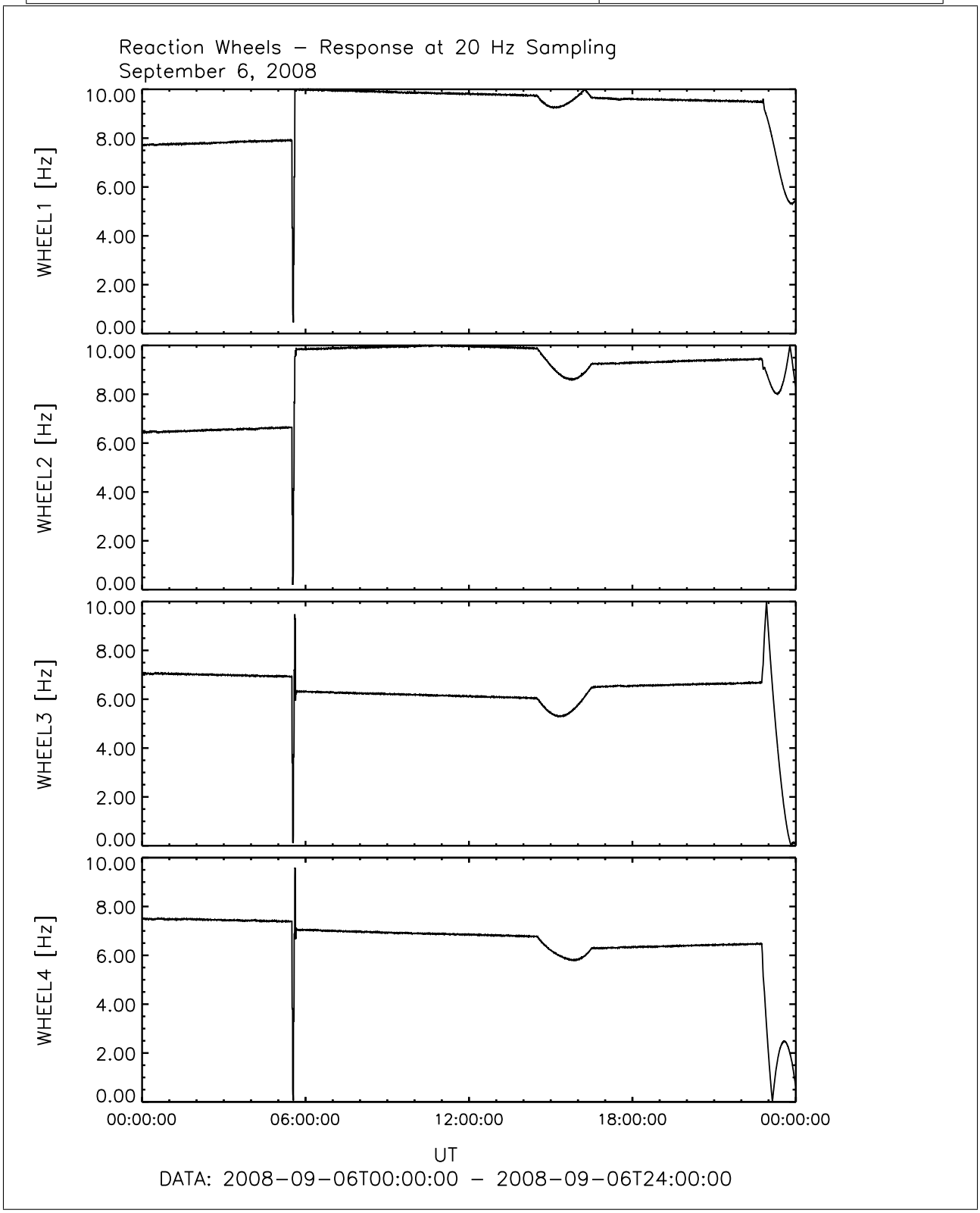

Figure 80: File: wheels_20Hz_Sampling2008-09-06T00-00

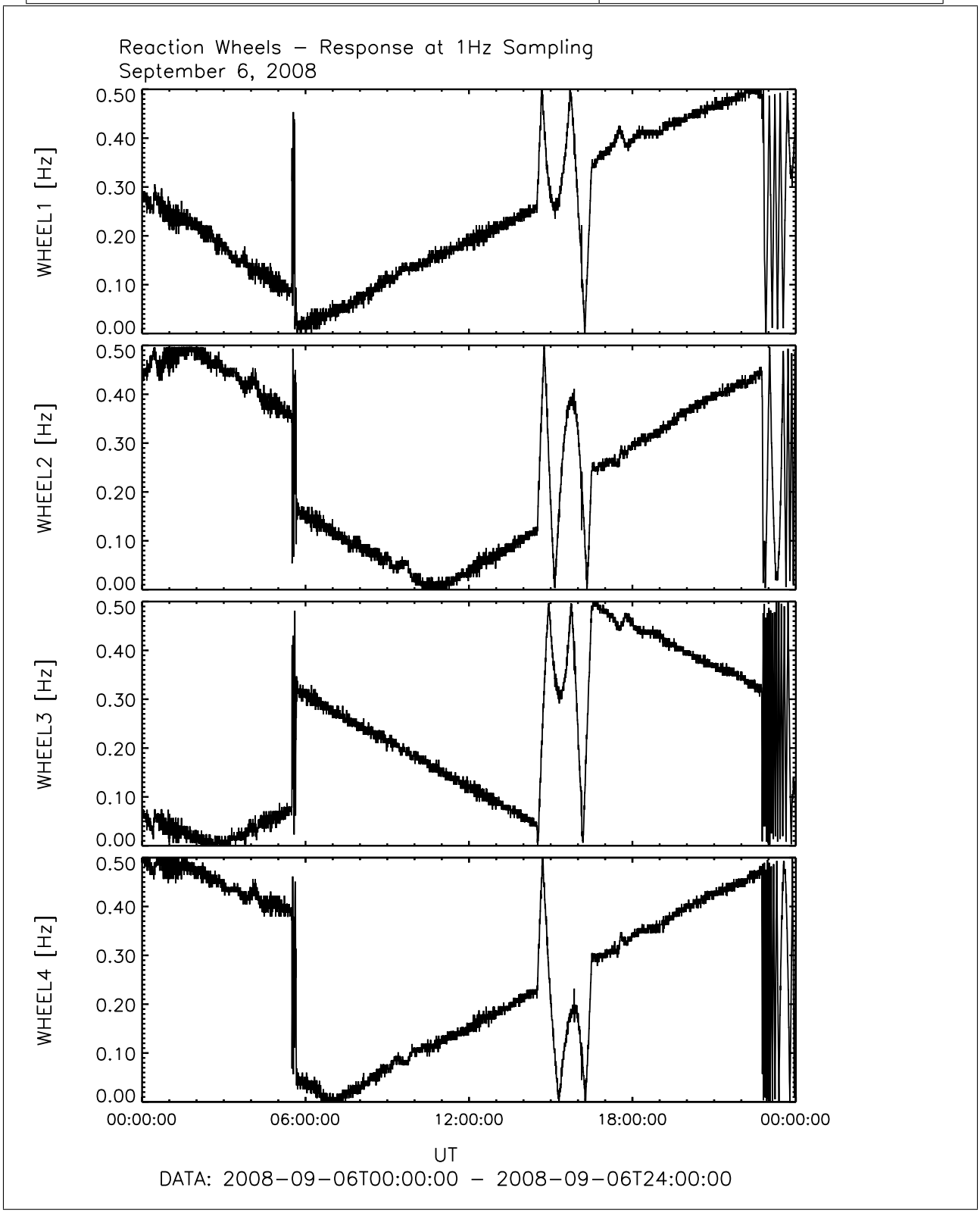

Figure 81: File: wheels_1Hz_Sampling2008-09-06T00-00

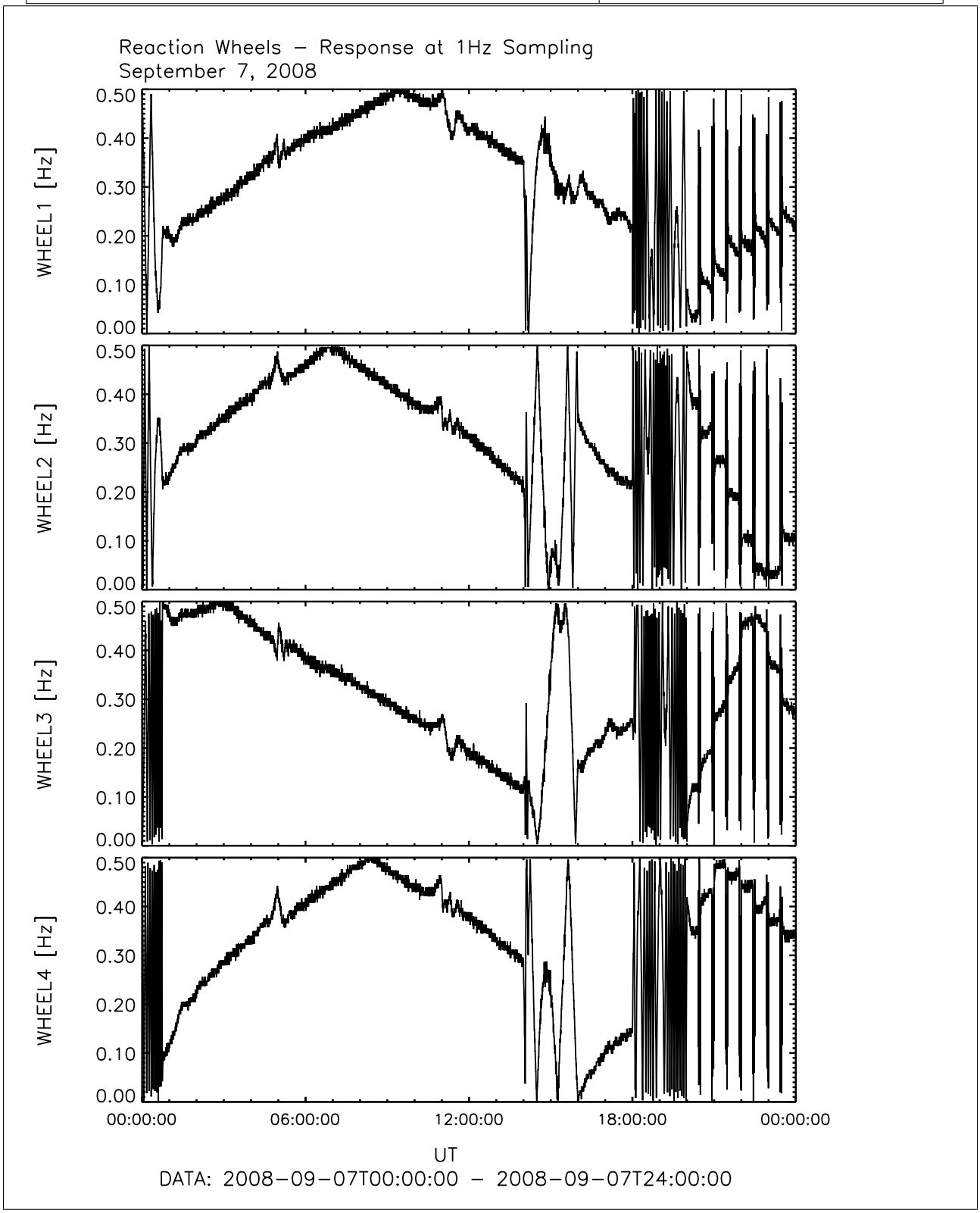

Figure 82: File: wheels_1Hz_Sampling2008-09-07T00-00

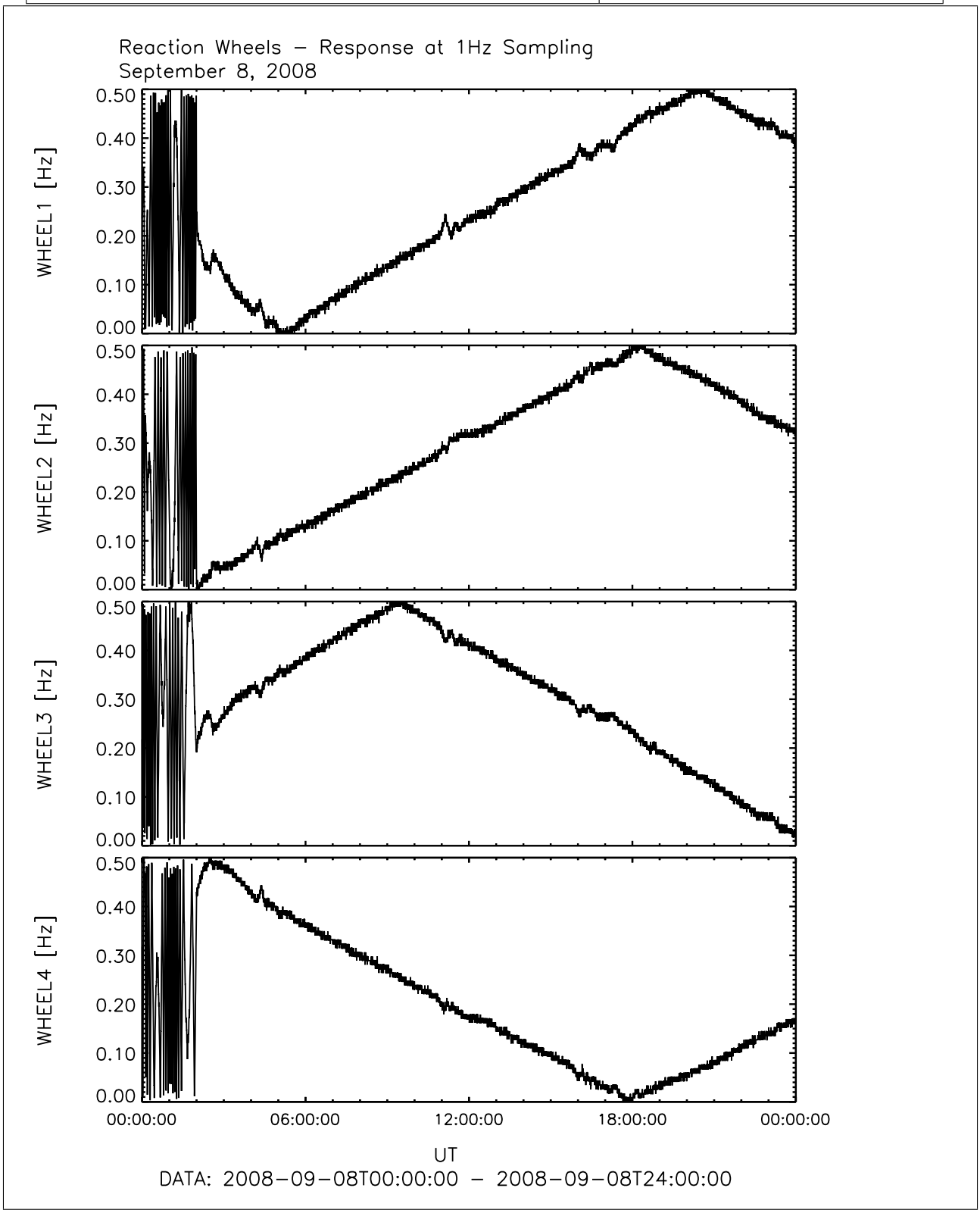

Figure 83: File: wheels_1Hz_Sampling2008-09-08T00-00

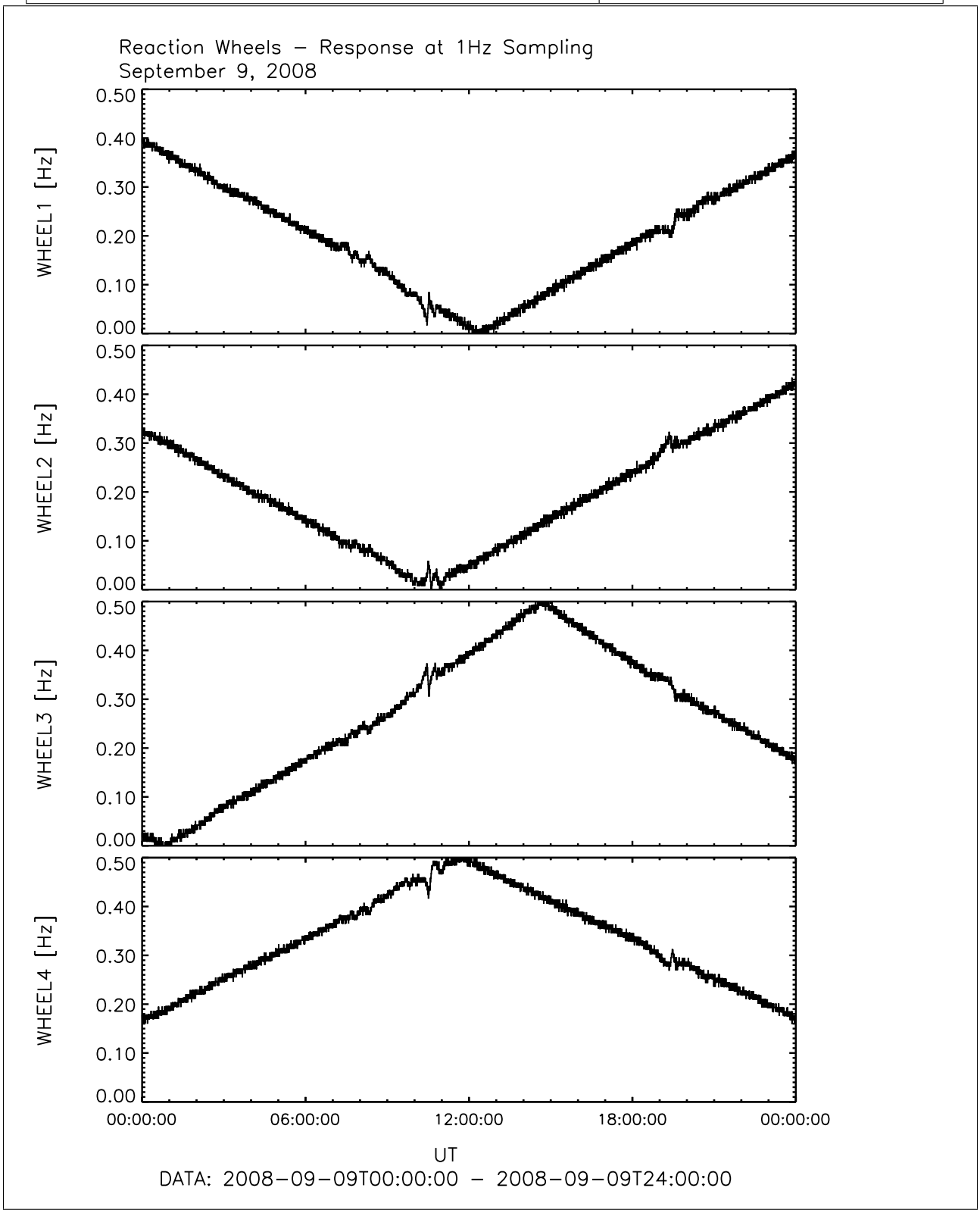

Figure 84: File: wheels_1Hz_Sampling2008-09-09T00-00

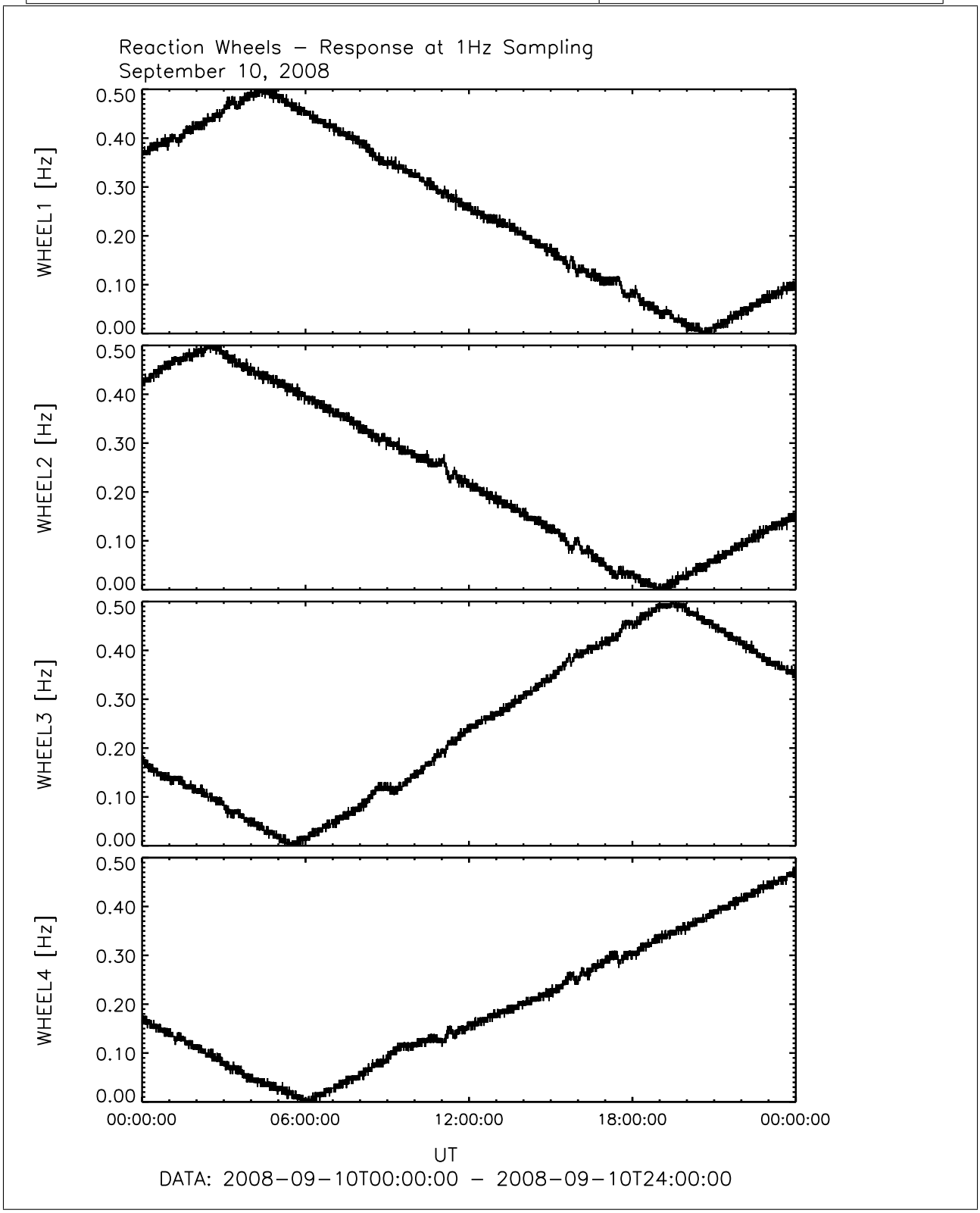

Figure 85: File: wheels_1Hz_Sampling2008-09-10T00-00

6.1 Plots of Reaction Wheel and LAP Disturbance corrected Data

The following plots show the dynamic spectra of the LEVEL_H data. These data have been purged from ROSETTAs reaction wheel disturbance and also from the disturbance of the LAP instrument. Plots are only shown for the primary sensor.

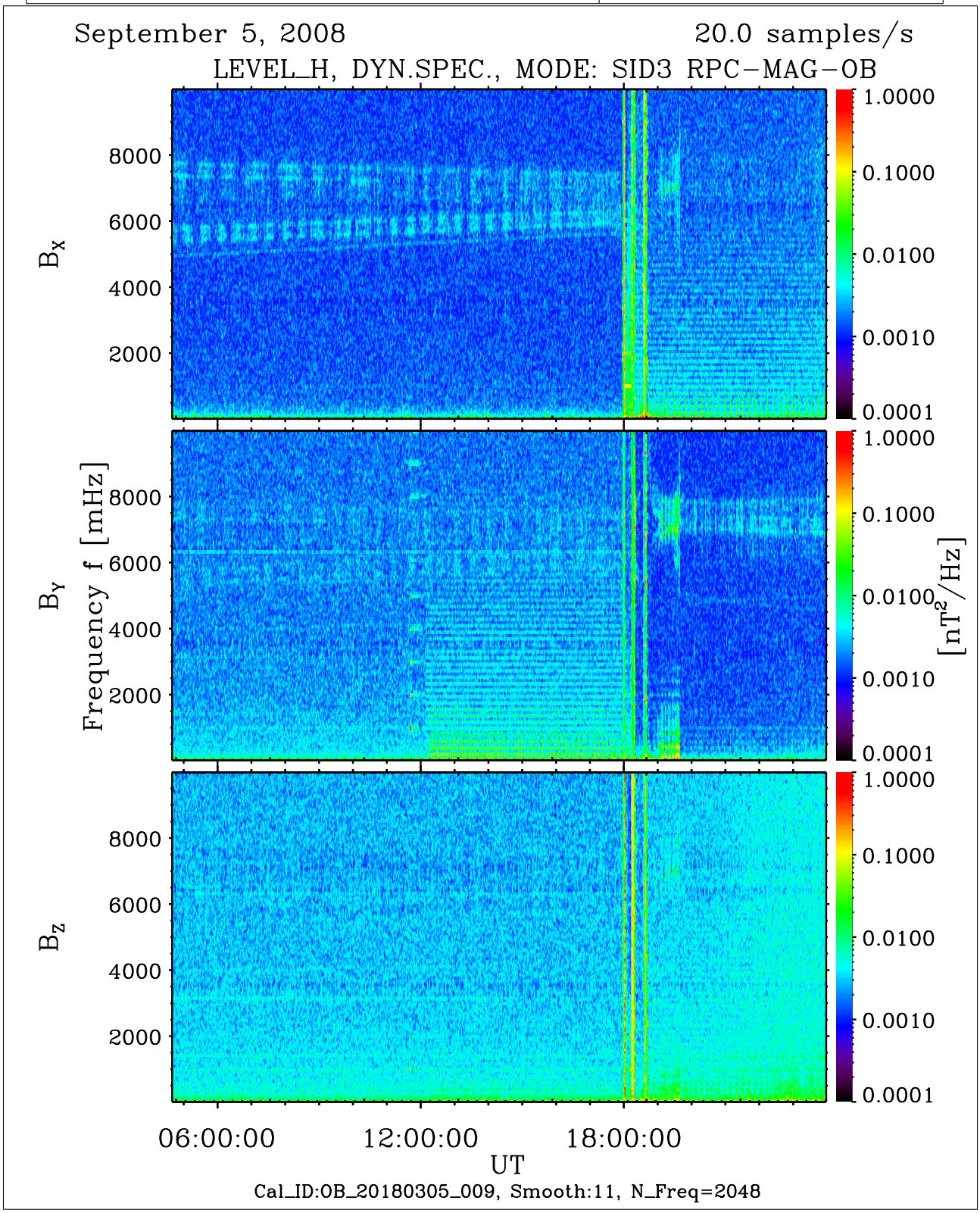

Figure 86: File: RPCMAG080905T0438_CLH_OB_M3_DS0_10000_009

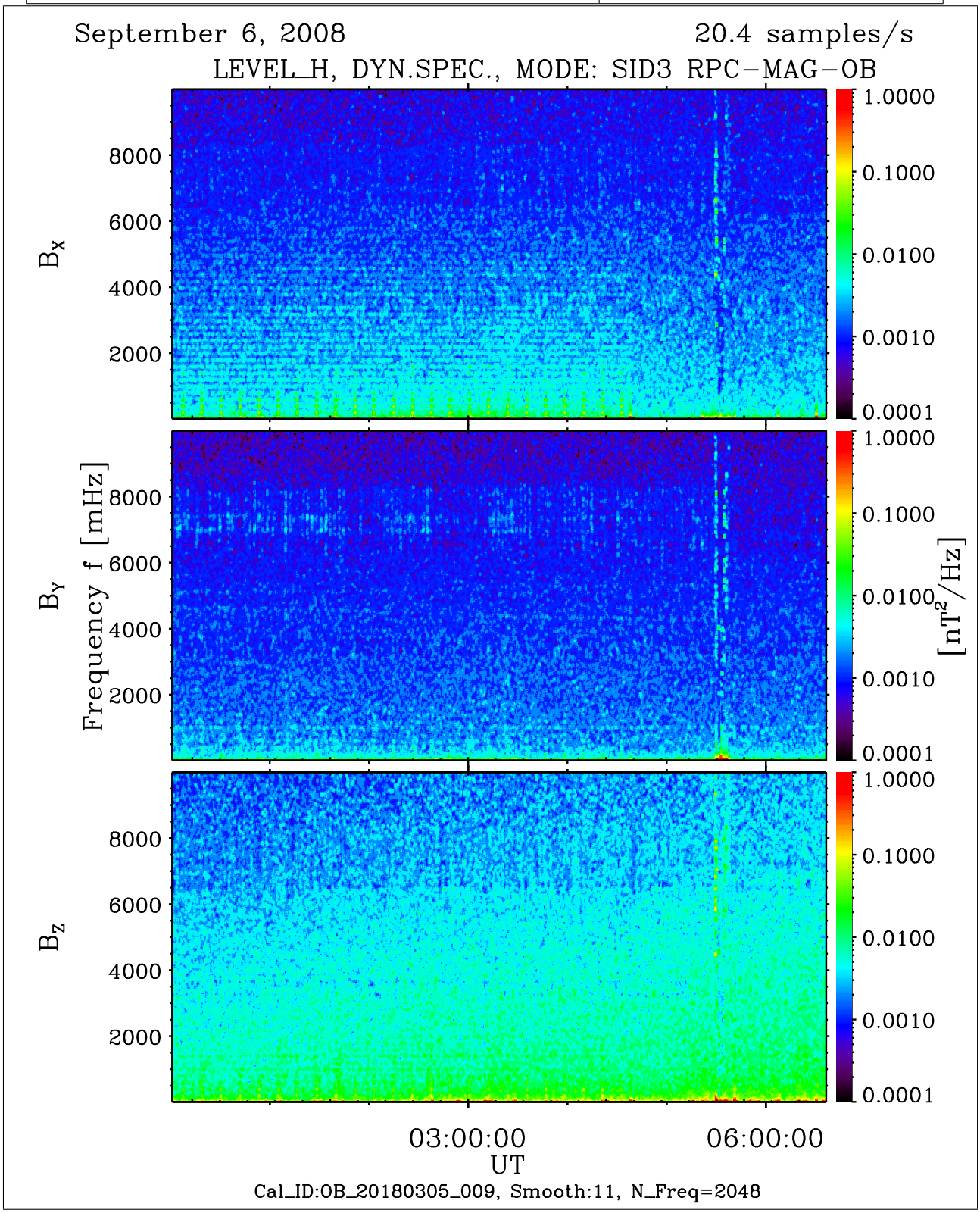

Figure 87: File: RPCMAG080906T0000_CLH_OB_M3_DS0_10000_009

7 Solar Array Rotation Angles and High Gain Antenna Orientation

To get an idea, whether the rotation of the Solar arrays or the movement of the High Gain Antenna (HGA) has an influence of the magnetic field data, the following plots have been generated. Each figure shows

- in the upper panel
  the rotation angle of the solar arrays (angle between the solar array normal and the spacecraft $x_{\mathrm{S/C}}$ axis
- in the two lower panels
  the projected rotation angle in the spacecraft $xy_{\mathrm{S/C}}$-Plane and the projected rotation angle in the spacecraft $xz_{\mathrm{S/C}}$-Plane. Both angles are displayed wrt. the x-axis.

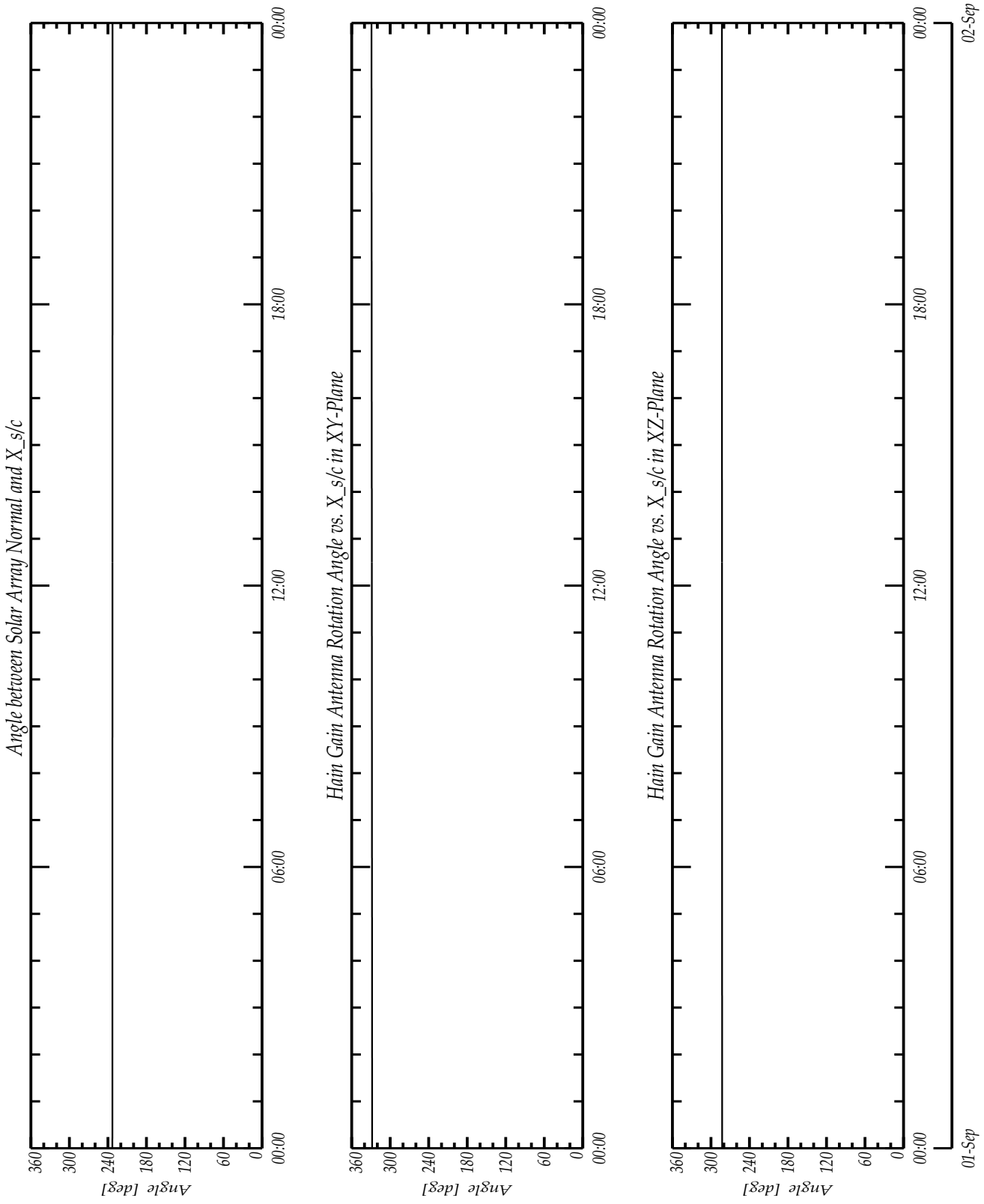

Figure 88: File: Solar Array and HGA Rotation Angles of 2008-09-01

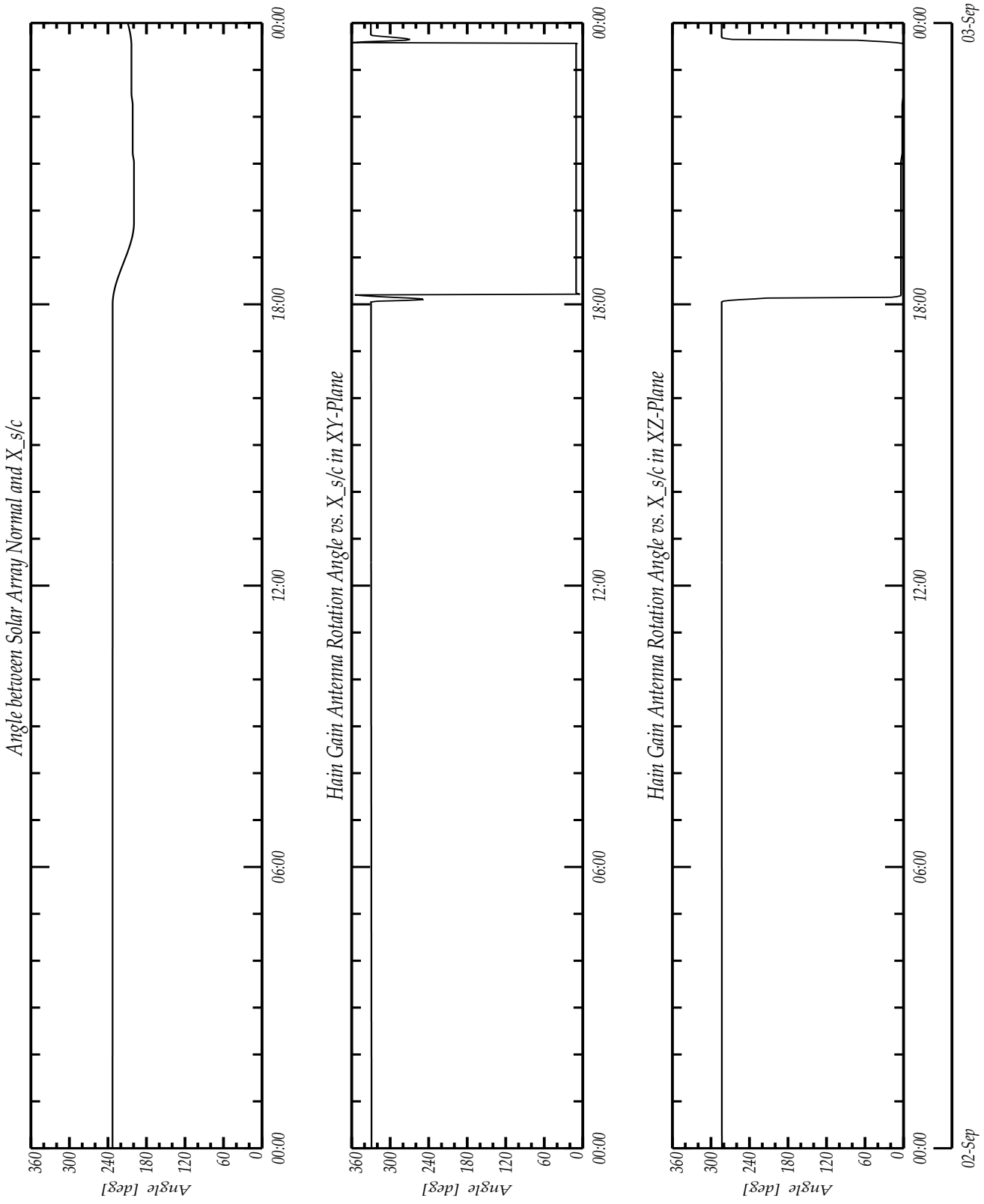

Figure 89: File: Solar Array and HGA Rotation Angles of 2008-09-02

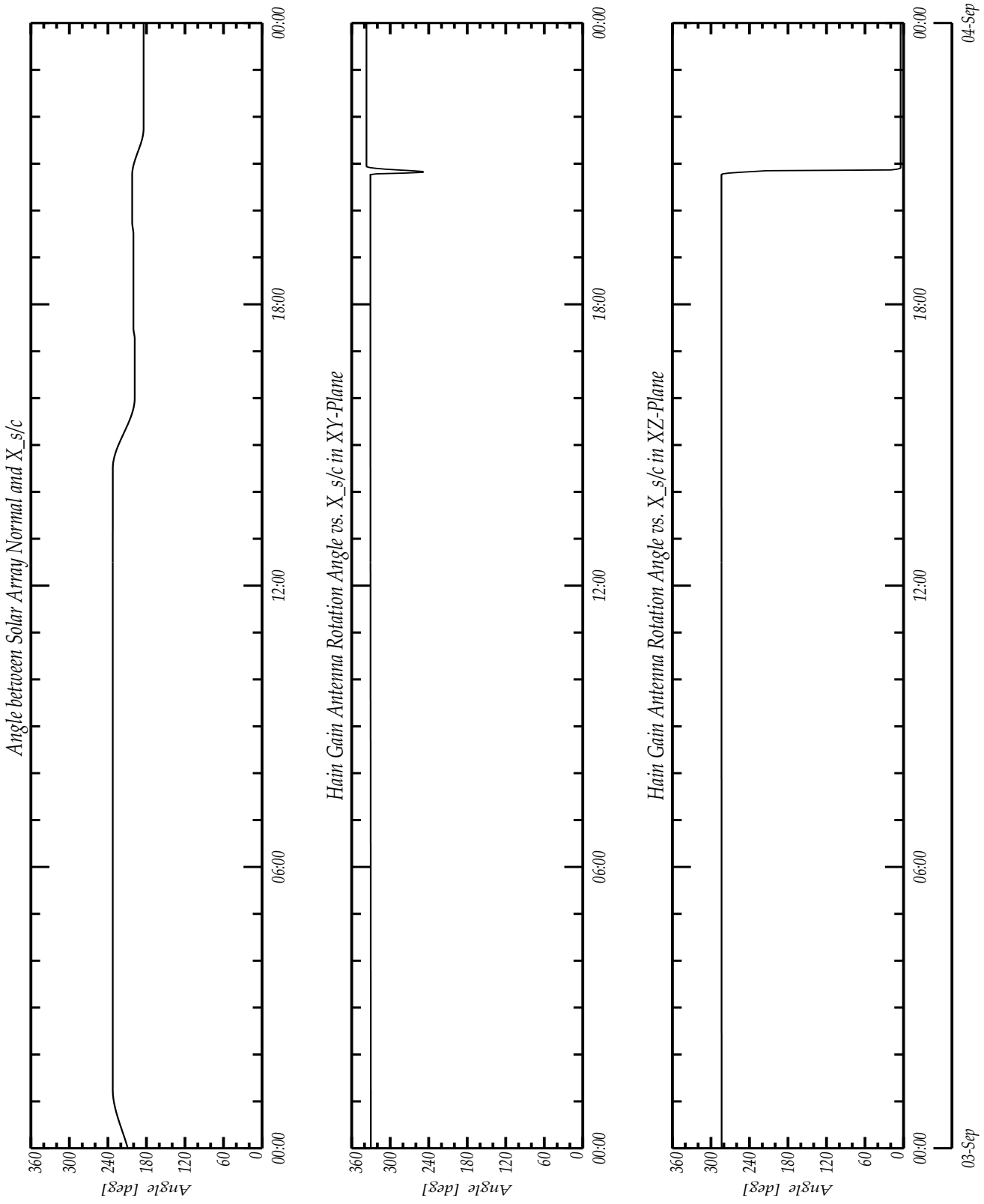

Figure 90: File: Solar Array and HGA Rotation Angles of 2008-09-03

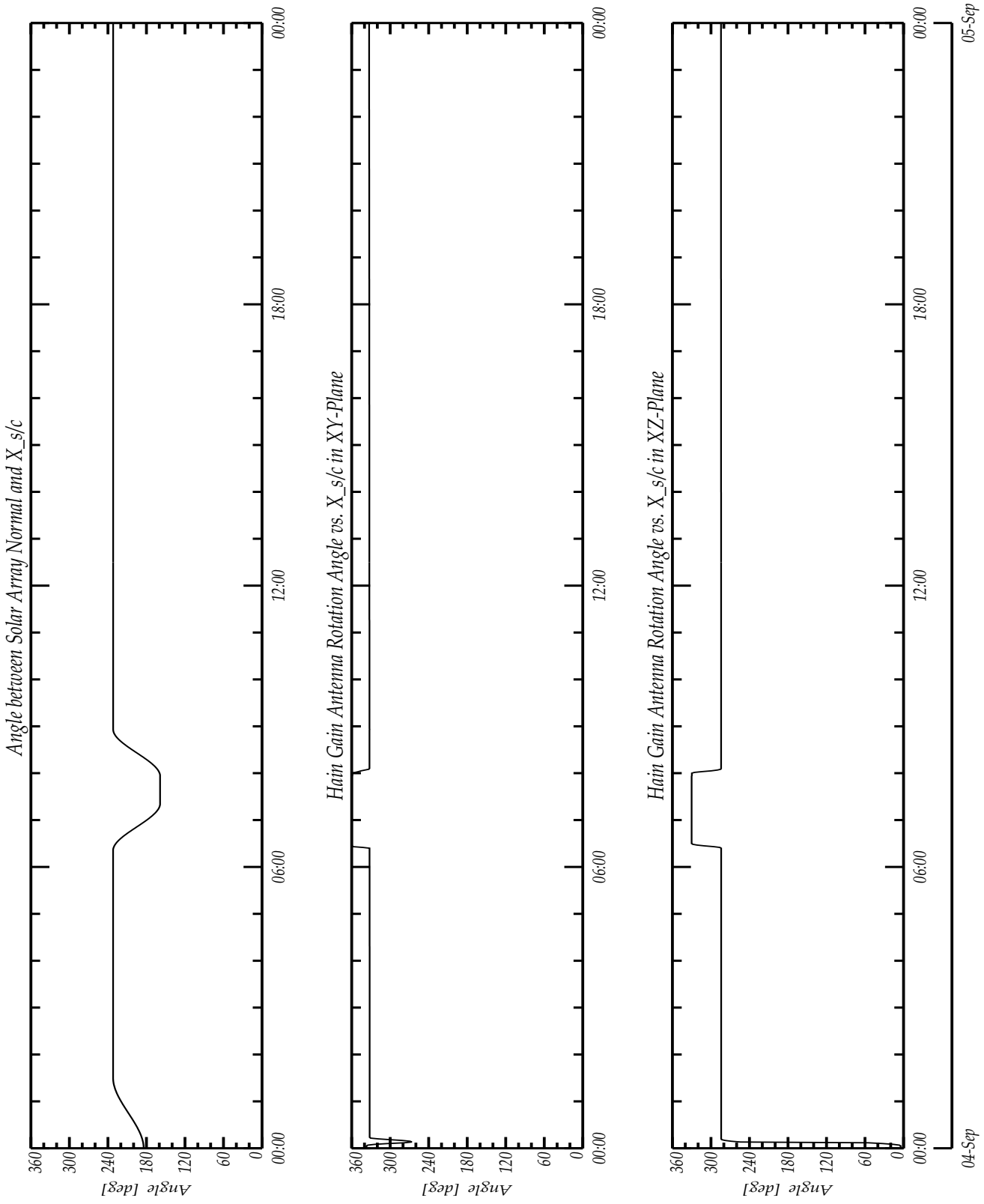

Figure 91: File: Solar Array and HGA Rotation Angles of 2008-09-04

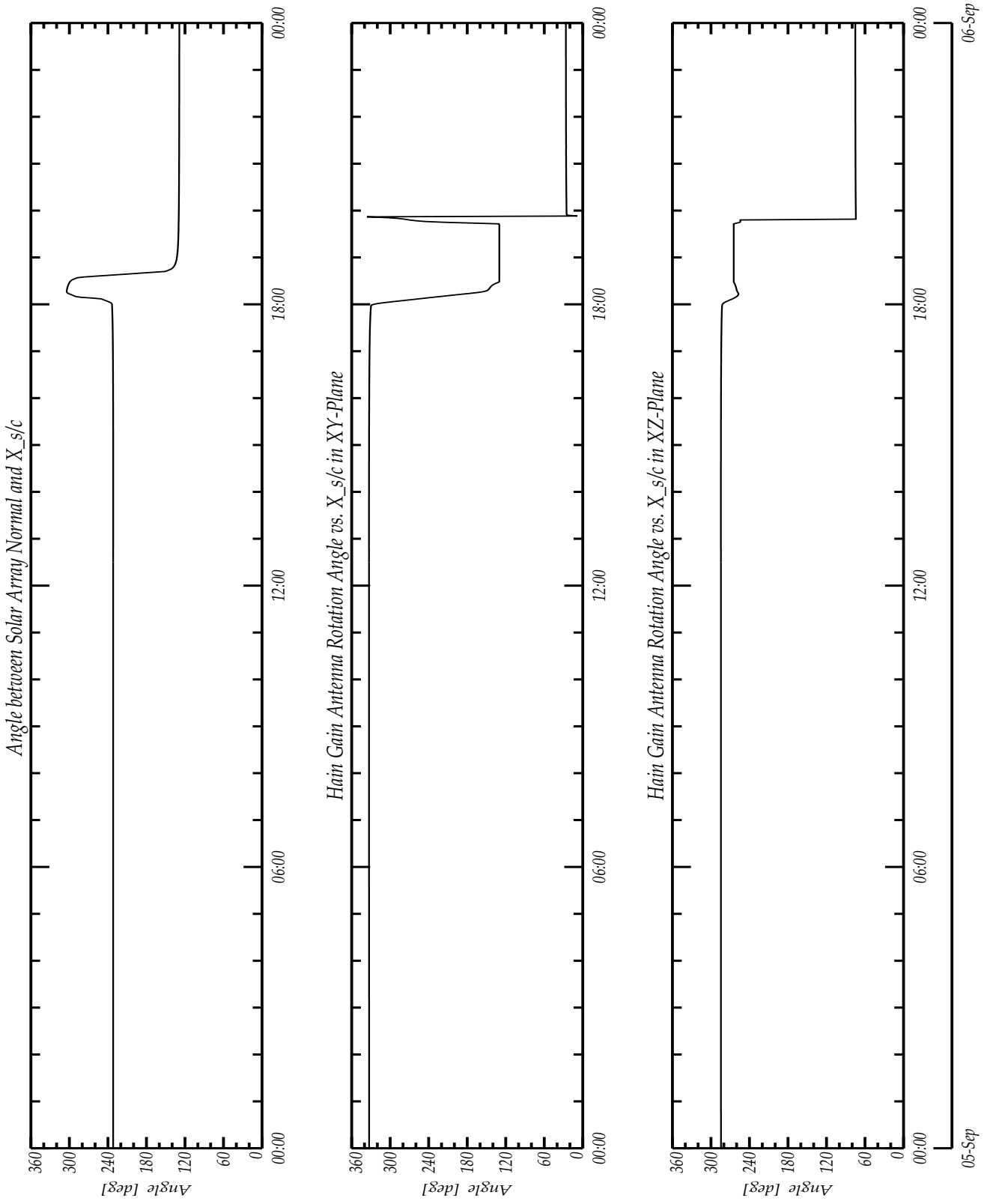

Figure 92: File: Solar Array and HGA Rotation Angles of 2008-09-05

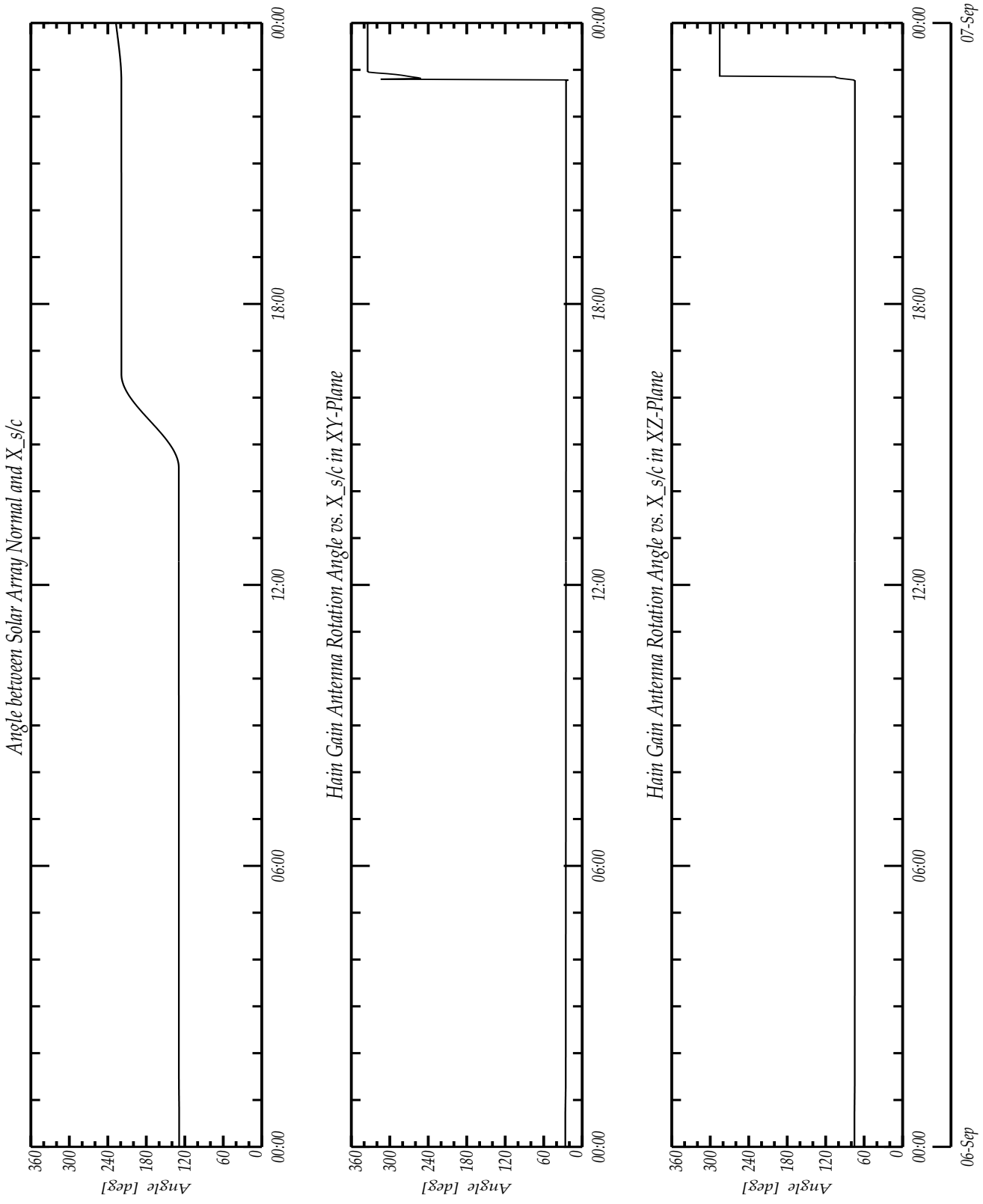

Figure 93: File: Solar Array and HGA Rotation Angles of 2008-09-06

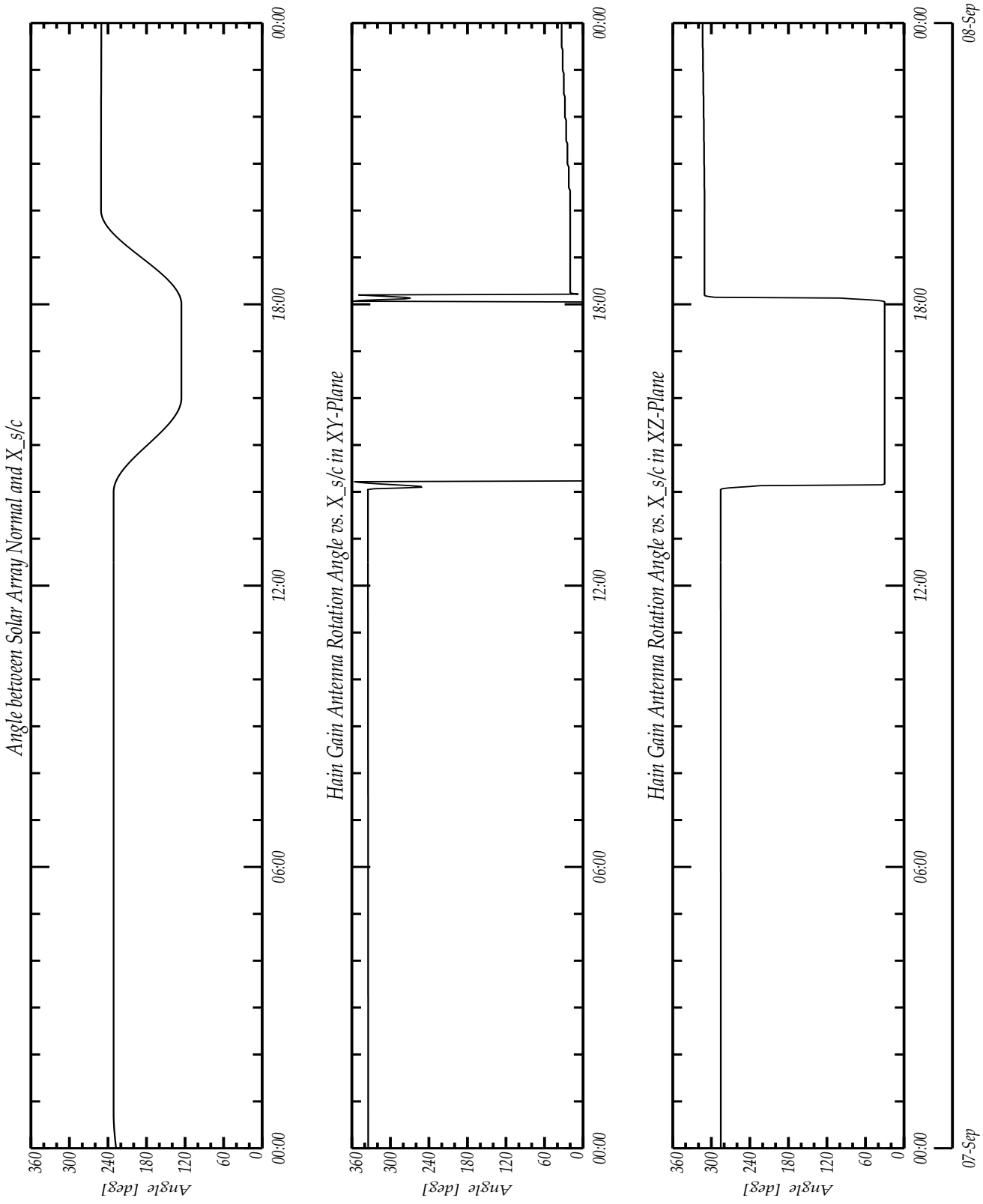

Figure 94: File: Solar Array and HGA Rotation Angles of 2008-09-07

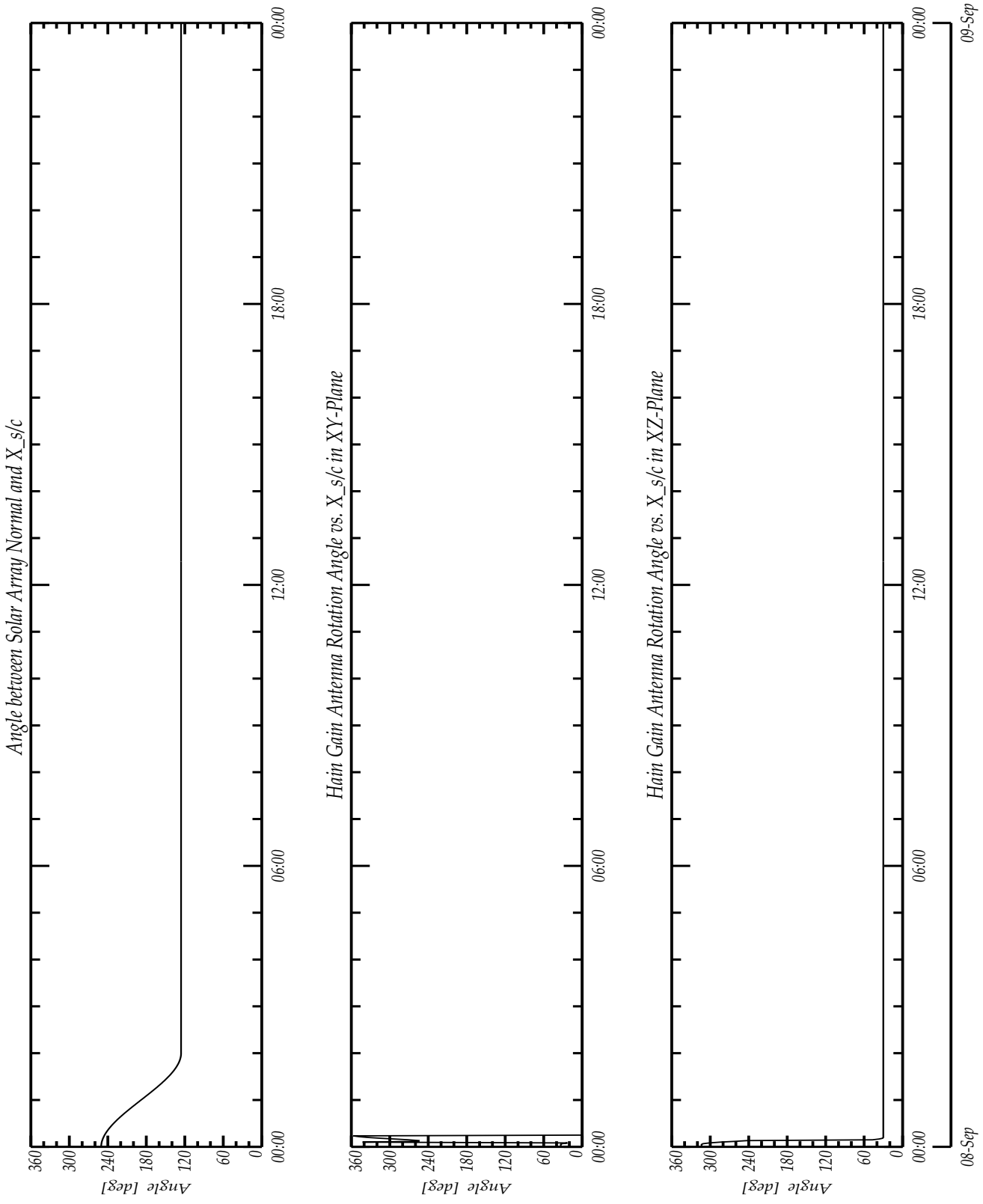

Figure 95: File: Solar Array and HGA Rotation Angles of 2008-09-08

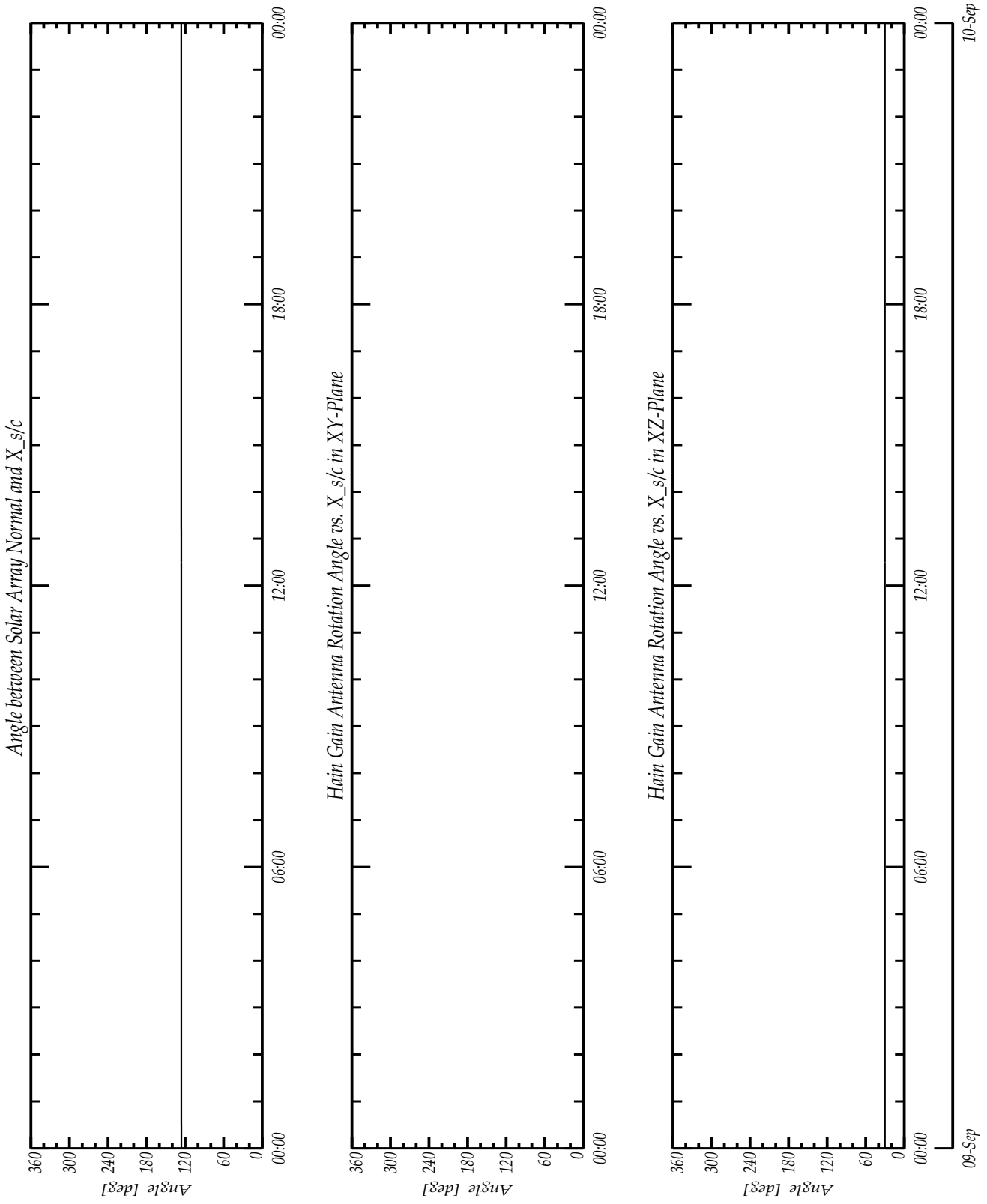

Figure 96: File: Solar Array and HGA Rotation Angles of 2008-09-09

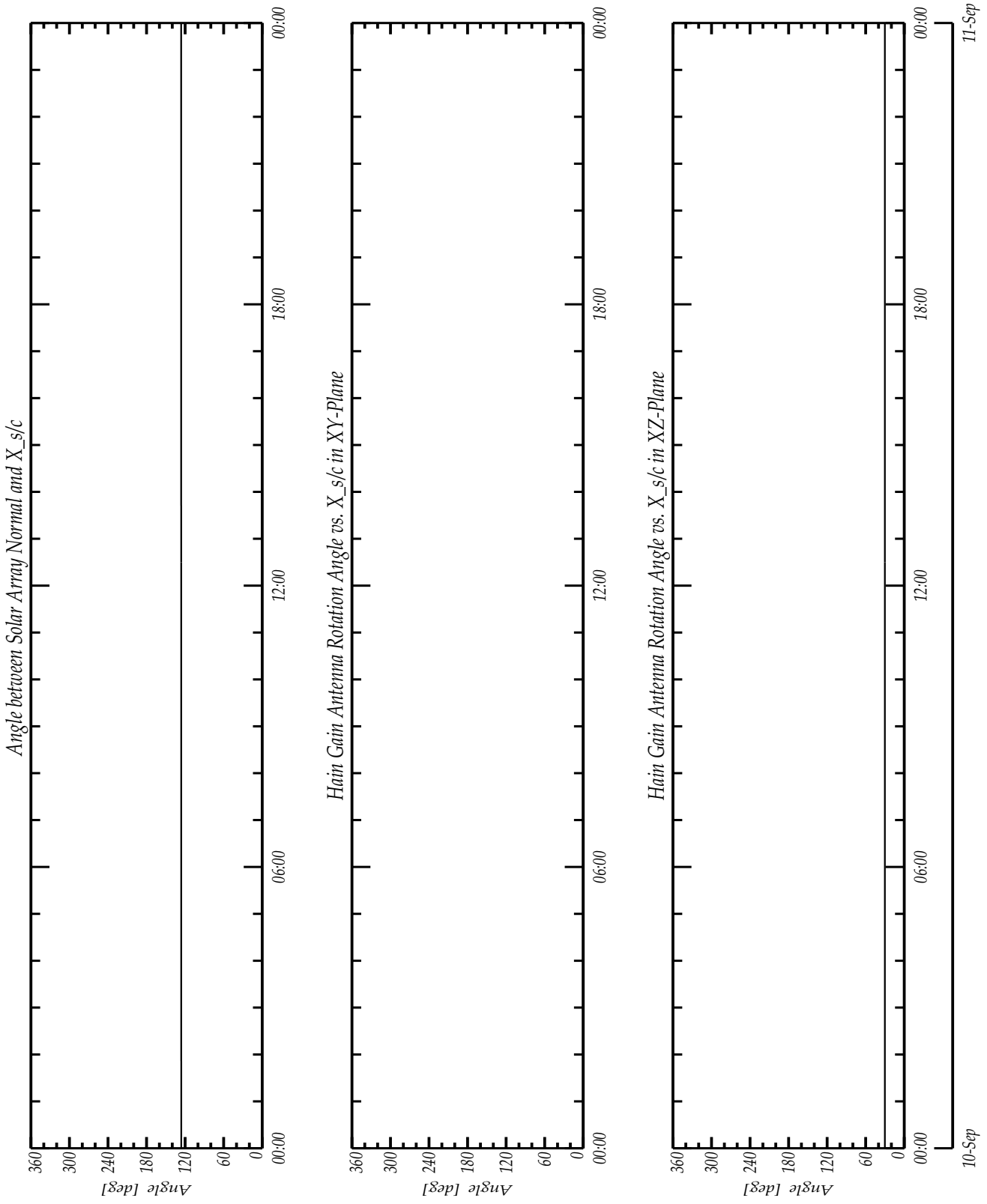

Figure 97: File: Solar Array and HGA Rotation Angles of 2008-09-10

8 Temperature profile during the FlyBy

The following figure shows the measured temperatures of the OB and IB sensor during the flyby. The lower panels of the graph show the angles between x–, y–, and z–axis of the s/c frame and the sun direction.

The analysis of these plots shows that - as expected - most of the temperature changes are related to attitude changes.

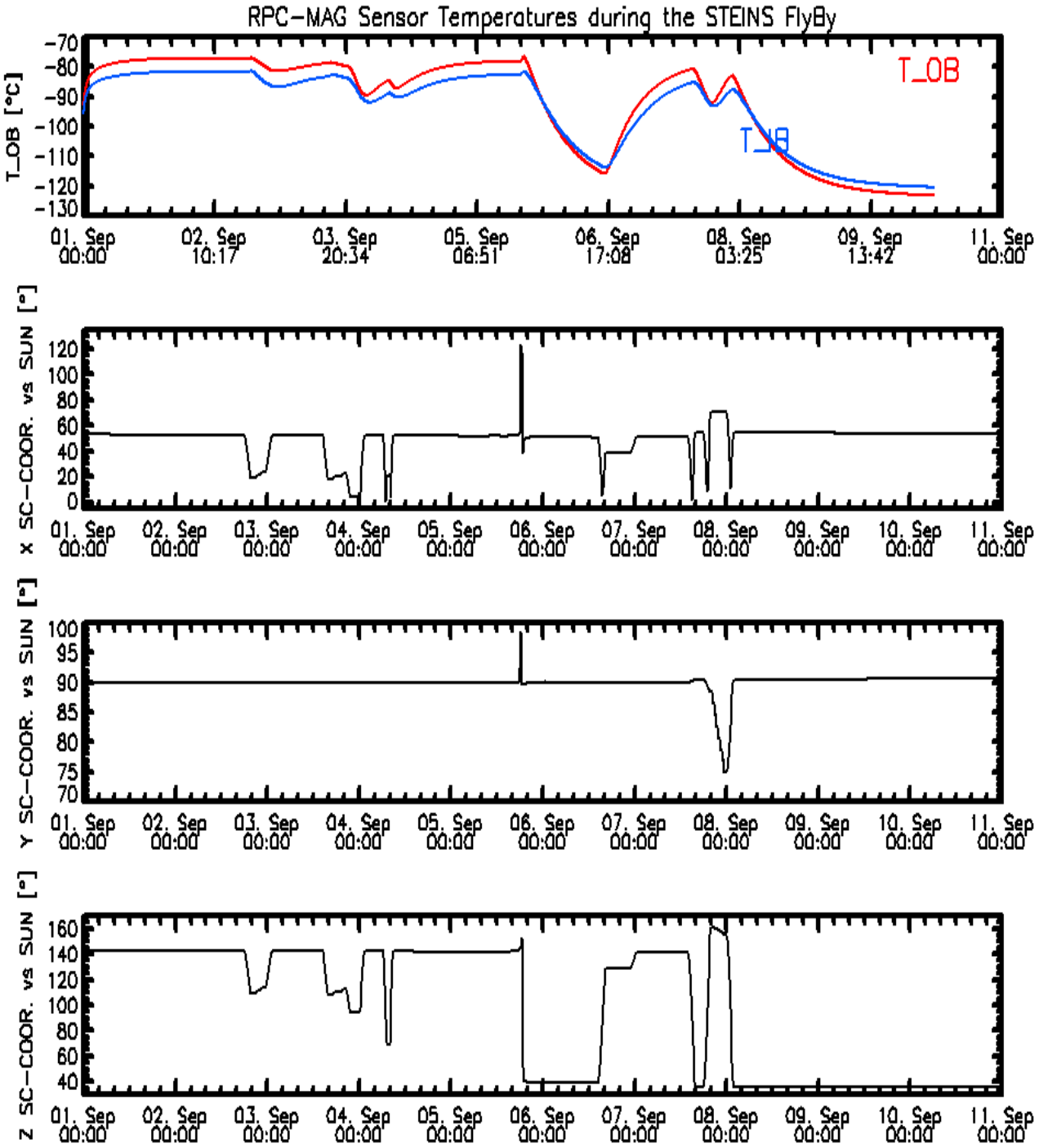

Figure 98: Measured Sensor Temperatures and attitudes during the STEINS FlyBy

9 Conclusions

- RPCMAG itself worked as expected.
- The data of the flyby are disturbed by pulsed MUPUS heater currents. The currents generate magnetic disturbances in the order of 2 nT (about 100 nT at the location of the ROMAP sensors)
- Reaction Wheel influence and the disturbance of of the LAP instrument can be seen whilst RPCMAG is operating in Burst mode.
- The comparison between IB and OB data showed that the measurements are very sensitive to specific temperature changes at the single sensors
- All flyby data are very disturbed. Disturbances occur in various time scales. The origin of the disturbance can not clearly be identified. MUPUS is one source but probably not the only one.
- Rotation of the solar array and movement of the High Gain Antenna cannot be seen in the magnetic field data.
- Last but not least: any signature of STEINS cannot be seen in the magnetic field data.
- The scientific results of this fly by have been published as:
  H.U. Auster; I. Richter; K.H. Glassmeier; G. Berghofer; C.M. Carr, U. Motschmann; Magnetic Field Investigations During ROSETTA's 2867 Steins Flyby, Planetary and Space Science, 2010